Full report

(รายงานฉบับสมบูรณ์)

Grant number: DBG5980004

Targeting of the FOXM1 signature for early diagnosis and treatment in cholangiocarcinoma

การมุ่งเป้า FOXM1 และเครือข่ายเพื่อวินิจฉัยและรักษามะเร็งท่อน้ำดี

Chawalit Pairojkul, et al

Faculty of Medicine

Khon Kaen University

---------- รายงานนี้ยังไม่เสร็จสิ้น ห้ามใช้ในการอ้างอิง ----------

สารบัญ

สารบัญภาพ

หน้า

สารบัญภาพ

หน้า

สารบัญภาพ

หน้า

สารบัญตาราง

หน้า

กิตติกรรมประกาศ

คณะผู้วิจัยขอขอบพระคุณสำนักงานกองทุนสนับสนุนการวิจัย (สกว.) ที่ริเริ่มทุนวิจัยพื้นฐานเชิงยุทธศาสตร์ (Strategic Basic Research Grant, DBG) และพิจารณามอบทุนให้กับคณะผู้วิจัย ซึ่งเป็นการขยายโอกาสและส่งเสริมความเข้มแข็งของกลุ่มวิจัย รวมทั้งมีโอกาสทำงานร่วมกับนักวิจัยจาก Imperial College London, United Kingdom

คณะผู้วิจัยขอขอบคุณสถาบันวิจัยมะเร็งท่อน้ำดีที่เอื้อเฟื้อตัวอย่างชีวภาพ ภาควิชาพยาธิวิทยา ภาควิชาชีวเคมี และภาควิชาศัลยศาสตร์ คณะแพทยศาสตร์ มหาวิทยาลัยขอนแก่น ที่สนับสนุนนักวิจัยให้สามารถทำวิจัยได้อย่างเต็มศักยภาพ ขอขอบคุณผู้ป่วยมะเร็งท่อน้ำดีที่ได้อุทิศตัวอย่างในการศึกษานี้ และผู้ช่วยนักวิจัยทุกท่านที่ให้ความร่วมมือในการวิจัยนี้เป็นอย่างดี

คณะผู้วิจัย

Full report (รายงานการวิจัยฉบับสมบูรณ์)

Grant number: DBG5980004

โครงการ : การมุ่งเป้า FOXM1 และเครือข่ายเพื่อวินิจฉัยและรักษามะเร็งท่อน้ำดี

Targeting the FOXM1 signature for early diagnosis and treatment in cholangiocarcinoma

บทสรุปสำหรับผู้บริหาร

โครงการการมุ่งเป้า FOXM1 และเครือข่ายเพื่อวินิจฉัยและรักษามะเร็งท่อน้ำดี ได้รับทุนพื้นฐานเชิงยุทธศาสตร์ จากฝ่ายวิชาการ สำนักงานกองทุนสนับสนุนการวิจัยเป็นเวลา 3 ปี โดยมี รศ. นพ. ชวลิต ไพโรจน์กุล เป็นหัวหน้านักวิจัยฝ่ายไทย ซึ่งได้พัฒนาความร่วมมือในการวิจัยกับ Prof. Eric Lam, Imperial College of Medicine, UK ผลการศึกษาวิจัย รวมถึงผลลัพธ์อื่นๆจากโครงการวิจัยเรื่องนี้ มีดังนี้

(1) ด้านวิชาการ ได้ค้นพบบทบาทและพิสูจน์ความสัมพันธ์ของ FOXM1 และเครือข่าย (FOXO3, FOXO4, FOXA1 และ FOXA3) ที่เกี่ยวข้องกับการพัฒนาการ การดื้อยา การแพร่กระจาย และระยะรอดชีพของผู้ป่วย ทั้งในลักษณะ oncogenic และ tumor suppressor เนื้อหาวิชาการเหล่านี้ได้รับการตีพิมพ์เผยแพร่ในวารสารวิชาการนานาชาติแล้ว 10 เรื่อง อยู่ระหว่าง revision 1 เรื่อง อยู่ในระหว่างเตรียมต้นฉบับ 4 เรื่อง รวม 15 เรื่อง (รายละเอียดในรายงาน)

(2) การพัฒนานักวิจัยรุ่นใหม่ การเลื่อนตำแหน่งทางวิชาการ: นักวิจัยในโครงการได้รับการกำหนดตำแหน่งวิชาการเป็น ผู้ช่วยศาตราจารย์ 4 คน และเตรียมเอกสารเพื่อยื่นกำหนดตำแหน่งรองศาสตราจารย์ 4 คน

(3) **บัณฑิต:** มีนักศึกษาที่จบปริญญาเอกและโทแล้วอย่างละ 1 คนและอยู่ในระหว่างทำวิทยานิพนธ์เพื่อสอบจบปริญญาเอกในปี 2020 อีก 2 คน มีนักวิจัยหลังปริญญาที่รับการฝึกอบรม 3 คน

(4) **รางวัลต่าง ๆ:** คณะนักวิจัยได้รับรางวัลระดับนานาชาติ 1 รางวัล ระดับสถาบันและระดับชาติจำนวน 8 รางวัล

(5) การสร้างกลุ่มวิจัย ภายใต้โครงการซึ่งมีนักวิจัยหลายระดับตั้งแต่นักวิจัยอาวุโส รุ่นกลาง และรุ่นใหม่ ทำให้เกิดการแลกเปลี่ยนเรียนรู้ข้ามศาสตร์ การได้รับการสนับสนุนด้านวิชาการและข้อมูลทางคลินิกต่าง ๆจากนักวิจัยสายแพทย์ การประชุมกลุ่มเป็นระยะ ทำให้สมาชิกกลุ่มสามารถขยายงานของตนเองและพัฒนาโครงการวิจัยภายใต้ความเชื่อมโยงของกลุ่มวิจัยได้ เป็นการสร้างบรรยากาศวิชาการและวิจัย และสังคมวิจัยที่มีความเอื้อเฟื้อช่วยเหลือกัน

โครงการนี้ได้ให้โอกาสนักวิจัยหลากรุ่นรวมกลุ่มกันเพื่อศึกษาหัวข้อเดียวกัน สามารถดำเนินการได้เกิน-ตามเป้าหมายหลายเรื่อง การสร้างผลงานในระยะแรกค่อนข้างช้ากว่าแผนเนื่องจาก FOXM1 เป็นโมเลกุลที่มีความซับซ้อน มีบทบาทหลากหลายและการควบคุมหลายระดับ ทำให้หลายการศึกษาไม่เป็นไปตามสมมุติฐานและต้องปรับแผนการวิจัย อย่างไรก็ตามเป็นโอกาสที่ทำให้ค้นพบความรู้ใหม่ที่ไม่ได้คาดไว้ก่อน ด้านความร่วมมือต่างประเทศไม่ราบรื่นในระยะหลัง เนื่องจากนักวิจัยต่างประเทศประสบปัญหาครอบครัวและการบริหารจัดการด้านการวิจัยของหน่วยงานต้นสังกัด ทำให้การแลกเปลี่ยนข้อมูล-การถ่ายทอดเทคโนโลยีรวมทั้งการสร้างผลงานร่วมกับนักวิจัยต่างประเทศต่ำกว่าที่คาดหวัง อย่างไรก็ตามคณะนักวิจัยไทยได้พยายามทำการวิจัยเพื่อให้ได้ผลงานตามเป้าหมาย

คณะนักวิจัยขอขอบพระคุณ ฝ่ายวิชาการ สำนักงานกองทุนสนับสนุนการวิจัย ที่ได้ริเริ่มโครงการวิจัยนำร่องนี้ และให้โอกาสได้สร้างผลงานด้านวิชาการที่เป็นองค์ความรู้ใหม่ ที่สามารถนำไปต่อยอดเพื่อสร้างคุณค่าที่เป็นรูปธรรมต่อไป

รศ. นพ. ชวลิต ไพโรจน์กุลและคณะนักวิจัย

Summarized report of UK collaborator

Research progress and Technology transfer: The project was officially started on 16th January 2016, but the proposed work plan was delayed until June 2016. This was due to the problem in recruiting a suitable postdoctoral fellow for the work and we have to obtained a new set of cholangiocarcinoma (CCA) cell lines from KKU to pursue the experiments described in the project.

We have firstly explored the comprehensive expression profile of proteins involved in FOXM1-FOXO3a axis among 5 human CCA cell lines. This work has been carried out by a PhD placement student from Khon Kaen University, Mr. Kitti Intuyod and Dr. Paula Saavedra-Garcia, the postdoc. They have explored the role of ER stress in CCA in relation to FOXM1 and FOXO3a and performed more work on drug resistance of CCA. For Mr. Kitti Intuyod, he has learnt a lot of molecular biology techniques and he has brought it back to Thailand to carry his project.

Since FOXM1 is one of the central regulators of a myriad of cancer development processes, this research will increase and foster a greater understanding of the biology of cancer. An understanding of the role and regulation of FOXM1 and its transcriptional targets in CCA will contribute towards the development of better diagnostics and treatment strategies for CCA.

Not only the novel knowledge on CCA gained, this project also strengthened the collaborative work between Thailand and UK researchers and served as bases for long-term collaboration between KKU and ICL. This project also provides future opportunities for further junior researcher exchanges between KKU and ICL. They will be exposed to cutting edge technology and stimulating research environment at ICL and KKU.

Collaborative activities between Thai collaborators and among MRC-TRF-sponsored CCA research groups: During this 3-year project, Professor Lam has visited the KKU group at Khon Kaen for 3 times. During his visit in 4-6 October 2016, KKU team presented him the progress of the project. The overview of the FOXM1 research project including conceptual framework, research plan and the outcomes were discussed and adjusted to comply the status of the project. During 12-15 February, 2017, Prof. Lam and his colleagues; Dr. Stefania Zona, a postdoctoral fellow and Ms. Catherine Yao, a PhD placement student, visited the Faculty of Medicine, KKU. The main discussion focused on the progress of Mr. Kitti Intuyod, a RGJ-PhD student under the supervision of Assoc. Prof. Somchai Pinla-or and Prof. Lam on “the effect of FOXM1 on chemotherapeutics response in CCA”. Apart from his visits, Prof Lam and Thai colleagues at KKU had several face to face meeting via SKYPE.

Professor Lam had also met with the other MRC-TRF-sponsored CCA research groups (Dave Bates, Anna Grabowska, Kiren Yacqub Usman, Kevin Gaston, and Sheela Padma Jayaraman) on 19th May, 2016 at Imperial College London to explore collaborations in order to provide added-values to the MRC-TRF

funding. The second meeting among the MRC-TRF-sponsored CCA research groups and the Thai representatives was held in Bangkok in September 2016.

Achievements:

• Mr. Kitti Intuyod completed his one-year placement in Prof Lam's laboratory. Prof Lam was a co-advisor with Dr. Somchai Pinlaor of Kitti Intuyod under the RGJ-PhD program supporting by TRF, Thailand, to study the "Treatment and chemoresistant of CCA". Dr. Kitti Intuyod was graduated his Ph.D. in Biomedical science program and is now a postdoctoral fellow of Prof. Somchai Pinlaor, at KKU.

• Two manuscripts were published under the collaborative works.

1. Together with Mr. Kitti Intuyod and Prof. Pinla-or: FOXM1 modulates 5-fluorouracil sensitivity in cholangiocarcinoma through thymidykate synthase (TYMS): implication of FOXM1-TYMS axis uncoupling in 5IFU resistance. Intuyod, K. et. al. Cell Death & Diseases journal, (Impact factor: 5.638).

2. Together with KKU team: O-GlcNAcylation mediates metastasis of cholangiocarcinoma through FOXO3 and MAN1A1 Chatchai Phoomak, Atit Silsirivani, Dayoung Park, Kanlayanee Sawanyawisuth, Kulthida Vaeteewoottacharn, Chaisiri Wongkham, Eric W. Lam, Chawalit Pairojkul, Carlito B. Lebrilla*, Sopit Wongkham* Oncogene 2018, 37:5648–5665. (Impact factor: 6.854)

.....

Full report (รายงานการวิจัยฉบับสมบูรณ์)

Grant number: DBG5980004

Project title: Targeting of the FOXM1 signature for early diagnosis and treatment in cholangiocarcinoma

การมุ่งเป้า FOXM1 และเครือข่ายเพื่อวินิจฉัยและรักษามะเร็งท่อน้ำดี

The Principle investigator: Assoc. Prof. Chawalit Pairojkul

Research activities

1. Expression of FOXM1 protein and mRNA in CCA patient tissues

We have done immunohistochemical analyses of Forkhead box M1 (FOXM1) expression in the tissue microarray (TMA) of CCA tissues from Thai patients (n = 113). The majority of CCA tissues expressed high FOXM1 (95/113; 84.07%) with cytoplasmic staining while 15.92% (18/113) showed negative for FOXM1 expression. The representative images for FOXM1 expression in the TMA are shown in Fig. 1-1A and 1-1B. The correlations between expression of FOXM1 and clinical findings of CCA patients were further analyzed. The univariate analysis indicated that expression of FOXM1 had no correlation with clinical features and survival of CCA patients (Table 1-1 and Fig. 1-2).

The human FOXM1 gene consists of 10 exons, two of which, exon Va (A1) and exon VIIa (A2) are alternatively spliced. These splices give rise to three distinct isoforms: FOXM1a, FOXM1b, and FOXM1c. FOXM1a, which harbors both exon Va and exon VIIa, is transcriptionally inactive owing to the disruption of its transactivation domain (TAD) by the latter exon. In comparison, both FOXM1b and FOXM1c, which has only exon Va, are transcriptionally active and can activate expression of their target genes (Fig. 1-3A). Based on the molecular feature of FOXM1, the expression of each FOXM1 isoform (a, b, and c) in CCA tissues from patients and their normal adjacent counterparts were further identified using end-point PCR. The results indicated that 70.00% of CCA tissues (n = 40) expressed FOXM1c and 25% expressed FOXM1b whereas none of adjacent normal tissues had FOXM1c. These findings demonstrated that FOXM1c was the major isoform found in CCA tissues. The survival analysis performed according to the Kaplan-Meier analysis method showed a significant correlation between

positive FOXM1c expression and shorter survival of CCA patients (P <0.05) (Fig. 1-3B). Univariate analysis indicated that metastasis status and FOXM1c expression were dependent factors for shorter survival of CCA patients (Tables 1-2). The multivariate analysis indicated that FOXM1c expression was an independent risk factor of poor prognosis of CCA patients (Table 1-2). This information is now under manuscript preparation.

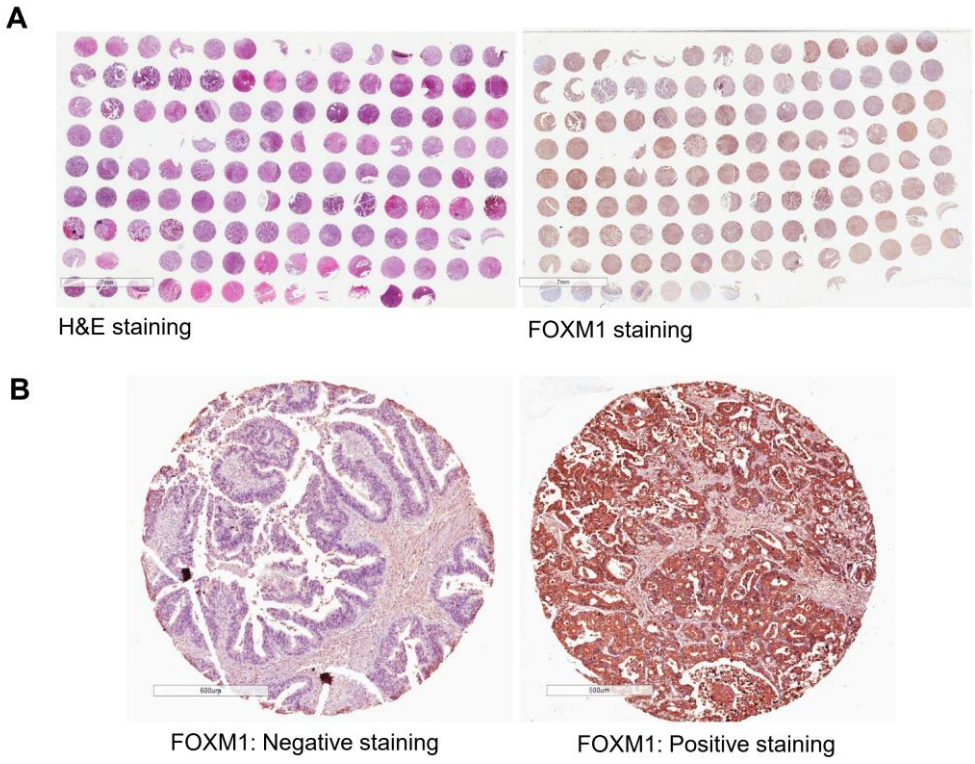

Figure 1-1. The expression of FOXM1 in CCA tissue microarray. (A) overview of hematoxylin and eosin (H&E) and FOXM1 staining in a homemade tissue microarray. (B) the representative picture of CCA tissues with negative and positive FOXM1 expression.

Table 1-1. Univariate analysis of FOXM1 protein expression in CCA tissues and the clinico-pathological findings of CCA patients.

Clinical parameters		FOXM1		p-value
		Negative	Positive	
SEX	Male	13	56	0.290
	Female	5	39	
AGE	< 56	10	42	0.376
	≥ 56	8	53	
Stage	1+2+3	12	46	0.168
	4A+4B	6	48	
Histopathological type	Papillary	7	45	0.484
	Mass forming	11	49	
p53	Negative	14	52	0.296
	Positive	4	28	

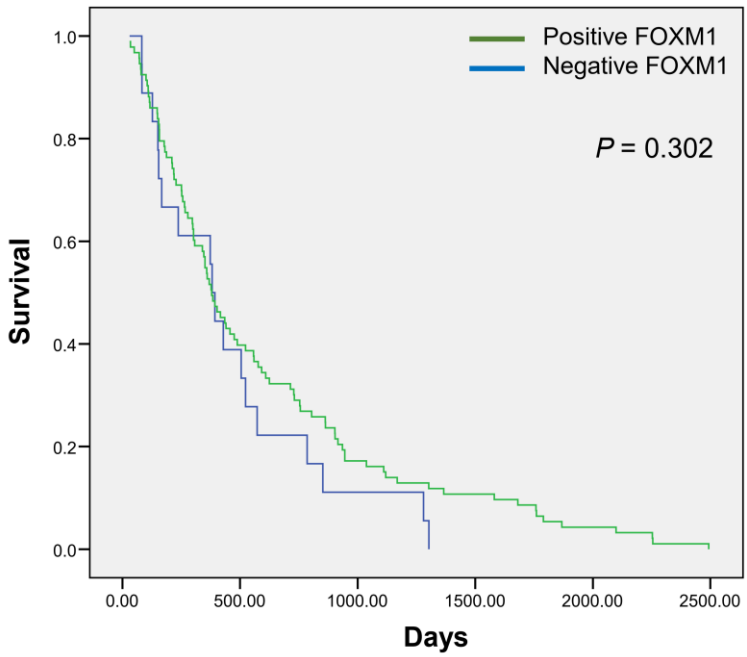

Figure 1-2. Relationship between FOXM1 expression and overall survival of CCA patients.

A

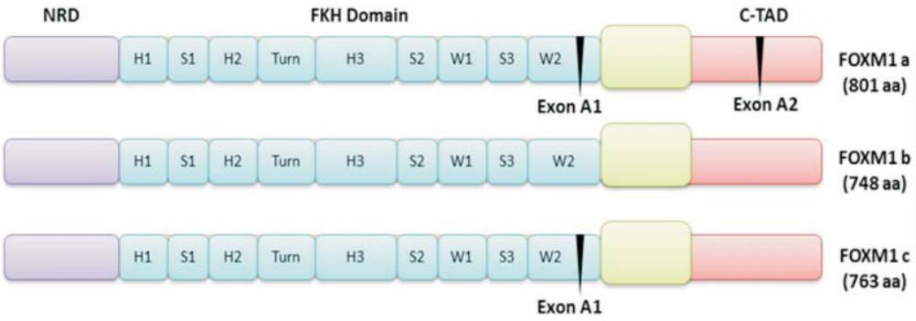

B

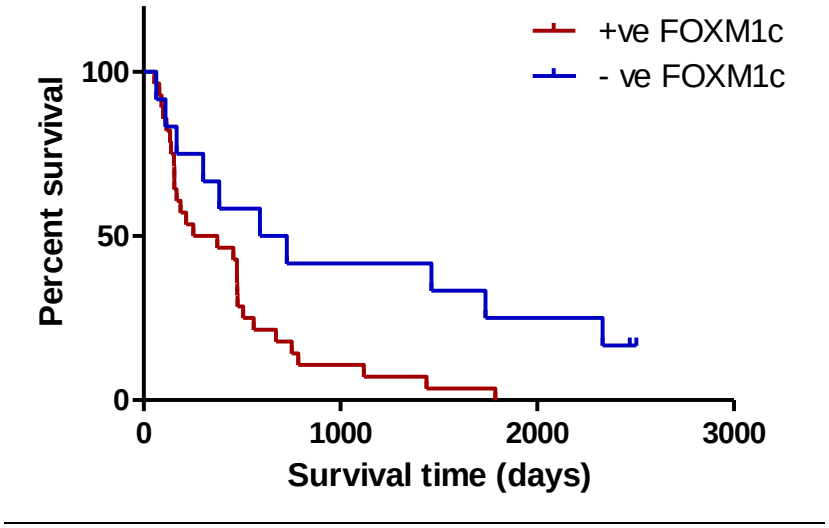

Figure 1-3. FOXM1c expression was associated with a shorter overall survival of CCA patients. A. Diagram illustrates human FOXM1 splice variants FOXM1A, FOXM1B, and FOXM1C. B. Survival analysis of patients based on FOXM1c expression in CCA tissues.

Table 1-2. Univariate and multivariate analysis of FOXM1c expression and clinico-pathological findings in CCA patients.

Variables		No. of patients	Univariable analysis			Multivariable analysis		
			HR	95% CI	*P*-Value	HR	95% CI	*P*-Value
Histological type	Non papillary	24	1.161	0.611 - 2.207	0.649	0.759	0.332 - 1.731	0.512
	Papillary	17						
Age (year)	≥ 57	23	0.993	0.525 - 1.878	0.983	0.725	0.297 - 1.773	0.481
	< 57	18						
Gender	Male	24	0.776	0.408 - 1.475	0.439	1.017	0.455 - 2.273	0.967
	Female	17						
Tumor size	≥ 6	26	1.426	0.736 - 2.764	0.293	1.403	0.627 - 3.141	0.41
	< 6	15						
Metastasis (n = 31)	Positive	24	2.441	0.906 - 6.580	0.078	1.577	0.613 - 4.059	0.345
	Negative	7						
FOXM1c	Positive	28	2.277	1.067 - 4.860	0.033*	3.389	1.092 - 10.513	0.035*
	Negative	13						

2. Effect of FOX axis on chemotherapeutics response in CCA

2.1 Role of FOXM1 on 5-fluorouracil sensitivity of cholangiocarcinoma (CCA)

Overexpression of FOXM1 mRNA in *O. viverrini*-associated CCA has been shown in previous cDNA array studies. To investigate further the role and regulation of Thymidylate Synthetase (TYMS) and FOXM1 in *O. viverrini*-associated CCA, the expression of TYMS and FOXM1 was determined by immunohistochemistry (IHC) in CCA tissue arrays. We found that 78% (88/113) of FOXM1 and 48% (54/113) of TYMS were upregulated in *O. viverrini*-associated cases (n = 113) (Fig. 2-1). The results highlighted that FOXM1 is commonly overexpressed in CCA, suggesting its involvement in CCA tumorigenesis. This finding also suggested that the FOXM1–TYMS axis might have a wider role in tumor progression, such as chemosensitivity, as TYMS is a cellular target of 5-FU, the first-line chemotherapeutic drug for CCA.

Correlated baseline expression of FOXM1 and TYMS in CCA cell lines

To explore the relationship between FOXM1, E2F1 and TYMS expression and their functional roles in CCA, western blot and real-time quantitative PCR (qPCR) analyses were performed to determine the baseline steady-state expression levels of FOXM1 and TYMS, as well as one of their known regulator E2F1, in four CCA cell lines. Consistent with the IHC results, western blot analysis revealed that in general FOXM1 was highly expressed and displayed good correlations with TYMS in CCA cells (Fig. 2-2A). Expression of E2F1 differed between the four cell lines and had little correlation with that of FOXM1 and TYMS, suggesting that FOXM1 and TYMS expression is not related to E2F1. Interestingly, TYMS expression was higher and FOXM1 expression lower in HuCCA compared to the other three CCA cell lines, KKU-D131, KKU-213 and KKU-214 (Fig. 2-2A). The mRNA levels of FOXM1, E2F1 and TYMS demonstrated good correlations with their protein levels in these CCA cells (Fig. 2-2B), indicating that the expression of these proteins are regulated primarily at the transcriptional level. Interestingly, the TYMS mRNA expression levels also demonstrated positive relationships with the FOXM1 in all but the HuCCA cell line, while E2F1 expression levels again did not appear to be associated with those of FOXM1 and TYMS in these CCA cell lines (Fig. 2-2B). Together, these results suggest that TYMS expression is regulated by FOXM1 but not by E2F1 in CCA cells. The discordance between FOXM1 and TYMS expression levels in HuCCA also suggests that TYMS expression is not coupled to FOXM1 regulation in this cell line.

A

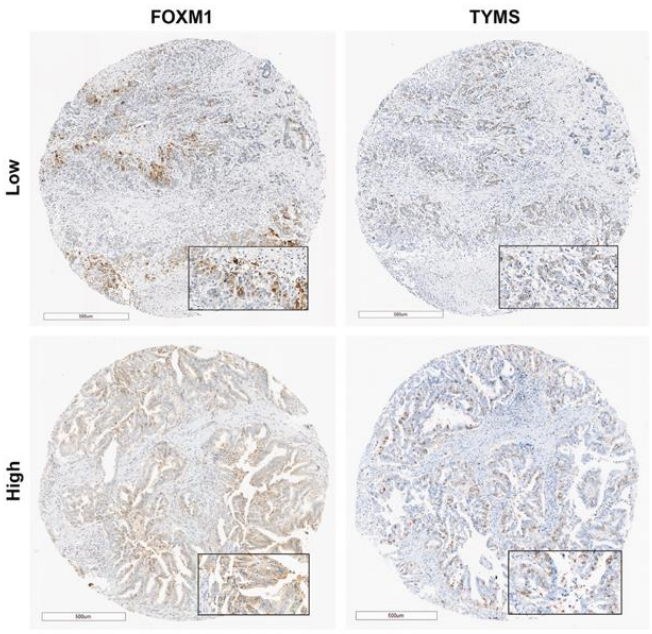

B

FOXM1 * TYMS Crosstabulation

Count

		TYMS		
		Negative	Positive	Total
FOXM1	Negative	19	6	25
	Positive	40	48	88
Total		59	54	113

Chi-Square Tests

	Value	df	Asymp. Sig. (2-sided)	Exact Sig. (2-sided)	Exact Sig. (1-sided)
Pearson Chi-Square	7.280(b)	1	.007		
Continuity Correction(a)	6.108	1	.013		
Likelihood Ratio	7.610	1	.006		
Fisher's Exact Test				.012	.006
Linear-by-Linear Association	7.216	1	.007		
N of Valid Cases	113				

a Computated only for a 2x2 table

b 0 cells (.0%) have expected count less than 5. The minimum expected count is 11.95.

Figure 2-1. Correlation of FOXM1 and TYMS expression in CCA tissues. CCA tissue arrays were prepared from 113 O. viverrini-associated CCA cases using tissue microdissection techniques. (A) Representative immunohistochemical staining images showing correlated FOXM1 (top) and TYMS (bottom) expression. (B) Staining results and Chi-square analysis. Chi-square statistical analysis was used to test the correlations between TYMS and FOXM1

expression of CCA patients using GraphPad Prism 7.0 and SPSS 16.0. In statistical analysis, *p < 0.05 was considered as significant.

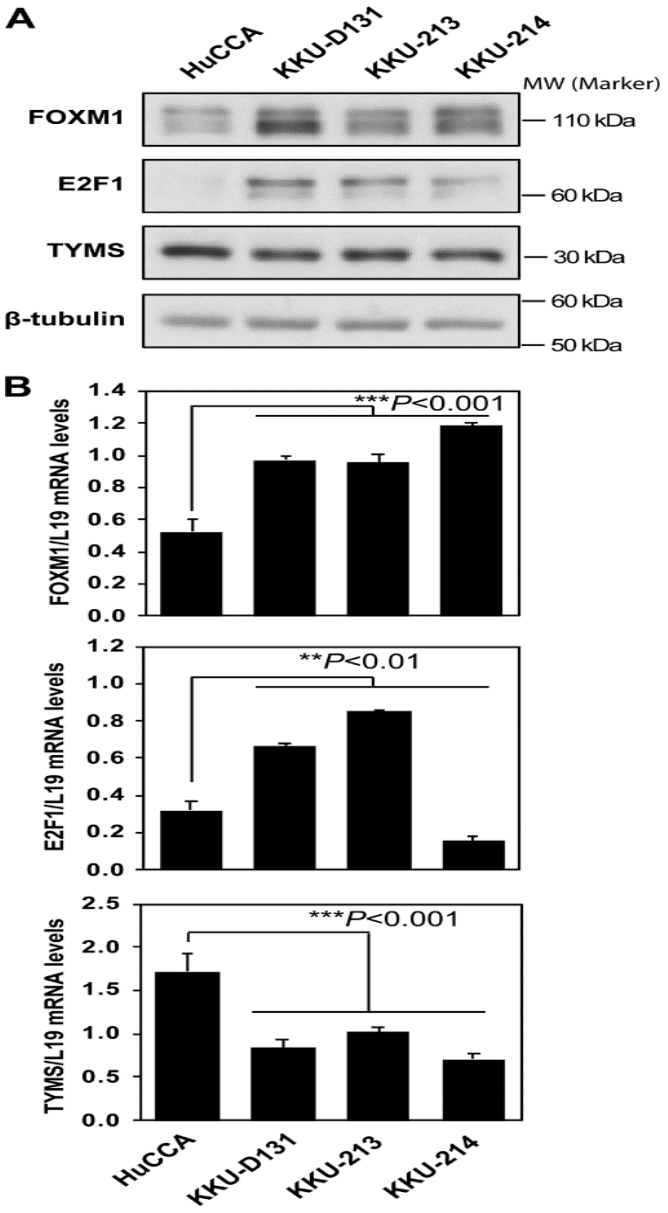

Figure 2-2. Baseline expression of FOXM1, E2F1 and TYMS in CCA cells. CCA cells were harvested and the expression of FOXM1, E2F1 and TYMS at the translation and transcription levels were investigated using (A) western blot and (B) RT-qPCR. The latter assay was carried out in triplicate, and data are presented as means ± S.E.M. Expression of each gene was normalized relative to L19. The RT-qPCR data were analyzed by one-way ANOVA with Fisher's Least Significant Difference (LSD) post-test. Double and triple asterisks (** and ***) indicate significant difference at $p < 0.01$ and $p < 0.001$, respectively, from HuCCA (n = 3).

HuCCA is a highly 5-FU-resistant CCA cell line

As TYMS is the direct cellular target of 5-FU, we next examined the four CCA cell lines, HuCCA, KKU-D131, KKU-213 and KKU-214, for their sensitivity to 5-FU using sulforhodamine B (SRB) assay. Viability of all CCA cell lines decreased in a dose-dependent manner after treatment with 5-FU after 24, 48 and 72 h; HuCCA remained the more resistant line compared with the other three and exhibited the highest IC_{50} (Fig. 2-3A). We next examined the sensitivity of the CCA cells to 5-FU by clonogenic assays. Consistently, clonogenic assays revealed that HuCCA was the most resistant cell line (Fig. 2-3B). The results also showed that these CCA cell lines are relatively resistant to 5-FU treatment, consistent with the observations in the clinic that most CCAs are resistant to genotoxic chemotherapy.

Coordinated FOXM1 and TYMS expression upon 5-FUtreatment in CCA cell lines

Since TYMS is an important target for 5-FU treatment and has previously been shown to be regulated by FOXM1 and E2F1, we therefore hypothesized that the expression levels of these proteins regulate 5-FU sensitivity. To test this conjecture, the four very 5-FU-resistant CCA cell lines were treated with a high dose of 100 μM 5-FU (see Fig. 2-3) over the course of 48 h, and the expression levels of FOXM1, E2F1 and TYMS proteins were examined by western blot analysis (Fig. 2-3C). Expression of FOXM1 in all four cell lines increased transient in a time-dependent manner and its expression level was the highest at 24 h posttreatment and declined thereafter, concomitant with a reduction in cell proliferation rates (Fig. 2-3A). This kinetics of FOXM1 expression is consistent with other cancer cells following treatment with genotoxic agents. Similarly, the expression of TYMS mirrored that of FOXM1 but at a slower kinetics in the CCA lines, except for HuCCA where TYMS was expressed consistently at comparatively higher levels throughout the time course. The active metabolite of 5-FU, FdUMP, binds to TYMS to form an inactive slower migrating FdUMP–TYMS complex, which inhibits the conversion of dUMP to dTMP. Notably, using a high dose of 100 μM 5-FU to treat the CCA cells, the majority of the TYMS-proteins were in the FdUMP-complexed inactive slower migrating (higher) forms following 5-FU treatment, and this lack of active unligated TYMS would lead to dNTP shortage and the cytotoxic DNA damage. Expression of E2F1 in all cell lines did not show good correlations with either FOXM1 or TYMS, indicating further that E2F1 does not control FOXM1 and TYMS expression or vice versa in response to 5-FU in these

CCA cells. These results also further suggest that FOXM1 regulates TYMS expression in CCA cells, except for the resistant HuCCA.

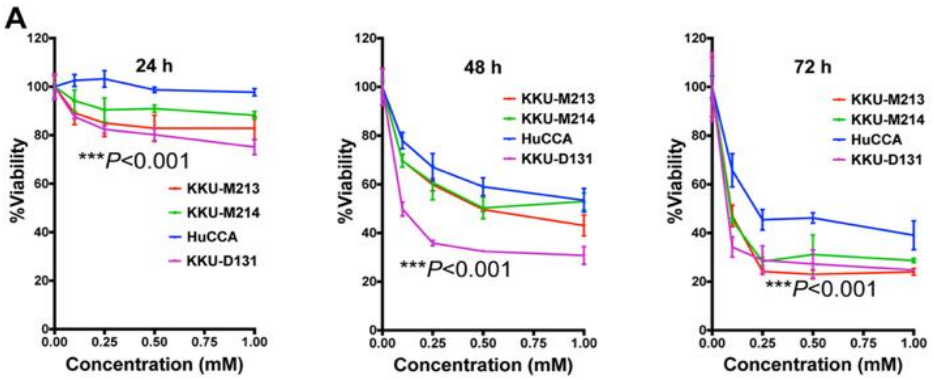

CCA cell lines	IC_{50} at 48 h (mM)	IC_{50} at 72 h (mM)
KKU-D131	0.013	0.008
KKU-M213	0.023	0.011
KKU-M214	0.033	0.014
HuCCA	0.042	0.026

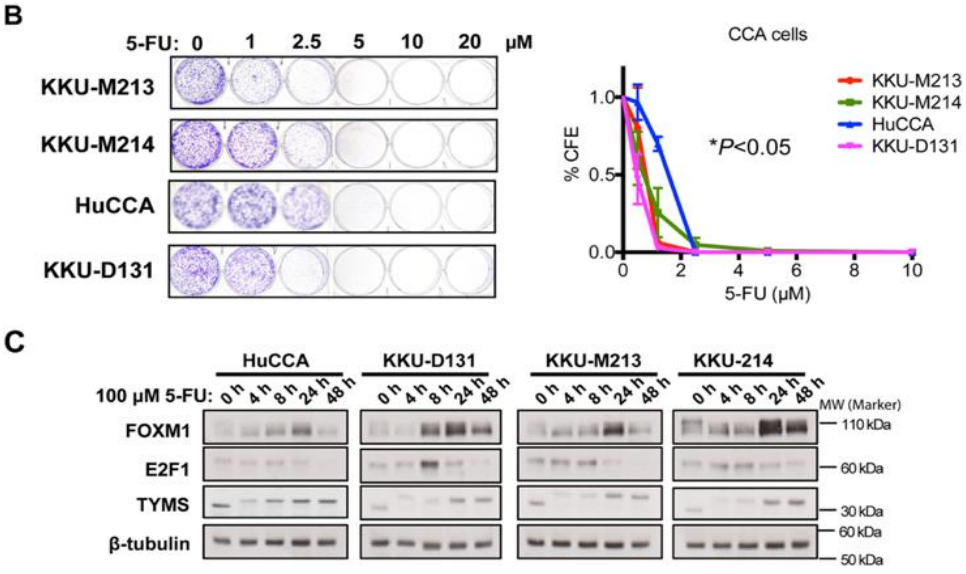

Figure 2-3. 5-FU treatment suppresses proliferation of CCA cells. CCA cells of HuCCA, KKU213, KKU214 and KKU-D131 lines were treated with different concentrations of 5-FU using DMSO as a vehicle. (A) Cell proliferation was assessed at 24, 48 and 72 h after 5-FU treatment using SRB assay. The experiment was carried out in triplicates and data are presented as means of the percentage of untreated control. The cell viability data were analyzed by two-way ANOVA with Fisher's Least Significant Difference (LSD) post-test (n = 3). The asterisks (***)

indicate significant difference at $p < 0.001$. (B) The CCA cells were analyzed for their sensitivity to 5-FU by clonogenic assays. After 48 h of incubation with the drugs, cells were cultured in fresh media, grown for around 14 days and stained with crystal violet. The graphs are representative of six experiments. Representative clonogenic images show the effects of 5-FU treatment. Data were analyzed by two-way ANOVA with Fisher's Least Significant Difference (LSD) post-test. The asterisk (*) indicates significant difference at $p < 0.05$. (C) Expression of FOXM1, E2F1 and TYMS in 5-FU-treated CCA cell lines in response to 5-FU. The CCA cell lines were treated with 100 μM of 5-FU over a period of 48 h. Cells were trypsinized at specific times and the expression of FOXM1, E2F1 and TYMS was determined using western blotting. β-Tubulin was used as a loading control. Representative western blot images are shown.

Silencing of FOXM1 reduced the 5-FU resistance and TYMS expression in KKU-D131 but not in HuCCA cells

To further investigate the role of FOXM1 in modulating the sensitivity of 5-FU in CCA cells, western blot analysis was performed on the most sensitive KKU-D131 and resistant HuCCA cells in the presence and absence of FOXM1 depletion. The result revealed that TYMS expression decreased upon FOXM1 depletion using small interfering RNA (siRNA) in the sensitive KKU-D131 but not in the resistant HuCCA cells, suggesting that TYMS is, at least partially, regulated by FOXM1 in the sensitive but not in the resistant CCA cells (Fig. 2-4A). By contrast, FOXM1 knockdown did not cause any substantial changes in E2F1 levels in both cell lines, further confirming that FOXM1 does not regulate E2F1. Clonogenic assay was then performed to investigate the effects of FOXM1 depletion on 5-FU sensitivity in HuCCA and KKU-D131 cells (Fig. 2-4B). Silencing of FOXM1 did not overtly affect 5-FU sensitivity of the resistant HuCCA cell line but caused a decrease in the clonogenicity of KKU-D131 (Fig. 2-4B), suggesting that FOXM1 plays a significant role in modulating TYMS expression and hence 5-FU sensitivity in the sensitive but not in the resistant CCA cells. FOXM1 was next overexpressed in KKU-D131 and HuCCA cells. The control and FOXM1-overexpressing CCA cells were then tested for their sensitivity to 5-FU. Western blot analysis revealed that FOXM1 was overexpressed in the FOXM1-transfected KKU-D131 and HuCCA cells, and TYMS expression was not affected by FOXM1 overexpression (Fig. 2-5A).

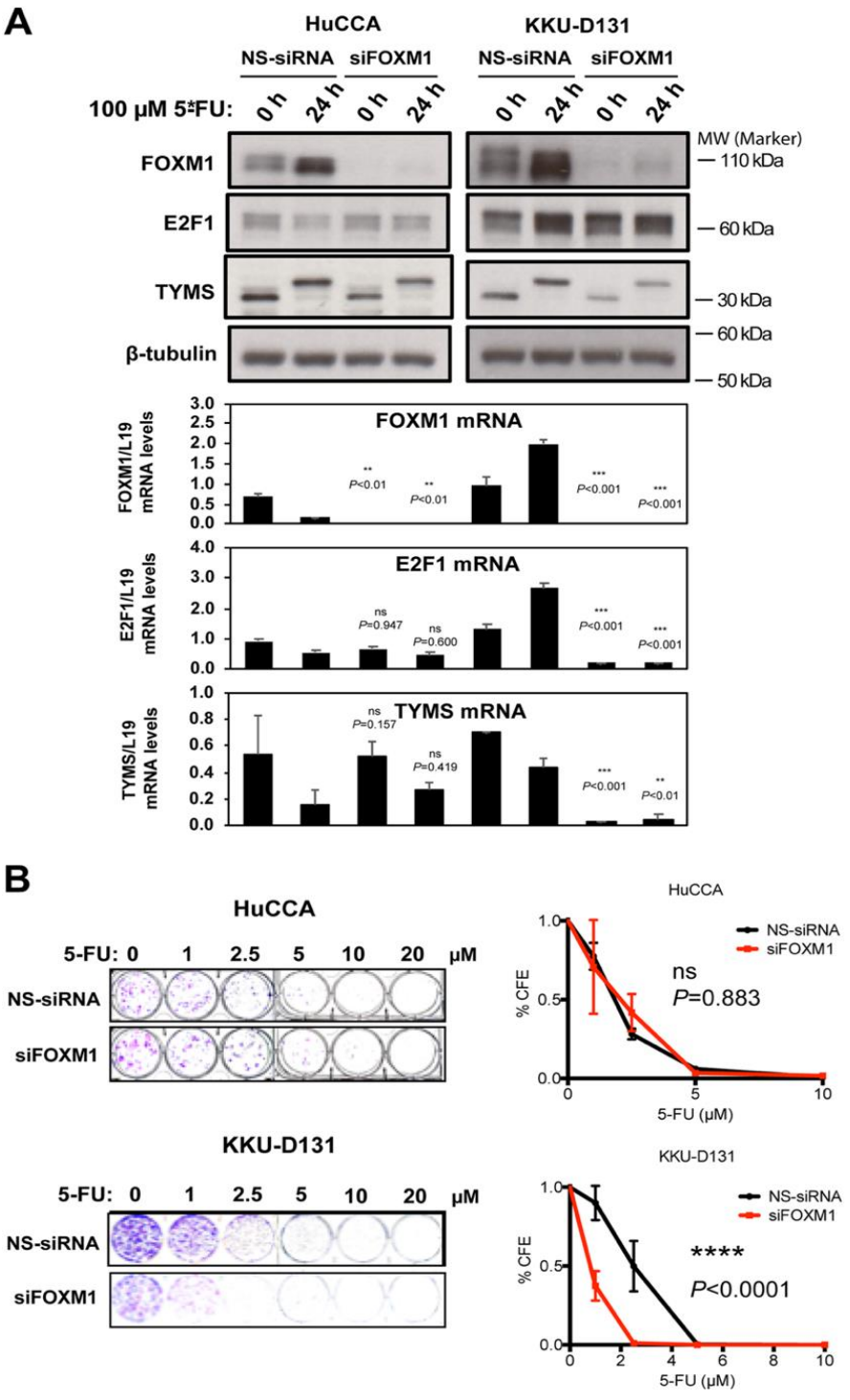

Figure 2-4. Effects of FOXM1 silencing on CCA cells in response to 5-FU treatment. FOXM1 expression in HuCCA and KKU-D131 cells was silenced using siRNA (siFOXM1) and non-silencing siRNA (NS-siRNA) was used as control. After 24 h, CCA cells were reseeded and grown overnight. (A) After treatment with 100 μM 5-FU for 24 h, cells were harvested and the expression levels

of FOXM1, E2F1 and TYMS were determined by western blot and RT-qPCR analysis. Western blot was performed using β-tubulin as loading control (upper panel). Expression of FOXM1, E2F1 and TYMS mRNA was also determined by RT-qPCR analysis using L19 as an internal control (lower panel). Data are presented as mean ± SEM (n > 3). RT-qPCR data were analysed by unpaired t tests. Double and triple asterisks (** and ***) indicate significant difference at $p < 0.01$ and $p < 0.001$, respectively, from the non-targeting siRNA-treated control cells; 'ns' indicates no significant difference. (B) Effect of FOXM1 silencing on 5-FU sensitivity was also investigated using clonogenic assays. Representative clonogenic images show the effects of FOXM1 silencing on the outcome of 5-FU treatment. Data are presented as mean ± SEM (n =3) and were analyzed by two-way ANOVA. The asterisks (****) indicate significant difference at $p < 0.0001$ from the non-targeting siRNA-treated control cells; 'ns' indicates no significant difference.

In concordance, clonogenic assay showed that ectopic overexpression of FOXM1 did not alter the sensitivity of either KKU-D131 or HuCCA cells to 5-FU (Fig. 2-5B). These results indicated that, although FOXM1 plays a vital role in the proliferation and 5-FU sensitivity of the KKU-D131, FOXM1 is already highly expressed and further overexpression would not induce additional TYMS expression and thereby 5-FU resistance. This notion is consistent with our earlier findings that FOXM1 is overexpressed in most CCA patient samples (Fig. 2-1) and cell lines (Fig. 2-2).

Unexpectedly, TYMS knockdown also resulted in a downregulation of FOXM1 expression (Fig. 2-6A), suggesting that TYMS might have a role in controlling the FOXM1 expression and FOXM1 as a sensor for TYMS activity and DNA damage, probably through the induction of DNA damage via blockage of replication fork progression. In addition, silencing of E2F1 by siRNA was also performed because expression of TYMS has previously been shown to be regulated by E2F1; however, E2F1 silencing did not affect the sensitivity of either HuCCA or KKU-D131 to 5-FU (Fig. 2-6B). Collectively, these data showed that TYMS expression levels determine the drug sensitivity in both sensitive and resistant CCA cells. In addition, the findings also supported the idea that FOXM1 regulates TYMS expression and thereby 5-FU sensitivity in CCA cells and that the uncoupling between FOXM1 and TYMS expression is linked to refractory to 5-FU in CCA cells.

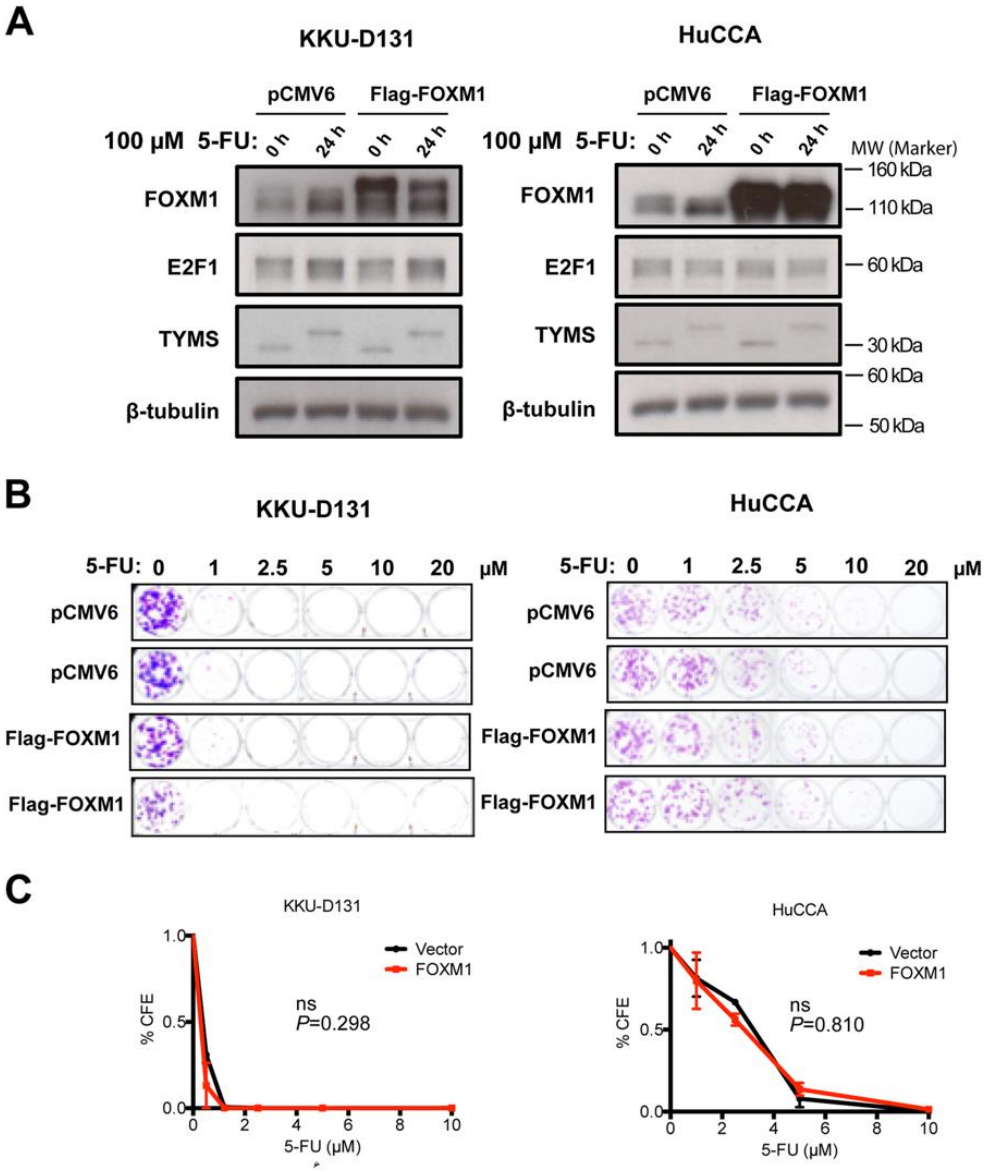

Figure 2-5. Effects of ectopic expression of FOXM1 in KKU-D131 and HuCCA cells in response to 5-FU treatment. FOXM1 expression in KKU-D131 cells was induced by transfection with FOXM1-pcDNA3.1 plasmid DNA. Plasmid DNA from parental vector was used as transfection controls. After 24 h, CCA cells were reseeded and grown overnight. (A) After treatment with 100 μM 5-FU for 24 h, cells were harvested and the expression levels of FOXM1, E2F1 and TYMS was determined by western blot analysis using β-tubulin as loading control. (B) Effects of FOXM1 overexpression on 5-FU toxicity was also investigated using a clonogenic assay. Representative clonogenic assay images show the effects of FOXM1 overexpression upon 5-FU treatment. (C) Data are presented as mean ± SEM (n =3) and were analyzed by two-way ANOVA. No significant difference is indicated by 'ns'.

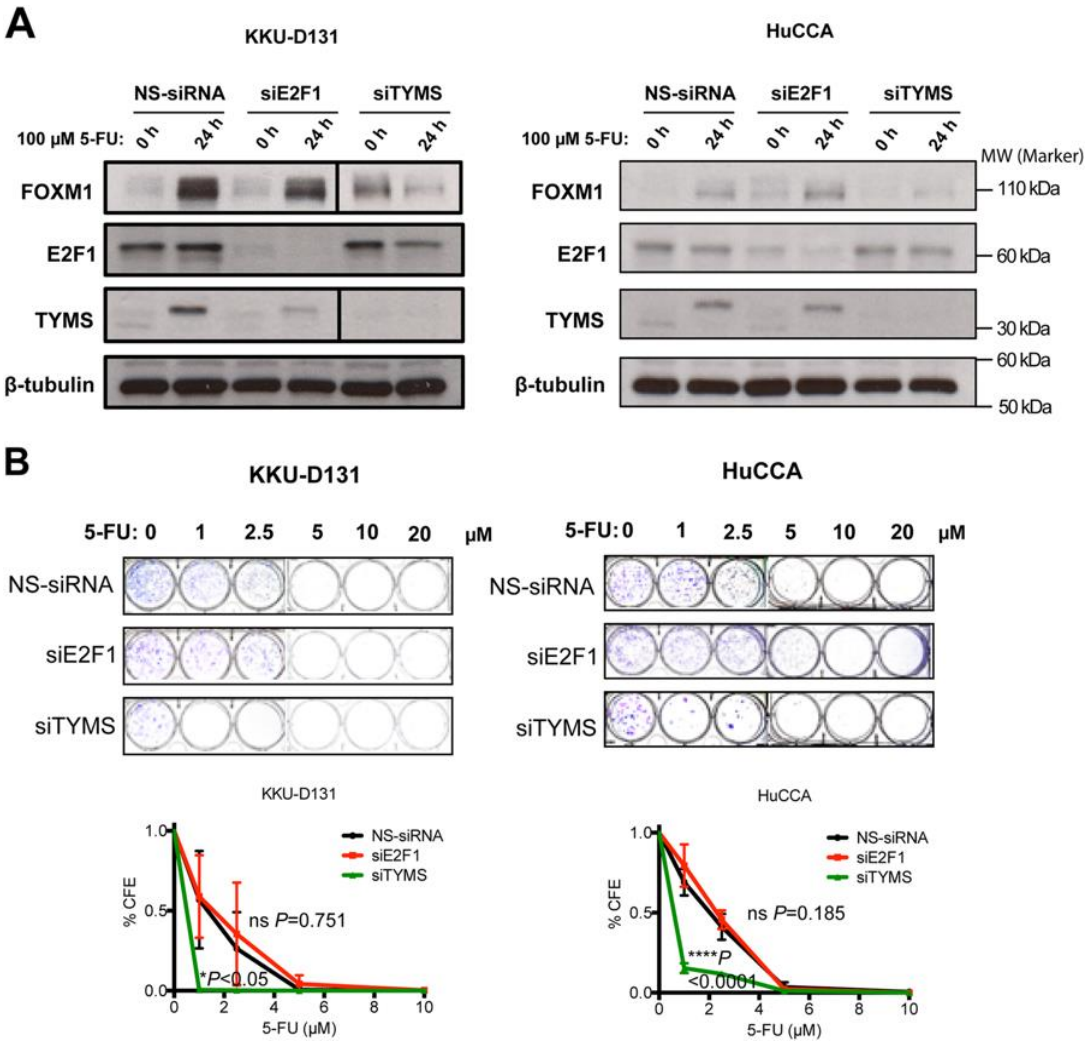

Figure 2-6. Effects of E2F1 and TYMS silencing on 5-FU treatment of CCA cells. Either E2F1 or TYMS expression in HuCCA cell was silenced using siRNA (siE2F1 or siTS). Non-silencing siRNA (NS-siRNA) was used as a control. After 24 h, HuCCA cells were reseeded and grown overnight. (A) After treatment with 100 μM 5-FU for 24 h, cells were harvested and the expression of FOXM1, E2F1 and TYMS was determined by western blot analysis using β-tubulin as loading control. (B) Effects of E2F1 and TYMS silencing on 5-FU toxicity was also investigated using a clonogenic assay. Representative clonogenic assay images show the effect on 5-FU treatment of silencing of either E2F1 or TYMS. Data are presented as mean ± SEM (n = 3) and were analyzed by two-way ANOVA. Single and triple asterisks (* and ****) indicates significant difference at $p < 0.05$ and $p < 0.001$, respectively, from the non-targeting siRNA-treated control cells; 'ns' indicates no significant difference.

FOXM1 modulates TYMS levels and 5-FU response in CCA cells

To further test the hypothesis that FOXM1 modulates 5-FU response through regulating TYMS expression levels in CCA, KKU-D131 and HuCCA cells were treated with a lower dose (20 μM) of 5-FU, which has differential cytotoxic effects on the comparatively more sensitive and resistant CCA cells (Fig. 2-7). As expected, in the comparatively more sensitive KKU-D131 both FOXM1 and TYMS protein and mRNA expression increased coordinately reaching a peak at 24 h posttreatment and decreased thereafter at 48 h. By contrast, despite the induction of FOXM1 expression in response to 5-FU in the resistant HuCCA cells, the expression of TYMS remained constantly high throughout the time course. Critically, in the sensitive KKU-D131 cells the majority of the TYMS proteins were in the FdUMP-complexed inactive slower migrating forms especially after the coordinated downregulation of FOXM1 and TYMS expression at 48 h following 5-FU treatment, and this lack of active unligated TYMS would lead to cytotoxic DNA damage. By comparison, in HuCCA cells the levels of TYMS remained relatively stable over the time course with a substantial proportion remaining in the uncomplexed and active faster migrating species, and the cells could still be able to process the dUMP to dTMP conversion for DNA replication (Fig. 2-7).

Differential binding of FOXM1 to endogenous TYMS promoter in 5-FU-sensitive and -resistant CCA cells

We next investigated the regulation of TYMS by FOXM1 at the promoter level. To this end, we first identified the putative FOXM1-binding regions from previously published FOXM1 chromatin-Immunoprecipitation–sequencing (ChIP-Seq) studies (Fig. 2-8). Both HuCCA and KKU-D131 cells were either untreated or treated with 5-FU for 24 and 48 h. To confirm further that FOXM1 binds to the endogenous TYMS promoter, we studied the occupancy of the endogenous TYMS promoter by FOXM1 using ChIP in the absence and presence of 24 or 48 h of 5-FU treatment in both cell lines. The ChIP analysis showed that FOXM1 is recruited to the endogenous Forkhead response element (FHRE) in both HuCCA and KKUD131 cells and its binding to the FHRE increases substantially in KKU-D131 but not in HuCCA in response to 5-FU (Fig. 2-8). Together, these findings suggest that TYMS is a direct transcriptional target of FOXM1 in CCA cells and that the incapacity of FOXM1 to modulate TYMS expression is due its inability to be efficiently recruited by the promoter of TYMS.

Summary

Our results evidently show that FOXM1, but not E2F-1, modulates TYMS expression and thereby 5-FU sensitivity in CCA cells. Our data also demonstrate that the FOXM1–TYMS axis plays a major role in mediating 5-FU sensitivity in CCA cells and its uncoupling may be linked to 5-FU resistance. Our findings suggest the FOXM1–TYMS axis is a determinant of 5-FU response and a target for designing more effective treatment for CCA patients. Since FOXM1 is overexpressed in almost all CCAs and may be essential for CCA tumorigenesis, FOXM1 and its downstream transcriptional signature might also be useful for prognosis prediction of CCA. These studies were concluded and published in Intuyod, K., P. Saavedra-Garcia, S. Zona, C. F. Lai, Y. Jiramongkol, K. Vaeteewoottacharn, C. Pairojkul, S. Yao, J. S. Yong, S. Trakansuebkul, S. Waraasawapati, V. Luvira, S. Wongkham, S. Pinlaor and E. W. Lam (2018). "FOXM1 modulates 5-fluorouracil sensitivity in cholangiocarcinoma through thymidylate synthase (TYMS): implications of FOXM1-TYMS axis uncoupling in 5-FU resistance." Cell Death Dis 9(12): 1185.

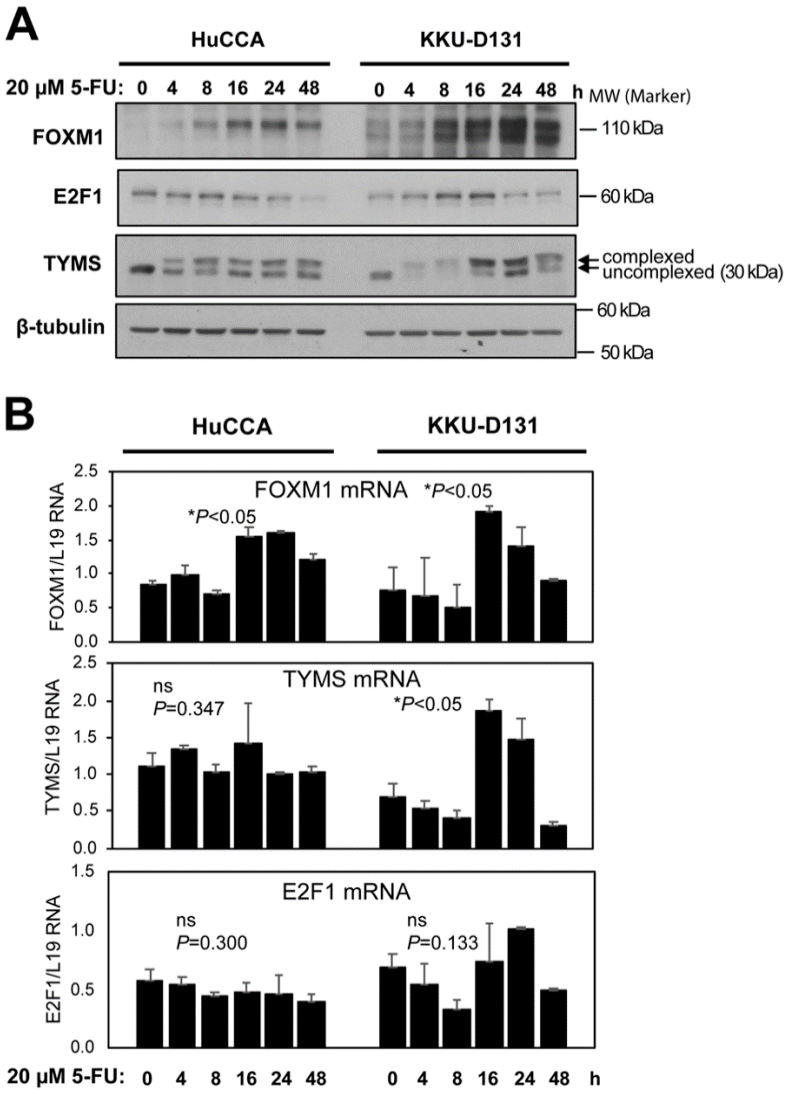

Figure 2-7. Expression of FOXM1, E2F1 and TYMS in CCA cell lines treated with a lower 20-μM dose of 5-FU. HuCCA and KKU-D131, the resistant and sensitive cell lines, respectively, were treated with 20 μM of 5-FU over a period of 48 h. Cells were trypsinized at specific times and the expression of FOXM1, E2F1 and TYMS was determined using western blotting. β-Tubulin was used as a loading control. (A) Expression of FOXM1, E2F1 and TYMS was determined by western blot analysis using β-tubulin as loading control. (B) Expression of FOXM1, E2F1 and TYMS mRNA was determined by RT-qPCR analysis using L19 as an internal control. Data are presented as mean ± SEM (n > 3). The RT-qPCR data were analyzed by one-way ANOVA. The asterisk (*) indicates significant difference at $p < 0.05$.

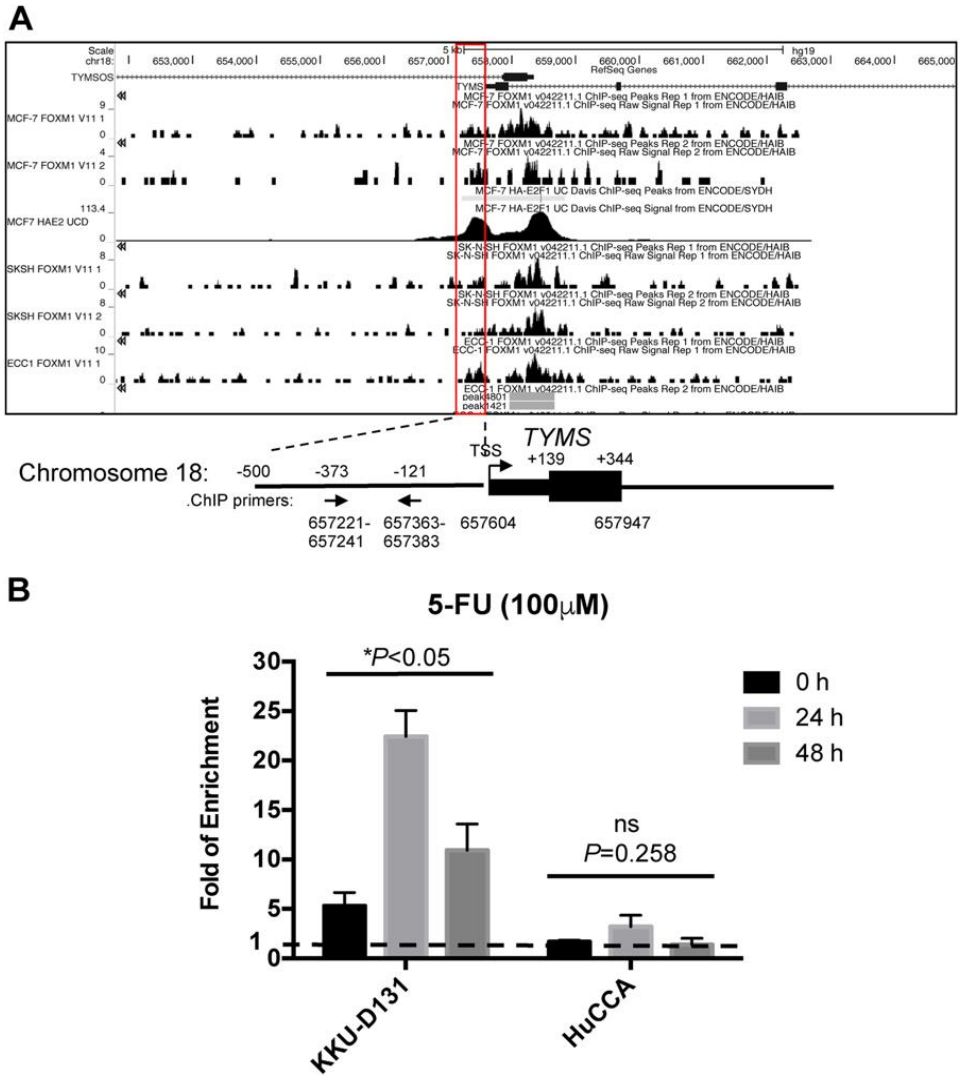

Figure 2-8. Analysis of FOXM1 binding on human TYMS promoter. (A) FOXM1-binding site on human TYMS promoter. ENCODE (the Encyclopedia of DNA Elements) project ChIP sequencing data of FOXM1 binding in the MCF-7, SKSH and ECC1 cells were used for predicting global genome-binding profiles for FOXM1 using the Integrative Genomics Viewer (Version 2.3.88) and the hg19 UCSC Genome Browser50. The predicted binding profiles of FOXM1 and the locations of the designed ChIP primer pairs are aligned to the human TYMS promoter. (B) KKU-D131 and HuCCA cells treated with 100 nM 5-FU for 0, 24 and 48 h were used for chromatin immunoprecipitation assays using the IgG as negative control and anti-FOXM1 antibody. After reversal of cross-linking, DNA was amplified by qRT–PCR, using primers amplifying the FOXM1 binding-site containing region. Data are presented as mean ± SEM (n = 4, each with >3 replicates) and were analyzed by two-way ANOVA. The asterisk (*) indicates significant difference at $p < 0.05$ and 'ns' no significant difference.

2.2 Role of FOXO4 on CCA cell biology

We utilized the parental KKU214 and drug resistant cell line KKU214^{GemR} to study the role of oncogenic transcription factor FOXO4 on gemcitabine treatment. Firstly, we compared the degree of gemcitabine resistant among KKU214 and KKU214^{GemR} using SRB assay. We found that the IC_{50} concentration of gemcitabine against KKU214^{GemR} cell line was obviously higher (X170 fold) than that parental KKU214 CCA cell line (Fig. 2-9). Clonogenic assay was also performed to confirm the finding in SRB assay. In agreement with SRB assay, clonogenic assay showed the resistant property of KKU214^{GemR} after treatment with gemcitabine (Fig. 2-10).

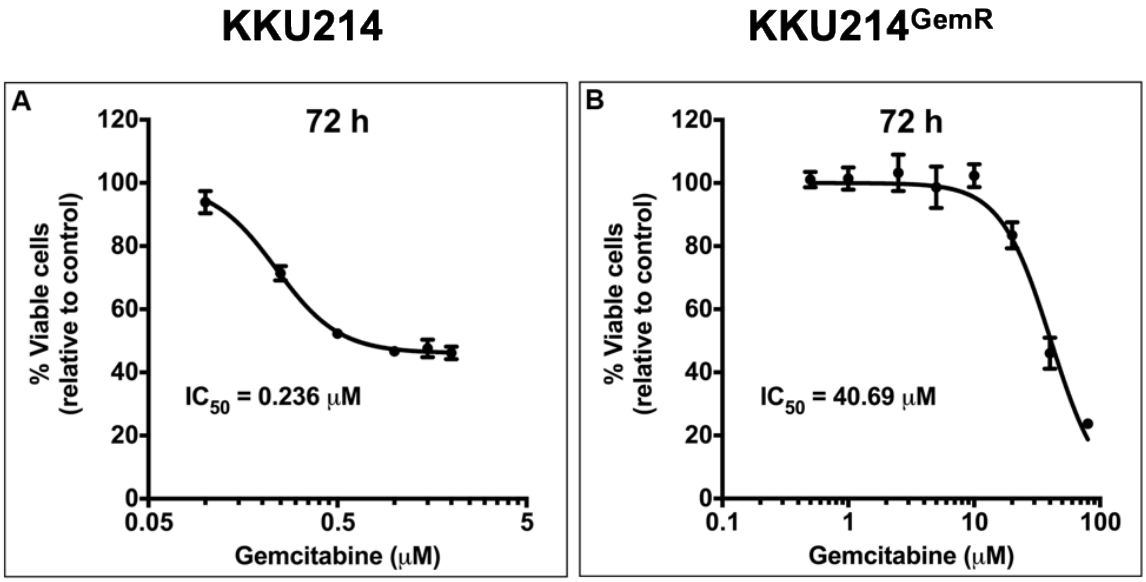

Figure 2-9. The IC_{50} values of gemcitabine against parental and gemcitabine-resistant CCA cell lines. (A) Parental (KKU214) and (B) gemcitabine-resistant CCA cell lines (KKU214^{GemR}) were treated with different concentrations of gemcitabine for indicated time periods. Then, percentage of cell proliferation was determined by the SRB assay compared to control, treatment (DMSO). The IC_{50} of gemcitabine on KKU214 and KKU214^{GemR} at 72 h post-treatment was calculated by using a dose-response curve analysis. Experiments were carried out in triplicate.

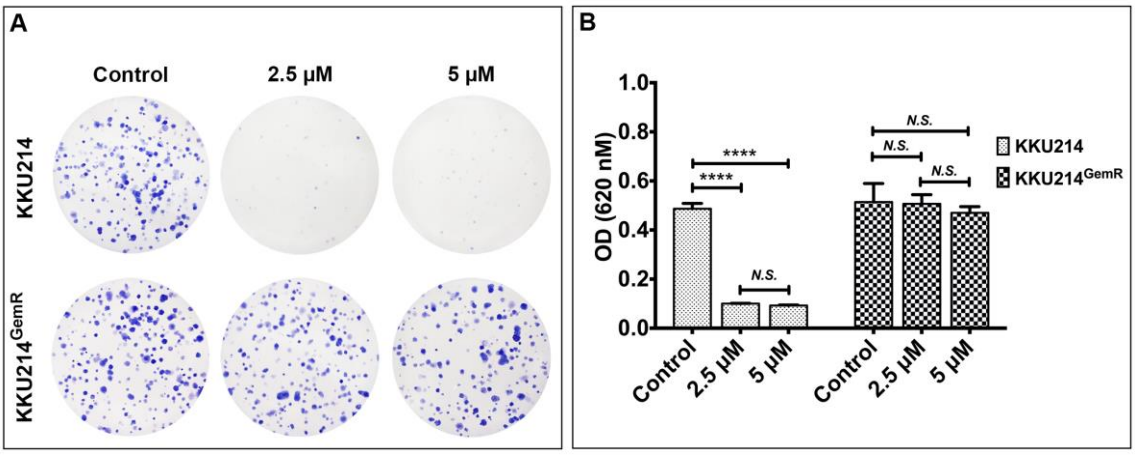

Figure 2-10. Gemcitabine treatment inhibits clonogenicity of KKU214 but not KKU214^{GemR}. (A) KKU214 and KKU214^{GemR} CCA cell lines were treated with gemcitabine at indicated doses for 48h . The cells were then subsequently maintained in normal growth medium for 14 days. The effect of gemcitabine treatment on colony formation of KKU214 and KKU214^{GemR} cell lines was determined by clonogenic assay. (B) Relative differences of colony formation of KKU214 and KKU214^{GemR} cell lines were investigated by dissolving stained colonies with 33% acetic acid and absorbance at optical density (OD) 620 nM was measured by ELISA reader. **** indicates a significant difference at $p<0.0001$. *N.S.* = no significant difference.

Next, we performed the RT-qPCR and Western blot analyses to explore the expression of FOXO4 at transcription and translation levels, respectively. RT-qPCR showed that FOXO4 expression in KKU214^{GemR} cell line was 300 times higher than that in KKU214 cell line (Fig 2-11A.). Relevantly, the Western blot analysis also demonstrated that FOXO4 was highly expressed in KKU214^{GemR} cell line but undetectable in KKU214 cell line (Fig. 2-11B). We next performed the Western blot analysis to explore the kinetic expression of FOXO4 and FOXs protein members after time course treatment with gemcitabine. We found that the expression of FOXM1 in KKU214 cell line was gradually increased and reach the highest level at 16 h post-gemcitabine treatment, and was declined thereafter. In KKU214^{GemR}, the different expression pattern of FOXM1 was observed and seemed that FOXM1 was not expressed in KKU214^{GemR} cell line (Fig 2-12.); however, this needed to be further confirmed by RT-qPCR. On the other hand, the expression of FOXO4 was not observed in parental KKU214 cell line but substantially increased in time-dependent manner in KKU214^{GemR} cell line. Interestingly, similar

pattern was also observed for Nanog protein, suggesting that there might be the association between FOXO4 and Nanog especially in drug-resistant cell line and this might involve in gemcitabine resistant of CCA cell line. For another FOX protein family, Western blot analysis illustrated that the expression of FOXO3a was decreased in time-dependent manner in KKU214 cell line whereas opposite finding was observed in KKU214^{GemR} cell line (Fig. 2-12). Hence, FOXO3a might also involve in gemcitabine response of CCA cell lines.

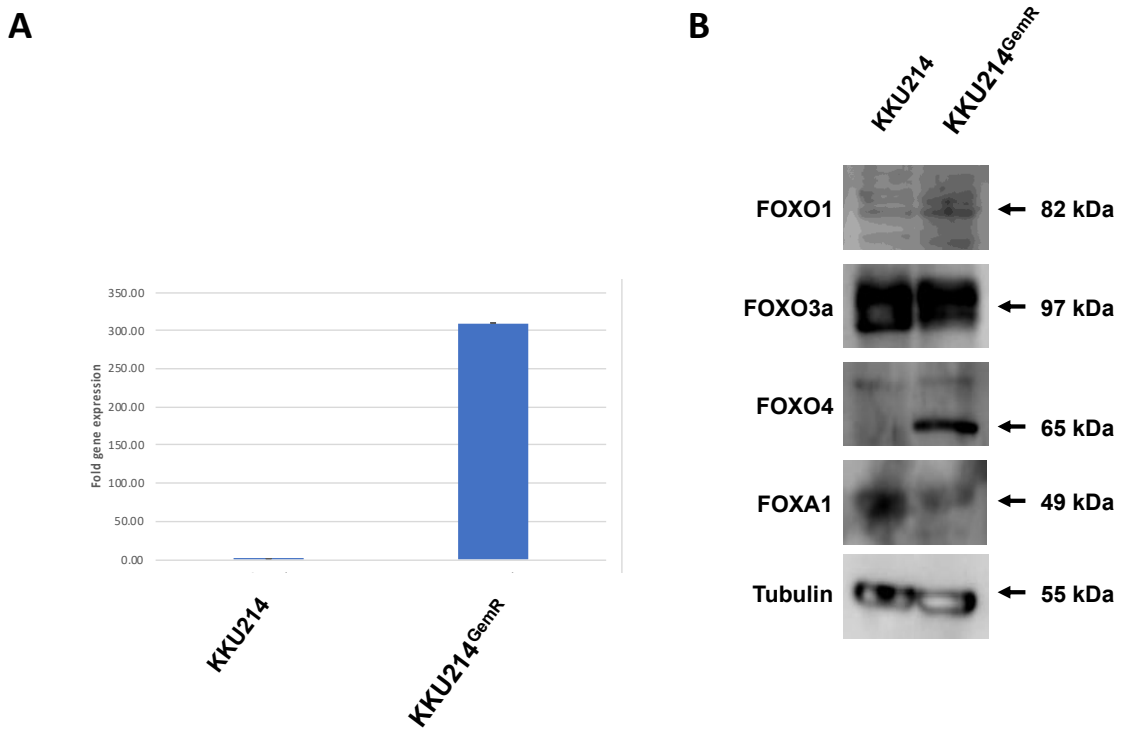

Figure 2-11. Baseline expression of FOXO4 and FOXs protein family in KKU214 and KKU214^{GemR} CCA cell lines. (A) CCA cells were harvested and the expression of FOXO4 at transcription level, relative to L19 gene, was determined by RT-qPCR. (B) The translational levels of FOXO1, FOXO3a, FOXO4 and FOXA1 were determined using Western blot analysis. β-tubulin was used as loading control.

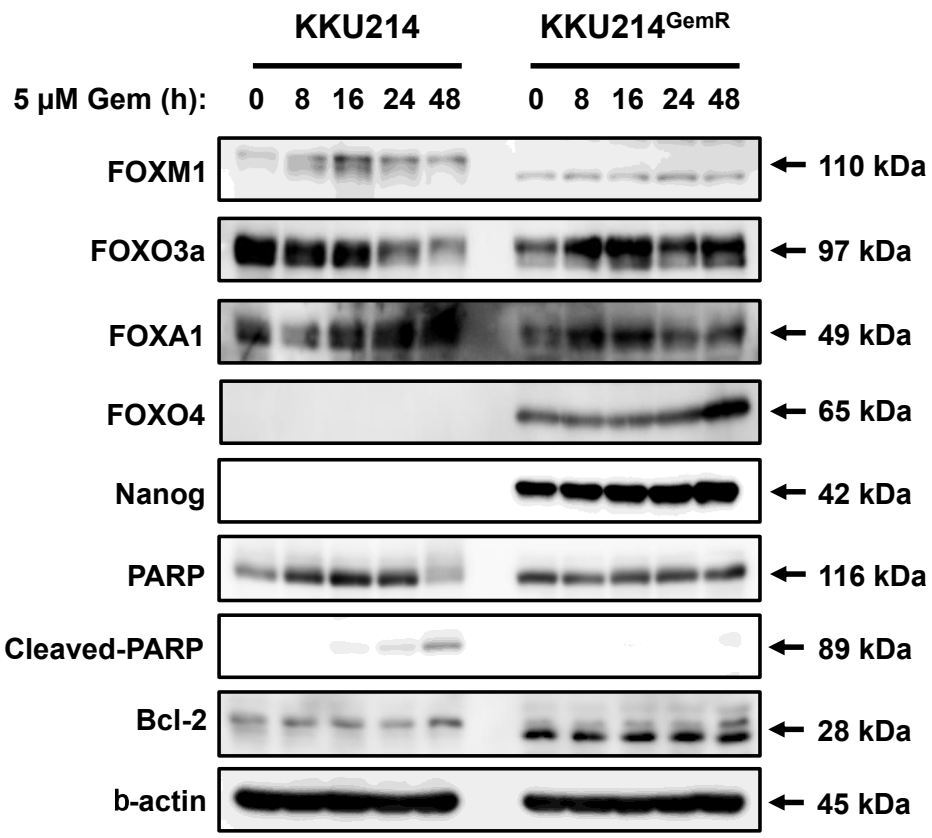

Figure 2-12. Gemcitabine treatment induces the changes of expression of FOX protein family and their related molecules. KKU214 and KKU214^{GemR} CCA cell lines were treated with 5 uM of gemcitabine with different time periods. After treatment at the designated time, cells were trypsinized and the dynamic expression of FOX protein family and their related molecules was determined by using Western blotting. β-actin was used as loading control. Gem = gemcitabine.

In order to test whether FOXO4 is involved in gemcitabine resistance of CCA cells, the expression of FOXO4 was inhibited by Crispr/Cas9 targeting FOXO4 gene. Western blot analysis showed that the expression of FOXO4 protein was dramatically decreased in Crispr/Cas9-FOXO4-transfected KKU214^{GemR} cells compared to mock transfection (Fig. 2-13). RT-qPCR analysis also confirmed that the FOXO4 expression was suppressed compared to mock transfection (data not shown). Interestingly, in transfected cells, the expression of Nanog protein was also reduced, highlighting the association of FOXO4 and Nanog in KKU214^{GemR} cells.

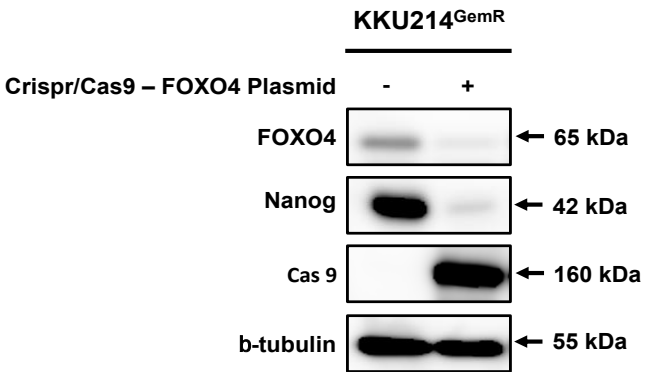

Figure 2-13. Expression of FOXO4 and Nanog in FOXO4-knocked out **KKU214^{GemR} CCA cell line.** KKU214^{GemR} cells were transfected with FOXO4-targeted Crispr/Cas9 plasmid DNA for 24 hr. The expression of FOXO4 and Nanog were determined using Western blot analysis. β-tubulin was used as loading control. Cas 9 expression was determined by Western blot analysis to indicate the success of transfection.

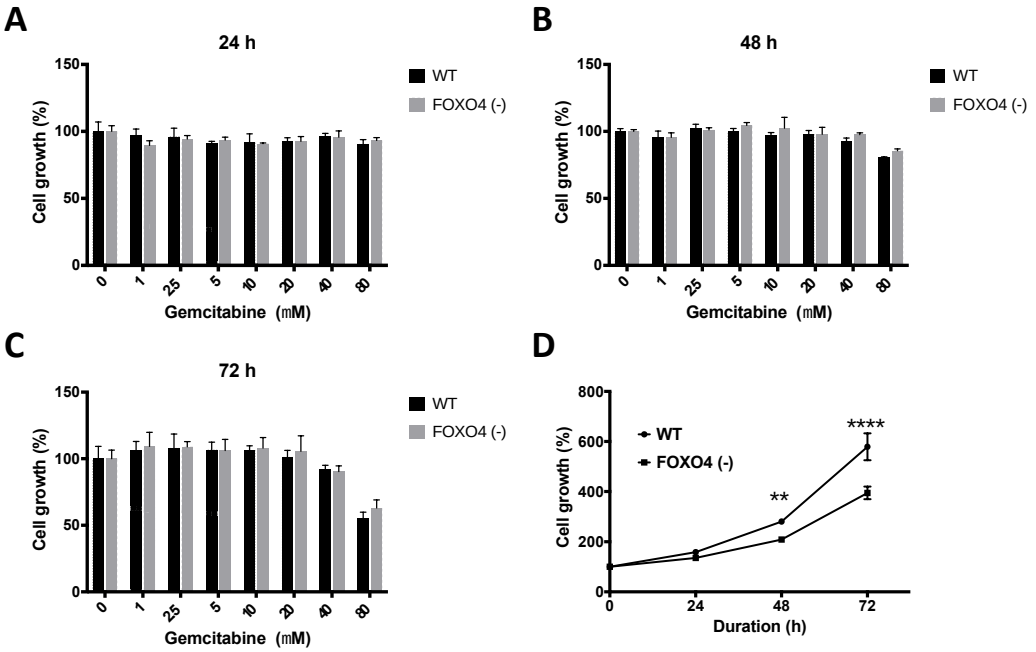

Figure 2-14. Effect of FOXO4 knock down on gemcitabine treatment and growth rate of KKU214^{GemR} CCA cell line. (A-C) FOXO4 wild type and FOXO4-knocked out KKU214^{GemR} cells were treated with different concentrations of gemcitabine for the indicated time periods. Then, percentage of cell proliferation was determined by the SRB assay compared to its control treatment (DMSO). (D) The growth rate at different time periods (0-72 h) of untreated FOXO4 wild type and FOXO4-knocked out KKU214^{GemR} cells was determined by the SRB assay. Experiments were carried out in triplicate.

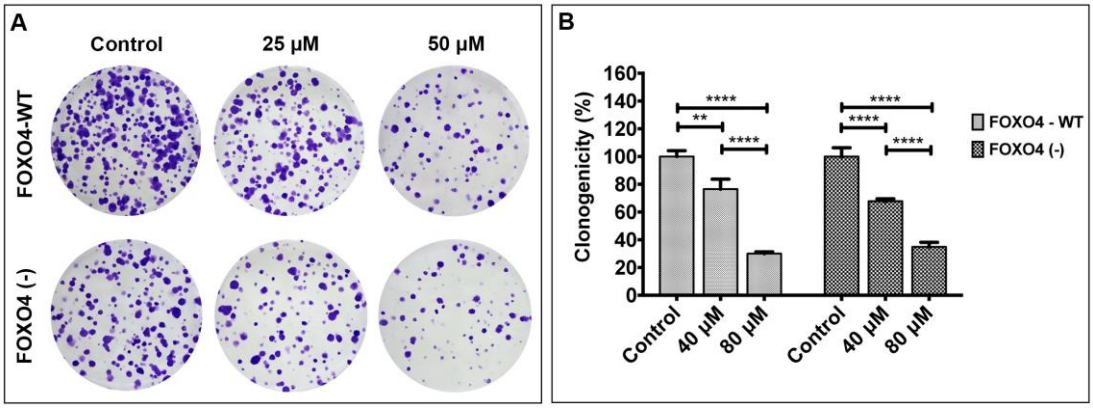

Figure 2-15. Effect of FOXO4 knock out **on clonogenicity of KKU214^{GemR} CCA cell line.** (A) FOXO4 wild type and FOXO4-knocked out KKU214^{GemR} cells were treated with gemcitabine at indicated doses for 48h. The cells were then subsequently maintained in normal growth medium for 14 days. The effect of gemcitabine treatment on colony formation of FOXO4 wild type and FOXO4-knocked out KKU214^{GemR} cells was determined by clonogenic assay. (B) Relative differences of colony formation between FOXO4 wild type and FOXO4-knocked down KKU214^{GemR} cells were investigated by dissolving stained colonies with 33% acetic acid and absorbance at optical density (OD) 620 nm was measured by ELISA reader. Percentage of clonogenicity was calculated in comparison to untreated control. ** and **** indicate the significant differences at $p<0.01$ and $p<0.0001$, respectively.

SRB assay demonstrated that the growth inhibitory effect of gemcitabine did not differ between mock transfection and FOXO-knocked out KKU214^{GemR} cells (Fig. 2-14A-C). However, the growth rate of FOXO-knocked out KKU214^{GemR} cells was lower than that control cells (Fig. 2-14D). This result was supported by the clonogenic assay (Fig. 2-15). Cell scratch assay demonstrated that suppression of FOXO4 reduced the migration of FOXO4-knocked out KKU214^{GemR} cells (Fig. 2-16), suggesting that FOXO4 did not involve in gemcitabine resistance but involved with CCA cell growth and migration. The underlyingly molecular mechanisms of these findings are under investigation.

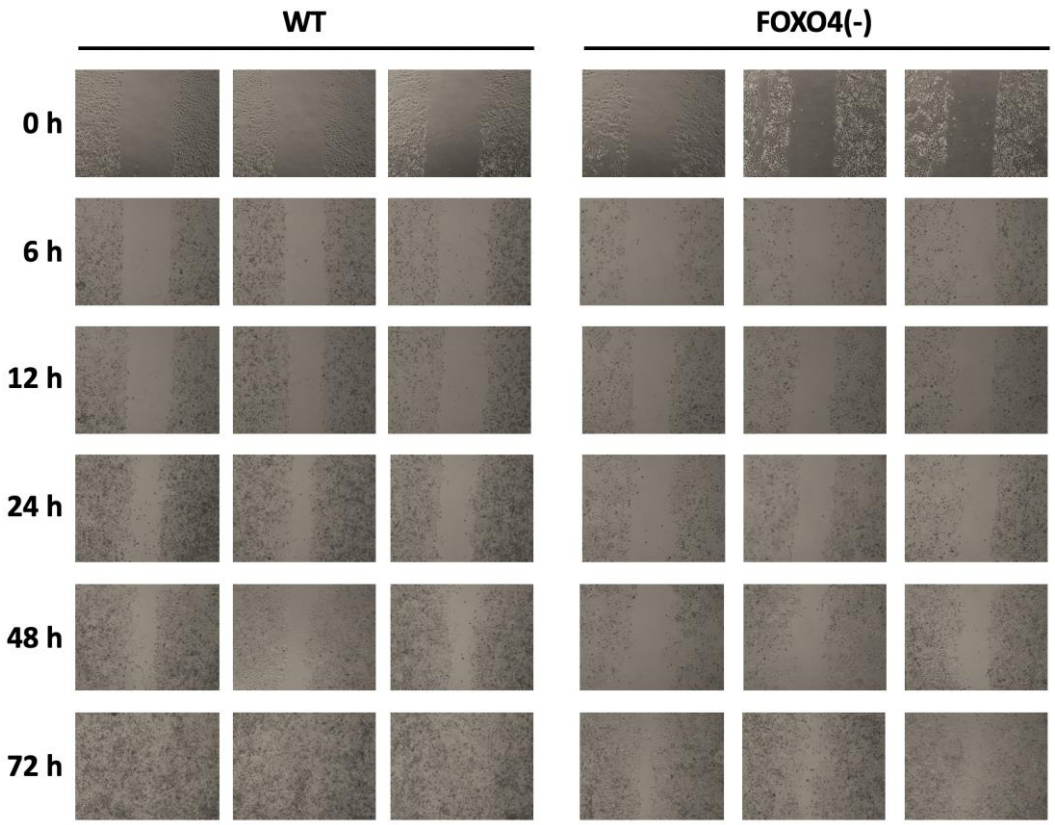

Figure 2-16. Effect of FOXO4 knock down on cell migration of KKU214^{GemR} CCA cell line. FOXO4 wild type and FOXO4-knocked down KKU214^{GemR} cells were seeded in 6-well plate. On the following day, a straight scratch was made using sterile P200 pipette tips. The cells were then washed with sterile PBS and further cultured in complete medium. Pictures were taken at the start of the experiment (0h) and 24, 48 and 72 h later. Experiment was performed in triplicate.

Summary

Our study indicated that FOXO4 was upregulated in gemcitabine resistant CCA cells, however, did not involve in gemcitabine resistance. FOXO4 may important in maintaining cell growth and migration of CCA cells in the presence of gemcitabine. Further investigation on the underlying molecular mechanisms is needed. This work is continuing to elucidate the function of FOXO4 and nanog in gemcitabine resistant CCA cells.

2.3 Application of anthocyanin (AC) on CCA cell and its role in sensitization of drug resistant CCA cells to gemcitabine treatment.

AC treatment inhibited proliferation and induced apoptosis of CCA cell lines.

Inhibition of tumor growth and induction of cellular apoptosis are important modes of action of most phytochemical agents. To determine whether AC exerts growth-inhibitory effect on CCA cell lines, and to determine relevant IC_{50} values, KKU213 and KKU214 were treated with various concentrations of AC. The SRB assay revealed that AC inhibited cell proliferation of both cell lines in dose- and time dependent manners (Fig. 2-17A and 2-17B). KKU214 cell line was more sensitive to AC treatment as its viability was completely inhibited by 600 ug/ml of AC after 48 h, whereas proliferation of KKU213 was completely inhibited by treatment with 800 ug/ml of AC. In agreement with this, non-linear regression analysis showed that IC50 values of AC for KKU213 and KKU214 were 620 and 540 ug/ml, respectively (Fig. 2-17C and 2-17D).

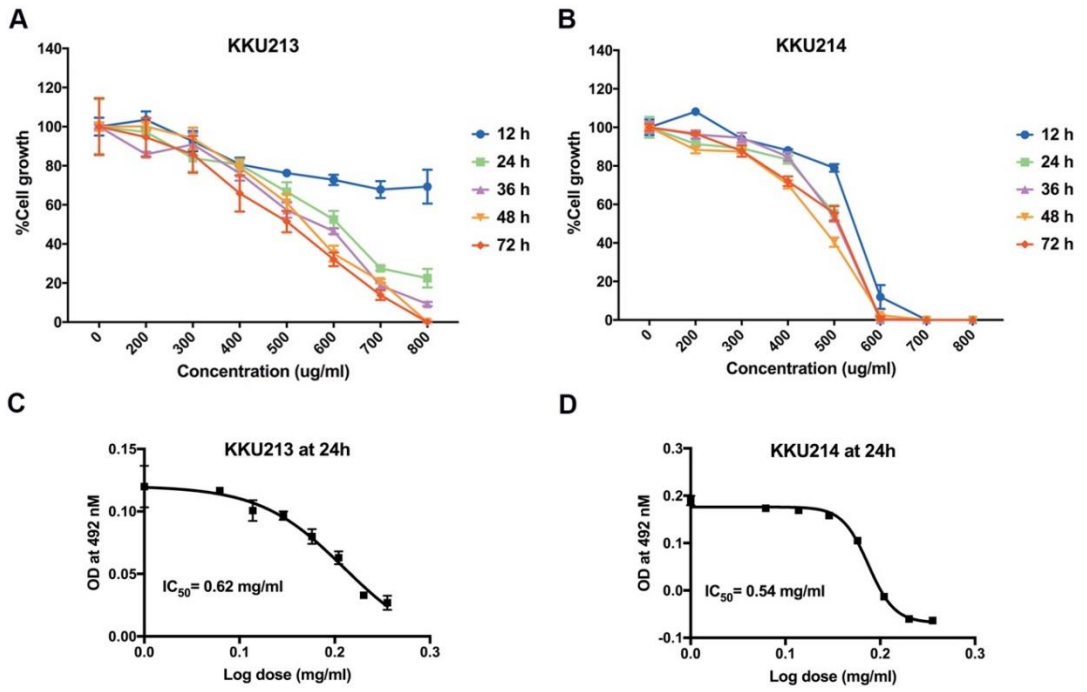

Figure 2-17. Anthocyanin complex (AC) inhibited cell growth of KKU213 and KKU214 CCA cell lines. (A, B) Two CCA cell lines (KKU213 and KKU214) were treated with different concentrations of AC for the indicated time periods. Then, percentage of cell proliferation was determined by the SRB assay compared to its control treatment (DMSO). (C, D) IC50 of AC on KKU213 and KKU214 at 24 h post-treatment was calculated by using a dose-response curve analysis. Experiments were carried out in triplicate. AC = anthocyanin complex.

Next, we investigated whether suppression of CCA cell growth by AC treatment is related to induction of apoptosis. We treated both cell lines with AC at dosages a bit lower than their IC_{50} values for 24 h and cellular apoptosis was investigated by flow cytometry. This revealed that cellular apoptosis was induced in a dose-dependent manner (Fig. 2-18). Slight increases (relative to controls) in rates of apoptosis of KKU213 and KKU214 were observed when treated with 300 and 250 ug/ml of AC, respectively (Fig. 2-18B and 2-18E). However, cellular apoptosis of both cell lines was dramatically induced when treated with 600 (KKU-213) or 500 ug/ml (KKU-214) of AC (Fig. 2-18C and 2-18F). These findings indicated that AC exhibited anti-CCA activity through suppression of proliferation and induction of cellular apoptosis.

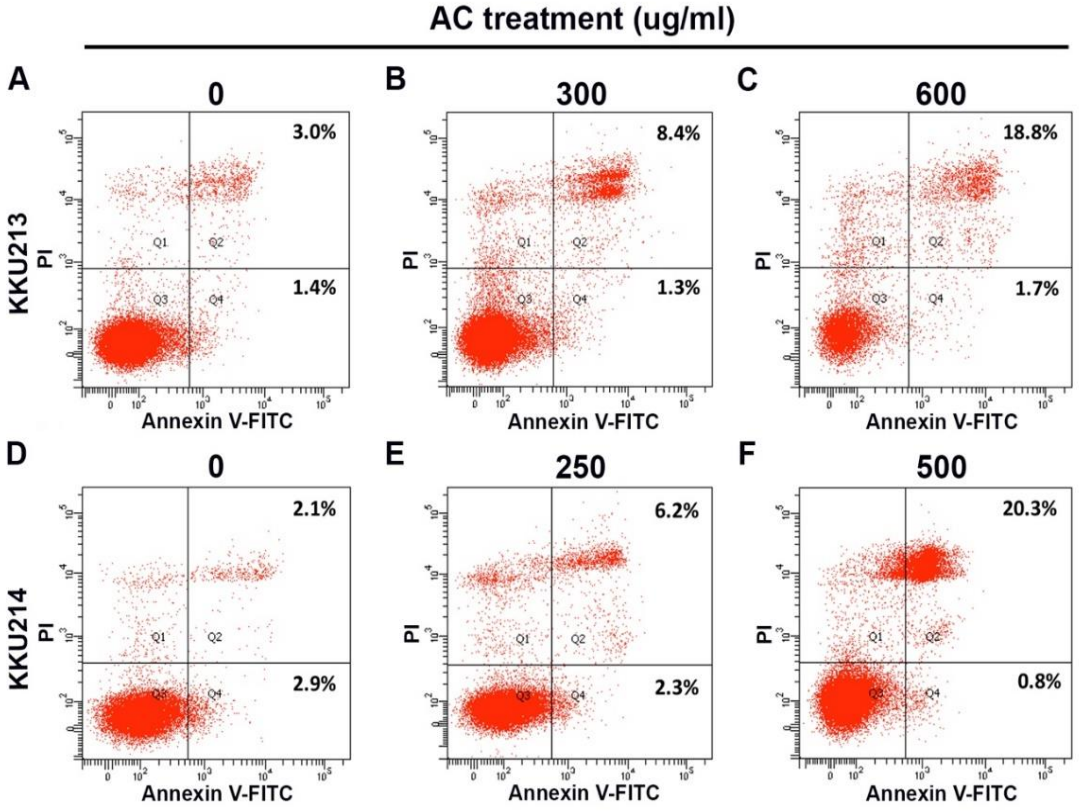

Figure 2-18. AC treatment induced cellular apoptosis of CCA cell lines. (A-C) KKU213 and (D-E) KKU214 were treated with AC at indicated doses for 24 h. Apoptotic cells were stained with Annexin V-FITC/PI solution and analysed by flow cytometry. DMSO at a final concentration of 1% was used as diluent control (0).

AC treatment inhibited colony formation of CCA cell lines.

The clonogenic assay is the method of choice to determine cell reproductive viability (ability of cells to produce progeny or ability of a single cell to form a colony) after treatment with radiation or a cytotoxic agent. We used this approach to determine the cytotoxic effects of AC treatment on CCA cell lines. Presence of AC significantly inhibited KKU-213 colony formation in a dose-dependent fashion compared to control group ($p<0.0001$, Fig. 2-19A and 2-19B). For KKU-214, colony formation was significantly inhibited only when treated with 500 ug/ml of AC ($p<0.0001$, Fig. 2-19A and 2-19C). Additionally, colony formation of KKU-214 treated with 500 ug/ml of AC was significantly lower than when treated with 250 ug/ml of AC ($p<0.0001$, Fig. 2-19C). This result indicated that AC-mediated reproductive death is one of the underlying mechanisms of AC against CCA.

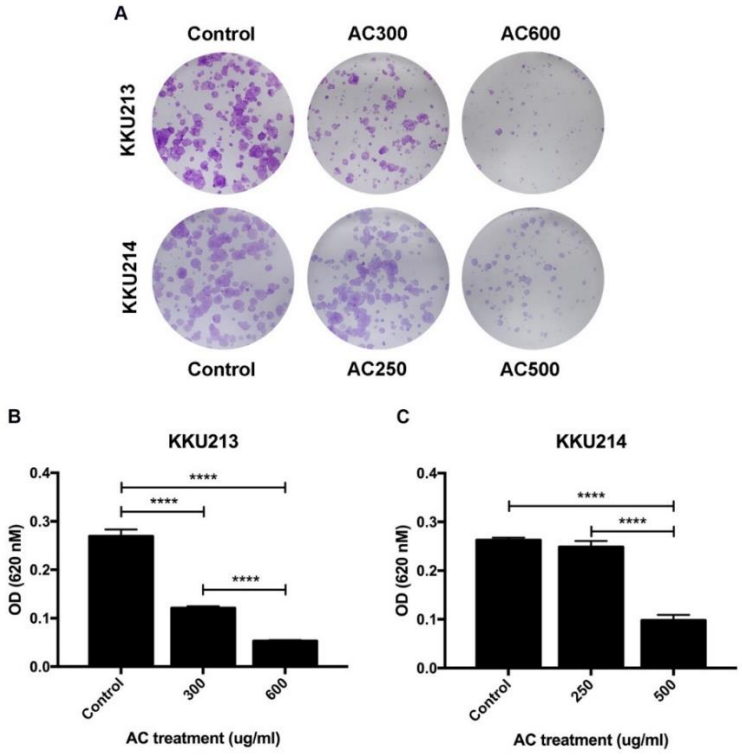

Figure 2-19. AC treatment reduced colony formation of CCA cell lines. (A) KKU-213 and KKU-214 cell lines were seeded in 6-well plates at a density of 1,000 cells/well and cultured with AC or DMSO (control) for 48 h. At day 14, colony formation was visualized by crystal violet staining and photographed with a digital camera. (B, C) Relative difference of colony formation of CCA cell lines was investigated by dissolving stained colonies with 33% acetic

acid and measuring absorbance at optical density (OD) 620 nM. **** indicates a significant difference at $p<0.0001$.

AC treatment induced mitochondrial superoxide production partly via suppression of Bcl-2 expression.

Induction of superoxide production in mitochondria is an important event in apoptosis induction. To investigate whether induction of mitochondrial superoxide production is involved in AC-induced apoptosis of CCA cell lines, both lines were treated with AC and mitochondria-specific superoxide was measured by flow cytometry. We found that superoxide production was slightly increased in mitochondria of KKU-213 and KKU-214 treated with 300 and 250 ug/ml of AC, respectively (Fig. 2-20B and 2-20E). However, treatment of KKU213 and KKU-214 cell lines with 600 and 500 ug/ml of AC, respectively, significantly induced superoxide production in mitochondria of both cell lines relative to controls ($p<0.001$, Fig. 2-20C and 2-20F, 2-20G and 2-20H).

Since superoxide production can be inhibited by anti-apoptotic Bcl-2 protein, we further investigated the expression of Bcl-2 protein in CCA cell lines. Western blot analysis revealed that expression of Bcl-2 protein mirrored superoxide production. Expression of Bcl-2 protein was decreased in AC-treated cell lines, especially in KKU-213 and KKU-214 treated with 600 and 500 ug/ml of AC, respectively, relative to DMSO-treated controls (Fig. 2-21). These results indicated that AC induced superoxide production-mediated apoptosis partly via inhibition of Bcl-2 protein expression.

AC treatment targeted pro-survival and endoplasmic reticulum stress (ER stress) response of CCA cell lines.

FOXM1 and NF-kB are well-known oncogenic proteins involved in the survival of cancers. We investigated the expression of these proteins in CCA cell lines after treated with AC for 24 h. Western blot analysis showed that expression of FOXM1 and the p65 subunit of NF-kB decreased in a dose-dependent manner in KKU-213 and KKU-214 cell lines treated with AC (Fig. 2-21). Notably, expression of these proteins was almost completely inhibited in KKU-213 and KKU-214 treated with 600 and 500 ug/ml of AC, respectively, compared with DMSO-treated controls (Fig. 2-21). Previous experiment has shown that AC treatment dramatically induces mitochondrial superoxide production. Excessive superoxide production can cause protein misfolding and ultimately induces ER stress. We therefore investigated the expression

of proteins in the PERK/eIF2α/ATF4 axis which is an important ER stress response pathway. Western blot analysis showed that expression of PERK, p-eIF2α (Ser 51) and ATF4 in both KKU-213 and KKU-214 decreased under AC treatment (Fig. 2-21). Notably, total eIF2α expression was not affected by AC treatment, suggesting that AC suppresses phosphorylation of eIF2α in these cell lines. In addition to FOXM1, p65 and the PERK/eIF2α/ATF4 axis, we found that PARP expression was also suppressed by AC treatment, particularly at the highest doses used (Fig. 2-21).

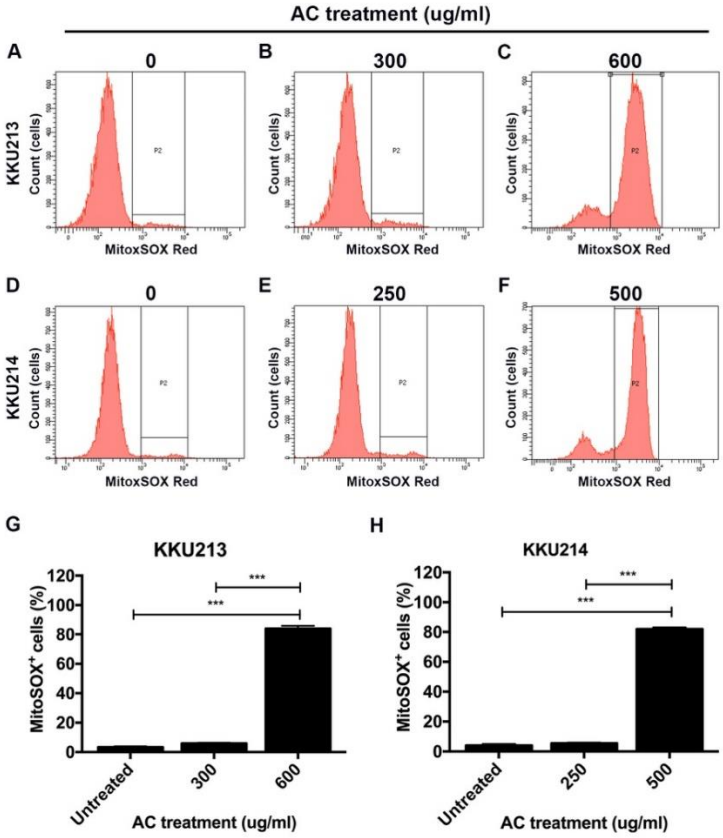

Figure 2-20. Mitochondrial superoxide production was dramatically induced by AC treatment. Mitochondrial superoxide production after AC treatment of (A-C) KKU-213 and (D-F) KKU-214 was measured by MitoSOX Red coupled with flow cytometry. A peak at P2 indicates superoxide production from mitochondria. Those cell lines treated with DMSO (1%) were used as diluent control. (G, H) Percentage of mitochondrial superoxide production was calculated

and plotted relative to the number of measured cells. *** indicates a significant difference at $p<0.001$.

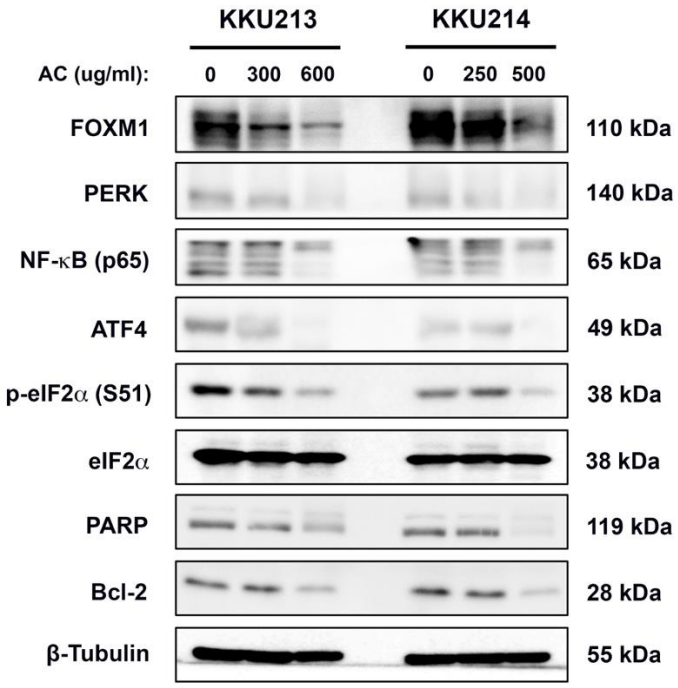

Figure 2-21. AC treatment downregulated the expression of several survival-related proteins and ER stress proteins. KKU-213 and KKU-214 were treated with AC for 24 h and cells were harvested and lysed by RIPA buffer. Expression of indicated proteins was investigated by Western blot analysis. β-tubulin expression was used as loading control.

AC treatment enhanced gemcitabine sensitivity of gemcitabine-resistant KKU214^{GemR} CCA cell line.

Resistance to chemotherapeutic treatment is an important obstacle for treatment of various cancers including CCA. Therefore, we attempted to investigate whether co-treatment with AC could enhance the effect of gemcitabine. The SRB assay revealed that the IC_{50} of gemcitabine against KKU-214GemR CCA cell line was 32.11 μM at 72 h whereas the IC_{50} of gemcitabine against the parental KKU-214 cell line was 0.40 μM at 72 h (data not shown), agreeing with a previous report. Treatment of KKU-214GemR with AC inhibited cell proliferation in dose- and time-dependent manners (Fig. 2-22A). For gemcitabine treatment alone, KKU-214^{GemR} cell growth was obviously inhibited by treatment with 40 μM for 48 h and 72 h (Fig. 2-22B). AC at a dose of 300 μg/ml which didn't show a growth inhibitory effect on KKU-214^{GemR},

was chosen for co-treatment with 20 or 40 μM of gemcitabine. As expected, both combinations significantly enhanced gemcitabine-mediated growth inhibition compared to treatments with single agents ($p<0.01$ for Gem20 vs AC300+Gem20; $p<0.001$ for Gem40 vs AC300+Gem40, Fig. 2-22C). Furthermore, clonogenic assay also depicted a significant enhancement of gemcitabine treatment when co-treated with AC ($p<0.05$, Fig. 2-22D). These results indicated that AC treatment significantly enhanced efficacy of gemcitabine against gemcitabine-resistant KKU-214^{GemR}.

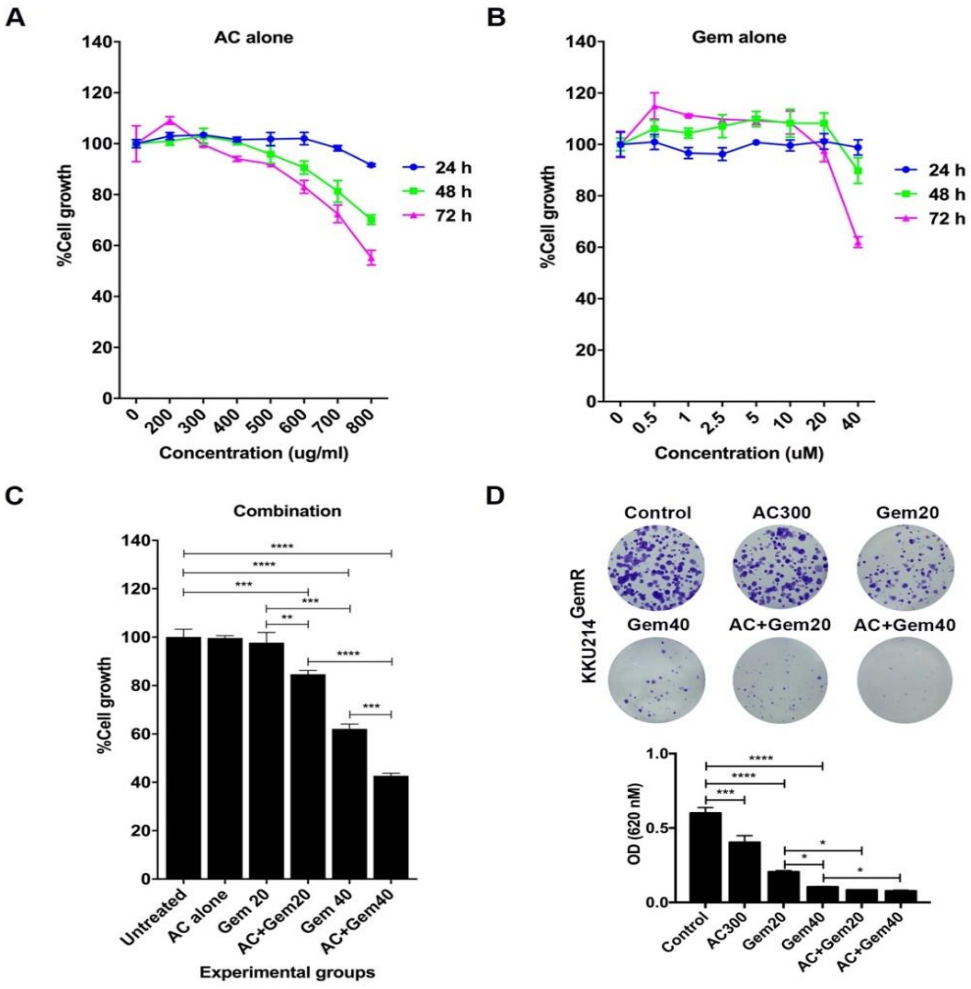

Figure 2-22. AC treatment sensitized the KKU-214GemR cell line to gemcitabine treatment. The KKU-214^{GemR} cell line was seeded in 96-well plates and treated with either (A) AC alone or (B) gemcitabine alone at indicated times. (C) Cells were treated with either the single agent (AC or gemcitabine) or a combination of AC (300 μg/ml) and gemcitabine (20 or 40 μM) for 72 h. Then, percentage of cell growth (relative to control) was determined using the SRB assay. Cell growth inhibition was clearly seen in the combination treatment compared

to treatment with either agent alone. (D) Effect of combinatorial treatment on colony formation of KKU214GemR cell line was also determined by the clonogenic assay. Relative difference of colony formation of KKU-214^{GemR} cell line was investigated by dissolving stained colonies with 33% acetic acid and absorbance at optical density (OD) 620 nM was measured by ELISA reader. *, **, *** and **** indicate a significant difference at $p<0.05$, $p<0.01$, $p<0.001$ and $p<0.0001$, respectively. Gem = gemcitabine.

Summary

Our study demonstrated that AC possesses cytotoxicity against CCA cell lines by suppression of cell growth and induction of apoptosis via downregulation of FOXM1, NF-kB the ER stress response and induction of mitochondrial superoxide production. AC also sensitizes KKU-214^{GemR} to gemcitabine treatment. Therefore, AC has potential as an alternative treatment agent and might assist in overcoming drug resistance of CCA when co-administered with other chemotherapeutic agents. This work was published in Intuyod, K., A. Priprem, C. Pairojkul, C. Hahnvajanawong, K. Vaeteewoottacharn, P. Pinlaor and S. Pinlaor (2018). "Anthocyanin complex exerts anti-cholangiocarcinoma activities and improves the efficacy of drug treatment in a gemcitabine-resistant cell line." Int J Oncol.

3. Roles of FOX axis on glycosylation in CCA

O-GlcNAcylation is an o-linked protein glycosylation with a single molecule of N-acetylglucosamine (GlcNAc). Unlike N-linked or other O-linked glycosylation, the modifications by O-GlcNAc are generally found in either cytoplasmic or nuclear proteins. The O-GlcNAcylation is a dynamic process modulated by two enzymes; O-linked β-N-acetylglucosaminyl transferase (OGT) and β-N-acetylglucosaminidase (OGA) to add or remove the GlcNAc from the proteins. The O-GlcNAcylation can regulate the protein behaviors via many mechanisms including protein phosphorylation, protein stability, protein-protein interaction, and protein expression which involves in many cellular processes. The aberration of this process can cause many human diseases, including cancer. We have studied the role of O-GlcNAcylation in CCA. After the treatment of CCA cell lines with OGA inhibitor, PUGNAc, the migration and invasion abilities were significantly increased in association with increasing of O-GlcNAcylation (Fig 3-1).

To understand the mechanism underlying effects of O-GlcNAcylation on migration and invasion of CCA cells, we have identified the O-GlcNAcylated proteins using O-GlcNAc affinity chromatography followed LC-MS/MS analysis. A multifaceted RNA/DNA-binding protein associated with pre-mRNA/mRNA metabolism and transport, namely hnRNP-K, was identified and selected for further studies. We have further investigated the effects of O-GlcNAcylation on the localization and expression of hnRNP-K by treating CCA cell lines with siOGT and PUGNAc. The results showed that suppression of O-GlcNAcylation by siOGT or enhancing O-GlcNAcylation by PUGNAc did not affect the expression of hnRNP-K in CCA cell lines (Fig. 3-2A). However, the localizing of hnRNP-K to nucleus in CCA cell lines is significantly suppressed after siOGT treatment (Fig. 3-2B), suggesting the role of O-GlcNAcylation in regulating functions and nuclear localization of hnRNP-K.

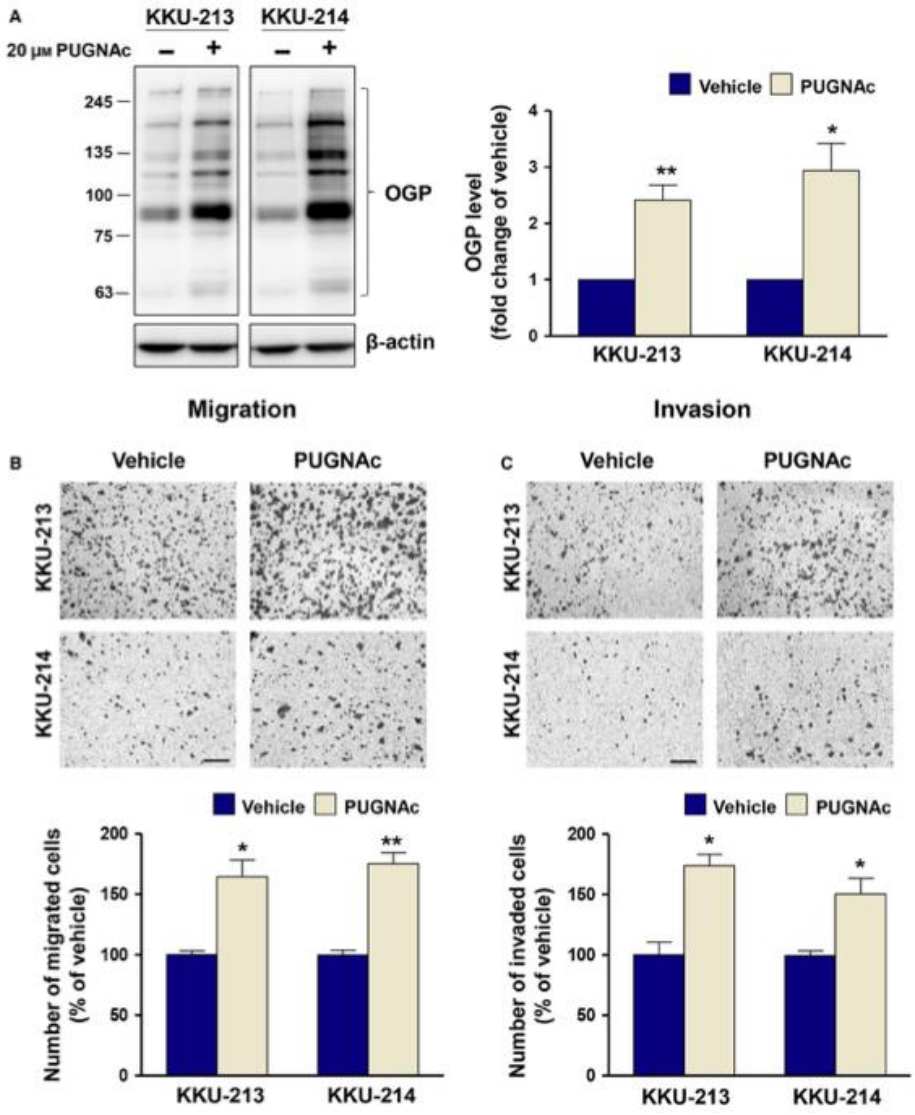

Figure 3-1. Effects of O-GlcNAcyaltion on migration and invasion of CCA cell lines.

CCA cell lines, KKU-213 and KKU-214, were treated with PUGNAc, an OGA specific inhibitor followed by (A) Determination of O-GlcNAcylation level by Western blotting, (B) migration and (C) invasion assays.

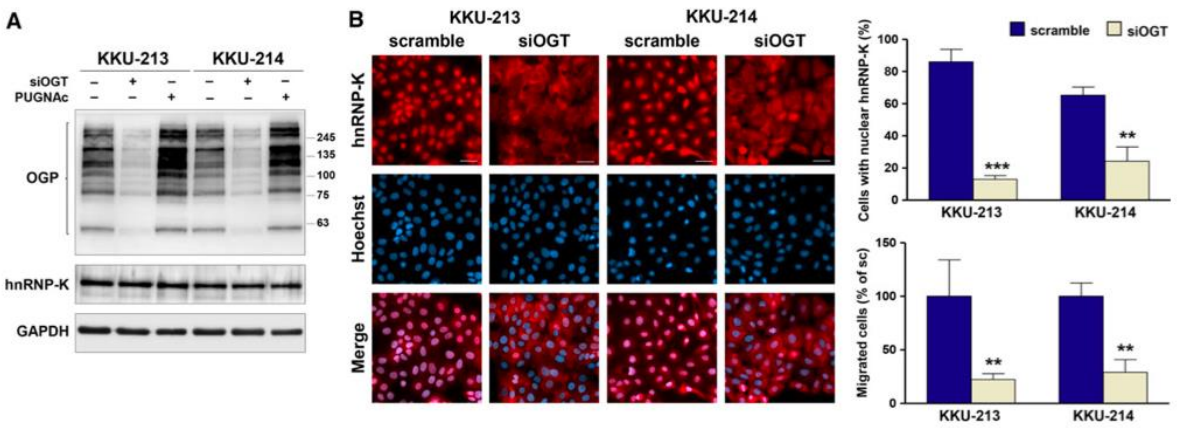

Figure 3-2. Role of O-GlcNAcylation in expression and localization of hnRNP-K. CCA cell lines, KKU-213 and KKU-214, were treated with siOGT or PUGNAc, (A) Determination of O-GlcNAcylation level and expression of hnRNAP-K by Western blotting, (B) localization of hnRNAP-K migration by immunofluorescent staining.

We further studied the role of hnRNP-K in CCA using specific siRNA. Knock down of hnRNAP-K by si-hnRNP-K significantly suppresses the proliferation, migration, and invasion of KKU-213 and KKU-214 CCA cell lines (Fig. 3-3).

Moreover, we further investigated whether O-GlcNAcylation can control other glycosylation processes such as N-glycosylation of the CCA cells. We have determined the N-glycan profiles in CCA cell lines and studied the effects of O-GlcNAcylation on the expression profile of N-glycans. Our data showed that siOGT treated CCA cells exhibited the low metastatic abilities with low expression of high mannose (Hex9HexNAc2) types of N-linked glycan (Fig.3-4A). While, the high metastatic CCA cell lines (KKU-213L5 and KKU-214L5) exhibited higher level of high mannose type N-glycans, comparing with their parental low metastatic KKU-213 and KKU-214 cell lines (Fig.3-4B). Lectin cytofluorescent staining using PSA, a lectin specific to mannose, showed that mannose-associated glycans wer dramatically reduced in siOGT treated cells, compared with controls (Fig. 3-4C) This information suggested the role of O-GlcNAcylation on mannose modification of N-glycans in CCA cell lines.

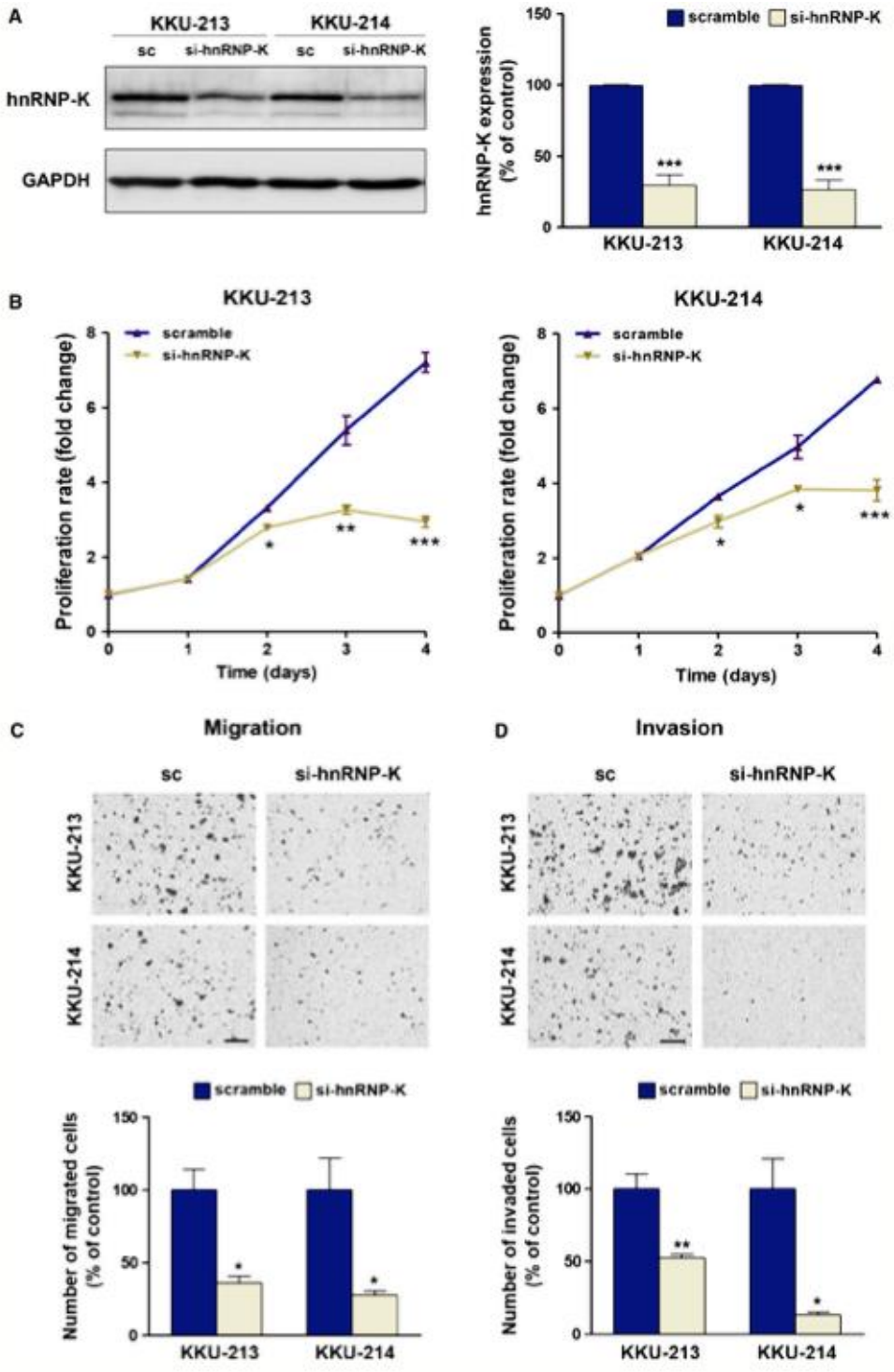

Figure 3-3. Role of hnRNP-K on proliferation, migration and invasion of CCA cell lines.

CCA cell lines, KKU-213 and KKU-214, were transfected with specific siRNA against hnRNP-K followed by (A) Determination of O-GlcNAcylation level by Western blotting, (B) migration and (C) invasion assays.

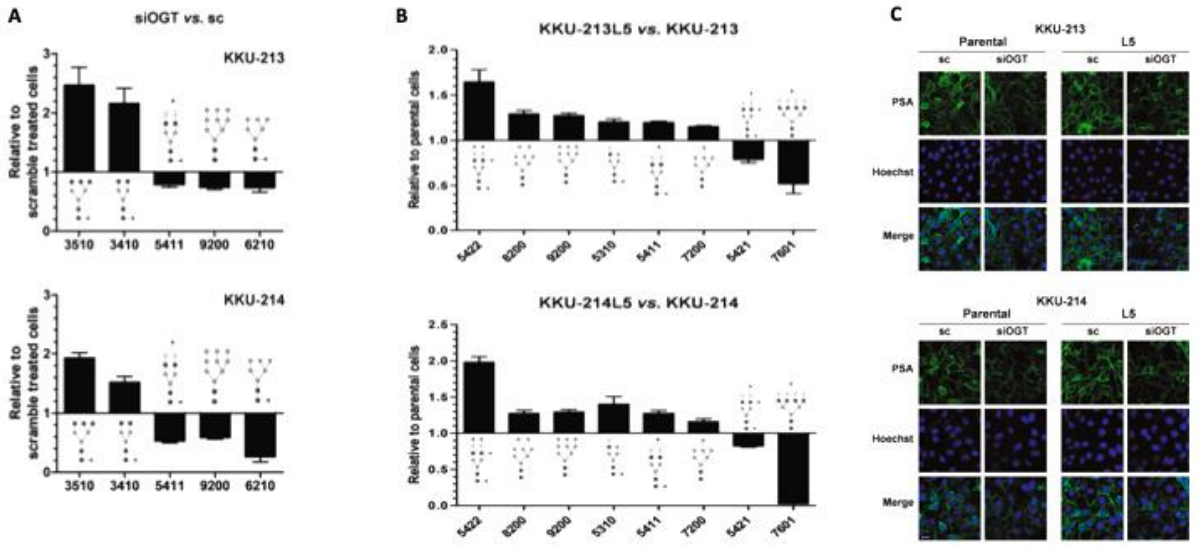

Figure 3-4. Effects of O-GlcNAcyaltion on expression of N-glycans in CCA cell lines.

siOGT treated KKU-213 and KKU-214 were compared with siControl (sc) and (B) High metastatic CCA cell lines (KKU-213L5 and KKU-214L5) were compared with their parental KKU-213 and KKU-214 cell lines, respectively. (C) PSA lectin fluorescent staining in siOGT treated KKU-213, KKU-213L5, KKU-214 and KKU-214 cells.

To address the roles of mannose modified glycans in CCA progression, *in vitro* functional assays; such as proliferation, migration, and invasion of CCA cell lines; were tested under the present of PSA lectin. Our data revealed that PSA can significant inhibit migration and invasion, but not proliferation, of CCA cell lines (Fig. 3-5).

We next explored the mechanism of which O-GlcNAcylation controls N-glycosyaltion. As it is known that an increasing of high mannose type N-glycans is mostly associated with decreasing of mannosidase, we therefore determined the expression of mannosidase 1A1 (MAN1A1) after siOGT treatment in CCA cell lines. The results showed that MAN1A1 was significant increased after knockdown of OGT (Fig. 3-6A). In addition, FOXO3A was also found to be increased in siOGT treated cells, comparing with siControl treated cells MAN1A1(Fig. 3-6A).

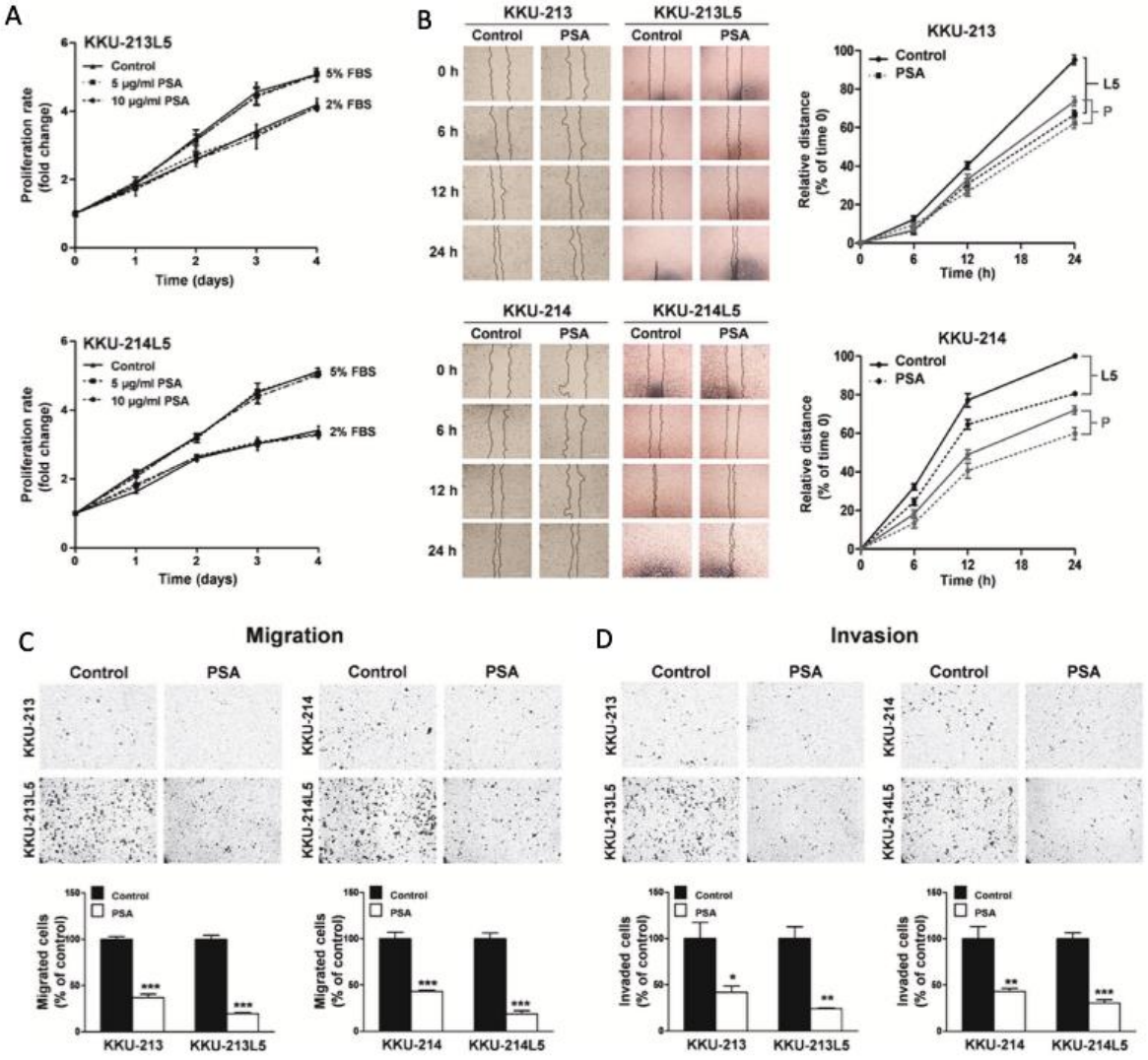

Figure 3-5. Effects of PSA on progression of CCA cell lines. CCA cell lines; KKU-213, KKU-213L5, KKU-214, and KKU-214L5; were treated by PSA followed by the *in vitro* (A) proliferation, (B) migration by wound healing assay, (C) migration by Boyden's chamber assay and (D) invasion assay.

As it is known that the expression of FOXO3 can be regulated by the activation of 3 kinase enzymes; Akt, Ekr, and Ikk. Therefore, the activation of these kinases under the suppressed O-GlcNAcylation condition were determined by western blot. Phospho-Akt and phospho-Erk were reduced in siOGT treated cells but not phospho-Ikk when compared with

the negative siRNA treated cells (Fig. 3-6B). The regulation of FOXO3a by O-GlcNAcylation may pass through the activation of Akt and Erk pathways.

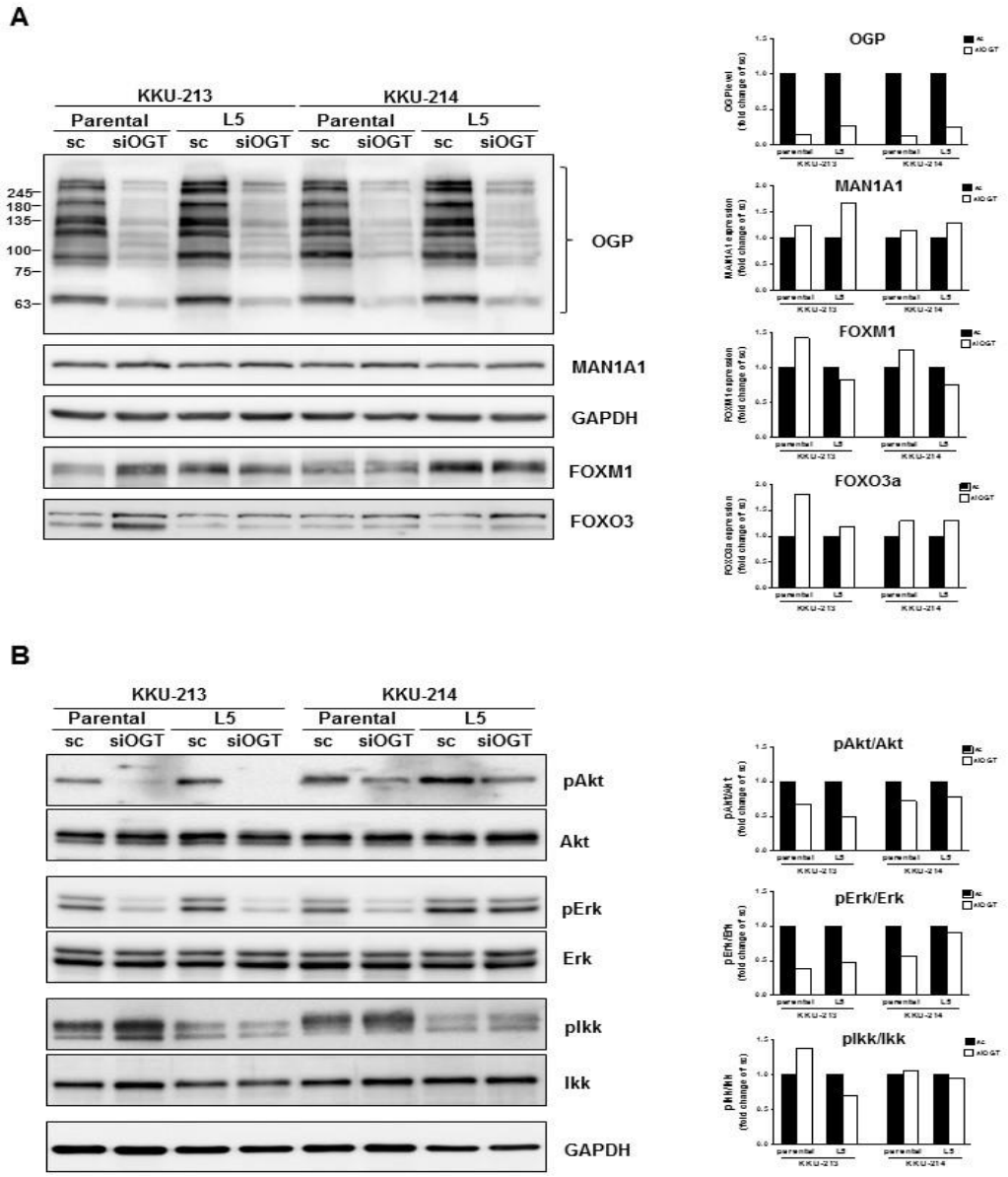

Figure 3-6. O-GlcNAcylation might regulate MAN1A1 expression via suppression of FOXO3a. The parental (KKU-213 and KKU-214) and highly metastatic (KKU-213L5 and KKU-214L5) CCA cells were treated with siOGT for 72h. (A) The expression of MAN1A1, FOXM1 and FOXO3a were determined. (B) The activation of Akt, Erk, and Ikk were detected with the western blot analysis of phosphorylated form.

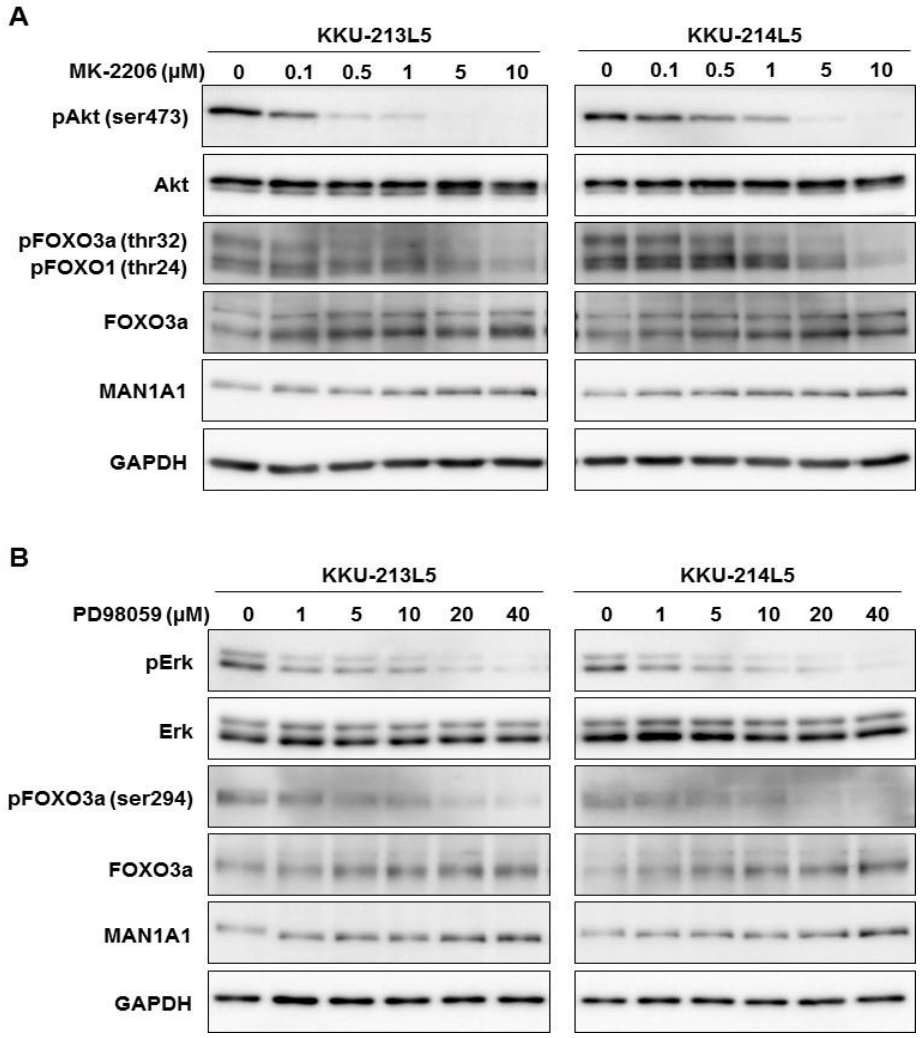

Figure 3-7. Akt and Erk activations regulated FOXO3a and MAN1A1 expressions. The levels of phospho-FOXO3 at thr-32 or ser-294, FOXO3a and MAN1A1 were determined in highly metastatic (KKU-213L5 and KKU-214L5) CCA cells were treated with various concentrations of (A) Akt inhibitor (MK-2206) or (B) Erk (PD98059) inhibitor.

As the O-GlcNAcylation modulated phosphorylation of Akt and Erk which might affect the expression of FOXO3a and MAN1A1. To prove this hypothesis, Akt inhibitor, MK-2206, and Erk inhibitor, PD98059, were applied. The highly metastatic (L5) CCA cells were treated with Akt inhibitor or Erk inhibitor at various concentrations for 24h and the expression of FOXO3a and MAN1A1 were determined. Akt inhibitor treatment could inhibit the phosphorylation of FOXO3a at thr-32 and could increase the expressions of FOXO3 and MAN1A1 (Fig. 3-7A). The

inhibition of phosphorylation of FOXO3 at ser-294 and the induction of FOXO3 and MAN1A1 expressions were also observed in Erk inhibitor treated cells (Fig. 3-7B).

In conclusion, as show in the figure below, the increasing of O-GlcNAcylation activated Akt and Erk phosphorylation which led to the increasing of FOXO3a phosphorylation. The elevation of FOXO3a phosphorylation by Akt and Erk resulted in increased of FOXO3a degradation which might affect the expression of MAN1A1 (Fig. 3-8). These data were published in Phoomak, C., A. Silsirivanit, D. Park, K. Sawanyawisuth, K. Vaeteewoottacharn, C. Wongkham, E. W. Lam, C. Pairojkul, C. B. Lebrilla and S. Wongkham (2018). "O-GlcNAcylation mediates metastasis of cholangiocarcinoma through FOXO3 and MAN1A1." Oncogene **37**(42): 5648-5665.

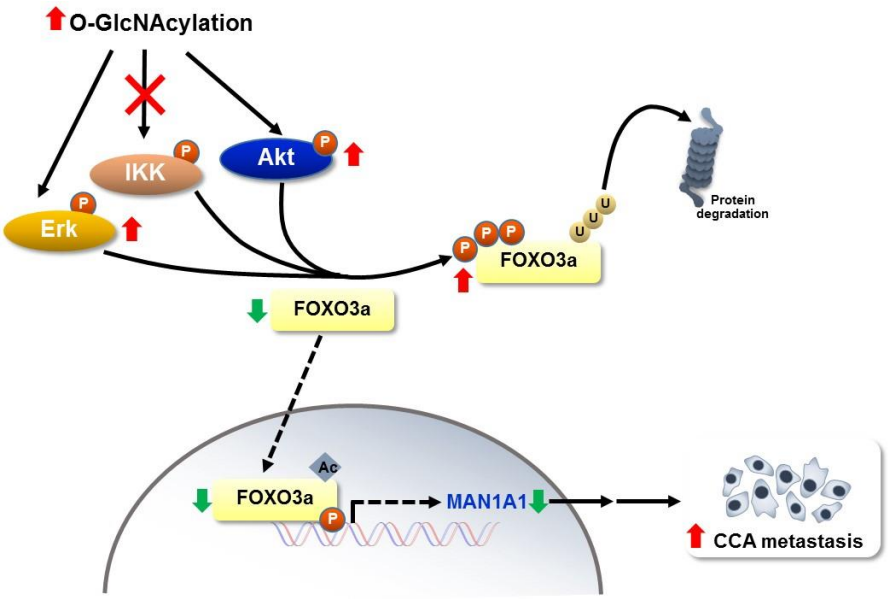

Figure 3-8. Mechanism of O-GlcNAcylation in regulating MAN1A1 expression. The speculated schematic diagram illustrates the mechanism of which O-GlcNAcylation regulates expression of MAN1A1 through the activation of FOXO3A.

4. Opposing roles of FOXA1 and FOXA3 in cholangiocarcinoma progression

FOXAs are transcriptions factors belong to FOX headbox family subfamily A that play roles in chromatin remodeling, metabolism and organogenesis including the development of liver. There are 3 isotopes of FOXAs including FOXA1/HNF3α (hepatocyte nuclear factor 3α), FOXA2/HNF3β and FOXA3/HNF3γ. FOXA1 (472 amino acids), FOXA2 (457 amino acids) and FOXA3 (350 amino acids) that involved in chromatin remodeling. Insight into the unique molecular basis of FOXAs function has been obtained from recent genetic and genomic data, which identify the FOXA proteins as 'pioneer factors' whose binding to promoters and enhancers enable chromatin access for other tissue-specific transcription factors. FOXA1, FOXA2 and FOXA3, have been found to play important roles in multiple stages of mammalian life, beginning with early development, continuing during organogenesis, and finally in metabolism and homeostasis in the adult. Hepatic oval cells or liver stem/progenitor cells have ability to differentiate into hepatocytes and cholangiocytes which is called “bipotential liver stem/progenitor cells”. The FOXA transcription factors play role in liver development by opening compacted chromatin structures within liver-specific target genes such as a hepatoblast marker alpha-fetoprotein (Afp), albumin and transthyretin. These suggested that FOXAs are involved in the bipotential liver stem developments and differentiations.

In this study, the expression patterns of FOXAs (FOXA1, FOXA2 and FOXA3) in CCA tissues (n = 74) were detected using immunohistochemistry. Then, the expression patterns were analyzed with clinical data including age, sex, metastasis status, and survival rates of the CCA patients. After that, FOXA1 and FOXA3 that are related with the aggressive clinical data such as poor prognosis and metastasis status were selected for the functional analysis in the CCA cell lines.

4.1 Expressions of FOXAs in CCA tissues

Expressions of FOXAs (light brown to dark brown) in CCA tissues were showed in Fig. 4-1. FOXAs were weakly detected in hepatocyte cells located at tumor adjacent areas. FOXA1 was highly detected in nucleus and cytoplasm of normal bile duct (NBD) cells adjacent to tumor tissues and some CCA cells in the tumor tissues as shown in Fig. 4-1 (upper panel). However, most of CCA tissues (72%; 53/74) had low expression of FOXA1. FOXA2 was detected

in the nucleus and cytoplasm of some cancer cells in the tumor tissues as shown in Fig. 4-1 (middle panel). 80% (59/74) of CCA tissues had low FOXA2 expression pattern. FOXA3 was highly detected in nucleus and cytoplasm of the cancer cells whereas it was weakly detected in the NBD at tumor adjacent areas. Most of CCA tissues (61%; 45/74) had high FOXA3 expression level.

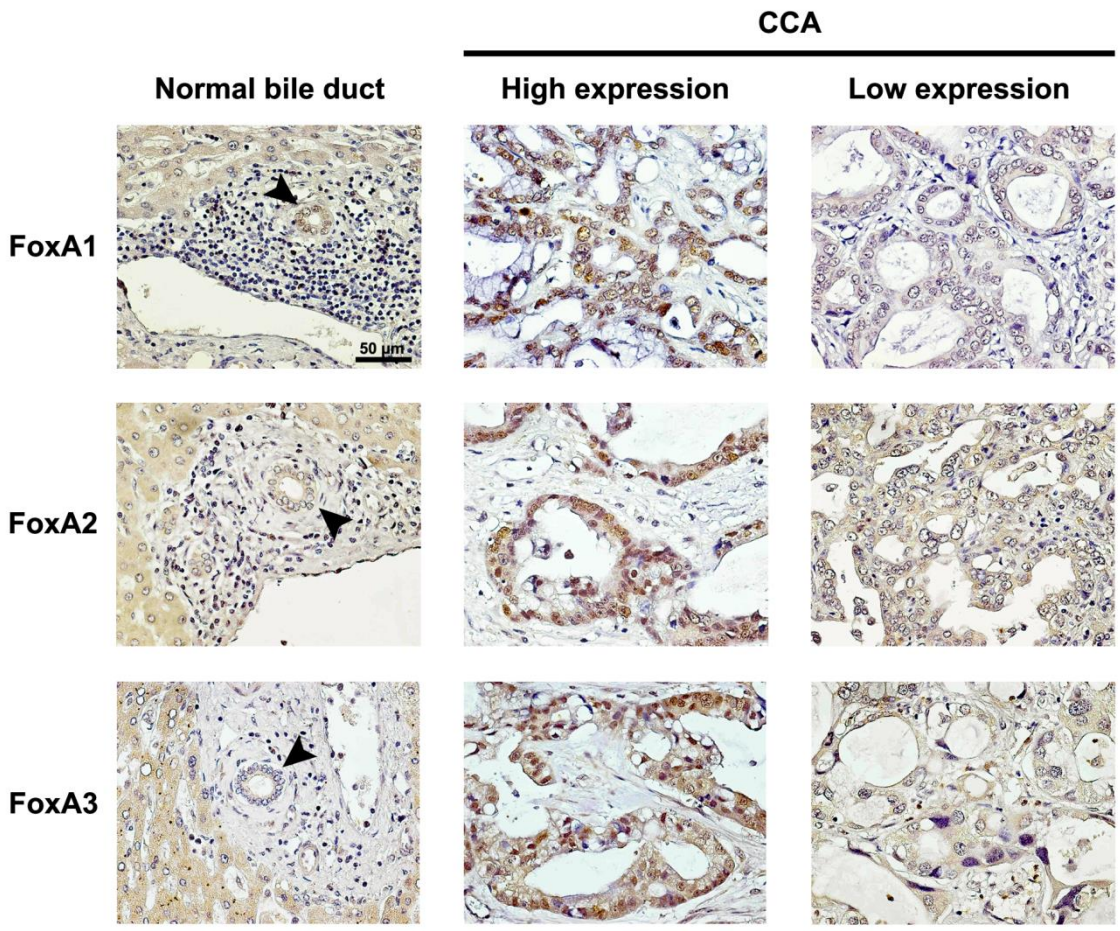

Figure 4-1. FOXA1, FOXA2 and FOXA3 expression patterns in NBD and CCA (high and low expressions) analyzed by IHC. Arrow heads indicate normal bile duct (NBD).

4.2 Correlations of FOXAs and clinicopathological data

The correlations of FOXAs expressions and clinicopathological data were showed in Table 4-1. The survival analyses of FOXAs expressions in CCA patients were presented in Fig. 4-2. Low FOXA1 expression pattern was significantly correlated with poor prognosis. The median survival of CCA patients with high FOXA1 expression was 364 days whereas those of patients with low FOXA1 expression was 256 days. FOXA2 expression was no correlated with

clinical data of CCA patients. Moreover, high expression of FOXA3 in CCA tissues was significantly correlated with metastasis status and patients' ages.

Table 4-1. Correlations of FOXA1, FOXA2 and FOXA3 expression patterns and clinic-pathological data *P-value < 0.05; analyzed by Pearson's Chi-square test

Clinical data	FOXA1			FOXA2			FOXA3		
	Low (n=53)	High (n=21)	*P-value	Low (n=59)	High (n=15)	*P-value	Low (n=29)	High (n=45)	*P-value
Age									
< 57	26	10	0.911	32	4	0.056	20	16	**0.005**
≥ 57	27	11		27	11		9	29	
Sex									
Male	37	14	0.792	41	10	0.833	19	32	0.612
Female	16	7		18	5		10	13	
Metastasis status									
Non-metastasis	24	9	0.850	27	6	0.688	18	15	**0.015**
Metastasis	29	12		32	9		11	30	
Median survival (days)	256	364	**0.031**	260	344	0.159	266	286	0.394

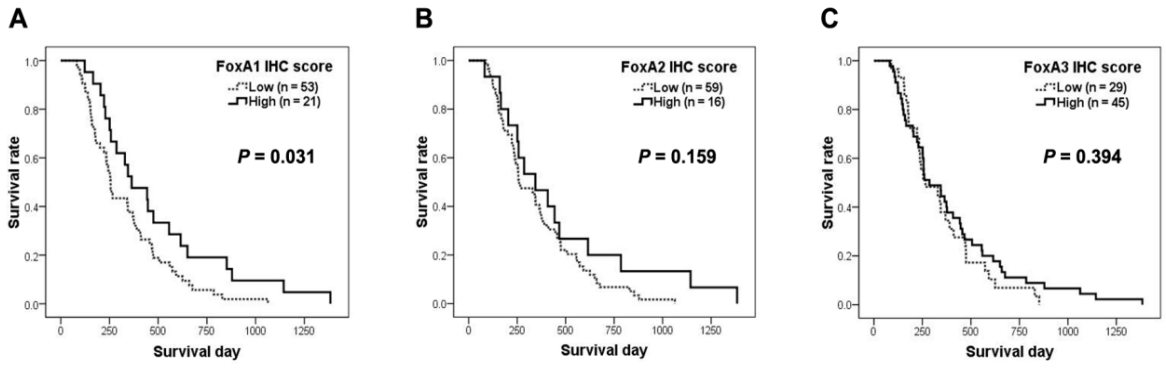

Figure 4-2 Survival analysis of FOXA1, FOXA2 and FOXA3 expression patterns in CCA patients

According to the data analysis, low FOXA1 expression was related with short survival rates and high FOXA3 expression was correlated with metastasis status of CCA patients. These results suggested that FOXA1 may relate with tumor suppressive roles whereas FOXA3 may involve in the induction of CCA progression. Therefore, FOXA1 and FOXA3 were further selected for the functional analyses in CCA cell lines (KKU-100 and KKU-213).

4.3 Functional analysis of CCA cell lines related to FOXA1 and FOXA3 baseline expression levels

The mRNA and protein expression levels of FOXA1 and FOXA3 were measured in KKU-100 and KKU-213 CCA cell lines using real time PCR and immunocytochemical analysis as shown in Figs. 4-3A, 4-3B, 4-3C and 4-3D. KKU-213 cell line had low FOXA1 expression and high FOXA3 expression compared to KKU-100 cell line. Moreover, KKU-213 cells were significantly increased in cell proliferation (Fig. 4-3E) and invasion (Fig. 4-3F and 4-3G) activities compared to KKU-100 cells. These results indicated that FOXA1 and FOXA3 baseline expressions may involve in the progression of CCA cells.

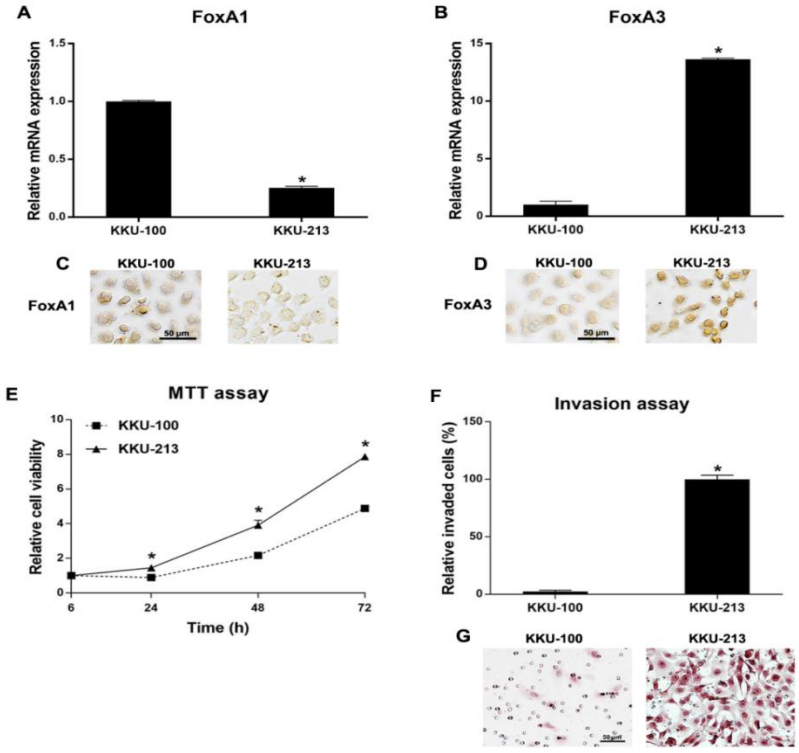

Figure 4-3 Cellular function analysis of KKU-100 and KKU-213. (A, B) mRNA expressions of FOXA1 and FOXA3 measured by real time PCR. (C, D) Protein expressions of FOXA1 and FOXA3 detected by immunocytochemistry. (E) Cell proliferation activities measured by MTT assay. (F)

Graphical represents invaded cells from cell invasion assy. (G) Hematoxylin-stained invaded cells under light microscope from cell invasion assay. *$P < 0.05$ analyzed by student t test.

4.4 Roles of FOXA1 in CCA cell line

KKU-213 had low FOXA1 expression levels was selected for FOXA1 over-expression experiments. KKU-213 cell line was transfected with the FOXA1 expression vector (FOXA1 vector) and the control vector (empty vector). After that, the cell proliferation and invasion activities were measured. FOXA1 mRNA and protein expression levels were significantly increased in the FOXA1-overexpressing cells compared to the control cells (Fig. 4-4A and 4-4B). The FOXA1-overexpressing KKU-213 cells were significantly reduced cell proliferation and invasion activities as shown in Fig. 4-4C, 4-4D and 4-4E. These results indicated that FOXA1 expression plays tumor suppressive roles in the cancer cell line.

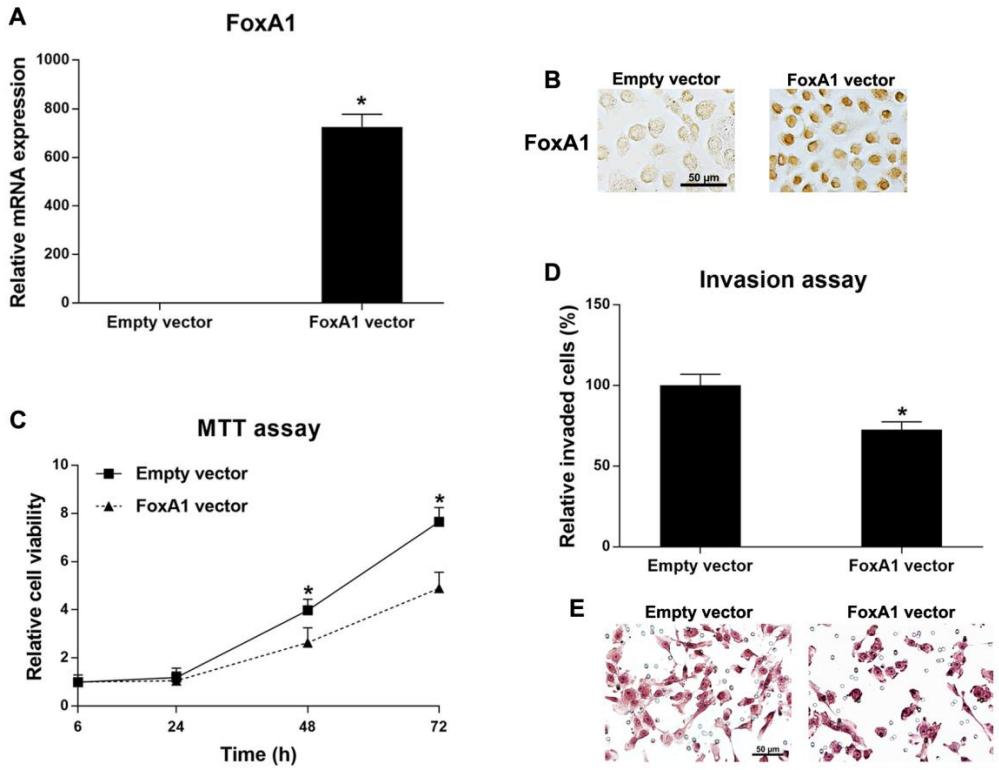

Figure 4-4. Functional analysis of FOXA1-overexpressing KKU-213 cells and the control cells. (A) mRNA expressions of FOXA1 measured by real time PCR. (B) Protein expressions of FOXA1 detected by immunocytochemistry. (C) Cell proliferation activities measured by MTT assay. (D) Graphical represents invaded cells from cell invasion assy. (E) Hematoxylin-stained invaded cells under light microscope from cell invasion assay. *$P < 0.05$, student t test.

4.5 Roles of FOXA3 in CCA cell line

KKU-213 had high FOXA3 expression level was selected for FOXA3-konckdown experiments. KKU-213 cell line was transfected with the specific siRNA for FOXA3 (siFOXA3) and the control siRNA (scramble). After that, the cell proliferation and invasion activities were measured. FOXA3 mRNA and protein expression levels were significantly decreased in the FOXA3-silencing cells compared to the control cells (Figure 4-5A and 4-5B). The FOXA3-silencing KKU-213 cells were significantly reduced cell proliferation and invasion activities as shown in Figure 4-5C, 4-5D and 4-5E. These results indicated that FOXA3 expression play significantly roles in CCA progression.

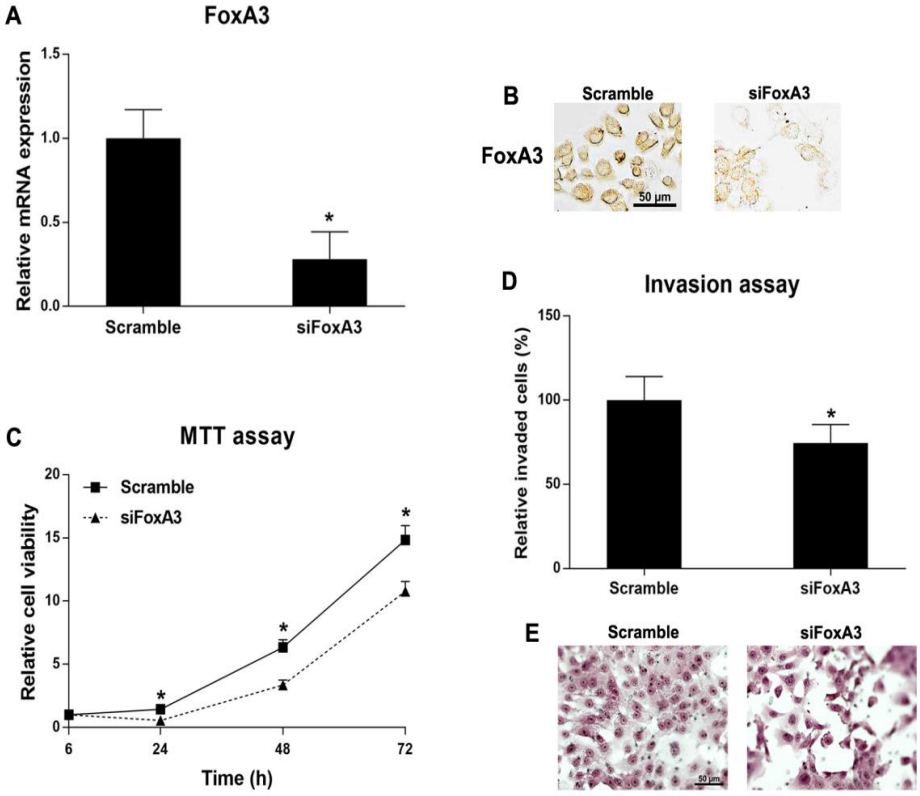

Figure 4-5 Functional analysis of FOXA3-silencing KKU-213 cells and the control cells. (A) mRNA expressions of FOXA3 measured by real time PCR. (B) Protein expressions of FOXA3 detected by immunocytochemistry. (C) Cell proliferation activities measured by MTT assay. (D) Graphical represents invaded cells from cell invasion assy. (E) Hematoxylin-stained invaded cells under light microscope from cell invasion assay. *$P < 0.05$ analyzed by student t test.

Summary

In this study, FOXAs expressions in human CCA tissues were detected using immunohistochemistry (IHC) and the functions of FOXAs in CCA cell lines were studied using specific knockdown and over-expression techniques. FOXA1 and FOXA2 were mainly localized in the nucleus of normal bile ducts (NBD) and some of the cancer cells. Low expression of FOXA1 in the CCA tissues (72%) was significantly correlated with poor prognosis. FOXA3 expression was localized in nucleus and cytoplasm of the cancer cells whereas it was slightly detected in NBD. High expression of FOXA3 in the cancer tissues (61%) was significantly related with high metastasis status. These suggest the different roles of FOXA1 and FOXA3 in CCA. Moreover, the FOXA1 over-expressing CCA cell line significantly reduced cell proliferation and invasion activities compare to the control cells. The FOXA3-knockdown-CCA cell line significantly decreased cell proliferation and invasion activities compare to the control cells. Taken all together, FOXA1 is down-regulated and has tumor suppressive roles in CCA whereas FOXA3 is up-regulated and has oncogenic roles in CCA. The manuscript is now under preparation for submission.

5. Effect of high glucose condition on FOXM1 expression and progression of cholangiocarcinoma cells.

To investigate the effect of high glucose on FOXM1 expression, CCA cells were cultured in normal glucose condition (NG; 5.6 mM) or High glucose media (HG; 25 mM). FOXM1 expression in these CCA cells were investigated using western blotting. The expression of FOXM1 between NG and HG cells of each cell line were compared. As shown in Fig. 5-1A, HG cells of all cell lines had significantly higher expression of FOXM1 than those in NG cells.

Silencing of FOXM1 expression using specific siRNA was performed in two CCA cell lines with high expression levels of FOXM1, KKU-213 and KKU-214. The siRNA specifically to FOXM1 effectively suppressed FOXM1 expression from 24 to 96 h in both HG cells of KKU-213 and KKU-214 (Fig. 5-1B). Suppression of FOXM1 expression (siFOXM1) did not affect rate of cell proliferation (Fig. 5-1C). However, suppression of FOXM1 expression markedly decreased number of migratory cells to 40% of those observed in KKU-213 and 20% of those in KKU-214 (Fig. 5-1D, $P < 0.001$). The same treatment could decrease the number of invaded cells of HG cells to 40% in KKU-213 and 30% in KKU-214 (Fig. 5-1E, $P < 0.001$). In addition, the protein expression levels of Epithelial to Mesenchymal Transition (EMT) proteins: E-cadherin and Claudin-1 for the epithelial markers; vimentin and slug for mesenchymal markers and Matrix metalloproteinase (MMP)-2 and 9 as the invasion markers were assessed in CCA cell lines using western blot analysis. As shown in Fig. 5-1F, slug and MMP-2 were down-regulated in siFOXM1 treated cells compared with the control cells.

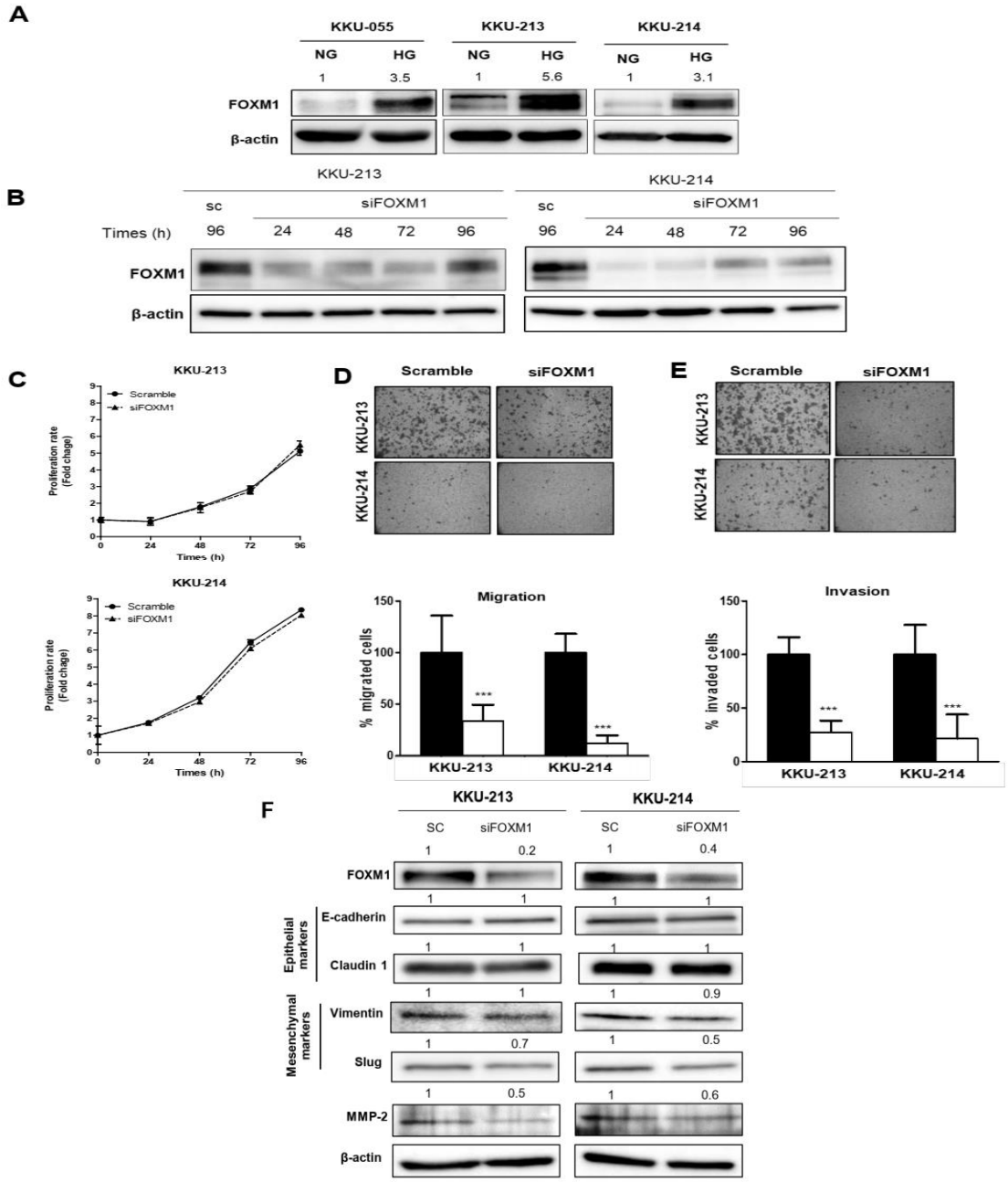

Figure 5-1 High glucose promotes CCA progression via activation of FOXM1 expression. (A) Expressions of FOXM1 protein in CCA cell lines, KKU-055, KKU-213 and KKU-214, in NG and HG cells. (B) Western blots of FOXM1 from siFOXM1 and scramble control (sc) treated cells from 24-96 h. Silencing of FOXM1 expression using siFOXM1 decreased levels of (C) cell proliferation, (D) migration and (E) invasion compared to those of scramble control cells. (F) Western blot analysis of epithelial markers (E-cadherin and Claudin-1), mesenchymal markers (vimentin and slug) and MMP-2 and MMP-9 were determined. Slug and MMP2 were decreased upon suppression of FOXM1 expression.

It is well known that STAT3 pathway is activated in many cancer types including CCA. It is possible that high glucose activates FOXM1 via STAT3 signal pathway. To define the STAT3 pathway that response to high glucose, the activation of STAT3 in HG vs. NG cells were compared using western blot. The activation of STAT3 were increased in HG cells (Fig. 5-2A). These results indicated that high glucose activated the phosphorylation of STAT3. To verify whether the activation of STAT3 affected progressive phenotypes observed under high glucose, Stattic, the specific inhibitor of STAT3 activation was used to diminish the action of STAT3. The HG cells of KKU-213 and KKU-214 were cultured in high glucose media in the presence of 1 μM of Stattic. The action of Stattic on inhibition of nuclear translocation of STAT3 was demonstrated by immunocytofluorescent staining (Fig. 5-2B). The effect of Stattic on CCA proliferation were also determined in KKU-213 and KKU-214 with 1 μM Stattic for 24, 48 and 72 h. The proliferation of CCA cells treated with Stattic was significantly suppressed in KKU-213 and KKU-214 (Fig. 5-2C). The effects of Stattic on migration and invasion ability of CCA cells were tested. The sub-cytoxicity dose (1 μM) of Stattic significantly reduced number of migrated cells of KKU- KKU-213 and KKU-214 to 30% and 60% of the controls (Fig. 5-2D). The same treatment of Stattic could inhibit number of invaded cells of KKU-213 and KKU-214 to 30% and 50% of the untreated cells (Fig. 5-2E).

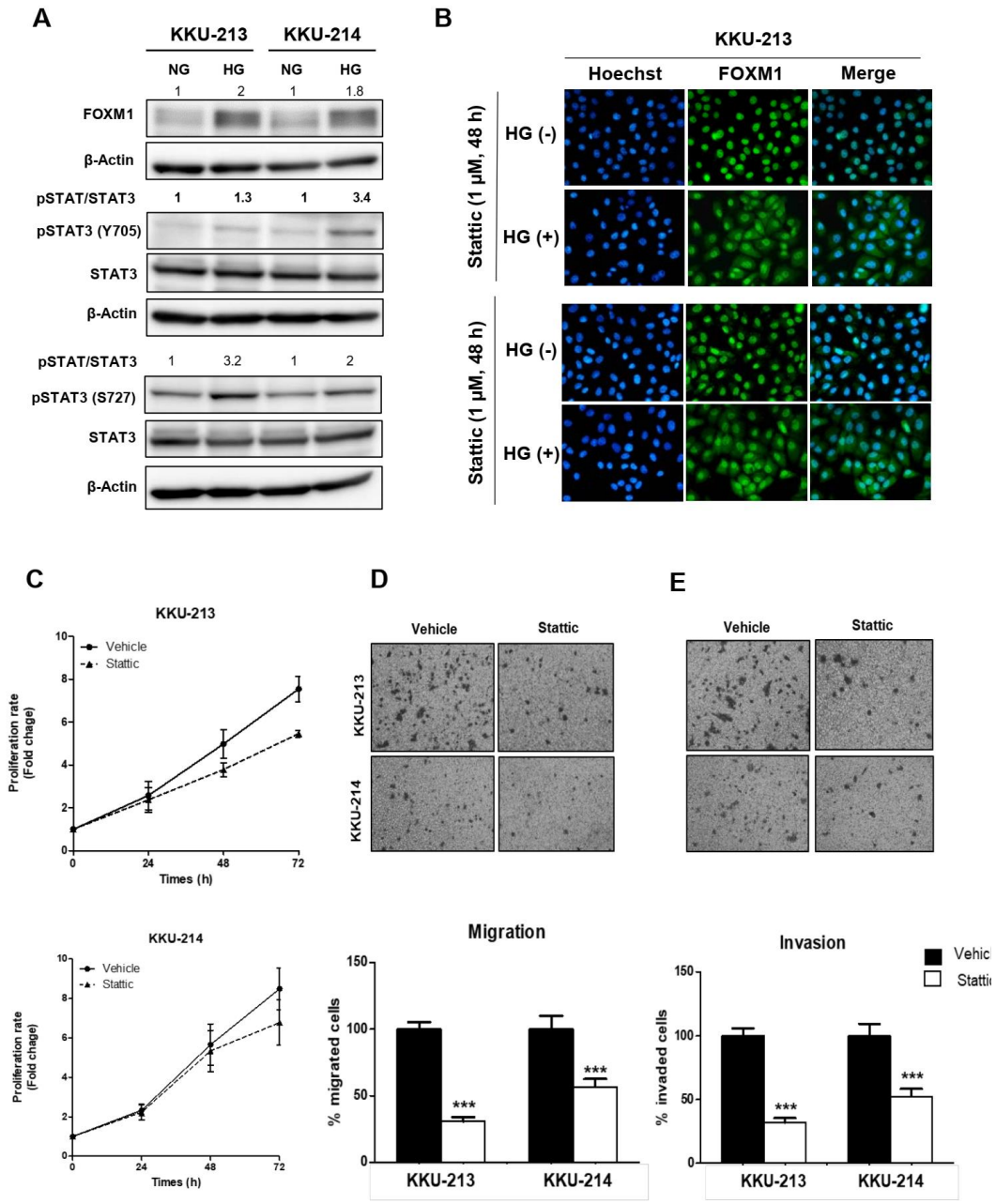

Figure 5-2 High glucose induces CCA progression via STAT3. (A) Phosphorylations of STAT3 (pSTAT3 of Y705 and S727) were verified in NG and HG cells of KKU-213 and KKU-214 using western blot analysis. Using STAT3 inhibitor reduces the enhancing effect of high glucose on CCA cells. The treatment of Stattic (STAT3 inhibitor) (B) inhibited nuclear translocation of STAT3 and p-STAT3 (S727) of HG cells. (C) significantly reduced proliferation, (D) migration and (E) invasion.

To understand the effect of high glucose enhances FOXM1 expression in CCA cells via STAT3, the nuclear translocation of was evaluated in the Stattic-treated KKU-213 and KKU-214 cells using immunocytofluorescent staining. As shown in Fig. 5-3A, the action of Stattic did not affect the nuclear localization of FOXM1 in KKU-213 and KKU-214. However, FOXM1 expression of KKU-213 and KKU-214 treated with Stattic were decreased compared with the control cells. In addition, Stattic treatment also suppressed expression of slug (Fig. 5-3B).

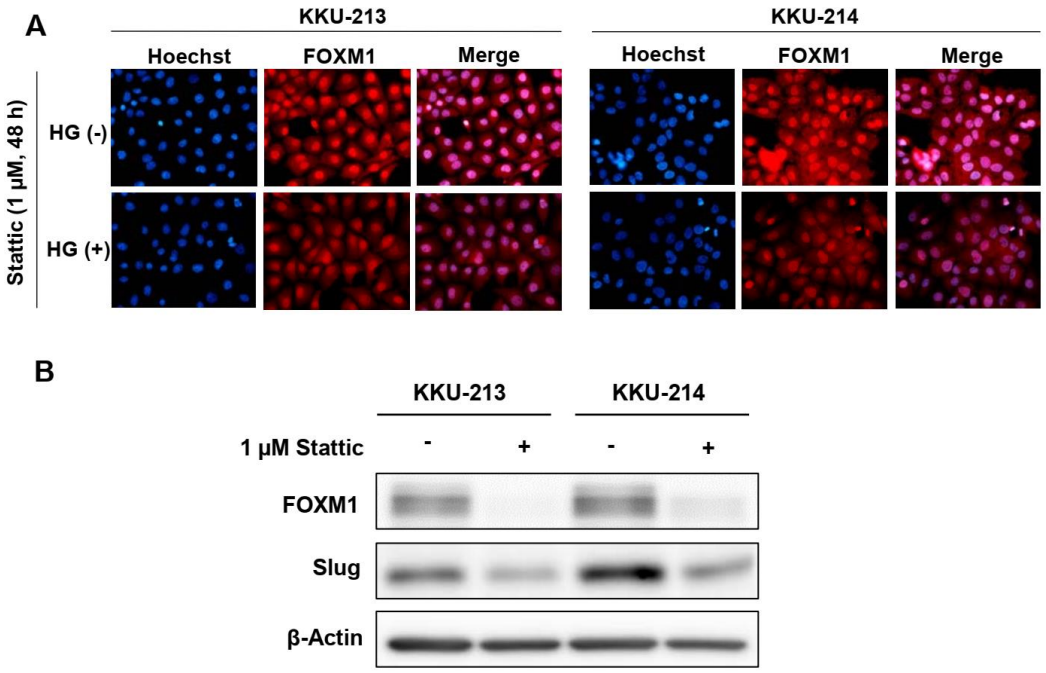

Figure 5-3 Effect of STAT3 inhibition on FOXM1 expression. HG cells of KKU-213 and KKU-214 were treated with 1 μM of Stattic for 48 h. (A) Nuclear localization of FOXM1 was demonstrated using immunocytofluorescent staining. (B) Level of FOXM1 and slug proteins were determined using western blot.

Summary This study revealed the molecular mechanism of FOXM1 associated CCA progression under high glucose condition. It was reported for the first time that high glucose enhanced aggressive phenotypes of CCA cells by upregulating FOXM1 expression and activation of STAT3. This work is now under preparation for submission.

Research Outputs

1. **Publications** (15)

1.1 Original articles (8)

Phoomak, C., A. Silsirivanit, D. Park, K. Sawanyawisuth, K. Vaeteewoottacharn, C. Wongkham, E. W. Lam, C. Pairojkul, C. B. Lebrilla and S. Wongkham (2018). "O-GlcNAcylation mediates metastasis of cholangiocarcinoma through FOXO3 and MAN1A1." Oncogene 37(42): 5648-5665. (IF = 7.519)

Intuyod, K., A. Priprem, C. Pairojkul, C. Hahnvajanawong, K. Vaeteewoottacharn, P. Pinlaor and S. Pinlaor (2018). Anthocyanin complex exerts anti-cholangiocarcinoma activities and improves the efficacy of drug treatment in a gemcitabine-resistant cell line. Int J Oncol. (IF = 3.079)

Intuyod, K., P. Saavedra-Garcia, S. Zona, C. F. Lai, Y. Jiramongkol, K. Vaeteewoottacharn, C. Pairojkul, S. Yao, J. S. Yong, S. Trakansuebkul, S. Waraasawapati, V. Luvira, S. Wongkham, S. Pinlaor and E. W. Lam (2018). "FOXM1 modulates 5-fluorouracil sensitivity in cholangiocarcinoma through thymidylate synthase (TYMS): implications of FOXM1-TYMS axis uncoupling in 5-FU resistance." Cell Death Dis 9(12): 1185.

Sawanyawisuth, K., C. Wongkham, C. Pairojkul and S. Wongkham (2018). “Translational cancer research towards Thailand 4.0.” Science Asia 44S:11-18.

Phoomak, C., D. Park, A. Silsirivanit, K. Sawanyawisuth, K. Vaeteewoottacharn, M. Detarya, C. Wongkham, C. B. Lebrilla and S. Wongkham (2019). "O-GlcNAc-induced nuclear translocation of hnRNP-K is associated with progression and metastasis of cholangiocarcinoma." Mol Oncol 13(2): 338-357.

Saengboonmee, C., K. Sawanyawisuth, Y. Chamgramol and S. Wongkham. (2018). “Prognostic biomarkers for cholangiocarcinoma and their clinical implications.” Expert Rev Anticancer Ther 18(6): 579-592.

Vaeteewoottacharn, K., C. Pairojkul, R. Kariya, K. Muisuk, K. Imtawil, Y. Chamgramol, V. Bhudhisawasdi, N. Khuntikeo, A. Pugkhem, O. T. Saeseow, A. Silsirivanit, C. Wongkham, S. Wongkham and S. Okada (2019). "Establishment of Highly Transplantable Cholangiocarcinoma Cell Lines from a Patient-Derived Xenograft Mouse Model." Cells 8(5).

P Dana, S Saisomboon, R Kariya, S Okada, S Obchoei, K Sawanyawisuth, C Wongkham, C Pairojkul, S Wongkham, K Vaeteewoottacharn. CD147 augmented monocarboxylate

transporters-1/4 expressions through modulation of Akt-FoxO3-NF-**K**B pathway promotes cholangiocarcinoma migration and invasion. Cellular Oncology (2019, IF = 4.761). (Article in press)

1.2 Review (2)

C Saengboonmee, K Sawanyawisuth, Y Chamgramol, S Wongkham, Prognostic biomarkers for cholangiocarcinoma and their clinical implications. Expert Review of Anticancer Therapy. 18(6), 2018. https://doi.org/10.1080/14737140.2018.1467760 (Impact Factor 2.212).

K Sawanyawisuth, C Wongkham, CPairojkul, St Wongkham. Translational Cancer Research Towards Thailand 4.0 Science Asia 44S (2018): 11–18 (SJR = 0.18).

1.3 Manuscripts under revision (1)

B Sripa, W Suebwai, K Vaeteewoottacharn, KSawanyawisuth, A Silsirivanit, W Kaewkong, K Muisuk, P Dana, C Phoomak, W Lert-itthiporn, V Luvira, C Pairojkul, Bin T Teh, S Wongkham, S Okada, Y Chamgramol. Functional and genetic characterization of three cell lines derived from a single tumor of an Opisthorchis viverrini-associated cholangiocarcinoma patient. Human cells (2019, IF = 2.109).

1.4 Manuscripts under preparation (4)

S Thaenkaewa, W Seubwai, C Phoomak, S Intramanee, P Dana, C Pairojkul, S Wongkham. High glucose promotes cholangiocarcinoma progression through STAT3/FOXM1 activations.

R Thanan et al. Role of FOXA1 and FOXA3 in progression of cholangiocarcinoma

N Klinhom-on, W Seubwai, W Lert-itthiporn, S Leung, S Thaenkaewa, S Wongkham. Transcriptomic analysis revealed FOXM1 as a modulator of claudin-1 in progression of cholangiocarcinoma.

Intuyod, K and S. Pinlaor et al. Role of FOXO4 in proliferation and progression of cholangiocarcinoma.

2. Human resource development

2.1 Academic promotion: Four junior researchers including Sakda Waraaswapati, Raynoo Thanan, Vor Luvira and Atit Silsirivanit have been promoted to be the assistant professors.

2.2 One PhD, two MSc students were graduated under the program. Two PhD candidates are going to graduate by the year 2020.

3. Outcomes

3.1 A set of tissue micro array (TMA) of 113 patients with cholangiocarcinoma was established under the project.

3.2 A set of tissue micro array (TMA) of 540 liver tissues from hamsters with cholangiocarcinoma was established under the project.

4. Awards

Awardee	Award titles	Organization
Assoc. Prof. Dr. Chawalit Pairojkul	AACR Team Science Award 2018	American Association for Cancer Research and Lilly Oncology
Prof. Dr. Sopit Wongkham	รางวัลเชิดชูเกียรติผู้อุทิศตนทำงานและเผยแพร่ความรู้ทางพันธุศาสตร์อย่างต่อเนื่อง และทำคุณประโยชน์ต่อประเทศ 2562	สมาคมพันธุศาสตร์ แห่งประเทศไทย
Prof. Dr. Sopit Wongkham	รางวัลอาจารย์ที่ปรึกษาดุษฎีนิพนธ์ระดับ ดีเด่น ปี 2561	Graduate School, Khon Kaen University
Prof. Dr. Somchai Pinlaor	รางวัลนักวิจัยดีเด่น ระดับเพชร 2561	มหาวิทยาลัยขอนแก่น
Prof. Dr. Somchai Pinlaor	รางวัลศิษย์เก่าดีเด่นด้านการวิจัยและเทคโนโลยี ปี 2561	คณะเทคนิคการแพทย์ มหาวิทยาลัยขอนแก่น
Prof. Dr. Somchai Pinlaor	รางวัลอาจารย์ที่ปรึกษาดุษฎีนิพนธ์ระดับ ดีเด่น ปี 2560	Graduate School, Khon Kaen University
Prof. Dr. Somchai Pinlaor	รางวัลอาจารย์ที่ปรึกษาดุษฎีนิพนธ์ระดับ ดี ปี 2559	Graduate School, Khon Kaen University
Asst. Prof. Dr. Wunchana Seubwai	Outstanding young researcher award 2018	Faculty of Medicine, Khon Kaen University
Dr. Kitti Intuyod	Outstanding thesis award 2018	Graduate School, Khon Kaen University

ภาคผนวก
ผลงานตีพิมพ์

Oncogene (2018) 37:5648–5665
https://doi.org/10.1038/s41388-018-0366-1

ARTICLE

O-GlcNAcylation mediates metastasis of cholangiocarcinoma through FOXO3 and MAN1A1

Chatchai Phoomak[1,2] · Atit Silsirivanit[1,2] · Dayoung Park[3,4] · Kanlayanee Sawanyawisuth[1,2] · Kulthida Vaeteewoottacharn[1,2] · Chaisiri Wongkham[1,2] · Eric W.-F. Lam[5] · Chawalit Pairojkul[2,6] · Carlito B. Lebrilla[3] · Sopit Wongkham[1,2]

Received: 17 August 2017 / Revised: 23 May 2018 / Accepted: 25 May 2018 / Published online: 18 June 2018

Abstract

The leading cause of death in cancer patients is metastasis, for which an effective treatment is still necessary. During metastasis, cancer cells aberrantly express several glycans that are correlated with poor patient outcome. This study was aimed toward exploring the effects of O-GlcNAcylation on membranous N-glycans that are associated with the progression of cholangiocarcinoma (CCA). Global O-GlcNAcylation in CCA cells was depleted using specific siRNA against O-GlcNAc transferase (OGT), which transfers GlcNAc to the acceptor proteins. Using an HPLC-Chip/Time-of-Flight (Chip/TOF) MS system, the N-glycans associated with O-GlcNAcylation were identified by comparing the membranous N-glycans of siOGT-treated cells with those of scramble siRNA-treated cells. In parallel, the membranous N-glycans of the parental cells (KKU-213 and KKU-214) were compared with those of the highly metastatic cells (KKU-213L5 and KKU-214L5). Together, these data revealed that high mannose ($Hex_9HexNAc_2$) and biantennary complex ($Hex_5HexNAc_4Fuc_1NeuAc_1$) N-linked glycans correlated positively with metastasis. We subsequently demonstrate that suppression of O-GlcNAcylation decreased the expression of these two N-glycans, suggesting that O-GlcNAcylation mediates their levels in CCA. In addition, the ability of highly metastatic cells to migrate and invade was reduced by the presence of *Pisum Sativum* Agglutinin (PSA), a mannose-specific lectin, further indicating the association of high mannose type N-glycans with CCA metastasis. The molecular mechanism of O-GlcNAc-mediated progression of CCA was shown to proceed via a series of signaling events, involving the activation of Akt/Erk (i), an increase in FOXO3 phosphorylation (ii), which results in the reduction of MAN1A1 expression (iii) and thus the accumulation of $Hex_9HexNAc_2$ N-glycans (iv). This study demonstrates for the first time the association between O-GlcNAcylation, high mannose type N-glycans, and the progression of CCA metastasis, suggesting a novel therapeutic target for treatment of metastatic CCA.

Introduction

Metastasis, a progressive process in which cancer cells develop the ability to colonize distant organs, is responsible for the majority of cancer deaths [1]. The occurrence of metastasis is particularly high for cholangiocarcinoma

Electronic supplementary material The online version of this article (https://doi.org/10.1038/s41388-018-0366-1) contains supplementary material, which is available to authorized users.

✉ Carlito B. Lebrilla
cblebrilla@ucdavis.edu

✉ Sopit Wongkham
sopit@kku.ac.th

[1] Department of Biochemistry, Faculty of Medicine, Khon Kaen University, Khon Kaen 40002, Thailand

[2] Cholangiocarcinoma Research Institute, Khon Kaen University, Khon Kaen 40002, Thailand

[3] Department of Chemistry, University of California, Davis, CA 95616, USA

[4] Department of Surgery, Beth Israel Deaconess Medical Center, Harvard Medical School, Boston, MA 02115, USA

[5] Department of Surgery and Cancer, Imperial Centre for Translational and Experimental Medicine, Imperial College London, London W12 0NN, UK

[6] Department of Pathology, Faculty of Medicine, Khon Kaen University, Khon Kaen 40002, Thailand

(CCA), a cancer of the bile duct. CCA is highly prevalent in southeast Asia and ranks among diseases with the highest mortality rates, following HIV and stroke [2–4]. At present, few effective treatments for advanced CCA outside of surgical resection is available to prolong the survival of the patients.

Modification of proteins via glycosylation is one of the most common post-translational processes that exercises key roles in homeostatic functions, e.g., inflammation, cell–cell interactions, morphogenesis, and immunity. Aberrant glycosylation is commonly found in cancer, some of which associate with metastatic processes [5–7]. The correlation between the membranous glycosylation and the progression of cancer has been collectively reported [8–11]. In CCA, several aberrant glycans and glycoproteins are correlated with CCA progression, such as carbohydrate antigen 19-9, carcinoembryonic antigen, mucin (MUC)1, MUC2, MUC5AC, serum α1β-glycoprotein, and several lectin-binding glycans [12–17].

O-GlcNAcylation is a form of protein modification, where a single moiety of *N*-acetylglucosamine (GlcNAc) is added to the target protein without further elongation or modification into more complex structures [18–20]. Modification with O-GlcNAc is a reversible process, in which GlcNAc is added to or removed from the amino acid Ser/Thr of a protein by O-GlcNAc transferase (OGT), or O-GlcNAcase (OGA), respectively [19]. Alterations of O-GlcNAcylation can dysregulate protein function, disrupting processes such as protein phosphorylation, stability, protein–protein interaction, and protein localization [21]. Accordingly, aberrant O-GlcNAcylation relates to a number of diseases, including cancer [22]. In particular, the increase of O-GlcNAcylation in tumor tissues has been shown to occur with the progression of cancers, including cancers of the breast, colon, liver, lung, pancreas and prostate [23] as well as CCA [24]. In contrast, suppression of OGT in CCA cells could decrease invasion and migratory capabilities [25]. Moreover, we have previously shown that CCA cells with high metastatic abilities have higher O-GlcNAcylation levels than those with low metastasis [26]. Nevertheless, how O-GlcNAcylation modulates progression of CCA metastasis remains unclear.

To our knowledge this study reports for the first time the molecular link between O-GlcNAcylation and membranous high mannose type N-glycans related to cancer progression. Comparing the glycomic data from siOGT treated and control cells with those from high and low metastatic cells, the metastatic-specific membranous N-glycans that were regulated by O-GlcNAcylation were identified. Subsequently, the molecular mechanism of how O-GlcNAcylation regulates the metastasis-related N-glycans were elucidated. These membranous N-glycans could be new prognostic markers or novel therapeutic targets for metastatic CCA.

Results

Expression of specific high mannose type N-glycans may be modulated by O-GlcNAcylation

We first investigated the involvement of O-GlcNAcylation in the membranous N-glycan expression. N-Glycan analysis was performed by graphitized carbon column chip-mounted nano-LC-MS. The N-glycan profiles of siOGT and control scramble siRNA (sc) treated cells were determined and compared. LC-MS analysis yielded nearly 130 N-glycans over a dynamic range of four orders of magnitude. The majority of membranous N-glycan on CCA cells were high mannose type N-glycans (Fig. 1a, b and Table S1). A ratio of N-glycan intensity of siOGT to sc higher than 1.2 was classified as up-regulated and a ratio lower than 0.8 were set as down-regulated. There were 16 N-glycans differentially expressed in KKU-213 and 31 in KKU-214 (Table S1). Among these, only five N-glycans were commonly altered when O-GlcNAcylation was suppressed in both KKU-213 and KKU-214 cells (Fig. 1c). Specifically, $Hex_9HexNAc_2$, $Hex_6HexNAc_2Fuc_1$, and $Hex_5HexNAc_4Fuc_1NeuAc_1$ were down-regulated, whereas $Hex_3HexNAc_5Fuc_1$ and $Hex_3HexNAc_4Fuc_1$ were up-regulated. The synthesis of these five N-glycans may be associated with O-GlcNAcylation in CCA cells.

Expressions of specific high mannose type N-glycans associate with metastatic ability of CCA cells

We next sought to identify the membranous N-glycans that may be correlated with metastasis. The expression profiles of the membranous N-glycans from two pairs of CCA cell lines with different metastatic potentials, the parental (KKU-213 and KKU-214) and the highly metastatic (KKU-213L5 and KKU-214L5) cells, were determined. A total of 136 N-glycans were found in both parental and highly metastatic CCA cells with different expression levels (Fig. 2a, b and Supplementary Table S2). There were 20 N-glycans differentially expressed between KKU-213 and KKU-213L5, and 30 N-glycans between KKU-214 and KKU-214L5 (Supplementary Table S2). Of these, eight differentially expressed N-glycans in both KKU-213L5 and KKU-214L5 were revealed. Six N-glycans were up-regulated ($Hex_5HexNAc_4Fuc_2NeuAc_2$, $Hex_8HexNAc_2$, $Hex_9HexNAc_2$, $Hex_5HexNAc_3Fuc_1$, $Hex_5HexNAc_4Fuc_1NeuAc_1$, and $Hex_7HexNAc_2$) while two were down-regulated ($Hex_5HexNAc_4Fuc_2NeuAc_1$ and $Hex_7HexNAc_6NeuAc_1$) (Fig. 2c). These eight N-glycans may associate with the metastatic abilities of CCA cells.

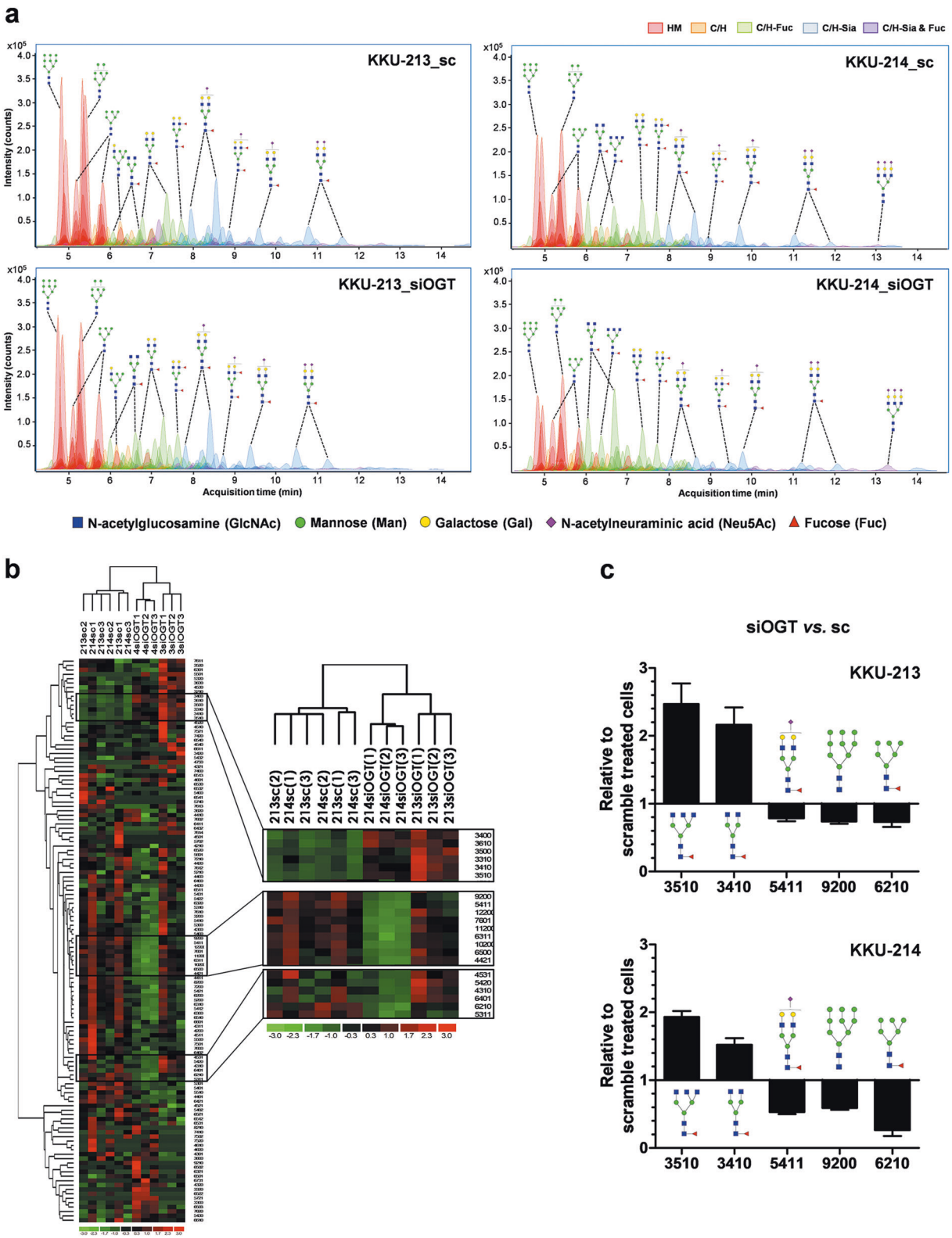

Fig. 1 Suppression of O-GlcNAcylation altered N-glycans expression in CCA cells. **a** Quantitative analysis of membranous N-glycans were determined using the Agilent MassHunter Qualitative analysis software. The colors of each peak represent the type of N-glycans; red for high mannose (HM) glycans; orange for undecorated complex/hybrid (C/H) glycans; green for fucosylated complex/hybrid (C/H−F) glycans; blue for sialylated complex/hybrid (C/H−S) glycans; and purple for fucosylated-sialylated complex/hybrid (C/H-FS) glycans. **b** Heat map represented numbers of differentially expressed N-glycans between scramble and siOGT-treated CCA cells (KKU-213 and KKU-214). Triplicate samples were analyzed. **c** The five N-glycans that were differentially expressed in both cell lines when O-GlcNAcylation was suppressed using siOGT

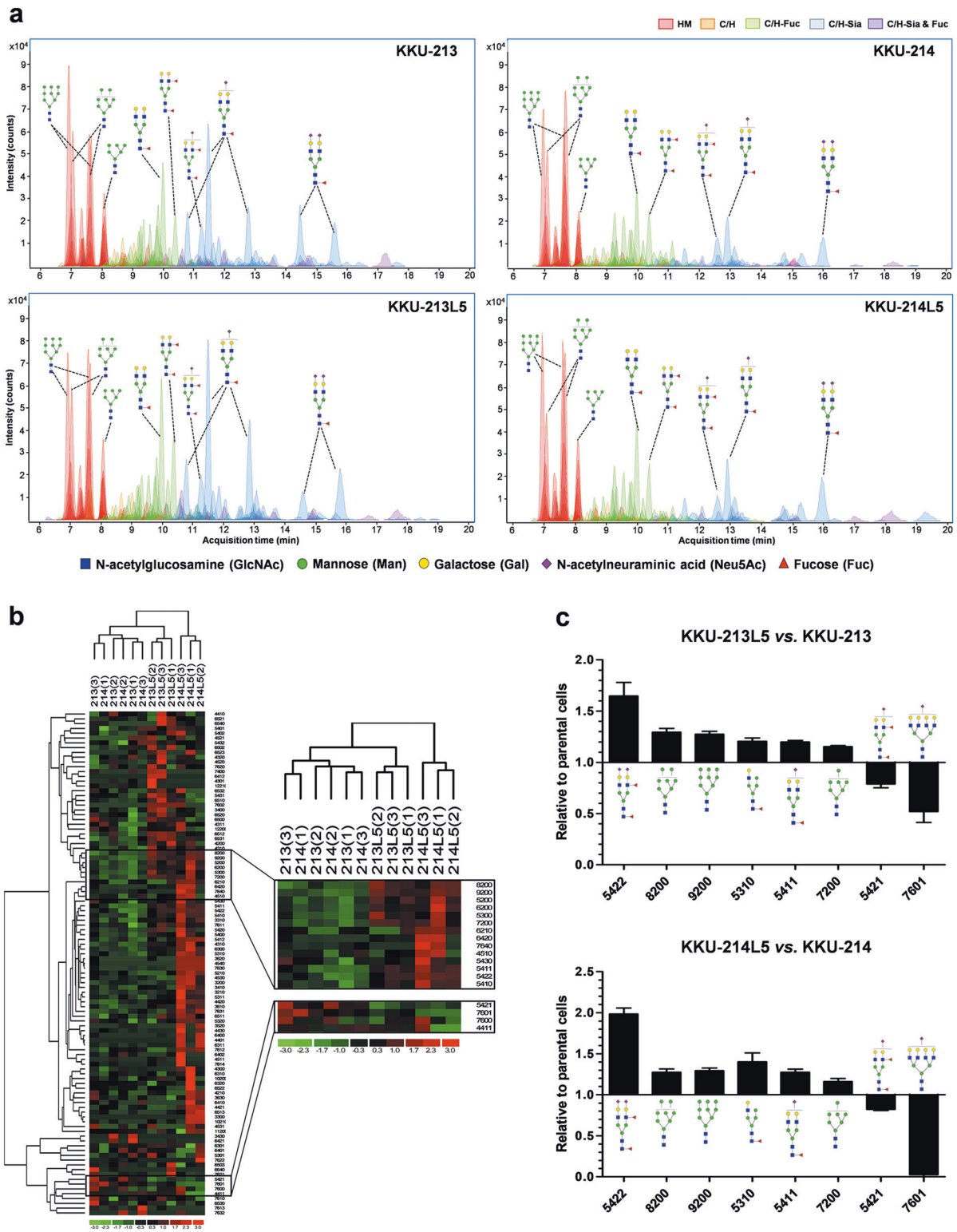

Fig. 2 N-glycan profiles of parental and highly metastatic CCA cells. The membranous N-glycans of parental (KKU-213 and KKU-214) and highly metastatic cells (KKU-213L5 and KKU-214L5) were compared. **a** Chromatograms of N-glycans released from CCA cells. The colors of each peak represent the type of N-glycans: red, high mannose (HM) glycans; orange, undecorated complex/hybrid (C/H) glycans; green, fucosylated complex/hybrid (C/H−F) glycans; blue, sialylated complex/hybrid (C/H−S) glycans; purple, fucosylated-sialylated complex/hybrid (C/H-FS) glycans. **b** Heat map represents the numbers of differentially expressed N-glycans between parental and highly metastatic CCA cells. Triplicate samples were analyzed. **c** Given the expression of parental cells (KKU-213 and KKU-214) as 1, eight N-glycans were differentially expressed in both highly metastatic CCA cells

Two membranous N-glycans are associated with metastatic activities and O-GlcNAcylation

To determine the N-glycans that may be involved in metastasis under the modulation of O-GlcNAcylation, the membranous N-glycans associated with O-GlcNAcylation (Fig. 1c) and those associated with metastatic potential (Fig. 2c) were aligned. As shown in Fig. 3a, $Hex_9HexNAc_2$ and $Hex_5HexNAc_4Fuc_1NeuAc_1$, two N-glycans were commonly found in both data sets. To confirm the structures of the predicted N-glycans, the structures of $Hex_9HexNAc_2$ and $Hex_5HexNAc_4Fuc_1NeuAc_1$ were analyzed using graphitized carbon column chip-mounted nano-LC-MS/MS. The predicted N-glycans were confirmed by MS/MS, as precursor *m/z* 942.33 for $Hex_9HexNAc_2$, a high mannose type N-glycan (Fig. 3b, upper panel) and precursor *m/z* 693.59 for $Hex_5HexNAc_4Fuc_1NeuAc_1$, a biantennary complex type N-glycan (Fig. 3b, lower panel).

Suppression of O-GlcNAcylation reduces expression of membranous high mannose type N-glycans

The high mannose type N-glycan, $Hex_9HexNAc_2$, was the highest abundant in CCA cells (Figs 1a and 2a) and therefore was selected for further study. To confirm the connection between the expression of the high mannose type N-glycans at the cell surface and intracellular O-GlcNAcylation, the expression of high mannose type N-glycans in the siOGT-treated *vs*. scramble siRNA-treated cells were determined. Both *Pisum Sativum* Agglutinin (PSA) and Concanavalin A (Con A) have been used to detect high mannose type N-glycan in several studies [27–30]. Our preliminary study using lectin-histochemistry of PSA and Con A in tumor tissues from CCA patients revealed that PSA but not Con A could differentiate non-metastatic from. metastatic CCA tissues (Supplementary Figure S1). The PSA signal was strongly positive in CCA tissues with metastasis, weaker in non-metastatic tissue, and negative with hepatocytes. Con A, in contrast, reacted strongly with both metastatic and non-metastatic CCA, as well as hepatocytes. On the basis of these observations, we selected to use PSA to detect high mannose type N-glycans in the subsequent study.

High mannose type N-glycans expressed at the cell surface were quantified using cytofluorescent staining of PSA, a mannose binding lectin. The specificity of PSA to mannosylate N-glycan was first determined using a sugar inhibition test. As shown in Fig. 3c, the PSA-cytofluorescent staining was localized at cell membranes. Adding 0.3 M D-mannose to neutralize the binding ability of PSA significantly diminish the staining signal of PSA. PSA-cytofluorescent staining was next performed and compared between the siOGT-treated cells and the scramble siRNA-treated cells. The PSA-cytofluorescent staining signals were reduced in siOGT-treated cells compared with those of scramble control cells (Fig. 3d). Similar patterns were observed for both parental and highly metastatic CCA cells. Quantitative analysis of the cytofluorescent signals are presented in Fig. 3e. The PSA-binding signals were significantly decreased in siOGT-treated cells ($P < 0.05$) and the reduction was more pronounced in the highly metastatic cells compared to the parental cells. These data connect the intracelluar O-GlcNAcylation to the expression of cell surface high mannose type N-glycans. In addition, higher basal PSA-binding signals of the highly metastatic cells compared to the parental cells were also observed in both cell lines (Fig. 3d, e) ($P < 0.05$). This may indicate the involvement of high mannose type N-glycans in the metastatic phenotype of CCA cells.

Cell surface high mannose type N-glycans promote progression of CCA metastasis

To demonstrate the association of cell surface high mannose type N-glycans with CCA progression, the surface high mannose type N-glycans were masked with PSA prior to metastatic activity assays. To prevent the possible cell aggregation caused by lectin binding, the appropriate concentration of PSA was first optimized. CCA cells were treated with 0–100 µg/ml of PSA for 1 h and the aggregated cells were determined under a microscope. No aggregated cells were observed at PSA 6.25–12.5 µg/ml (Supplementary Figure S2), therefore, PSA at 5 and 10 µg/ml were used to neutralize high mannose glycans at the cell surface. As shown in Fig. 4a, PSA treatment had no effect on growth of CCA cells either in the presence of 2% or 5% fetal bovine serum (FBS). The highly metastatic cells exhibited higher migration capability than the parental cells as shown in the wound scratch and migration assays (Fig. 4b, c). CCA cells treated with 10 µg/ml of PSA did decrease the cell migration abilities of both parental and highly metastatic cells, but to a lesser extent in the parental cells. In the wound scratch assay, PSA treatment extended the time of wound closing of highly metastatic cells from 12 h to more than 24 h (Fig. 4b). Moreover, treated cells with PSA significantly decreased the migratory abilities of the parental cells to 40% and those of highly metastatic cells to 20% relatively to the control cells ($P < 0.001$) (Fig. 4c). Similar effects were observed in the invasion assay. PSA treatment markedly decreased the number of invaded cells by 42–43% for parental cells ($P < 0.05$; $P < 0.01$) and 25–30% for highly metastatic cells ($P < 0.01$; $P < 0.001$) in both cell lines (Fig. 4d). These data highlight the significance of the surface high mannose type N-glycans in promoting the progression of CCA metastasis.

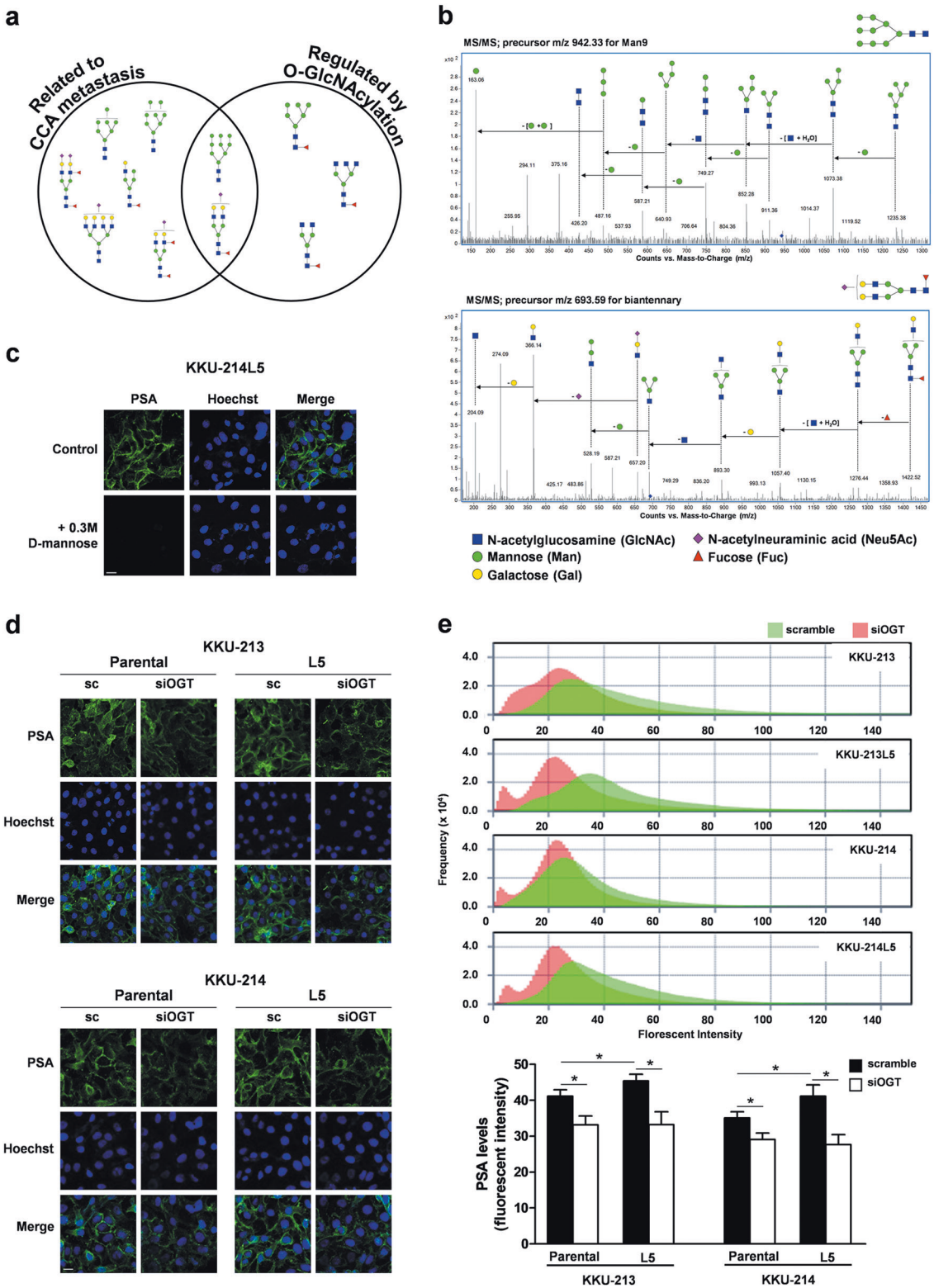

Fig. 3 The expression levels of membranous N-glycans were modulated by O-GlcNAcylation. **a** Expression of high mannose type N-glycan, $Hex_9HexNAc_2$ and biantennary complex type N-glycan, $Hex_5HexNAc_4Fuc_1NeuAc_1$, were found to be associated with metastatic ability and O-GlcNAcylation. **b** The MS/MS spectra confirmed glycan structures of both N-glycans; high mannose type (*m/z* 942.33) and for biantennary complex type (*m/z* 693.59). **c** PSA-cytofluorescence stained high mannose glycans at the cell membrane. The specificity of PSA to mannosylated glycan was proved by sugar inhibition test. **d** PSA-cytofluorescent staining was reduced in siOGT-treated cells. **e** Histograms and graphs represent the quantitative levels of PSA-fluorescent signals. The results are mean ± SEM of one representative from two independent experiments; $*P < 0.05$, student's *t* test

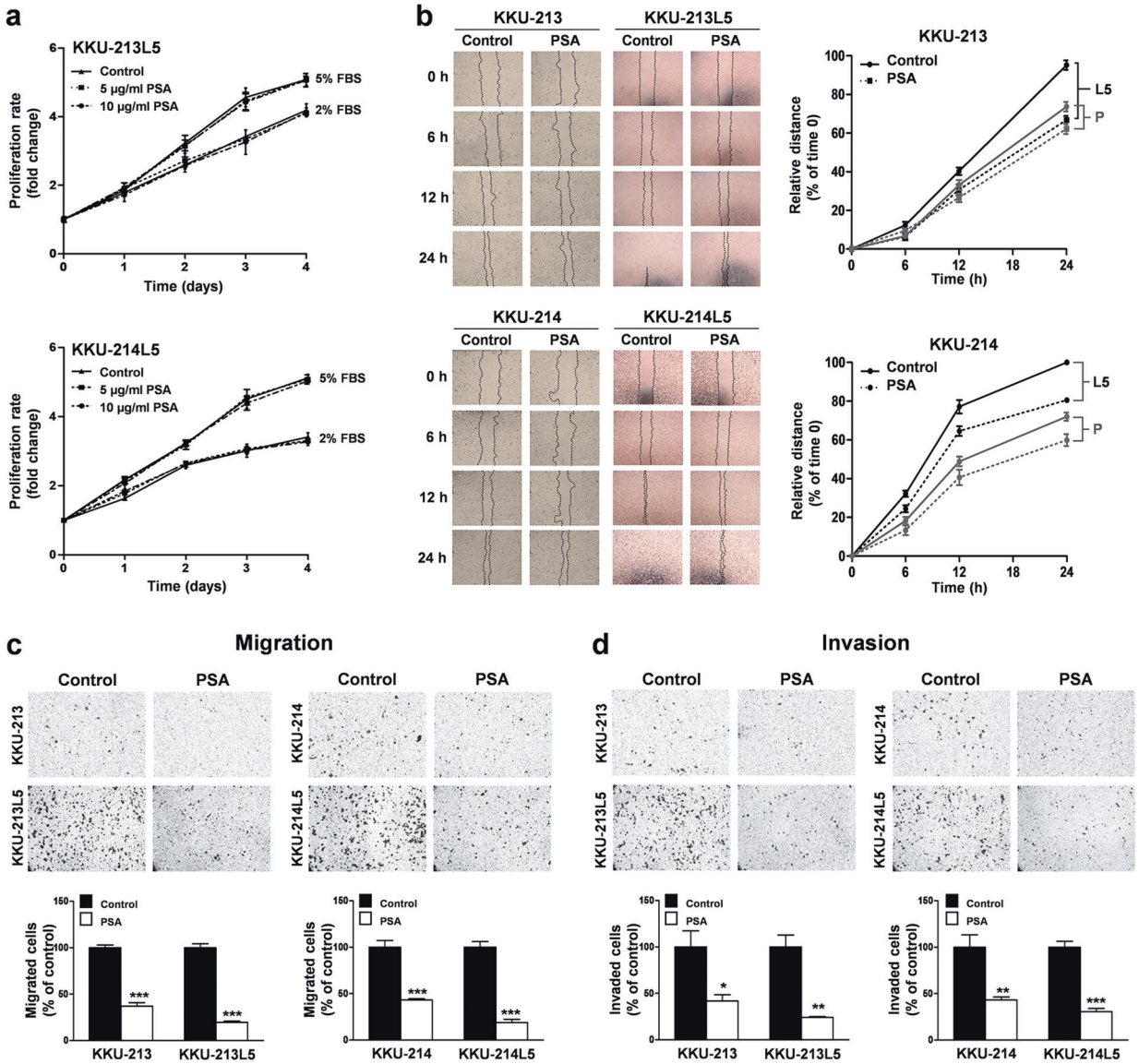

Fig. 4 PSA treatment reduced migration and invasion abilities of CCA cells. Treatment of PSA in the parental cells, KKU-213 and KKU-214, and highly metastatic CCA cells, KKU-213L5 and KKU-214L5, for 24 h had no effect on (**a**) cell proliferation, but significantly affected (**b**, **c**) cell migration and (**d**) invasion. The numbers of migrated and invaded cells were compared with the non-treated control cells given as 100%. The results are mean ± SEM of two independent experiments; $*P < 0.05$, $**P < 0.01$, $***P < 0.001$, student's *t* test

O-GlcNAcylation upregulates high mannose type N-glycans via decreasing MAN1A1 and FOXO3 expression

The molecular mechanisms by which O-GlcNAcylation controlled the expression level of high mannose type N-glycans were further explored. The biosynthesis of all N-glycans starts in the endoplasmic reticulum (ER), and the elongation process for the peripheral glycan moieties occurs in the Golgi apparatus [18, 31]. The core N-glycan structure is mannosylated in the ER to yield $Hex_9HexNAc_2$, trimmed back by α1,2-mannosidases, e.g., α1,2-mannosidase IA (MAN1A1) in the Golgi apparatus to form $Hex_5HexNAc_2$, and further elongated to hybrid and complex types (Fig. 5a). Therefore, the accumulation of $Hex_9HexNAc_2$ is likely due to the decrease in expression of MAN1A1. We first tested whether MAN1A1 expression was modulated via O-GlcNAcylation. The expression of MAN1A1 was determined in the parental and highly metastatic CCA cells treated with siOGT. As shown in Fig. 5b, siOGT significantly reduced the level of O-GlcNAcylation as determined by the levels of O-GlcNAcylated proteins (OGP). Compared to untreated cells, siOGT treatment dramatically reduced O-GlcNAcylation of the parental cells 0.20-fold and of the highly metastatic cells 0.25 fold. Suppression of O-

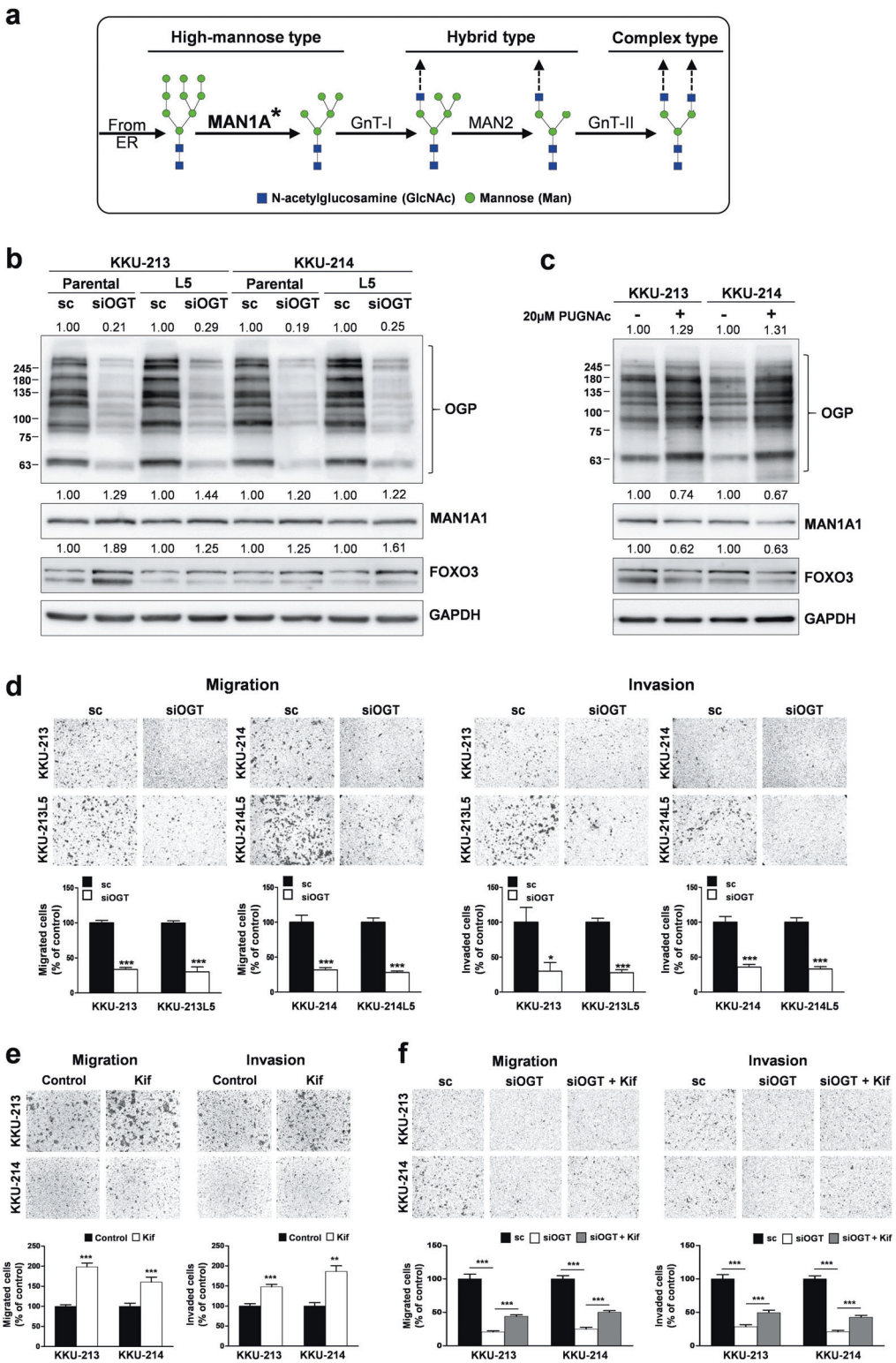

GlcNAcylation indeed increased expression of MAN1A1 in all siOGT-treated cells. In contrast, inhibition of OGA by PUGNAc, elevated O-GlcNAcylation and decreased MAN1A1 expression compared with those of control cells (Fig. 5c). The data supports the link between O-GlcNAcylation levels and MAN1A1 expression.

As FOXO3, a member of Forkhead box (FOX) transcriptional factors, has been suggested to regulate MAN1A1

◀ **Fig. 5** O-GlcNAcylation regulated migration and invasion abilities of CCA cells via FOXO3 and MAN1A1 expression. **a** N-linked glycan synthesis pathway in Golgi apparatus. **b** siOGT effectively suppressed O-GlcNAcylation in parental (KKU-213 and KKU-214) and highly metastatic (KKU-213L5 and KKU-214L5) CCA cells as the levels of O-GlcNAcylated proteins (OGP) were reduced. The siOGT treatment suppressed expression of MAN1A1 and FOXO3. **c** PUGNAc treatment could increase OGP and reduce the expression of MAN1A1 and FOXO3 in the parental cells. GAPDH was used as the loading control, data represent one of two independent experiments. **d** Suppression of O-GlcNAcylation by siOGT reduced migration and invasion abilities of parental and highly metastatic CCA cells. **e** Inhibition of MAN1A1 activity using kifunensine (Kif) enhanced migration and invasion abilities of CCA cells. **f** The inhibition effect of siOGT on CCA migration/invasion could be reversed by Kif treatment. The results are mean ± SEM of one representation from two independent experiments; $*P < 0.05$, $**P < 0.01$, $***P < 0.001$, student's t test

expression (http://www.sabiosciences.com/chipqpcrsearch.php), we next tested whether FOXO3 expression was also modulated by O-GlcNAcylation. Similar to MAN1A1, the expression of FOXO3 increased in all siOGT-treated cells and decreased in PUGNAc treated cells (Fig. 5b, c). The data imply that O-GlcNAcylation affects MAN1A1 expression by modulating FOXO3 expression.

To reveal whether O-GlcNAcylation affects CCA metastasis, the progression of the parental and highly metastatic CCA cells were compared in siOGT and scramble siRNA-treated cells. siOGT treatment suppressed O-GlcNAcylation and reduced the migration and invasion abilities of both parental and highly metastatic CCA cells ($P < 0.001$) (Fig. 5d). To demonstrate whether MAN1A1 affects migration and invasion of CCA cells, MAN1A1 activity was inhibited using kifunensine, a specific inhibitor of mannosidase 1. As demonstrated in Fig. 5e, the migration/invasion abilities of kifunensine treated cells were significantly increased relatively to those of the control cells. Moreover, the inhibition effect of OGT silencing on the reduction of migration and invasion could be rescued by kifunensine treatment ~2 fold compared to siOGT-treated cells (Fig. 5f). These data support the connection of O-GlcNAc modifcation and MAN1A1 with the migration and invasion capabilities of CCA cells.

O-GlcNAcylation regulates MAN1A1 expression via activating Akt/Erk signaling and modulating FOXO3 stability

We further elucidated how O-GlcNAcylation regulates expression of MAN1A1 via FOXO3. The activations of Akt, Erk, and Ikk, which are modulated by O-GlcNAc modification and are the major kinases that regulate the expression of FOXO3 [32], were proposed to be the connection between O-GlcNAcylation and FOXO3. The phosphorylations of Akt, Erk, and Ikk were hence determined in the siOGT-treated cells. As shown in Fig. 6a, the levels of pAkt/Akt and pErk/Erk, but not pIkk/Ikk, were markedly decreased in the OGT knocked down cells. All the data at this stage indicated that suppression of O-GlcNAcylation inhibits the activation of Akt and Erk, which subsequently upregulates FOXO3 activity and MAN1A1.

We next explored whether activation of Akt and Erk directly modulates FOXO3 expression. An allosteric inhibitor of Akt, MK-2206, was used to inhibit Akt activity in the high metastatic CCA cells. In the presence of MK-2206, phosphorylation of Akt was reduced in a dose dependent manner. As a result, phosphorylation of FOXO3 at Thr-32 was suppressed, whereas expression of total FOXO3 and MAN1A1 were dependently increased with increasing doses of MK-2206 (Fig. 6b). Similar observations were obtained when PD98059 (2′-amino-3′-methoxyflavone), a selective MEK inhibitor, was used to inhibit Erk activation. Phosphorylation of Erk was reduced by PD98059 treatment in a dose dependent fashion. The treatment also decreased phosphorylation of FOXO3 at Ser-294 and increased expression of FOXO3 and MAN1A1 (Fig. 6c). The inactivation of Akt and Erk signaling pathways had no effect on the status of O-GlcNAcylation in CCA cells (Figure S3). These results demonstrate the direct effects of Akt and Erk activation on FOXO3 and MAN1A1 expression.

As Akt phosphorylation of FOXO3 has been shown to increase the degradation of FOXO3, we next explored whether Akt affects FOXO3 stability in CCA cells. The stability of FOXO3 was determined following cyclohexamide (CHX) treatment. As shown in Fig. 6d, the stability of FOXO3 was prolonged by MK-2206 treatment, with a half-life of ~5 h for MK-2206 treated cells and ~1.5 h for the control cells. Together, Akt/Erk inhibitors inactivated Akt/Erk phosphorylation, resulting in the reduction of FOXO3 phosphorylation, which in turn increased the stability of FOXO3 and expression of MAN1A1.

To demonstrate the link between Akt activation and the function of MAN1A1 on CCA progression, we first investigated the migration and invasion of CCA cells in the presence of an Akt inhibitor, MK-2206. As shown in Fig. 6e, MK-2206 treatment markedly decreased the migration of CCA to 40% and 60% in KKU-213L5 and KKU-214L5, respectively. Moreover, these effects could be reversed by inhibiting MAN1A1 activity using kifunensine. Treatment of cells with MK-2206 and kifunensine significantly increased the motility 1.4–2 folds higher than those of MK-2206 treated cells ($P < 0.001$). Similar results were observed for their invasion abilities (Fig. 6f). Collectively, our data show that O-GlcNAcylation promotes progression of CCA metastasis via activation of Akt, which consequently represses FOXO3 and MAN1A1 expression.

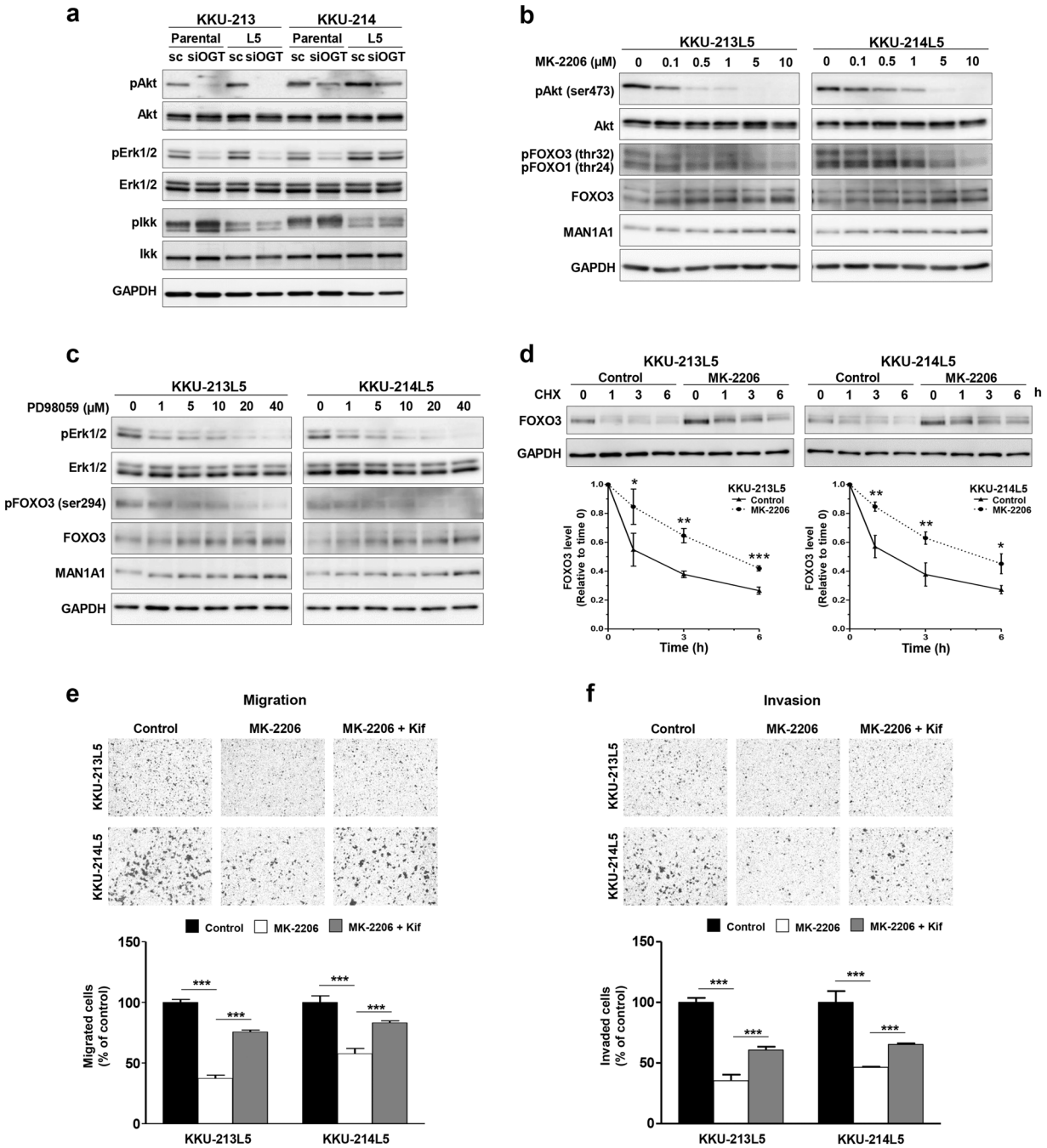

Fig. 6 O-GlcNAcylation regulated activations of Akt and Erk and expression of FOXO3 and MAN1A1. OGT was suppressed in parental (KKU-213 and KKU-214) and highly metastatic (KKU-213L5 and KKU-214L5) CCA cells using siOGT. **a** siOGT treatment inactivated the phosphorylation of Akt and Erk but not Ikk. **b** The modulations of Akt and Erk on FOXO3 expression were revealed using Akt and Erk inhibitors. CCA cells were treated with various concentrations of Akt inhibitor, MK-2206 and (**c**) Erk inhibitor, PD98059, for 24 h. The expression of pAkt/Akt, pErk/Erk, phospho-FOXO3, FOXO3 and MAN1A1 were determined using western blotting. **d** The MK-2206-treated L5 CCA cells were incubated with 20 μM of cycloheximide (CHX) for 1, 3, and 6 h. FOXO3 levels at each time point were determined using western blotting and compared with those of the untreated control cells. The data are represented as the mean ± SD from three independent experiments. Inhibition of Akt activation significantly reduced (**e**) migration and (**f**) invasion abilities of CCA cells and these effects could be rescued by kifunensine (Kif) treatment. The results are mean ± SEM of one representative from two independent experiments. $^{*}P < 0.05$; $^{**}P < 0.01$; $^{***}P < 0.001$, student's *t* test

FOXO3 positively regulates MAN1A1 expression in CCA cells

As the level of MAN1A1 expression corresponded well with FOXO3 expression, we further questioned whether FOXO3 is a direct modulator of MAN1A1 expression. We first verified the association of FOXO3 and MAN1A1 by determination of MAN1A1 expression in siFOXO3 treated cells. siFOXO3 treatment effectively suppressed FOXO3 and MAN1A1 expression in both parental and highly metastatic CCA cells (Fig. 7a). Suppression of FOXO3 expression could also significantly suppress expression levels of MAN1A1 mRNA and protein ($P < 0.001$, Fig. 7b).

To prove the direct regulation of FOXO3 on MAN1A1 expression, chromatin immunoprecipitation (ChIP) assay was performed. The primer sequences were designed to cover the binding region of FOXO3 on *MAN1A1* gene as revealed by EpiTect ChIP qPCR Primers (Fig. 7c). ChIP assay was conducted in the parental cells, in the presence and absence of siFOXO3 and MK-2206. The positive binding of FOXO3 on *MAN1A1* gene was detected, as shown in Fig. 7d and Aupplementary Figure S4. Moreover, suppression of FOXO3 by siFOXO3 reduced the FOXO3-binding level, whereas increase of FOXO3 by inhibiting Akt activity using MK-2206 significantly enhanced the FOXO3 binding on the endogenous *MAN1A1* gene in both KKU-213 and KKU-214 cell lines. Taken together, this information suggests for the first time that FOXO3 is a positive direct regulator of MAN1A1.

Association of O-GlcNAcylation, high-mannose type N-glycans and MAN1A1 observed in the in vitro studies were confirmed in patients' tissues

Upon demonstrating the correlation of OGP, OGT, MAN1A1 and PSA with cell migration/invasion of CCA cell lines (Figs 3–5), we next explored whether the same could be observed in CCA tissues of patients. Immunohistochemistry of OGP, OGT, MAN1A1 and PSA-histochemistry were performed in five each of non-metastasis and metastasis CCA cases. As shown in Fig. 8a, b, the expression of OGP, OGT and PSA were elevated in CCA tissues with metastasis compared to those with non-metastatic CCA. In contrast, MAN1A1 expression in CCA tissues with metastasis was lower than that in non-metastatic CCA. The correlation of OGP, OGT, MAN1A1 and PSA levels in CCA tissues were determined using Spearman rank correlation coefficient. As shown in Fig. 8c, OGP had a positive correlation with expression of OGT and PSA but had a negative correlation with expression of MAN1A1. In addition, OGT expression was correlated with OGP levels while PSA signal was negatively correlated with MAN1A1 expression. These in vivo data confirmed the associations of

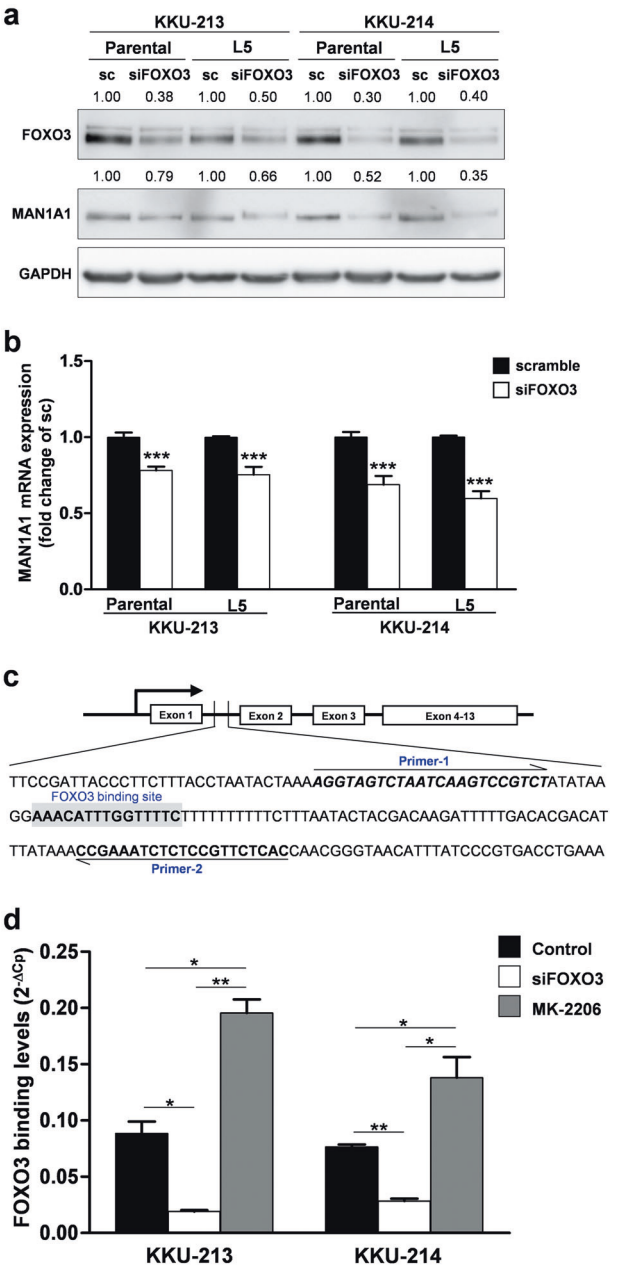

Fig. 7 FOXO3 is a positive regulator of MAN1A1. CCA cells were treated with siFOXO3 for 48 h. The expression of FOXO3 and MAN1A1 were determined using western blots and real-time PCR. Compared with scramble (sc) treated cells, suppression of FOXO3 using siFOXO3 decreased expression of FOXO3 and expression levels of (**a**) MAN1A1 protein and (**b**) MAN1A1 mRNA. GAPDH was used as the loading control. **c** Schematic illustrations of the locations of primers and FOXO3-binding region on the *MAN1A1* gene used in the ChIP assays. **d** Chromatin immunoprecipitation (ChIP) assay was used to determine the direct binding of FOXO3 on *MAN1A1* gene. To confirm the binding activity of FOXO3 on *MAN1A1* gene, ChIP assays of cells treated with siFOXO3 and MK-2206 for 24 h were performed and compared to those of control cells. The results are one representation from two independent experiments. $*P < 0.05$, $**P < 0.01$, $***P < 0.001$, student's t test

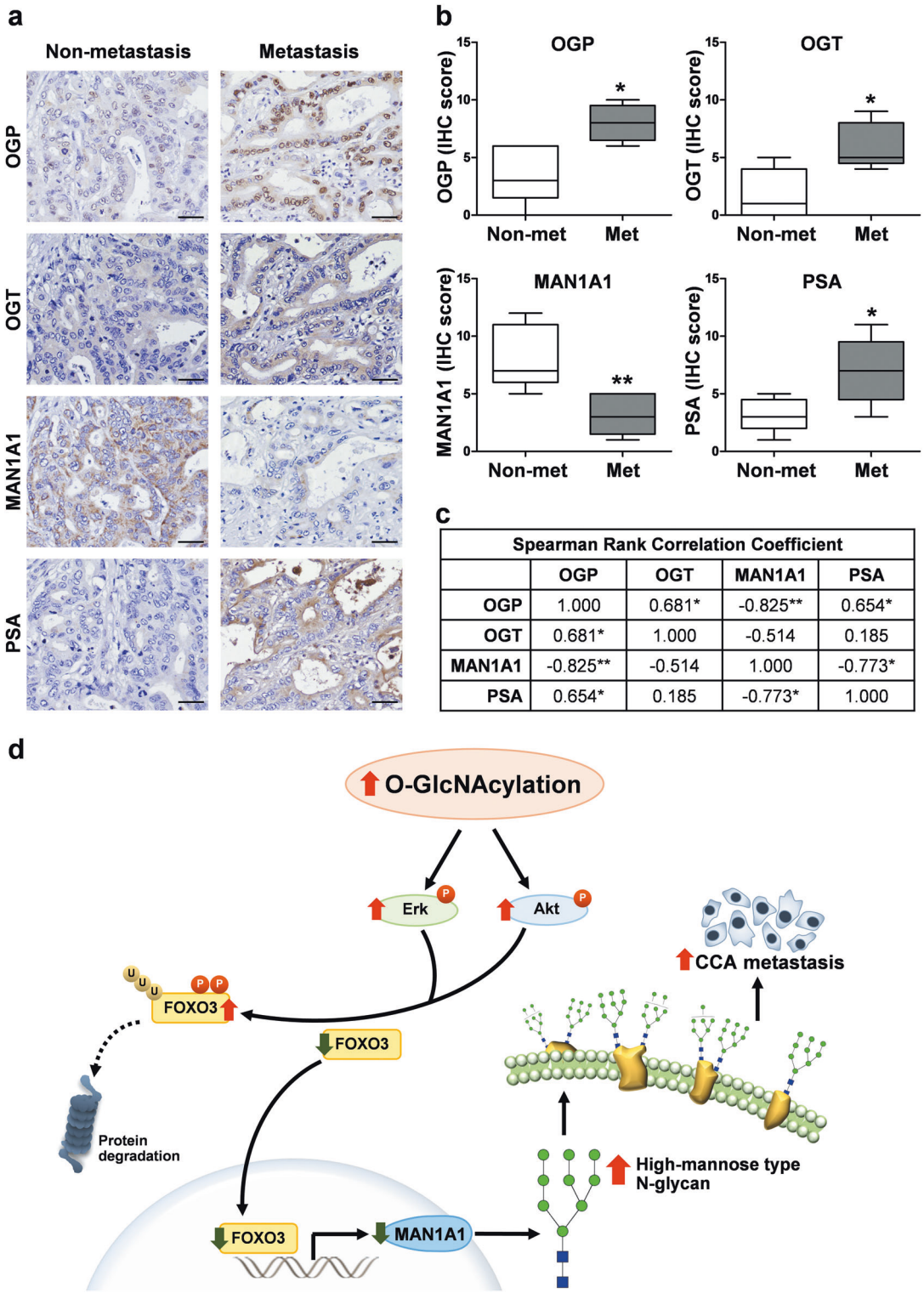

Spearman Rank Correlation Coefficient				
	OGP	OGT	MAN1A1	PSA
OGP	1.000	0.681*	-0.825**	0.654*
OGT	0.681*	1.000	-0.514	0.185
MAN1A1	-0.825**	-0.514	1.000	-0.773*
PSA	0.654*	0.185	-0.773*	1.000

Fig. 8 CCA tissues with metastasis exhibit high expression of OGP, OGT, and strong PSA binding, with low MAN1A1. **a** The expression of OGP, OGT, MAN1A1 and PSA were determined using IHC staining non-metastatic ($n = 5$) and metastatic ($n = 5$) CCA tissues. Bars indicate 20 μm. **b** Mean expression of OGP, OGT and PSA in metastatic CCA (Met) are significantly higher than that in non-metastatic CCA (Non-met). The opposite was observed for MAN1A1 expression (*$P < 0.05$, **$P < 0.01$; Mann–Whitney test). **c** The correlations between OGP, OGT, MAN1A1 and PSA levels were shown by Spearman's rank correlation test (*$P < 0.05$, **$P < 0.01$). **d** Schematic diagram demonstrates the mechanism of O-GlcNAcylation augmenting metastasis of CCA cells via increasing high mannose type N-glycans. Elevation of O-GlcNAcylation activates Akt and Erk activities, which further induces phosphorylation of FOXO3. The phosphorylation of FOXO3 by Akt or Erk leads to proteolytic degradation of FOXO3. The decrease of FOXO3 may cause the reduction of MAN1A1 expression, leading to the elevation of high mannose type N-glycans on the cell surface. The increase of the high mannose type N-glycan, Man 9, can promote CCA metastasis

O-GlcNAcylation, high-mannose type N-glycan and MAN1A1 observed in the in vitro studies.

Discussion

The glycan moieties of glycoproteins and glycolipids on cell membrane play several important biological roles. Incomplete synthesis and neo-synthesis of glycans are commonly found in cancer cells [33]. The regulation of glycan synthesis, however, is not well understood. The rationale of this study for the contribution of O-GlcNAcylation on regulation of N-glycans was initiated from several observations. First, elevation of O-GlcNAcylation enhances CCA progression [25, 26]. Second, increase of several membranous N-glycans are related to progression of cancer [34–36]. Finally, O-GlcNAcylation can regulate many transcriptional factors that modulate the expression of several proteins including enzymes. These lines of evidence led us to hypothesize that O-GlcNAcylation may enhance progression of CCA by modulation of membranous N-glycans via glycan synthesizing enzymes.

Our study is the first report to demonstrate that O-GlcNAcylation, an intracellular glycosylation, can modulate the expression of a cell surface high mannose type N-glycan, $Hex_9HexNAc_2$, and consequently promote progression of CCA cells. The molecular link between O-GlcNAcylation and high mannose type N-glycans via activation of Akt/Erk, and expression of FOXO3 and MAN1A1 was elucidated. Moreover, the direct regulation of MAN1A1 expression by FOXO3 was first evidenced in this study.

Overexpression of OGT in tumor tissues and the association between high O-GlcNAcylation and poor patients' outcome have been previously reported in CCA [24]. The in vitro study indicated that the abilities of CCA cells to migrate and invade could be monitored by modulating O-GlcNAcylation levels [25]. In addition, higher level of O-GlcNAc modification in highly metastatic CCA cells than the parental cells were hitherto observed [26]. In the present study, we further demonstrate the molecular pathway by which O-GlcNAcylation modulates progression of CCA. As the glycan moieties of membrane proteins have a significant function in adhesion of cell–cell/cell–matrix, cell invasion and migration, we postulated that O-GlcNAcylation modulates specific glycan moieties of membrane proteins. Comparing the glycomic data of membranous N-glycans between low and highly metastatic CCA cells and between siOGT treated and scramble control cells suggested a membranous high mannose type N-glycan, $Hex_9HexNAc_2$, and a biantennary complex type N-glycan, $Hex_5HexNAc_4Fuc_1NeuAc_1$, to be associated with metastatic activity and be mediated by O-GlcNAcylation. Up to our search, this study is the primary report of the link between O-GlcNAcylation and the expression of high mannose type N-glycans.

Normally, mammalian cells scarcely express cell surface high mannose type N-glycans [37], with the exemption of stem cells and macrophages [38]. In the current study, these N-glycans were the highest abundant N-glycans found on the membranous glycoproteins of CCA cells, indicating dynamic changes of glycosylation in CCA progression. In the current study, the significant increase of $Hex_9HexNAc_2$ level in the highly metastatic cells was evident from the glycomic analysis data (Fig. 2c) and PSA-cytofluorescence signals (Fig. 3e). The involvement of high mannose type N-glycans and progression of CCA cells was confirmed by the PSA neutralizing experiment. Masking high mannose type N-glycans with PSA, a mannose binding lectin, significantly reduced the capabilities of CCA cells in migration and invasion. Notably, the effect of PSA inhibition on migration and invasion was more obvious in highly metastatic cells than in the parental cells. This implies that the magnitude of high mannose type N-glycans is positively related to the progression of CCA metastasis. The association of overexpression of $Hex_9HexNAc_2$ with metastasis has been reported in several types of cancers [34–36]. In addition, $Hex_8HexNAc_2$ glycan was also stated in pancreatic tumor tissues [39].

O-GlcNAcylation, an intracellular glycosylation, is involved in key cellular processes, including nutrient sensing, stress response, transcription-translation, signal transduction, and proteolysis by proteasome [21]. To our knowledge, the connection of O-GlcNAc modification and the $Hex_9HexNAc_2$ expression has never been reported. We demonstrate that reduction of O-GlcNAcylation with siOGT significantly reduced cell surface high mannose type N-glycans. To elucidate how O-GlcNAcylation modulates the level of $Hex_9HexNAc_2$, we first focused on the expression of MAN1A1, as it is the enzyme that mediates $Hex_9HexNAc_2$ processing by removing 3 terminal mannose residues from $Hex_9HexNAc_2$. Suppression of O-GlcNAcylation using siOGT elevated the expression level of MAN1A1 and consequently reduced the level of $Hex_9HexNAc_2$. Conversely, induction of O-GlcNAcylation using an OGA inhibitor, PUGNAc, decreased the expression of MAN1A1. These data support our hypothesis that O-GlcNAcylation can regulate the level of surface N-glycan via modulating the expression of glycan synthesizing enzymes, namely MAN1A1. The significance of O-GlcNAcylation and MAN1A1 on the progression of CCA metastasis was confirmed by the facts that reduction of O-GlcNAcylation markedly suppressed the migratory and invasion abilities of both parental and highly metastatic CCA cells (Fig. 5d), whereas inhibition of MAN1A1 activity by kifunensine

increased the observed functions (Fig. 5e). We further show O-GlcNAcylation modulates the progression of CCA metastasis via MAN1A1 by the finding that reduction of CCA metastasis by siOGT treatment could be reversed by inhibiting MAN1A1 activity using kifunensine (Fig. 5f).

We next explored how O-GlcNAcylation regulates MAN1A1 expression. Our previous study demonstrated that O-GlcNAcylation could activate Akt signaling and promote progression of CCA metastasis [25]. This information supports our finding that FOXO3, a transcriptional factor under Akt and Erk activation, is a transcriptional factor of MAN1A1. Our data led us to propose that FOXO3 is a transcriptional factor that linked O-GlcNAcylation and Akt and Erk activation to MAN1A1 expression. We demonstrate the link between FOXO3 and expression of MAN1A1 by the findings that suppression of FOXO3 expression decreased the expression level of MAN1A1 in both parental and highly metastatic cells. In addition, the analysis of EpiTect ChIP qPCR Primers assay suggested FOXO3 as a possible transcriptional regulator of *MAN1A1*. The ChIP assay showed that FOXO3 could bind to the *MAN1A1* gene and that DNA binding of FOXO3 correlated well with the expression levels of FOXO3, especially in the FOXO3 suppressed cells or Akt inhibited cells. These data demonstrated for the first time that FOXO3 is a positive transcriptional activator of MAN1A1.

The association of O-GlcNAcylation and FOXO3 expression was further shown to be via Akt and Erk activation. First, suppression of O-GlcNAcylation using siOGT was able to inhibit the activation of Akt and Erk in both parental and highly metastatic CCA cells. Second, inhibiting activities of Akt and Erk by their specific inhibitors reduced the phosphorylation of FOXO3 at Thr-32 and Ser-294, leading to the increased expression of FOXO3 and hence MAN1A1.

In agreement with our findings, the association of O-GlcNAc modification and increased metastatic ability has been shown in several types of cancers. Activation of PI3K/Akt and MAPK/Erk pathways have been demonstrated to be the link between O-GlcNAcylation and metastatic ability of various cancer cells, including thyroid anaplastic cancer [40] and breast cancer [41]. It has been shown that elevation of O-GlcNAcylation by OGA inhibition or overexpression of OGT could increase Akt phosphorylation at Ser-473 in thyroid anaplastic cancer cells [40]. In addition, suppression of O-GlcNAcylation by siOGT decreased O-GlcNAcylation and phosphorylation of Akt in breast cancer cells [41]. In primary mouse vascular smooth muscle cells, O-GlcNAcylation of Akt at Thr-430 and Thr-479 promoted Akt phosphorylation at Ser-473 and consequently induced vascular calcification [42].

Furthermore, similar to our finding, earlier reports suggest that activation of Akt and Erk promotes cancer progression via downregulation of FOXO3 [32] in breast cancer [43] and uveal melanoma cancer cells [44]. The mechanism by which Erk activation promotes breast cancer progression via inhibition of FOXO3 expression has also been shown to be through MDM2-mediated degradation [45]. This evidence is consistent with our study that suppression of Akt using the protein synthesis inhibitor cycloheximide increases the expression level of FOXO3 by stabilizing the protein. The connection between Akt activation and MAN1A1 on CCA progression has also been demonstrated for the first time in this study. Inhibition of Akt activity markedly inhibited migration and invasion of highly metastatic CCA cells and these effects could be rescued by inhibiting MAN1A1 activity using kifunensine (Fig. 6e, f).

The correlation between MAN1A1 expression and metastasis has been reported in liver cancer. Lower expression of MAN1A1 in HCCLM3, MHCC97H, and MHCC97L, the metastatic hepatoma cells than Hep3B, the non-metastatic hepatoma cells was reported [46]. Moreover, high expression of MAN1A1 was correlated with a better outcome of breast cancer patients [47]. The regulation of MAN1A1 in cancer, however, is still unclear. It has been shown in melanoma, liver, breast and cervical cancers that aberrant expression of MAN1A1 is associated with the status of methylation at promoter region [48]. Expression level of MAN1A1 was shown to be modulated via FOXO3 in the present study. MAN1A1 and FOXO3 expression in CCA tissues and their association with clinical pathological features of the patients should be explored to support the in vitro findings of this study. Moreover, further investigation is needed on the roles of the biantennary structure, $Hex_5HexNAc_4Fuc_1$-$NeuAc_1$, as well as the truncated complex N-glycans, $Hex_5HexNAc_3Fuc_1$ and $Hex_5HexNAc_4Fuc_1$, in O-GlcNAc-mediated CCA progression.

Our earlier studies demonstrated the increase of O-GlcNAcylation in CCA tissues with negative relationship to survival of CCA patients [24]. In addition, elevation of O-GlcNAcylation has been shown to increase progressiveness of CCA metastasis via activation of Akt and Erk [25]. In the current study, the molecular link between O-GlcNAcylation and CCA progression was further shown to be via increasing of the membranous high mannose type N-glycan, $Hex_9HexNAc_2$. O-GlcNAcylation activates the PI3K/Akt and MAPK/Erk signaling pathways which negatively regulates the expression level of FOXO3 leading to the decreased expression of MAN1A1 and accumulation of $Hex_9HexNAc_2$ (Fig. 8d). These findings reveal new perspectives of $Hex_9HexNAc_2$ as a candidate marker and therapeutic target for CCA.

Materials and methods

Antibodies and reagents

Antibodies were obtained from several sources: anti-O-GlcNAc (RL-2, #MA1-072) from Pierce Biotechnology (Rockford, IL); anti-MAN1A1 (#M-3694) from Sigma-Aldrich (St. Louis, MO); anti-pAkt (ser-473, #9271s), anti-Akt, anti-pFOXO3 (ser-294, #5538s), and anti-pFOXO3 (thr-32, #9464s) from Cell Signaling (Danvers, MA); anti-Erk (K-23, #sc-94), anti-pErk (E-4, #sc-7383), anti-pIkk (T23, #sc-101706), and anti-Ikk (H470, #sc-7607) from Santa Cruz Biotechnology; anti-FOXO3 (#07–702) and anti-GAPDH (#MAB-374) from Merck Millipore (Billerica, MA). Akt inhibitor, MK-2206 dihydrochloride (#sc-364537) was from Santa Cruz Biotechnology (Santa Cruz, CA) and Erk inhibitor, PD98059 (#9900) was obtained from Cell Signaling (Danvers, MA). PNGase-F (#P0704) was purchased from New England Biolabs (Ipswich, MA), *Pisum Sativum* Agglutinin (PSA, #L-1050), biotinylated PSA (#B-1055), biotinylated Concanavalin A (#B-1005) were obtained from Vector Laboratories (Burlingame, CA). Mannosidase I inhibitor, kifunensine (#K1140), OGA inhibitor, [O-(2-Acetamido-2-deoxy-D-glucopyranosylidenamino)-N-phenylcarbamate; PUGNAc, #A7229], and cycloheximide (CHX, #C104450) were purchased from Sigma-Aldrich.

Cell culture and treatments

KKU-213 and KKU-214, the CCA cell lines were provided from the Japanese Collection of Research Bioresources (JCRB) Cell Bank, Osaka, Japan. Highly metastatic CCA sublines; KKU-213L5 and KKU-214L5 were established from the parental cells, KKU-213 [49] and KKU-214 [50]. All cells were cultured in HAM's F-12 (Gibco, NY) containing 10% fetal bovine serum (Gibco) and 1% antibiotic-antimycotic (Gibco), under the standard protocol at 37 °C and 5% CO_2.

OGA inhibitor, PUGNAc, was used to enhance O-GlcNAcylation level in CCA cells. CCA cells, (8×10^5 cells) in a 6 cm-culture dish were treated with 20 µM PUGNAc for 24 h prior to further experiments.

Cycloheximide (CHX) a protein synthesis inhibitor, was used to determine protein stability. Adherent CCA cells (3×10^5 cells/well) in a 6-well plate were treated with 20 µg/ml of CHX for the indicated time.

Kifunensine, a mannosidase 1 inhibitor, was used to inhibit the MAN1A1 activity. After plating 8×10^5 cells per well in a 6 cm-culture dish for 24 h, 20 µg/ml of kifunensine was added in each well and the plates were cultured further for 48 h before subjecting to further experiments.

PSA neutralization test was used to neutralize cell surface mannosylated N-glycans. CCA cells (3×10^5 cells) were treated with 10 µg/ml of PSA in a complete media for 24 h at 37 °C prior to further experiments.

OGT- and FOXO3- siRNA-treated cells

The level of O-GlcNAcylation was modulated by suppressing OGT expression using specific siRNA as described previously [51]. The negative control siRNA (scramble siRNA, QIAGEN, Hilden, Germany) was used as the control. Similar procedures were performed for siFOXO3 [52].

Preparation of membrane fraction and purification of membranous N-glycans

The membrane fraction was harvested according to the standard procedure [53] with minor modification. In brief, CCA cells were homogenized in 20 mM HEPES-KOH, pH 7.4 containing 0.25 M sucrose and 1:100 protease inhibitor, using probe sonication (25 Amplitude, pulsed on 5 s and off 10 s for 5 times). Cell nuclei were fractionated by centrifugation at $2000 \times g$, for 10 min. Then, the membrane fraction was separated by 3 times of ultra-centrifugation at $200{,}000 \times g$, 45 min. The final pellet was collected as the membrane fraction and total N-glycans were released using 1000 U of PNGase-F at 37 °C in a microwave reactor (CEM Corporation, Matthews, NC) at 20 watts for 10 min. The released N-glycans were enriched and purified by porous graphitized carbon solid-phase extraction as described previously [48]. The unbound fraction was first eluted with 9 ml of pure water and the bound N-glycan fraction was eluted with 4 ml of 40% ACN and 0.1% TFA in pure water.

Glycomic analysis of membranous N-glycans

Samples were reconsitituted in 30 µl pure water and composition of glycans were analyzed by Agilent HPLC-Chip/Time-of-Flight (Chip/TOF) MS system (Agilent Technologies, Santa Clara, CA) as previously reported [48]. The enrichment column was conditioned with 3% ACN and 0.1% formic acid (FA) in water. Sample (5 µl) was injected at 4.0 µl/min using a 6 °C maintained autosampler. The mass spectra were analyzed using Agilent MassHunter Qualitative Analysis software and the extracted compound chromatograms (ECC) were determined using the Molecular Feature Extractor algorithm. Each compound was identified using an in-house retrosynthetic library [54]. Area under the peaks was used for relative quantitation.

Cell aggregation test

To select the appropriated concentration of *Pisum Sativum* Agglutinin (PSA), a mannose recognition lectin, cell

aggregation test was first tested. In a 24-well plate, KKU-213L5 of 5×10^4 cells per well were incubated in a serum free Ham's F-21 media containing 0–100 µg/ml of PSA for 1 h. The aggregated cells were visualized using a light microscope. The highest PSA concentration that did not initiate aggregated cells was selected for further studies.

PSA-cytofluorescence staining

A solution of 4% paraformaldehyde was used to fix the cells for 30 min prior to block the non-specific binding with 0.5% BSA in PBS for 5 min. Cells were then incubated with 0.01 mg/ml of biotinylated PSA (Vector Laboratories) at 4 °C, overnight and 1 h at room temperature with 1:500 streptavidin-FITC (Invitrogen, UK). Hoechst 33342 (Molecular probe, Invitrogen) was used to stain the nuclei and the fluorescent image was visualized using a ZEISS LSM 800 Confocal Laser Scanning Microscope (Zeiss, Oberkochen, Germany). The intensities of the fluorescent signals were analyzed using ZEN 2.1 software (Zeiss).

Cell proliferation

Viable cells in a 96-well plate were determined continuously for 4 days using the MTT proliferation assay (Moleular probes, Eugene, OR) as previously described [25]. Proliferation rate (fold change from control) was determined as OD of treatment/mean OD of control.

Cell migration and invasion

The Boyden chamber assay (8.0 µm pore size, Corning Incorporated, Corning, NY) was used to determine the migration and invasion as previously described [25]. For invasion assay, the upper chambers were pre-coated overnight with 100 µl of 0.4 mg/ml Matrigel (BD Matrigel™, BD biosciences). At least 5 microscopic fields of 10 × objective were determined for migrated and invaded cells. Triplicate tests per experiment were performed.

Western blot analysis

Cell lysate (30–50 µg) in a NP-40 lysis buffer was loaded onto a 10% SDS-PAGE and the separated proteins were electro-transferred onto a PVDF membrane. The immunoreactivity and captured signal were determined as mentioned previously [25]. Amount of proteins in cell lysates were measured with Bradford reagent (Bio-rad laboratories, Hercules, CA) as described by the manufacturer.

RNA extraction and real-time reverse transcriptase polymerase chain reaction (RT-PCR)

Total RNA extraction and cDNA conversion were performed as described previously [25]. PCR reactions were performed using 40 ng cDNA, 0.4 µM of the specific forward and reverse primers for MAN1A1 (5′-GTGGACAGTGGGGTCAACAT-3′ and 5′-GCTGCTAGACTTGCGGATCA-3′) in a total of 10 µl LightCycle 480® SYBR green I master mix (Roche Diagnostic, Mannheim, Germany), using the LightCycle 480® real-time PCR system (Roche Diagnostic). β-actin expression was analyzed as an internal control. Gene expression levels were determined using LightCycle 480® Relative Quantification software (Roche Diagnostic).

Chromatin immunoprecipitation (ChIP) assay

ChIP assay was performed using the EZ-ChIP™ chromatin immunoprecipitation kit (17–371, Upstate, Millipore Corporation) as suggested by the manufacturer. Briefly, after treating cells with siFOXO3 or Akt inhibitor, the DNA and proteins were crosslinked using formaldehyde at a final concentration of 1% (v/v) in culture media. The cells were sonicated on ice with 5 sets of 15 s pulses on and 10 s pulses off using Ultrasonic homogenizer (sonic VCX 750, Sonics & Materials inc., CT), equipped with a 2 mm tip and set to 30% power. The FOXO3-bound DNA was precipitated with 3 µg/ml of anti-FOXO3 antibody. Rabbit IgG was used as an isotype control. The chromatin-antibody complexes were captured with Protein G-Agarose containing Salmon Sperm DNA. After washing, the DNA–protein cross-links that bound to Protein G-Agarose were eluted using elution buffer, and the complexes were reversed at 65 °C overnight in 0.2 M NaCl. Protein was removed from the DNA using proteinase K at 45 °C for 1 h. The DNA was purified using a spin column. The FOXO3-binding site on *MAN1A1* gene in the purified DNA and input genomic DNA were analyzed by real-time PCR, using the primer sequences; primer-1, 5′-TCCATCAGATTAGTTCAGGCAGA-3′ and primer-2, 5′-CACTCTTGCCTCTCTAAAGCC-3′ as suggested by EpiTect ChIP qPCR Primers (http://sabiosciences.com/chipqpcrsearch.php). The results of FOXO3 binding are normalized against the input DNA.

Immunohistochemistry

The immunohistochemistry (IHC) experiments were performed using formalin-fixed paraffin-embed liver tissues from histologically proven CCA patients which were obtained from the specimen bank of Cholangiocarcinoma Research Institute at Khon Kaen University (Khon Kaen,

Thailand). Each subject gave informed consent and the study protocol was certified by the Ethics Committee for Human Research at Khon Kaen University (HE581369).

Expression levels of OGP, OGT, PSA and MAN1A1 in 10 CCA tissues (non-metastasis ($n = 5$) and metastasis ($n = 5$) CCA) were determined using IHC staining according to the standard protocol [26]. The signals were amplified using the EnVision-system-HRP (Dako, Glostrup, Denmark). The immunoreactivity signals were developed using diaminobenzidine (Sigma-Aldrich). The IHC score was determined as described previously. Two independent assessors scored the levels of IHC staining signal blindly without prior knowledge of clinical parameters.

Statistical analysis

At least two independent experiments and with two biological replicates were performed in all experiments. GraphPad Prism® 5.0 software (GraphPad software, Inc., La Jolla, CA) was used for statistical analysis. $P < 0.05$ was considered as statistical significance.

Acknowledgements This project was co-supported by the Thailand Research Fund and Medical Research Council-UK (Newton Fund) project no. DBG5980004, and National Research University grant, Khon Kaen University (NRU592010), a scholarship under the Post-Doctoral Training Program from Research Affairs and Graduate School, Khon Kaen University, Thailand (59151) and National Institutes of Health (USA) R01GM049077. EW-FL work is supported by MRC (MR/N012097/1), CRUK (A12011), Breast Cancer Now (2012MayPR070; 2012NovPhD016), the Cancer Research UK Imperial Centre, Imperial ECMC and NIHR Imperial BRC.

Compliance with ethical standards

Conflict of interest The authors declare that they have no conflict of interest.

References

1. Steeg PS. Targeting metastasis. Nat Rev Cancer. 2016;16:201–18.
2. Sripa B, Pairojkul C. Cholangiocarcinoma: lessons from Thailand. Curr Opin Gastroenterol. 2008;24:349–56.
3. Patel T. Cholangiocarcinoma. Nat Clin Pract Gastroenterol Hepatol. 2006;3:33–42.
4. Uttaravichien T, Bhudhisawasdi V, Pairojkul C, Pugkhem A. Intrahepatic cholangiocarcinoma in Thailand. J Hepatobiliary Pancreat Surg. 1999;6:128–35.
5. Li X, Wang X, Tan Z, Chen S, Guan F. Role of glycans in cancer cells undergoing epithelial-mesenchymal transition. Front Oncol. 2016;6:33.
6. Varki A, Freeze HH. Glycans in acquired human diseases. In: Varki A, Cummings RD, Esko JD, Freeze HH, Stanley P, Bertozzi CR, et al, editors. Essentials of glycobiology. 2nd ed. NY: Cold Spring Harbor; 2009; p. 601–16.
7. Varki A, Kannagi R, Toole BP. Glycosylation changes in cancer. In: Varki A, Cummings RD, Esko JD, Freeze HH, Stanley P, Bertozzi CR, et al, editos. Essentials of glycobiology. 2nd ed. NY: Cold Spring Harbor; 2009; p. 617–32.
8. Christie DR, Shaikh FM, Lucas JAt, Lucas JA 3rd, Bellis SL. ST6Gal-I expression in ovarian cancer cells promotes an invasive phenotype by altering integrin glycosylation and function. J Ovarian Res. 2008;1:3.
9. Handerson T, Camp R, Harigopal M, Rimm D, Pawelek J. Beta1,6-branched oligosaccharides are increased in lymph node metastases and predict poor outcome in breast carcinoma. Clin Cancer Res. 2005;11:2969–73.
10. Litynska A, Przybylo M, Pochec E, Kremser E, Hoja-Lukowicz D, Sulowska U. Does glycosylation of melanoma cells influence their interactions with fibronectin? Biochimie. 2006;88:527–34.
11. Takahashi M, Kuroki Y, Ohtsubo K, Taniguchi N. Core fucose and bisecting GlcNAc, the direct modifiers of the N-glycan core: their functions and target proteins. Carbohydr Res. 2009;344:1387–90.
12. Silsirivanit A, Araki N, Wongkham C, Pairojkul C, Narimatsu Y, Kuwahara K, et al. A novel serum carbohydrate marker on mucin 5AC: values for diagnostic and prognostic indicators for cholangiocarcinoma. Cancer. 2011;117:3393–403.
13. Matsuda A, Kuno A, Nakagawa T, Ikehara Y, Irimura T, Yamamoto M, et al. Lectin Microarray-based sero-biomarker verification targeting aberrant O-linked glycosylation on mucin 1. Anal Chem. 2015;87:7274–81.
14. Higashi M, Yonezawa S, Ho JJ, Tanaka S, Irimura T, Kim YS, et al. Expression of MUC1 and MUC2 mucin antigens in intrahepatic bile duct tumors: its relationship with a new morphological classification of cholangiocarcinoma. Hepatology. 1999;30:1347–55.
15. Tolek A, Wongkham C, Proungvitaya S, Silsirivanit A, Roytrakul S, Khuntikeo N, et al. Serum alpha1beta-glycoprotein and afamin ratio as potential diagnostic and prognostic markers in cholangiocarcinoma. Exp Biol Med. 2012;237:1142–9.
16. Indramanee S, Silsirivanit A, Pairojkul C, Wongkham C, Wongkham S. Aberrant glycosylation in cholangiocarcinoma demonstrated by lectin-histochemistry. Asian Pac J Cancer Prev. 2012;13(Suppl):119–24.
17. Anderson CD, Pinson CW, Berlin J, Chari RS. Diagnosis and treatment of cholangiocarcinoma. Oncologist. 2004;9:43–57.
18. Ghazarian H, Idoni B, Oppenheimer SB. A glycobiology review: carbohydrates, lectins and implications in cancer therapeutics. Acta Histochem. 2011;113:236–47.
19. Hart GW, Housley MP, Slawson C. Cycling of O-linked beta-N-acetylglucosamine on nucleocytoplasmic proteins. Nature. 2007;446:1017–22.
20. Zachara NE, Hart GW. Cell signaling, the essential role of O-GlcNAc! Biochim Biophys Acta. 2006;1761:599–617.
21. Butkinaree C, Park K, Hart GW. O-linked beta-N-acetylglucosamine (O-GlcNAc): Extensive crosstalk with phosphorylation to regulate signaling and transcription in response to nutrients and stress. Biochim Biophys Acta. 2010;1800:96–106.
22. Hart GW, Slawson C, Ramirez-Correa G, Lagerlof O. Cross talk between O-GlcNAcylation and phosphorylation: roles in

signaling, transcription, and chronic disease. Annu Rev Biochem. 2011;80:825–58.
23. de Queiroz RM, Carvalho E, Dias WB. O-GlcNAcylation: the sweet side of the cancer. Front Oncol. 2014;4:132.
24. Phoomak C, Silsirivanit A, Wongkham C, Sripa B, Puapairoj A, Wongkham S. Overexpression of O-GlcNAc-transferase associates with aggressiveness of mass-forming cholangiocarcinoma. Asian Pac J Cancer Prev. 2012;13(Suppl):101–5.
25. Phoomak C, Vaeteewoottacharn K, Sawanyawisuth K, Seubwai W, Wongkham C, Silsirivanit A, et al. Mechanistic insights of O-GlcNAcylation that promote progression of cholangiocarcinoma cells via nuclear translocation of NF-kappaB. Sci Rep. 2016;6:27853.
26. Phoomak C, Vaeteewoottacharn K, Silsirivanit A, Saengboonmee C, Seubwai W, Sawanyawisuth K, et al. High glucose levels boost the aggressiveness of highly metastatic cholangiocarcinoma cells via O-GlcNAcylation. Sci Rep. 2017;7:43842.
27. Kaku H, Goldstein IJ, Oscarson S. Interactions of five D-mannose-specific lectins with a series of synthetic branched trisaccharides. Carbohydr Res. 1991;213:109–16.
28. Pilobello KT, Slawek DE, Mahal LK. A ratiometric lectin microarray approach to analysis of the dynamic mammalian glycome. Proc Natl Acad Sci USA. 2007;104:11534–9.
29. Zhao Y, Li J, Wang J, Xing Y, Geng M. Role of cell surface oligosaccharides of mouse mammary tumor cell lines in cancer metastasis. Indian J Biochem Biophys. 2007;44:145–51.
30. Lucena MC, Carvalho-Cruz P, Donadio JL, Oliveira IA, de Queiroz RM, Marinho-Carvalho MM, et al. Epithelial–mesenchymal transition induces aberrant glycosylation through hexosamine biosynthetic pathway activation. J Biol Chem. 2016;291:12917–29.
31. Stanley P, Schachter H, Taniguchi N. N-glycans. In: Varki A, Cummings RD, Esko JD, Freeze HH, Stanley P, Bertozzi CR, et al, editors. Essentials of glycobiology. 2nd ed. NY: Cold Spring Harbor; 2009; p. 101–14.
32. Coomans de Brachene A, Demoulin JB. FOXO transcription factors in cancer development and therapy. Cell Mol Life Sci. 2016;73:1159–72.
33. Kannagi R, Yin J, Miyazaki K, Izawa M. Current relevance of incomplete synthesis and neo-synthesis for cancer-associated alteration of carbohydrate determinants--Hakomori's concepts revisited. Biochim Biophys Acta. 2008;1780:525–31.
34. de Leoz ML, Young LJ, An HJ, Kronewitter SR, Kim J, Miyamoto S, et al. High-mannose glycans are elevated during breast cancer progression. Mol Cell Proteom. 2011;10(M110):002717.
35. Zhang X, Wang Y, Qian Y, Wu X, Zhang Z, Liu X, et al. Discovery of specific metastasis-related N-glycan alterations in epithelial ovarian cancer based on quantitative glycomics. PLoS ONE. 2014;9:e87978.
36. Park HM, Hwang MP, Kim YW, Kim KJ, Jin JM, Kim YH, et al. Mass spectrometry-based N-linked glycomic profiling as a means for tracking pancreatic cancer metastasis. Carbohydr Res. 2015;413:5–11.
37. Tao SC, Li Y, Zhou J, Qian J, Schnaar RL, Zhang Y, et al. Lectin microarrays identify cell-specific and functionally significant cell surface glycan markers. Glycobiology. 2008;18:761–9.
38. Morishima S, Morita I, Tokushima T, Kawashima H, Miyasaka M, Omura K, et al. Expression and role of mannose receptor/terminal high-mannose type oligosaccharide on osteoclast precursors during osteoclast formation. J Endocrinol. 2003;176:285–92.
39. Powers TW, Neely BA, Shao Y, Tang H, Troyer DA, Mehta AS, et al. MALDI imaging mass spectrometry profiling of N-glycans in formalin-fixed paraffin embedded clinical tissue blocks and tissue microarrays. PLoS One. 2014;9:e106255.
40. Zhang P, Wang C, Ma T, You S. O-GlcNAcylation enhances the invasion of thyroid anaplastic cancer cells partially by PI3K/Akt1 pathway. Onco Targets Ther. 2015;8:3305–13.
41. Liu Y, Cao Y, Pan X, Shi M, Wu Q, Huang T, et al. O-GlcNAc elevation through activation of the hexosamine biosynthetic pathway enhances cancer cell chemoresistance. Cell Death Dis. 2018;9:485.
42. Heath JM, Sun Y, Yuan K, Bradley WE, Litovsky S, Dell'Italia LJ, et al. Activation of AKT by O-linked N-acetylglucosamine induces vascular calcification in diabetes mellitus. Circ Res. 2014;114:1094–102.
43. Chen S, Han Q, Wang X, Yang M, Zhang Z, Li P, et al. IBP-mediated suppression of autophagy promotes growth and metastasis of breast cancer cells via activating mTORC2/Akt/FOXO3a signaling pathway. Cell Death Dis. 2013;4:e842.
44. Yan F, Liao R, Farhan M, Wang T, Chen J, Wang Z, et al. Elucidating the role of the FoxO3a transcription factor in the IGF-1-induced migration and invasion of uveal melanoma cancer cells. Biomed Pharmacother. 2016;84:1538–50.
45. Yang JY, Zong CS, Xia W, Yamaguchi H, Ding Q, Xie X, et al. ERK promotes tumorigenesis by inhibiting FOXO3a via MDM2-mediated degradation. Nat Cell Biol. 2008;10:138–48.
46. Liu T, Zhang S, Chen J, Jiang K, Zhang Q, Guo K, et al. The transcriptional profiling of glycogenes associated with hepatocellular carcinoma metastasis. PLoS ONE. 2014;9:e107941.
47. Milde-Langosch K, Karn T, Schmidt M, zu Eulenburg C, Oliveira-Ferrer L, Wirtz RM, et al. Prognostic relevance of glycosylation-associated genes in breast cancer. Breast Cancer Res Treat. 2014;145:295–305.
48. Vojta A, Samarzija I, Bockor L, Zoldos V. Glyco-genes change expression in cancer through aberrant methylation. Biochim Biophys Acta. 2016;1860:1776–85.
49. Uthaisar K, Vaeteewoottacharn K, Seubwai W, Talabnin C, Sawanyawisuth K, Obchoei S, et al. Establishment and characterization of a novel human cholangiocarcinoma cell line with high metastatic activity. Oncol Rep. 2016;36:1435–46.
50. Saentaweesuk W, Araki N, Vaeteewoottacharn K, Silsirivanit A, Seubwai W, Talabnin C et al. Activation of Vimentin is Critical to Promote a Metastatic Potential of Cholangiocarcinoma Cells. Oncol Res. 2017. https://doi.org/10.3727/096504017X15009778205068.
51. Zhu Q, Zhou L, Yang Z, Lai M, Xie H, Wu L, et al. O-GlcNAcylation plays a role in tumor recurrence of hepatocellular carcinoma following liver transplantation. Med Oncol. 2012;29:985–93.
52. Lin C, Wu Z, Lin X, Yu C, Shi T, Zeng Y, et al. Knockdown of FLOT1 impairs cell proliferation and tumorigenicity in breast cancer through upregulation of FOXO3a. Clin Cancer Res. 2011;17:3089–99.
53. Park D, Arabyan N, Williams CC, Song T, Mitra A, Weimer BC, et al. Salmonella typhimurium enzymatically landscapes the host intestinal epithelial cell (IEC) surface glycome to increase invasion. Mol Cell Proteom. 2016;15:3653–64.
54. Kronewitter SR, An HJ, de Leoz ML, Lebrilla CB, Miyamoto S, Leiserowitz GS. The development of retrosynthetic glycan libraries to profile and classify the human serum N-linked glycome. Proteomics. 2009;9:2986–94.

Anthocyanin complex exerts anti-cholangiocarcinoma activities and improves the efficacy of drug treatment in a gemcitabine-resistant cell line

KITTI INTUYOD[1,2], AROONSRI PRIPREM[3], CHAWALIT PAIROJKUL[2,4], CHARIYA HAHNVAJANAWONG[2,5,6], KULTHIDA VAETEEWOOTTACHARN[2,7], PORNTIP PINLAOR[2,8] and SOMCHAI PINLAOR[2,9]

[1]Biomedical Science Program, Graduate School; [2]Cholangiocarcinoma Research Institute, Faculty of Medicine; [3]Department of Pharmaceutical Technology, Faculty of Pharmaceutical Science; Departments of [4]Pathology and [5]Microbiology; [6]Center of Excellence for Innovation in Chemistry; [7]Department of Biochemistry, Faculty of Medicine; [8]Centre for Research and Development in Medical Diagnostic Laboratory, Faculty of Associated Medical Sciences; [9]Department of Parasitology, Faculty of Medicine, Khon Kaen University, Khon Kaen 40002, Thailand

Received August 7, 2017; Accepted March 1, 2018

DOI: 10.3892/ijo.2018.4306

Abstract. Cholangiocarcinoma (CCA) is a deleterious bile duct tumor with poor prognosis and is relatively resistant to chemotherapy. Therefore, alternative or supplementary agents with anticancer and chemosensitizing activities may be useful for the treatment of CCA. A novel anthocyanin complex (AC) nanoparticle, developed from extracts of cobs of purple waxy corn and petals of blue butterfly pea, has exhibited chemopreventive potential *in vivo*. In the present study, the anti-CCA activities of AC and their underlying molecular mechanisms were investigated further *in vitro* using a CCA cell line (KKU213). The potential use of AC as a chemosensitizer was also evaluated in a gemcitabine-resistant CCA cell line (KKU214^{GemR}). It was demonstrated that AC treatment suppressed proliferation of KKU213 CCA cells in dose- and time-dependent manners. AC treatment also induced apoptosis and mitochondrial superoxide production, decreased clonogenicity of CCA cells, and downregulated forkhead box protein M1 (FOXM1), nuclear factor-κB (NF-κB) and pro-survival protein B-cell lymphoma-2 (Bcl-2). The expression of endoplasmic reticulum (ER) stress-response proteins, including protein kinase RNA-like ER kinase, phosphorylated eIF2α, eukaryotic initiation factor 2α and activating transcription factor 4, also decreased following AC treatment. It was also identified that AC treatment inhibited KKU214^{GemR} cell proliferation in dose- and time-dependent manners. Co-treatment of KKU214^{GemR} cells with low doses of AC together with gemcitabine significantly enhanced efficacy of the latter against this cell line. Therefore, it is suggested that AC treatment is cytotoxic to KKU213 cells, possibly via downregulation of FOXM1, NF-κB, Bcl-2 and the ER stress response, and by induction of mitochondrial superoxide production. AC also sensitizes KKU214^{GemR} to gemcitabine treatment, which may have potential for overcoming drug resistance of CCA.

Correspondence to: Professor Somchai Pinlaor, Department of Parasitology, Faculty of Medicine, Khon Kaen University, Khon Kaen 40002, Thailand
E-mail: psomec@kku.ac.th

Abbreviations: AC, anthocyanin complex; AEBSF, 4-(2-aminoethyl) benzenesulfonyl fluoride hydrochloride; ATF4, activating transcription factor 4; BCA, bicinchoninic acid; CCA, cholangiocarcinoma; DMEM, Dulbecco's modified Eagle's medium; DMSO, dimethyl sulfoxide; ER, endoplasmic reticulum; FBS, fetal bovine serum; FOXM1, forkhead box protein M1; HBSS, Hank's balanced salt solution; NF-κB, nuclear factor-κB; PERK, protein kinase RNA-like endoplasmic reticulum kinase; eIF2α, eukaryotic initiation factor 2α; PVDF, polyvinylidene difluoride; RIPA, radioimmunoprecipitation assay; SRB, sulforhodamine B.

Key words: anthocyanin complex, chemosensitizer, cholangiocarcinoma, forkhead box protein M1, endoplasmic reticulum stress, gemcitabine

Introduction

Cholangiocarcinoma (CCA) is a bile-duct tumor that is rare in the majority of countries (1,2), but which has a far greater incidence in the Greater Mekong sub-region of southeast Asia, particularly in northeastern Thailand, where the prevalence of the small human liver fluke *Opisthorchis viverrini* is high (3). *O. viverrini* is classified as a group I carcinogen by the International Agency for Research on Cancer (4). Infection with this fluke causes chronic inflammation, leading to periductal fibrosis and ultimately contributing to the development of CCA (5,6). In northeastern Thailand, CCA is the major primary liver cancer, with its management costing US$120 million annually (5,7). Clinical presentation is typically observed at a late stage and therefore the majority of patients with CCA cannot be cured by surgical resection (8,9). Furthermore, the disease is able to develop resistance to standard chemotherapeutic drugs over time (10). Therefore, using phytochemicals with anti-inflammatory and anticancer

activities to treat cancer or to enhance the efficacy of other chemotherapeutic drugs, may be an alternative approach for the management of CCA and help to avoid drug-resistance (11-13).

Anthocyanins are the water-soluble flavonoids responsible for the blue, purple and red colors in a number of fruits, flowers and leaves (14). Anthocyanins exhibit anti-inflammatory, anti-angiogenesis, antioxidant and anti-proliferative effects, and thus have a number of medical applications (15-18). Among these are prevention and treatment of cancer (19,20). Previous studies have demonstrated that the consumption of anthocyanin-rich foods is associated with a decreased risk of chronic diseases, including cardiovascular disease, arthritis and diabetes mellitus, and development of esophageal, colon, lung and skin cancers (17,21).

Cyanidin and delphinidin glycosides are the most abundant and well-studied anthocyanins with potential anticancer activity (22-24). However, a major obstacle in the use of anthocyanins is that they are unstable and prone to degradation (25). Previously, cyanidin and delphinidin were isolated from cobs of purple waxy corn (*Zea mays* L. var. *ceritina Kulesh*) and petals of blue butterfly pea (*Clitoria ternatea* L.) and were manipulated to form a complex with turmeric extract and other trace elements (26) to increase their stability and activity. This novel anthocyanin complex (AC) nanoparticle exhibited anti-inflammatory and anti-fibrotic effects in an *O. viverrini*-infected hamster model, establishing its potential for chemoprevention of CCA (26). However, the utility for CCA treatment has not yet been investigated.

The aim of the present study was to demonstrate the application of AC for CCA treatment. Anticancer activities of AC and the potential underlying molecular mechanisms against CCA were investigated *in vitro* using a CCA cell line. The effect of combined treatment of AC and gemcitabine against the gemcitabine-resistant CCA cell line ($KKU214^{GemR}$) was also investigated. The results of the present study provide an insight into the promising use of AC phytochemical products for the treatment of CCA.

Materials and methods

Chemicals and reagents. AC was prepared as described previously (26). In brief, aqueous extracts of purple waxy corn cobs and blue butterfly pea petals were mixed with turmeric (*Curcuma longa*) extract (7:2:1) in the presence of 100 mM caffeic acid and piperine (Sigma Aldrich; Merck KGaA, Darmstadt, Germany) and 2 mM zinc sulfate (Ajax Finechem; Thermo Fisher Scientific, Inc., Waltham, MA, USA). Thereafter, the mixture was cooled and dried to yield of AC. Only one batch of AC was used throughout the present study to avoid batch-to-batch variation. Dulbecco's modified Eagle's medium (DMEM), penicillin/streptomycin, trypsin-EDTA and fetal bovine serum (FBS) were purchased from Gibco; Thermo Fisher Scientific, Inc. 4-(2-Aminoethyl) benzenesulfonyl fluoride hydrochloride (AEBSF), dimethyl sulfoxide (DMSO), sulforhodamine B (SRB) and the broad-spectrum caspase inhibitor quinolone-Val-Asp-difluorophenoxymethyl ketone (Q-VD-OPh) were purchased from Sigma-Aldrich; Merck KGaA. Rabbit anti-protein kinase RNA-like endoplasmic reticulum (ER) kinase (PERK; cat. no. 5683), anti-p65 (cat. no. 8242), anti-activating transcription factor 4 (ATF4; cat. no. 11815), anti-phosphorylated eukaryotic initiation factor 2α (p-eIF2α; cat. no. 3398) (Ser^{51}), anti-eIF2α (cat. no. 9722), anti-poly(ADP-ribose) polymerase (PARP; cat. no. 9542), anti-B-cell lymphoma-2 (Bcl-2; cat. no. 2872), anti-caspase-3 (cat. no. 9662) and anti-β-tubulin (cat. no. 2128) and radioimmunoprecipitation assay (RIPA) buffer were purchased from Cell Signaling Technology, Inc. (Danvers, MA, USA). Rabbit anti-forkhead box M1 (FOXM1; cat. no. sc-502) (C-20) was obtained from Santa Cruz Biotechnology, Inc. (Dallas, TX, USA). Horseradish peroxidase (HRP)-conjugated goat anti-rabbit IgG (cat. no. 111-035-003) secondary antibody was purchased from Jackson ImmunoResearch, Inc. (West Grove, PA, USA). A dead-cell apoptosis kit [Annexin V/propidium iodide (PI)], Pierce™ bicinchoninic acid (BCA) protein assay kit, Hank's balanced salt solution (HBSS) and MitoSOX™ Red mitochondrial superoxide indicator were obtained from Thermo Fisher Scientific, Inc. ECL™ Prime western blotting detection reagent and polyvinylidene difluoride (PVDF) membrane were obtained from GE Healthcare (Chicago, IL, USA).

Human CCA cell lines. The KKU213 CCA cell line was established from Thai CCA patients as described previously (27). The gemcitabine-resistant CCA cell line $KKU214^{GemR}$ was established previously by exposure to stepwise increases in the concentration of gemcitabine as described previously (28). It should be noted that the parental line of $KKU214^{GemR}$ cells appears to be a KKU213 cell derivative (web.expasy.org/cellosaurus/CVCL_M264). However, due to the fact that $KKU214^{GemR}$ cells were induced to be a gemcitabine-resistant CCA cell line, it would not have any bearing on the results of the present study. The cell lines were maintained in DMEM supplemented with 10% FBS, 100 U/ml penicillin and 100 μg/ml streptomycin at 37˚C in a humidified incubator containing 10% CO_2. $KKU214^{GemR}$ cells were cultured in the presence of gemcitabine to maintain its resistant phenotype, but were cultured in a drug-free medium for one passage prior to performing experiments.

Assessment of half-maximal inhibitory concentration (IC_{50}) of AC. The IC_{50} was assessed using the SRB assay. For instance, KKU213 cells were seeded at 2,000 cells/well in flat-bottomed 96-well plates (Corning Inc., Corning, NY, USA). The following day, the cells were incubated with either DMSO (diluent control) or various concentrations of AC (100-800 μg/ml) dissolved in DMSO for 12, 24, 36 and 48 h at 37˚C in a humidified incubator containing 10% CO_2. Cells were fixed with ice-cold 40% trichloroacetic acid at 4˚C for 1 h. Following washing three times with running tap water, 0.4% (w/v) SRB solution in 1% acetic acid was added and incubated further for 1 h at room temperature. Excess SRB solution was removed by washing with 1% acetic acid and SRB was dissolved by adding 10 mM Tris buffer. Absorbance at 492 nm was determined using an ELISA plate reader (Tecan Group Ltd., Männedorf, Switzerland). The absorbance at 492 nm of DMSO-treated cells was used as control. For $KKU214^{GemR}$ cells, the same procedure was performed, but the cells were treated with either single agent (300 μg/ml AC; 20 or 40 μM gemcitabine) or a combination of AC (300 μg/ml) and gemcitabine (20 or 40 μM) for 24, 48 and 72 h.

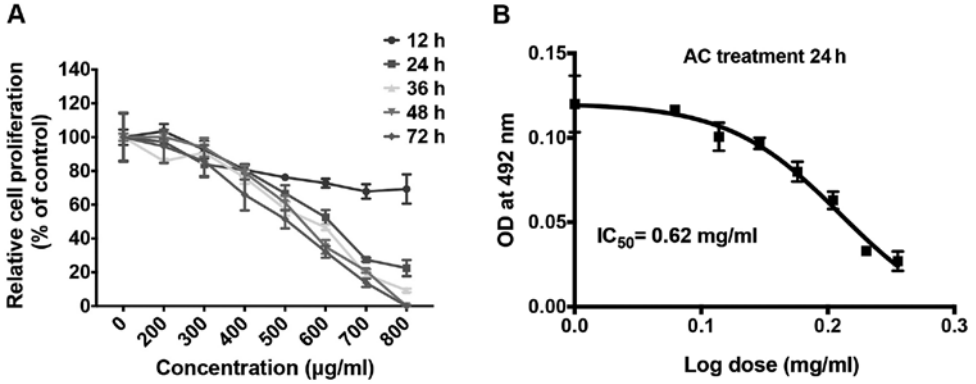

Figure 1. AC inhibits proliferation of the KKU213 CCA cell line. (A) KKU213 CCA cells were treated with different concentrations of AC for the indicated time periods. The percentage of cell proliferation was determined using the SRB assay compared with its control treatment (dimethyl sulfoxide). (B) IC_{50} of AC on KKU213 cells at 24 h post-treatment was calculated using a dose-response curve analysis. Experiments were carried out in triplicate. AC, anthocyanin complex; CCA, cholangiocarcinoma; SRB, sulforhodamine B; IC_{50}, half-maximal inhibitory concentration; OD, optical density.

Assessment of cellular apoptosis. Cellular apoptosis was determined by Annexin V/PI staining according to the manufacturer's protocol. In brief, following trypsinization and washing with sterile PBS, ~10^6 KKU213 cells were resuspended in 1X binding buffer. Annexin V/PI solution was added prior to incubation at room temperature in the dark for 15 min. Stained cells were detected using a BD FACSCanto II flow cytometer and analyzed using BD FACSDiva software (version 6.1.3) (both from BD Biosciences, San Jose, CA, USA).

Plasmid transfection. The pCMV4-p65 plasmid was a gift from Professor Warner Greene, Gladstone Institute of Virology and Immunology, San Francisco, CA, USA (Addgene plasmid #21966). In total ~2x10^6 KKU213 cells were seeded into 10-cm cell culture dishes for 24 h, prior to transfection with pCMV4-p65 plasmid using X-tremeGENE HP (Roche Diagnostics, Basel, Switzerland), according to the manufacturer's protocol. Cells were then harvested at 24 h post-transfection for further experiments.

Clonogenic assay. CCA cells were seeded into 6-well plates at a density of 1,000 cells/well overnight prior to drug treatment. Cells were treated with different concentrations of AC (100-800 μg/ml) and incubated for 48 h at 37˚C in a humidified incubator containing 10% CO_2. In the case of $KKU214^{GemR}$ cells, cells were treated with either a single agent (300 μg/ml AC; 20 or 40 μM gemcitabine) or a combination of AC (300 μg/ml) and gemcitabine (20 or 40 μM). The culture medium was changed every 2 days and cells were cultured for a further 14 days. Finally, cells were fixed with 4% paraformaldehyde and stained with 0.5% crystal violet. Stained cells were dissolved with 33% acetic acid and absorbance at 620 nm was measured using an ELISA reader (Tecan Group Ltd.).

Measurement of mitochondrial superoxide production. Mitochondrial superoxide production was determined using MitoSOX Red mitochondrial superoxide indicator, according to the manufacturer's protocol. In brief, CCA cells were trypsinized, washed once and resuspended in HBSS with Ca^{2+}/Mg^{2+}. Subsequently, 4 μM MitoSOX Red solution was added and the mixture was incubated at 37˚C for 30 min in the dark. CCA cells were centrifuged at 600 x g for 5 min at room temperature and washed with 1 ml HBSS/Ca^{2+}/Mg^{2+}. Finally, CCA cells were resuspended in HBSS/Ca^{2+}/Mg^{2+} and the fluorescence intensity at 575 nm was measured using a flow cytometer (BD Biosciences).

Western blot analysis. Protein was extracted from CCA cells using RIPA buffer (50 mM Tris/HCl, 150 mM NaCl, 1% Nonidet P-40, 0.5% sodium deoxycholate, 0.1% SDS and 1 mM AEBSF) and the protein concentration was determined using the BCA assay. Subsequently, 20 μg protein was separated by SDS-PAGE (7 or 12% gels) and then transferred onto a PVDF membrane. Following blocking with 5% bovine serum albumin in Tris-buffered saline containing 0.05% Tween-20, membranes were incubated with primary antibodies against PERK, p65, ATF4, p-eIF2α (Ser^{51}), eIF2α, PARP, caspase-3, Bcl-2 and β-tubulin (all 1:1,000) overnight at 4˚C. Following washing, membranes were incubated with secondary antibody (1:3,000) and the chemiluminescent reaction was developed using ECL™ Prime blotting detection reagent. Immunoreactivity bands were captured using the ImageQuant™ LAS4000 mini imager (GE Healthcare).

Statistical analysis. Data are expressed as the mean ± standard deviation. Student's t-test and analysis of variance and Tukey's test were performed to determine differences among experimental groups using SPSS (version 13.0; SPSS, Inc., Chicago, IL, USA). $P<0.05$ was considered to indicate a statistically significant difference. Non-linear regression analysis was performed to determine the IC_{50} values using GraphPad Prism (version 6; GraphPad Software, Inc., La Jolla, CA, USA).

Results

AC treatment inhibits proliferation and induces caspase-independent apoptosis of the CCA cell line. Inhibition of tumor growth and induction of cellular apoptosis are important modes of action of the majority of phytochemical agents. To determine whether AC exerts proliferation-inhibitory effects on CCA cells, and to determine relevant IC_{50} values, KKU213 cells were treated with various concentrations of AC. The SRB assay revealed that AC inhibited cell proliferation in this cell

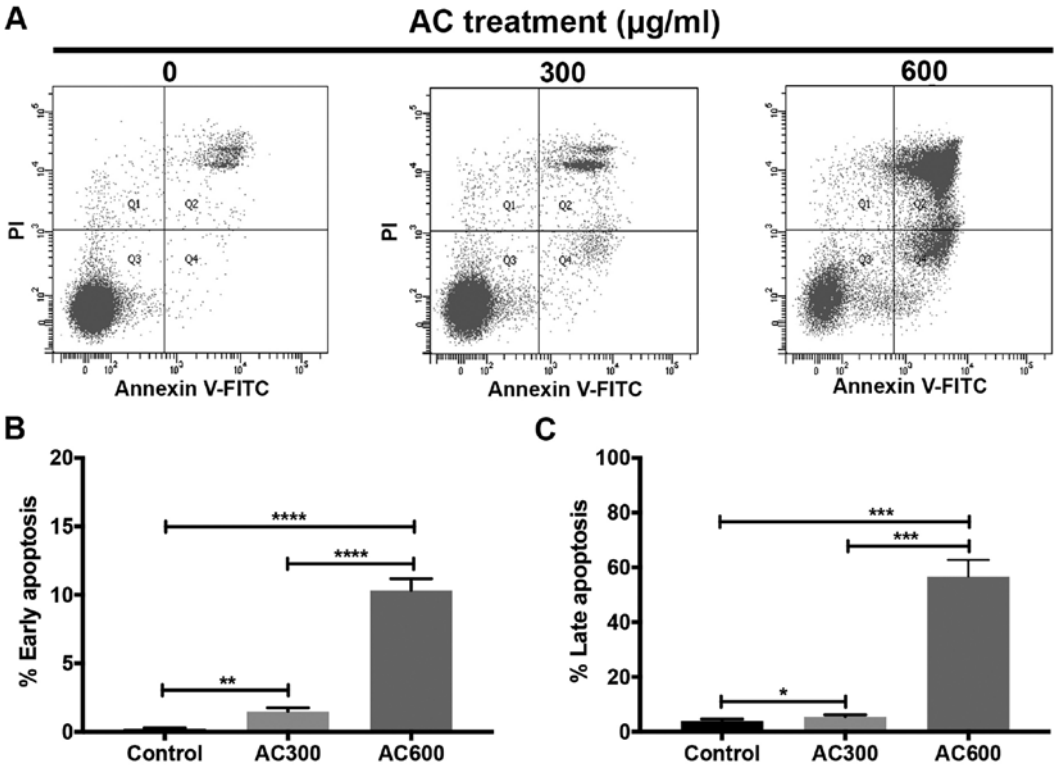

Figure 2. AC treatment induces apoptosis of CCA cells. (A) KKU213 cells were treated with AC at the indicated doses for 24 h. Apoptotic cells were stained with Annexin V-FITC/PI solution and analyzed by flow cytometry. Dimethyl sulfoxide at a final concentration of 0.1% was used as diluent control (0). (B) Percentages of early apoptosis and (C) late apoptosis of AC-treated KKU213 cells were calculated from three independent experiments. *P<0.05, **P<0.01, ***P<0.001 and ****P<0.0001. AC, anthocyanin complex; FITC, fluorescein isothiocyanate; PI, propidium iodide.

line in a dose- and time-dependent manner (Fig. 1A). The proliferation of KKU213 cells was completely inhibited by treatment with 800 μg/ml AC after 48 h. Non-linear regression analysis identified that the IC_{50} value of AC for KKU213 was 620 μg/ml (Fig. 1B).

It was subsequently investigated whether suppression of CCA cell proliferation by AC treatment is associated with induction of apoptosis. KKU213 cells were treated with 300 or 600 μg/ml AC for 24 h, and cellular apoptosis was investigated using flow cytometry (Fig. 2A). The results revealed that early (1.50±0.27% for AC300 and 10.33±0.83% for AC600) (Fig. 2B) and late (5.50±0.66% for AC300 and 56.70±6.05% for AC600) (Fig. 2C) apoptosis was significantly induced dose-dependently in AC-treated groups compared with the control group. These results indicated that AC exhibited cytotoxicity against CCA cells through the induction of cellular apoptosis. Levels of cleaved caspase-3, a protein marker for cellular apoptosis, was also assayed using western blotting. Cleaved caspase-3 was not observed in AC-treated KKU213 cells, but was detected in a gemcitabine-treated group (Fig. 3A). In addition, a pan-caspase inhibitor (Q-VD-OPh) was combined with AC treatment to test whether cell death was due to a caspase-independent pathway. A clonogenic assay demonstrated that treatment with 2 and 10 μM Q-VD-OPh, identified to prevent caspase activation (29), did not affect cell viability of the KKU213 cells (Fig. 3C). Notably, Q-VD-OPh treatment was not able to prevent cell death when combined with AC treatment (Fig. 3D and E), indicating that caspase-independent cell death was occurring in AC-treated CCA cells.

AC treatment inhibits colony formation of the CCA cell line. The clonogenic assay is the method of choice to determine cell reproductive viability (ability of cells to produce progeny or ability of a single cell to form a colony) following treatment with radiation or a cytotoxic agent (30,31). This approach was employed to determine the cytotoxic effects of AC treatment on a CCA cell line (Fig. 4A). Consistent with the results of the SRB assay, the presence of AC significantly inhibited KKU213 colony formation in a dose-dependent manner compared with the control group (P<0.0001) (Fig. 4B). This result indicated that the AC-mediated decrease in reproductive viability is one of the underlying molecular mechanisms of AC against CCA.

AC treatment induces mitochondrial superoxide production partly via suppression of Bcl-2 expression. Induction of superoxide production in mitochondria is an important event in the induction of apoptosis (32). To investigate whether induction of mitochondrial superoxide production is involved in AC-induced apoptosis of CCA cells, KKU213 cells were treated with AC, and levels of mitochondria-specific superoxide were determined using flow cytometry. Minimal superoxide production was detected in the control group; however, production was slightly increased in KKU213 cells treated with 300 μg/ml AC (Fig. 5). Treatment with 600 μg/ml AC significantly induced superoxide production in the mitochondria of KKU213 cells relative to the control group (P<0.001) (Fig. 5).

Since superoxide production may be inhibited by the anti-apoptotic Bcl-2 protein (32), the expression of Bcl-2 protein was investigated further in KKU213 CCA cells. Western blot

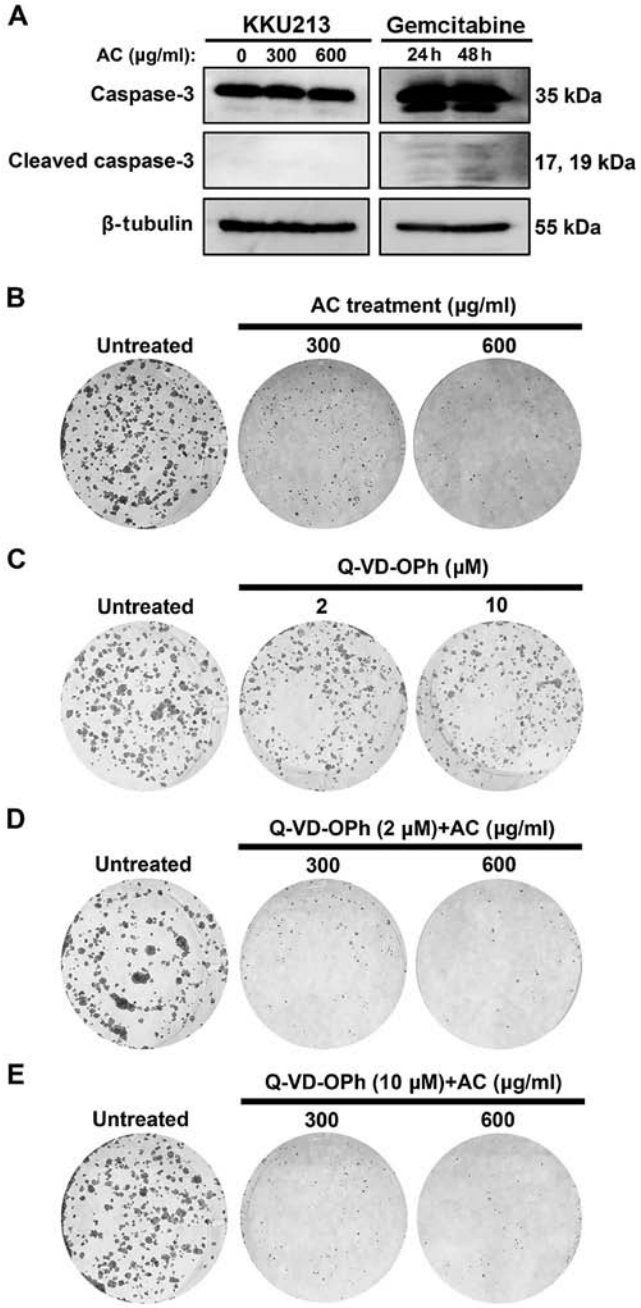

Figure 3. Pan-caspase inhibitor Q-VD-OPh does not protect KKU213 cells from AC-induced cell death. (A) Western blot analysis was performed to determine the expression of caspase-3 and its cleaved form in AC-treated KKU213 cells compared with cells treated with gemcitabine. β-tubulin was used as a loading control. The viability of KKU213 cells following (B) AC treatment, (C) Q-VD-OPh treatment and the combination of (D) 2 μM and (E) 10 μM Q-VD-OPh with AC treatment was determined using a clonogenic assay. Q-VD-OPh, quinolone-Val-Asp-difluorophenoxymethyl ketone; AC, anthocyanin complex.

analysis revealed that the expression of Bcl-2 protein mirrored superoxide production. Expression of Bcl-2 protein decreased in the AC-treated group, particularly when 600 μg/ml AC was used, relative to the DMSO-treated control (Fig. 6). These results indicated that AC induced superoxide production-mediated apoptosis partly via the inhibition of Bcl-2 protein expression.

AC treatment targets pro-survival and endoplasmic reticulum stress (ER stress) response of the CCA cell line. FOXM1 and NF-κB are well-known oncogenic proteins involved in the survival of cancer cells (33,34). The expression of these proteins was determined in the CCA cell line following treatment with AC for 24 h. Western blot analysis revealed that expression of FOXM1 and the p65 subunit of NF-κB decreased in a dose-dependent manner in KKU213 cells treated with AC (Fig. 6). Notably, expression of these proteins was almost completely inhibited in KKU213 cells treated with 600 μg/ml AC compared with the DMSO-treated control (Fig. 6). Additionally, KKU213 cells were transfected with p65 plasmid DNA and the influence of p65 induction on AC treatment of KKU213 cells was determined using a clonogenic assay. The p65 subunit of NF-κB was successfully induced in KKU213 as identified using western blot analysis (Fig. 7A). However, the clonogenic assay revealed that p65 overexpression did not affect the viability of KKU213 cells compared with non-transfected and mock-transfected controls (Fig. 7B and C). This implies that AC is a potent inducer of apoptosis against CCA cells, and that induction of a pro-survival transcription factor was not able to protect CCA cells from cell death following AC treatment. A previous study has identified that AC treatment dramatically induced mitochondrial superoxide production; excessive superoxide production may cause protein misfolding and ultimately induce ER stress (35). Therefore, the expression of proteins in the PERK/eIF2α/ATF4 axis, which is an important ER stress-response pathway, was investigated. Western blot analysis revealed that expression of PERK, p-eIF2α (Ser^{51}) and ATF4 in KKU213 cells decreased following AC treatment (Fig. 6). Notably, total eIF2α expression was not affected by AC treatment, suggesting that AC suppresses phosphorylation of the eIF2α protein. In addition to FOXM1, p65 and the PERK/eIF2α/ATF4 axis, it was identified that PARP expression was also suppressed by AC treatment, particularly at the highest dose used (Fig. 6).

AC treatment increases gemcitabine sensitivity of the gemcitabine-resistant KKU214^{GemR} CCA cell line. Resistance to chemotherapeutic treatment is an important obstacle for the treatment of various types of cancer, including CCA (36). Therefore, whether co-treatment with AC was able to enhance the effect of gemcitabine was investigated. The SRB assay revealed that the IC_{50} of gemcitabine against the KKU214^{GemR} CCA cell line was 32.11 μM at 72 h, whereas the IC_{50} of gemcitabine against the parental KKU214 cell line was 0.40 μM at 72 h (data not shown), agreeing with a previous study (28). Treatment of KKU214^{GemR} cells with AC inhibited cell proliferation in a dose- and time-dependent manner (Fig. 8A). For gemcitabine treatment alone, KKU214^{GemR} cell proliferation was markedly inhibited by treatment with 40 μM for 72 h (Fig. 8B). AC at a dose of 300 μg/ml, which did not exert a proliferation-inhibitory effect on KKU214^{GemR} cells, was selected for co-treatment with 20 or 40 μM gemcitabine. As expected, the two combinations significantly enhanced gemcitabine-mediated proliferation inhibition compared with treatments with single agents ($P<0.01$ for 20 μM gemcitabine vs. 300 μg/ml AC+20 μM gemcitabine; $P<0.001$ for 40 μM gemcitabine vs. 300 μg/ml AC+40 μM gemcitabine) (Fig. 8C). Furthermore, the clonogenic assay also identified a significant enhancement of gemcitabine treatment when co-treated with AC ($P<0.05$) (Fig. 8D). Annexin V/PI

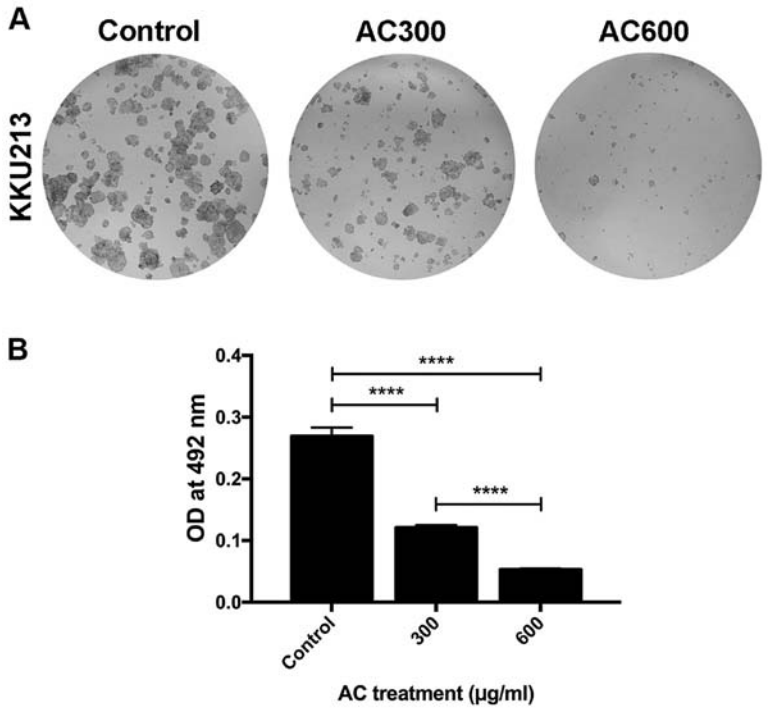

Figure 4. AC treatment decreases colony formation of CCA cells. (A) KKU213 cells were seeded in 6-well plates at a density of 1,000 cells/well and cultured with AC or dimethyl sulfoxide (control) for 48 h. At day 14, colony formation was visualized by crystal violet staining and images were captured using a digital camera. (B) Relative difference of colony formation of CCA cells was investigated by dissolving stained colonies with 33% acetic acid and determining the OD at 620 nm. ****P<0.0001. AC, anthocyanin complex; CCA, cholangiocarcinoma; OD, optical density.

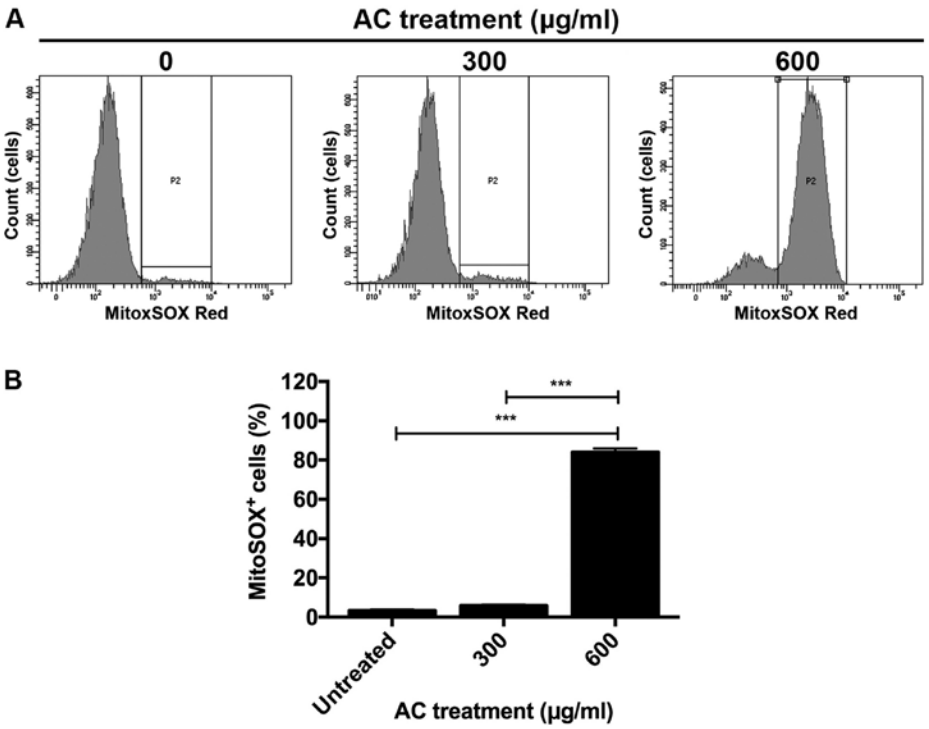

Figure 5. Mitochondrial superoxide production is markedly induced by AC treatment. (A) Mitochondrial superoxide production following AC treatment of KKU213 cells was determined using MitoSOX Red coupled with flow cytometry. A peak at P2 indicates superoxide production from mitochondria. Cells treated with dimethyl sulfoxide (0.1%) were used as diluent control. Experiments were performed in triplicate. (B) The percentage of mitochondrial superoxide production was calculated and plotted relative to the number of cells measured. ***P<0.001. AC, anthocyanin complex.

staining coupled with flow cytometry was used to detect apoptotic cells following combination treatment of KKU214^{GemR} cells. Administration of AC (300 μg/ml) and gemcitabine (40 μM) significantly induced early apoptosis of these cells compared with single treatments and the control group (P<0.0001) (Fig. 9). These results indicated that AC treatment

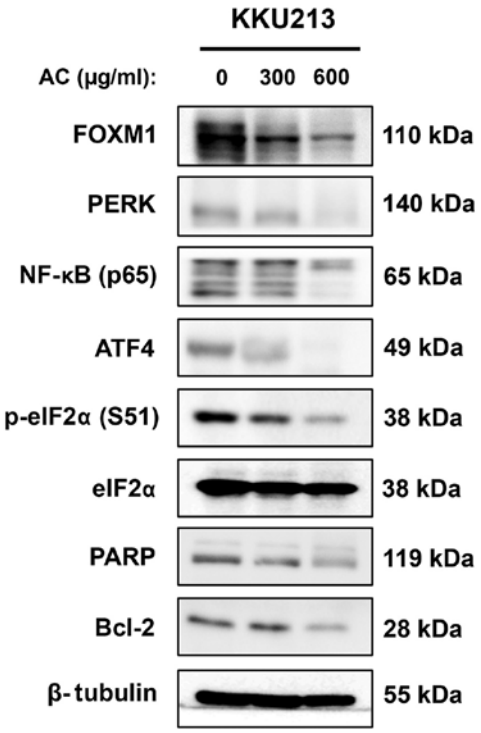

Figure 6. AC treatment downregulates the expression of a number of survival-associated proteins and endoplasmic reticulum stress proteins. KKU213 cells were treated with AC for 24 h prior to western blotting. β-tubulin expression was used as loading control. AC, anthocyanin complex; FOXM1, forkhead box M1; PERK, protein kinase RNA-like endoplasmic reticulum kinase; NF-κB, nuclear factor-κB; ATF4, activating transcription factor 4; eIF2α, eukaryotic initiation factor 2α; p-eIF2α, phosphorylated eIF2α; PARP, poly(ADP-ribose) polymerase; Bcl-2, B-cell lymphoma-2.

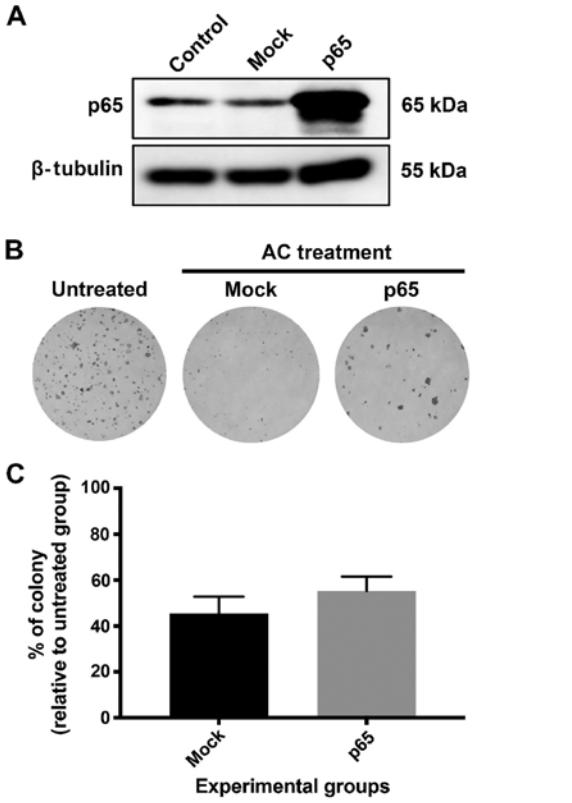

Figure 7. Overexpression of p65 NF-κB does not affect the anticancer activity of AC in the KKU213 cell line. Expression of p65 NF-κB was induced in KKU213 cells using a combination of pCMV4-p65 plasmid DNA and X-tremeGENE HP. (A) The expression of p65 in p65-transfected cells was detected by western blot analysis compared with control and mock transfections. (B) The effect of p65 overexpression on AC treatment was determined using a clonogenic assay. (C) Relative difference of colony formation of KKU213 cell line was investigated by dissolving stained colonies with 33% acetic acid and determining the optical density at 620 nm. NF-κB, nuclear factor-κB; AC, anthocyanin complex.

significantly enhanced the efficacy of gemcitabine against the gemcitabine-resistant KKU214^{GemR} cell line.

Discussion

Several previous studies have demonstrated that anthocyanins exert anticancer activity against various types of cancer, including HCC, melanoma, colon cancer, lung cancer and breast cancer (37-39). In our previous study, we developed a novel AC, which primarily consisted of extracts of purple corn cobs, blue butterfly peas and turmeric (26). The combination of these exhibited increased antioxidant activity and increased thermal stability compared with that of individual extracts (26). In the present study, to the best of our knowledge, we have identified, for the first time, anti-CCA activity of AC, which exhibited cytotoxicity against a CCA cell line through the suppression of cell proliferation and induction of caspase-independent apoptosis probably via increased mitochondrial superoxide production. Furthermore, AC also suppressed the expression of a number of oncogenic proteins that have previously been reported to be upregulated in CCA, including FOXM1, NF-κB and ER stress-response proteins. The potential underlying molecular mechanisms of AC treatment on CCA cells are summarized in Fig. 10. AC was able to potentiate gemcitabine treatment against the gemcitabine-resistant KKU214^{GemR} cell line. We therefore hypothesize that AC has a potential function as an alternative or supplementary treatment for CCA.

cDNA analysis of *O. viverrini*-associated CCA clinical samples revealed that FOXM1 was highly expressed, being the second most abundant gene in these samples (40). FOXM1 has been implicated primarily in cell proliferation and survival, as well as in cancer progression (34). In the present study, suppression of cell proliferation and induction of cellular apoptosis following AC treatment were observed alongside downregulation of FOXM1 expression. These results suggest that suppression of FOXM1 is, in part, the mode of action of AC against CCA. To the best of our knowledge, the present study is the first to identify the effects of cyanidin and delphinidin on FOXM1 expression. However, a previous study demonstrated that curcumin, an important bioactive compound in turmeric extract, was able to suppress FOXM1 (41). Therefore, suppression of FOXM1 using AC treatment is potentially mediated by either anthocyanin(s) (cyanidin and/or delphinidin) or turmeric extract or both. In addition to FOXM1, western blot analysis also demonstrated the downregulation of NF-κB in AC-treated CCA cells. NF-κB is a well-known transcription factor associated with inflammation and cancer (42-44). A previous study has identified that NF-κB, particularly its p65 subunit, was overexpressed in *O. viverrini*-associated CCA tumor tissues. Furthermore, treatment with dehydroxymethylepoxyquinomicin inhibited CCA cell proliferation and induced apoptosis

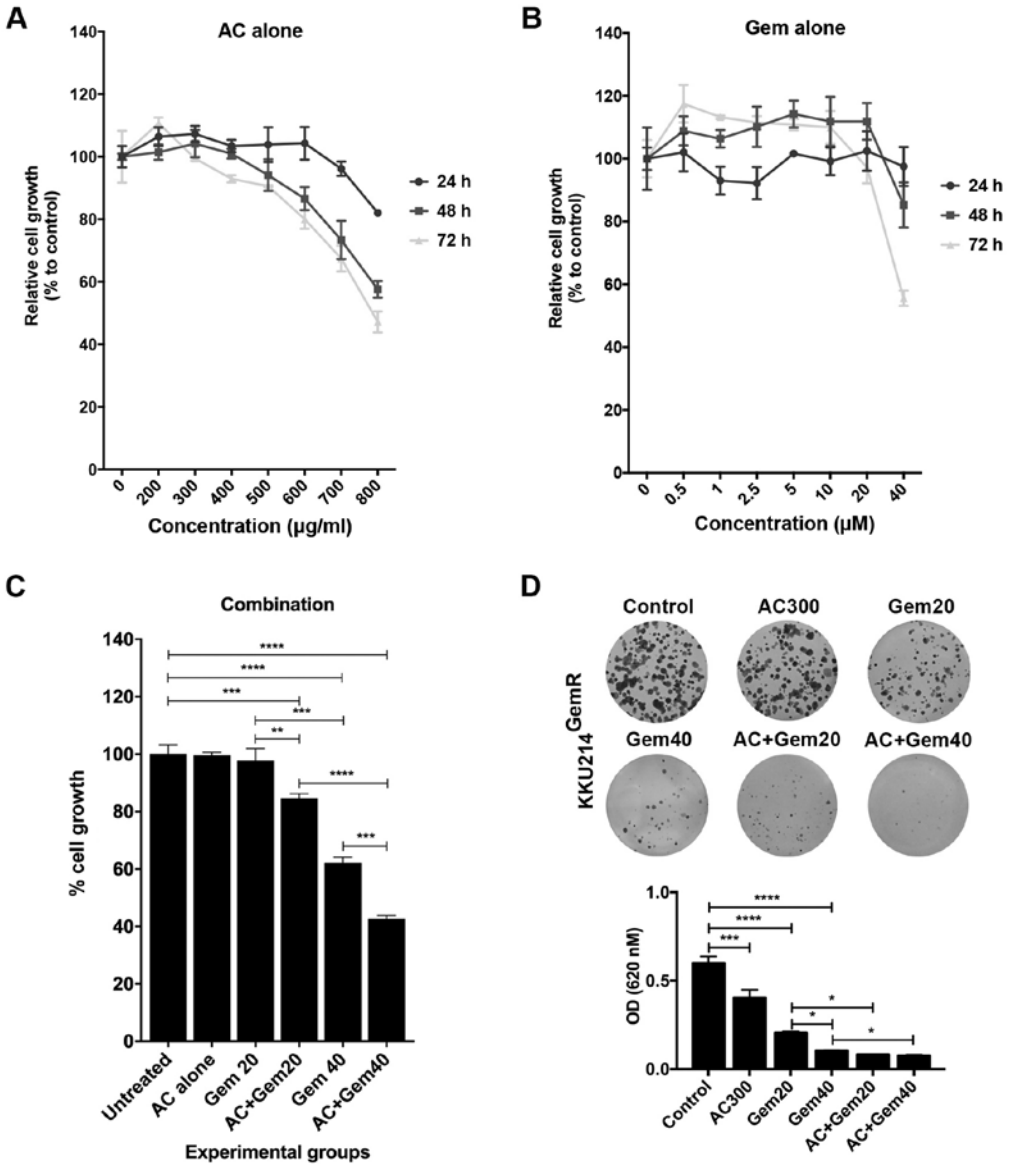

Figure 8. AC treatment sensitizes the KKU214^{GemR} cell line to gemcitabine treatment. KKU214^{GemR} cells were seeded in 96-well plates and treated with either (A) AC alone or (B) gemcitabine alone at indicated times. (C) Cells were treated with either the single agent (AC or gemcitabine) or a combination of AC (300 μg/ml) and gemcitabine (20 or 40 μM) for 72 h. The percentage of cell proliferation (relative to control) was determined using the SRB assay. Inhibition of cell proliferation was observed in the combination treatment compared with treatment with either agent alone. (D) Effect of combined treatment on colony formation of KKU214^{GemR} cells was also determined using the clonogenic assay. The relative difference in colony formation of KKU214^{GemR} cells was investigated by dissolving stained colonies with 33% acetic acid and absorbance at the OD at 620 nm was determined using an ELISA reader. *P<0.05, **P<0.01, ***P<0.001 and ****P<0.0001. AC, anthocyanin complex; Gem, gemcitabine; OD, optical density.

in KKU213 cells via the suppression of NF-κB and Bcl-2 proteins (45). The results of the present study are in general agreement with this previous study, demonstrating that the p65 subunit of NF-κB and Bcl-2 were also suppressed concurrently with induction of apoptosis in the AC-treated KKU213 CCA cell line. Cyanidin and delphinidin are known to suppress the expression of NF-κB and Bcl-2 (46,47). Furthermore, the turmeric extract in AC was also identified to suppress NF-κB and Bcl-2 (48,49). Therefore, we hypothesized that cyanidin, delphinidin and turmeric extract in AC may synergistically inhibit NF-κB and Bcl-2. Curcumin, an important active ingredient in turmeric extract, is able to inhibit NF-κB expression and induce cancer cell apoptosis. AC, composed of purple corn cob, blue butterfly pea and turmeric extracts at a ratio of 7:2:1, contains ~60 μg turmeric extract per 600 μg/ml AC. In its standard form, turmeric contains 5% curcumin, implying that there is ~3 μg or 8 μM curcumin in 60 μg turmeric extract. In our previous study, we identified that significant suppression of proliferation, induction of apoptosis (4% of the cell population compared with the untreated control) and suppression of pro-survival proteins in the KKU213 cell line were only observed when treated with 50 μM curcumin (49). The synergistic effect of combining different anthocyanins was also demonstrated previously (50,51). These results support our hypothesis that the cytotoxicity of AC against CCA cells is mediated by synergism of cyanidin, delphinidin and turmeric extract. Notably, in the present study, the function of p65 on AC treatment of KKU213 cells was also determined using p65 plasmid DNA transfection coupled with a clonogenic assay. Although p65 was successfully induced in KKU213 cells, the clonogenic assay revealed that

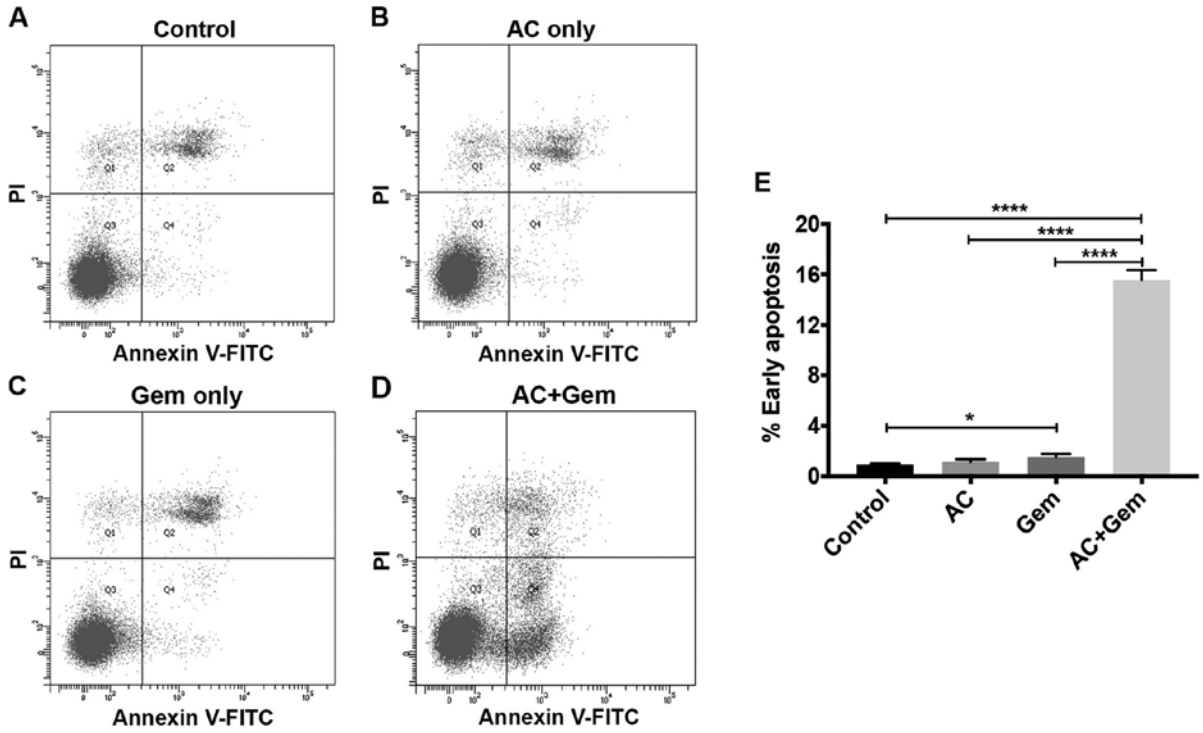

Figure 9. Combination of AC and gemcitabine treatment induces early apoptosis of the KKU214^{GemR} cell line. KKU214^{GemR} cells were treated with (A) 0.1% dimethyl sulfoxide, (B) AC (300 μg/ml) or (C) gemcitabine (40 μM), or (D) a combination of AC (300 μg/ml) and gemcitabine (40 μM) for 72 h. Apoptotic cells were stained with Annexin V-FITC/PI solution and analyzed using flow cytometry. (E) The percentage of cells undergoing early apoptosis was calculated from three independent experiments. *P<0.05 and ****P<0.0001. AC, anthocyanin complex; FITC, fluorescein isothiocyanate; PI, propidium iodide; Gem, gemcitabine.

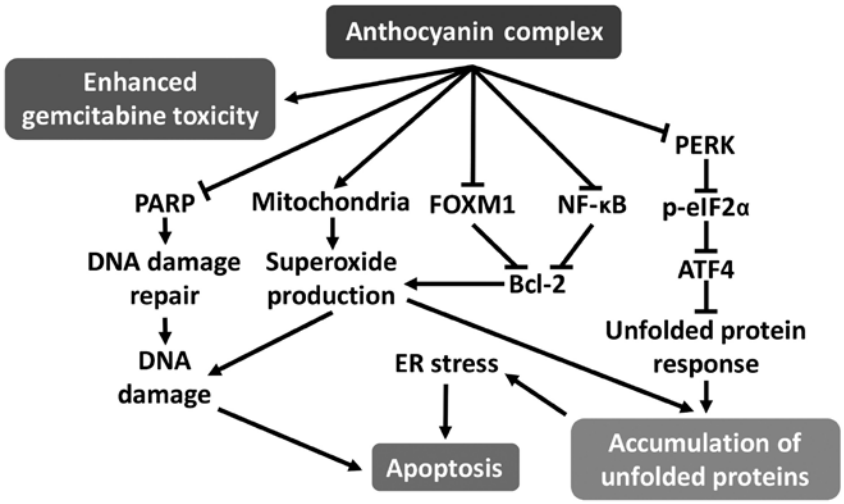

Figure 10. Schematic diagram of the postulated mechanism of AC against CCA cell lines. AC treatment downregulates FOXM1 and NF-κB expression, leading to suppression of Bcl-2 expression. AC treatment also stimulates superoxide production from mitochondria, in part due to Bcl-2 suppression, since this protein serves a function in inhibiting superoxide production from mitochondria. Massive superoxide production leads to DNA damage. Inhibition of the DNA damage-repair protein PARP by AC treatment may induce DNA damage-mediated apoptosis. In addition to DNA damage, superoxide production may result in the induction of protein misfolding or of unfolded proteins, accumulation of which stimulates the UPR in the ER. AC treatment inhibits the primary UPR pathway (PERK/eIF2α/ATF4), leading to ER stress and induction of apoptosis. AC, anthocyanin complex; CCA, cholangiocarcinoma; FOXM1, forkhead box M1; NF-κB, nuclear factor-κB; Bcl-2, B-cell lymphoma-2; PARP, poly(ADP-ribose) polymerase; UPR, unfolded protein response; ER, endoplasmic reticulum; PERK, protein kinase RNA-like ER kinase; eIF2α, eukaryotic initiation factor 2α; ATF4, activating transcription factor 4.

induction of pro-survival transcription factor expression was not able to protect KKU213 cells from apoptosis following AC treatment. Failure of NF-κB to prevent cell death has also been demonstrated in tumor necrosis factor α-induced apoptosis in the HeLa cell line (52). Furthermore, failure to escape apoptosis following p65 induction may be because AC treatment induces CCA cell apoptosis through multiple pathways. Therefore, AC is a potent apoptosis inducer against CCA cells.

AC treatment also markedly induced superoxide production from mitochondria in KKU213 cells. Mitochondrial superoxide has been demonstrated as an inducer of apoptosis (32). Apoptosis induced in this manner is consistent with a previous

study demonstrating that diphenyleneiodonium induces mitochondrial superoxide-mediated apoptosis (53). Notably, in the present study, cleaved PARP (data not shown) and cleaved caspase-3 were not observed after 24 h of AC treatment in CCA cell lines, suggesting that caspase-independent cell death occurred without activating Bcl-2-associated X protein, cytochrome *c* and caspase-3 (54). Caspase-independent cell death was also indicated by treatment with a combination of AC and pan-caspase inhibitor (Q-VD-OPh): addition of Q-VD-OPh was not able to protect CCA cells from AC-mediated cell death. The defects in the caspase activation pathway are common in cancer, leading to resistance to certain pro-apoptotic stimuli (55). Therefore, triggering caspase-independent cell death is one of the novel approaches to treat cancer (56). Therefore, in addition to CCA, the AC may be useful for the treatment of cancer, particularly that with the ability to evade caspase-dependent cell death. Decreasing PARP expression in CCA cell lines was observed following AC treatment. This result may be explained by the fact that this protein is involved in DNA damage repair (57). Induction of mitochondrial superoxide production was able to induce DNA damage (58,59), suggesting that decreasing of PARP expression after AC treatment could lead to a decrease in DNA damage repair by PARP. Therefore, we hypothesize that AC-treated cells underwent apoptosis via DNA damage-induced caspase-independent cell death (60).

Superoxide in mitochondria may be converted into H_2O_2 and diffuse into the cytoplasm. H_2O_2 may be catalyzed further to form other highly reactive oxygen species (ROS). Under basal physiological conditions, ROS accumulation may be prevented by cellular antioxidant defense mechanisms (61). However, excessive ROS production caused by excessive mitochondrial superoxide production triggers disturbance of ER redox homeostasis, thus aggravating the accumulation of misfolded or unfolded proteins in the ER or ER stress (62). The process known as the unfolded protein response (UPR) is thus activated to restore ER homeostasis (63). However, if ER stress is severe or prolonged, it may induce cell death (64). The PERK/eIF2α/ATF4 axis is important in UPR signaling during ER stress (65). PERK activates the phosphorylation of eIF2α at Ser^{51}, resulting in global translation inhibition (66), but induces the expression of ATF4 (67) to overcome ER stress. The results of the present study identified downregulation of PERK/eIF2α/ATF4 in an AC-treated CCA cell line. Therefore, we hypothesize that AC treatment induces ER stress and eventual cell death via the stimulation of mitochondrial superoxide production and suppression of PERK/eIF2α/ATF4 axis-mediated UPR. This hypothesis is supported by previous studies demonstrating that inhibition of PERK or eIF2α rendered cells susceptible to ER stress-mediated cell death (68-70). Furthermore, a recent study has demonstrated that activation of PERK and eIF2α was inhibited in cyanidin-treated cells (71).

Drug resistance is a major barrier for chemotherapy in a number of types of cancer, including CCA. Enhancement of chemotherapeutic drug treatment and chemosensitization of cancer cells by plant polyphenols have been the focus of much work and discussion (72). In the present study, the effect of co-treatment of AC and gemcitabine against a gemcitabine-resistant $KKU214^{GemR}$ cell line was investigated. It was identified that $KKU214^{GemR}$ cells were ~80-fold more resistant to gemcitabine compared with its parental cell line. However, the combination of AC with gemcitabine significantly enhanced the efficacy of gemcitabine against $KKU214^{GemR}$ cells compared with single agent treatment. Although the potential of AC against a CCA cell line as well as its potential as a chemosensitizer in a gemcitabine-resistant CCA cell line have been demonstrated in the present study, these results have not been verified in an animal model of CCA. Therefore, the anticancer activity of AC should be investigated further in xenograft mouse or liver fluke-induced hamster CCA models. Furthermore, the anticancer potential of AC requires testing in diverse cancer cell types to support its potential use as an alternative or supplementary treatment for cancer, particularly CCA. Additionally, high-throughput approaches, including RNA sequencing, are required to explore the precise mechanisms underlying anticancer and chemosensitization activities of AC.

In conclusion, the results of the present study demonstrated that AC possesses cytotoxicity against CCA cell lines by suppression of cell proliferation and induction of caspase-independent apoptosis possibly via downregulation of FOXM1, NF-κB and the ER stress response, and by induction of mitochondrial superoxide production. AC also sensitizes $KKU214^{GemR}$ cells to gemcitabine treatment. Therefore, AC has potential as an alternative treatment agent and may assist in overcoming drug resistance of CCA when co-administered with other chemotherapeutic agents.

Acknowledgements

The authors thank Miss Sucharat Limsitthichaikoon for assisting with AC preparation and the Research Instrument Unit, Faculty of Medicine, Khon Kaen University, Khon Kaen, Thailand, for technical and facility support.

Funding

This study was supported in part by the Thailand Research Fund (TRF) and Khon Kaen University through Royal Golden Jubilee PhD joint funding program (grant no. PHD/0166/2553) and also by the TRF and Medical Research Council (MRC) UK via TRF-MRC Joint Health Research (grant no. DBG5980004) and Khon Kaen University Research Fund (grant no. KKU600701).

Availability of data and materials

The data sets generated during the study are available from the corresponding author on reasonable request.

Authors' contributions

SP and KI mainly designed, performed the research and wrote the manuscript. KI analyzed the data, and AP, CP, CH, KV and PP helped to prepare and provided materials, and analyzed the data. All authors have read and approved the final version of the manuscript.

Ethics approval and consent to participate

Not applicable.

Consent for publication

Not applicable.

Competing interests

The authors declare that they have no competing interests.

References

1. Banales JM, Cardinale V, Carpino G, Marzioni M, Andersen JB, Invernizzi P, Lind GE, Folseraas T, Forbes SJ, Fouassier L, *et al*: Expert consensus document: Cholangiocarcinoma: Current knowledge and future perspectives consensus statement from the European Network for the Study of Cholangiocarcinoma (ENS-CCA). Nat Rev Gastroenterol Hepatol 13: 261-280, 2016.
2. Kirstein MM and Vogel A: Epidemiology and risk factors of cholangiocarcinoma. Visc Med 32: 395-400, 2016.
3. Sripa B and Pairojkul C: Cholangiocarcinoma: Lessons from Thailand. Curr Opin Gastroenterol 24: 349-356, 2008.
4. IARC: A Review of Human Carcinogens: *Opisthorchis viverrini* and *Clonorchis sinensis*. IARC Monogr Eval Carcinog Risks Hum 100B: 341-370, 2012.
5. Sripa B, Brindley PJ, Mulvenna J, Laha T, Smout MJ, Mairiang E, Bethony JM and Loukas A: The tumorigenic liver fluke *Opisthorchis viverrini* - multiple pathways to cancer. Trends Parasitol 28: 395-407, 2012.
6. Prakobwong S, Pinlaor S, Yongvanit P, Sithithaworn P, Pairojkul C and Hiraku Y: Time profiles of the expression of metalloproteinases, tissue inhibitors of metalloproteases, cytokines and collagens in hamsters infected with *Opisthorchis viverrini* with special reference to peribiliary fibrosis and liver injury. Int J Parasitol 39: 825-835, 2009.
7. Loaharanu P and Sornmani S: Preliminary estimates of economic impact of liver fluke infection in Thailand and the feasibility of irradiation as a control measure. Southeast Asian J Trop Med Public Health 22 (Suppl 22): 384-390, 1991.
8. Khan SA, Davidson BR, Goldin R, Pereira SP, Rosenberg WM, Taylor-Robinson SD, Thillainayagam AV, Thomas HC, Thursz MR and Wasan H; British Society of Gastroenterology: Guidelines for the diagnosis and treatment of cholangiocarcinoma: Consensus document. Gut 51 (Suppl 6): VI1-VI9, 2002.
9. Anderson CD, Pinson CW, Berlin J and Chari RS: Diagnosis and treatment of cholangiocarcinoma. Oncologist 9: 43-57, 2004.
10. Valle J, Wasan H, Palmer DH, Cunningham D, Anthoney A, Maraveyas A, Madhusudan S, Iveson T, Hughes S, Pereira SP, *et al*; ABC-02 Trial Investigators: Cisplatin plus gemcitabine versus gemcitabine for biliary tract cancer. N Engl J Med 362: 1273-1281, 2010.
11. Surh YJ: Cancer chemoprevention with dietary phytochemicals. Nat Rev Cancer 3: 768-780, 2003.
12. Wang H, Khor TO, Shu L, Su ZY, Fuentes F, Lee JH and Kong AN: Plants vs. cancer: A review on natural phytochemicals in preventing and treating cancers and their druggability. Anticancer Agents Med Chem 12: 1281-1305, 2012.
13. Singh CK, Siddiqui IA, El-Abd S, Mukhtar H and Ahmad N: Combination chemoprevention with grape antioxidants. Mol Nutr Food Res 60: 1406-1415, 2016.
14. Castañeda-Ovando A, Pacheco-Hernández ML, Páez-Hernández ME, Rodríguez JA and Galán-Vidal CA: Pacheco-Hernández MdL, Páez-Hernández ME, Rodríguez JA and Galán-Vidal CA: Chemical studies of anthocyanins: A review. Food Chem 113: 859-871, 2009.
15. Cerletti C, De Curtis A, Bracone F, Digesù C, Morganti AG, Iacoviello L, de Gaetano G and Donati MB: Dietary anthocyanins and health: Data from FLORA and ATHENA EU projects. Br J Clin Pharmacol 83: 103-106, 2017.
16. Lin BW, Gong CC, Song HF and Cui YY: Effects of anthocyanins on the prevention and treatment of cancer. Br J Pharmacol 174: 1226-1243, 2017.
17. Li D, Wang P, Luo Y, Zhao M and Chen F: Health benefits of anthocyanins and molecular mechanisms: Update from recent decade. Crit Rev Food Sci Nutr 57: 1729-1741, 2017.
18. Yousuf B, Gul K, Wani AA and Singh P: Health benefits of anthocyanins and their encapsulation for potential use in food systems: A Review. Crit Rev Food Sci Nutr 56: 2223-2230, 2016.
19. Nichenametla SN, Taruscio TG, Barney DL and Exon JH: A review of the effects and mechanisms of polyphenolics in cancer. Crit Rev Food Sci Nutr 46: 161-183, 2006.
20. Umar Lule S and Xia W: Food phenolics, pros and cons: A Review. Food Rev Int 21: 367-388, 2005.
21. Wang LS and Stoner GD: Anthocyanins and their role in cancer prevention. Cancer Lett 269: 281-290, 2008.
22. Yang X, Luo E, Liu X, Han B, Yu X and Peng X: Delphinidin-3-glucoside suppresses breast carcinogenesis by inactivating the Akt/HOTAIR signaling pathway. BMC Cancer 16: 423, 2016.
23. Chen PN, Chu SC, Chiou HL, Kuo WH, Chiang CL and Hsieh YS: Mulberry anthocyanins, cyanidin 3-rutinoside and cyanidin 3-glucoside, exhibited an inhibitory effect on the migration and invasion of a human lung cancer cell line. Cancer Lett 235: 248-259, 2006.
24. Kamei H, Kojima T, Hasegawa M, Koide T, Umeda T, Yukawa T and Terabe K: Suppression of tumor cell growth by anthocyanins in vitro. Cancer Invest 13: 590-594, 1995.
25. Eiro MJ and Heinonen M: Anthocyanin color behavior and stability during storage: Effect of intermolecular copigmentation. J Agric Food Chem 50: 7461-7466, 2002.
26. Intuyod K, Priprem A, Limphirat W, Charoensuk L, Pinlaor P, Pairojkul C, Lertrat K and Pinlaor S: Anti-inflammatory and anti-periductal fibrosis effects of an anthocyanin complex in *Opisthorchis viverrini*-infected hamsters. Food Chem Toxicol 74: 206-215, 2014.
27. Tepsiri N, Chaturat L, Sripa B, Namwat W, Wongkham S, Bhudhisawasdi V and Tassaneeyakul W: Drug sensitivity and drug resistance profiles of human intrahepatic cholangiocarcinoma cell lines. World J Gastroenterol 11: 2748-2753, 2005.
28. Wattanawongdon W, Hahnvajanawong C, Namwat N, Kanchanawat S, Boonmars T, Jearanaikoon P, Leelayuwat C, Techasen A and Seubwai W: Establishment and characterization of gemcitabine-resistant human cholangiocarcinoma cell lines with multidrug resistance and enhanced invasiveness. Int J Oncol 47: 398-410, 2015.
29. Kuželová K, Grebeňová D and Brodská B: Dose-dependent effects of the caspase inhibitor Q-VD-OPh on different apoptosis-related processes. J Cell Biochem 112: 3334-3342, 2011.
30. Franken NA, Rodermond HM, Stap J, Haveman J and van Bree C: Clonogenic assay of cells in vitro. Nat Protoc 1: 2315-2319, 2006.
31. Puck TT and Marcus PI: Action of x-rays on mammalian cells. J Exp Med 103: 653-666, 1956.
32. Cai J and Jones DP: Superoxide in apoptosis. Mitochondrial generation triggered by cytochrome *c* loss. J Biol Chem 273: 11401-11404, 1998.
33. Piva R, Belardo G and Santoro MG: NF-kappaB: A stress-regulated switch for cell survival. Antioxid Redox Signal 8: 478-486, 2006.
34. Myatt SS and Lam EW: The emerging roles of forkhead box (Fox) proteins in cancer. Nat Rev Cancer 7: 847-859, 2007.
35. Cao SS and Kaufman RJ: Endoplasmic reticulum stress and oxidative stress in cell fate decision and human disease. Antioxid Redox Signal 21: 396-413, 2014.
36. Holohan C, Van Schaeybroeck S, Longley DB and Johnston PG: Cancer drug resistance: An evolving paradigm. Nat Rev Cancer 13: 714-726, 2013.
37. Longo L, Platini F, Scardino A, Alabiso O, Vasapollo G and Tessitore L: Autophagy inhibition enhances anthocyanin-induced apoptosis in hepatocellular carcinoma. Mol Cancer Ther 7: 2476-2485, 2008.
38. Neto CC, Amoroso JW and Liberty AM: Anticancer activities of cranberry phytochemicals: An update. Mol Nutr Food Res 52 (Suppl 1): S18-S27, 2008.
39. Rugină D, Hanganu D, Diaconeasa Z, Tăbăran F, Coman C, Leopold L, Bunea A and Pintea A: Antiproliferative and apoptotic potential of cyanidin-based anthocyanins on melanoma cells. Int J Mol Sci 18: 949-959, 2017.
40. Jinawath N, Chamgramol Y, Furukawa Y, Obama K, Tsunoda T, Sripa B, Pairojkul C and Nakamura Y: Comparison of gene expression profiles between *Opisthorchis viverrini* and non-*Opisthorchis viverrini* associated human intrahepatic cholangiocarcinoma. Hepatology 44: 1025-1038, 2006.
41. Zhang JR, Lu F, Lu T, Dong WH, Li P, Liu N, Ma DX and Ji CY: Inactivation of FoxM1 transcription factor contributes to curcumin-induced inhibition of survival, angiogenesis, and chemosensitivity in acute myeloid leukemia cells. J Mol Med (Berl) 92: 1319-1330, 2014.
42. Karin M: Nuclear factor-kappaB in cancer development and progression. Nature 441: 431-436, 2006.

43. Hoesel B and Schmid JA: The complexity of NF-κB signaling in inflammation and cancer. Mol Cancer 12: 86, 2013.
44. Baldwin AS Jr: The NF-kappa B and I kappa B proteins: New discoveries and insights. Annu Rev Immunol 14: 649-683, 1996.
45. Seubwai W, Wongkham C, Puapairoj A, Khuntikeo N, Pugkhem A, Hahnvajanawong C, Chaiyagool J, Umezawa K, Okada S and Wongkham S: Aberrant expression of NF-κB in liver fluke associated cholangiocarcinoma: Implications for targeted therapy. PLoS One 9: e106056, 2014.
46. Hafeez BB, Siddiqui IA, Asim M, Malik A, Afaq F, Adhami VM, Saleem M, Din M and Mukhtar H: A dietary anthocyanidin delphinidin induces apoptosis of human prostate cancer PC3 cells in vitro and in vivo: Involvement of nuclear factor-kappaB signaling. Cancer Res 68: 8564-8572, 2008.
47. Hecht SS, Huang C, Stoner GD, Li J, Kenney PM, Sturla SJ and Carmella SG: Identification of cyanidin glycosides as constituents of freeze-dried black raspberries which inhibit anti-benzo[a]pyrene-7,8-diol-9,10-epoxide induced NFkappaB and AP-1 activity. Carcinogenesis 27: 1617-1626, 2006.
48. Kim JH, Gupta SC, Park B, Yadav VR and Aggarwal BB: Turmeric (*Curcuma longa*) inhibits inflammatory nuclear factor (NF)-κB and NF-κB-regulated gene products and induces death receptors leading to suppressed proliferation, induced chemosensitization, and suppressed osteoclastogenesis. Mol Nutr Food Res 56: 454-465, 2012.
49. Prakobwong S, Gupta SC, Kim JH, Sung B, Pinlaor P, Hiraku Y, Wongkham S, Sripa B, Pinlaor S and Aggarwal BB: Curcumin suppresses proliferation and induces apoptosis in human biliary cancer cells through modulation of multiple cell signaling pathways. Carcinogenesis 32: 1372-1380, 2011.
50. Rahman MM, Ichiyanagi T, Komiyama T, Hatano Y and Konishi T: Superoxide radical- and peroxynitrite-scavenging activity of anthocyanins; structure-activity relationship and their synergism. Free Radic Res 40: 993-1002, 2006.
51. Kausar H, Jeyabalan J, Aqil F, Chabba D, Sidana J, Singh IP and Gupta RC: Berry anthocyanidins synergistically suppress growth and invasive potential of human non-small-cell lung cancer cells. Cancer Lett 325: 54-62, 2012.
52. Casanelles E, Gozzelino R, Marqués-Fernández F, Iglesias-Guimarais V, Garcia-Belinchón M, Sánchez-Osuna M, Solé C, Moubarak RS, Comella JX and Yuste VJ: NF-κB activation fails to protect cells to TNFα-induced apoptosis in the absence of Bcl-xL, but not Mcl-1, Bcl-2 or Bcl-w. Biochim Biophys Acta 1833: 1085-1095, 2013.
53. Li N, Ragheb K, Lawler G, Sturgis J, Rajwa B, Melendez JA and Robinson JP: DPI induces mitochondrial superoxide-mediated apoptosis. Free Radic Biol Med 34: 465-477, 2003.
54. Kondo K, Obitsu S, Ohta S, Matsunami K, Otsuka H and Teshima R: Poly(ADP-ribose) polymerase (PARP)-1-independent apoptosis-inducing factor (AIF) release and cell death are induced by eleostearic acid and blocked by alpha-tocopherol and MEK inhibition. J Biol Chem 285: 13079-13091, 2010.
55. Fernald K and Kurokawa M: Evading apoptosis in cancer. Trends Cell Biol 23: 620-633, 2013.
56. Mathiasen IS and Jäättelä M: Triggering caspase-independent cell death to combat cancer. Trends Mol Med 8: 212-220, 2002.
57. Herceg Z and Wang ZQ: Functions of poly(ADP-ribose) polymerase (PARP) in DNA repair, genomic integrity and cell death. Mutat Res 477: 97-110, 2001.
58. Schieber M and Chandel NS: ROS function in redox signaling and oxidative stress. Curr Biol 24: R453-R462, 2014.
59. Dizdaroglu M, Jaruga P, Birincioglu M and Rodriguez H: Free radical-induced damage to DNA: Mechanisms and measurement. Free Radic Biol Med 32: 1102-1115, 2002.
60. Borges HL, Linden R and Wang JY: DNA damage-induced cell death: Lessons from the central nervous system. Cell Res 18: 17-26, 2008.
61. Murphy MP: How mitochondria produce reactive oxygen species. Biochem J 417: 1-13, 2009.
62. Higa A and Chevet E: Redox signaling loops in the unfolded protein response. Cell Signal 24: 1548-1555, 2012.
63. Schröder M and Kaufman RJ: ER stress and the unfolded protein response. Mutat Res 569: 29-63, 2005.
64. Xu C, Bailly-Maitre B and Reed JC: Endoplasmic reticulum stress: Cell life and death decisions. J Clin Invest 115: 2656-2664, 2005.
65. Ron D: Translational control in the endoplasmic reticulum stress response. J Clin Invest 110: 1383-1388, 2002.
66. Shi Y, Vattem KM, Sood R, An J, Liang J, Stramm L and Wek RC: Identification and characterization of pancreatic eukaryotic initiation factor 2 alpha-subunit kinase, PEK, involved in translational control. Mol Cell Biol 18: 7499-7509, 1998.
67. Harding HP, Novoa I, Zhang Y, Zeng H, Wek R, Schapira M and Ron D: Regulated translation initiation controls stress-induced gene expression in mammalian cells. Mol Cell 6: 1099-1108, 2000.
68. Scheuner D, Song B, McEwen E, Liu C, Laybutt R, Gillespie P, Saunders T, Bonner-Weir S and Kaufman RJ: Translational control is required for the unfolded protein response and in vivo glucose homeostasis. Mol Cell 7: 1165-1176, 2001.
69. Harding HP, Zhang Y, Bertolotti A, Zeng H and Ron D: Perk is essential for translational regulation and cell survival during the unfolded protein response. Mol Cell 5: 897-904, 2000.
70. Rajesh K, Krishnamoorthy J, Kazimierczak U, Tenkerian C, Papadakis AI, Wang S, Huang S and Koromilas AE: Phosphorylation of the translation initiation factor eIF2α at serine 51 determines the cell fate decisions of Akt in response to oxidative stress. Cell Death Dis 6: e1591, 2015.
71. Thummayot S, Tocharus C, Suksamrarn A and Tocharus J: Neuroprotective effects of cyanidin against Aβ-induced oxidative and ER stress in SK-N-SH cells. Neurochem Int 101: 15-21, 2016.
72. Garg AK, Buchholz TA and Aggarwal BB: Chemosensitization and radiosensitization of tumors by plant polyphenols. Antioxid Redox Signal 7: 1630-1647, 2005.

Intuyod et al. *Cell Death and Disease* (2018)9:1185
https://doi.org/10.1038/s41419-018-1235-0

Cell Death & Disease

ARTICLE Open Access

FOXM1 modulates 5-fluorouracil sensitivity in cholangiocarcinoma through thymidylate synthase (TYMS): implications of FOXM1–TYMS axis uncoupling in 5-FU resistance

Kitti Intuyod[1,2,3], Paula Saavedra-García[1], Stefania Zona[1], Chun-Fui Lai[1], Yannasittha Jiramongkol[1], Kulthida Vaeteewoottacharn[3,4], Chawalit Pairojkul[3,5], Shang Yao[1], Jay-Sze Yong[1], Sasanan Trakansuebkul[1], Sakda Waraasawapati[3,5], Vor Luvira[3,6], Sopit Wongkham[3,4], Somchai Pinlaor[3,7] and Eric W.-F. Lam[1]

Abstract

Fluorouracil (5-FU) is the first-line chemotherapeutic drug for cholangiocarcinoma (CCA), but its efficacy has been compromised by the development of resistance. Development of 5-FU resistance is associated with elevated expression of its cellular target, thymidylate synthase (TYMS). E2F1 transcription factor has previously been shown to modulate the expression of FOXM1 and TYMS. Immunohistochemical (IHC) analysis revealed a strong correlated upregulation of FOXM1 (78%) and TYMS (48%) expression at the protein levels in CCA tissues. In agreement, RT-qPCR and western blot analyses of four human CCA cell lines at the baseline level and in response to high doses of 5-FU revealed good correlations between FOXM1 and TYMS expression in the CCA cell lines tested, except for the highly 5-FU-resistant HuCCA cells. Consistently, siRNA-mediated knockdown of FOXM1 reduced the clonogenicity and TYMS expression in the relatively sensitive KKU-D131 but not in the highly resistant HuCCA cells. Interestingly, silencing of TYMS sensitized both KKU-D131 and HuCCA to 5-FU treatment, suggesting that resistance to very high levels of 5-FU is due to the inability of the genotoxic sensor FOXM1 to modulate TYMS expression. Consistently, ChIP analysis revealed that FOXM1 binds efficiently to the TYMS promoter and modulates TYMS expression at the promoter level upon 5-FU treatment in KKU-D131 but not in HuCCA cells. In addition, E2F1 expression did not correlate with either FOXM1 or TYMS expression and E2F1 depletion has no effects on the clonogenicity and TYMS expression in the CCA cells. In conclusion, our data show that FOXM1 regulates TYMS expression to modulate 5-FU resistance in CCA and that severe 5-FU resistance can be caused by the uncoupling of the regulation of TYMS by FOXM1. Our findings suggest that the FOXM1–TYMS axis can be a novel diagnostic, predictive and prognostic marker as well as a therapeutic target for CCA.

Introduction

Opisthorchiasis, a hepatobiliary disease caused by infection with a small human liver fluke *Opisthorchis viverrini*, is a major health problem in Southeast Asia, predominantly in Thailand, Lao PDR, South Vietnam and Cambodia. *O. viverrini* infection has been proven to be associated with cholangiocarcinoma (CCA) development[1]. At least 6 million people are currently infected with *O. viverrini* and thus

Correspondence: Somchai Pinlaor (psomec@kku.ac.th) or Eric W.-F. Lam (eric.lam@imperial.ac.uk)
[1]Department of Surgery and Cancer, Imperial College London, Imperial College London, Hammersmith Hospital Campus, London W12 0NN, UK
[2]Biomedical Science Program, Graduate School, Khon Kaen University, Khon Kaen 40002, Thailand
Full list of author information is available at the end of the article.
Edited by P. Bouillet

SPRINGER NATURE CDDpress

at risk for CCA[2]. Extensive research has revealed that *O. viverrini* infection induces inflammation, leading to periductal fibrosis and ultimately cholangiocarcinogenesis in patients[2–5]. Currently, surgical resection is the most effective treatment for operable cases but most CCA patients are inoperable[6,7], resulting in poor prognosis. Despite chemotherapy, particularly with the first-line drug 5-fluorouracil (5-FU), resistance eventually develops over time[8–10]. Therefore, an understanding of the mechanism involved in the development of 5-FU resistance is urgently needed for predicting and for improving treatment efficacy.

Previous cDNA microarray studies have revealed the upregulation of Forkhead box M1 (FOXM1) mRNA levels in tumour specimens derived from *O. viverrini*-associated CCA patients[11]. FOXM1 is a potent oncogenic transcription factor involved in normal development and also progression of numerous cancer types[12]. Furthermore, FOXM1 is crucial for chemotherapeutic drug response and resistance in many cancers[13–15] and is therefore an attractive target for therapeutic intervention[15]. Thymidylate synthase (TYMS) is an enzyme involved in DNA synthesis process. It catalyses the conversion of deoxyuridine monophosphate (dUMP) to deoxythymidine monophosphate (dTMP) and a target of 5-FU chemotherapy. Specifically, the active metabolite of 5-FU, fluorodeoxyuridine monophosphate (FdUMP) binds to the active site of for dUMP on TYMS, leading to the formation of an inactive FdUMP–TYMS complex and inhibition of the conversion of dUMP to dTMP. This causes deoxynucleotide (dNTP) pool imbalance and, ultimately, DNA damage and cell death[16]. Upregulation of *TYMS* gene has been reported following 5-FU treatment in human CCA cell lines[17]; however, its steady-state mRNA levels in human CCA tissues are not significantly correlated with the response to 5-FU[18]. Like FOXM1, the transcription factor E2F1 is a potent oncogene involved in cell cycle progression, DNA-damage response, drug resistance and apoptosis[19–21]. Both FOXM1 and TYMS have been reported to be the target genes of the E2F1 transcription factor[20,22–24]. Based on these previous findings, we therefore hypothesized that FOXM1 and E2F1 may coordinately modulate 5-FU sensitivity by targeting TYMS in CCA. Hitherto, the functional roles of FOXM1 and TYMS in the development of 5-FU resistance in *O. viverrini*-associated CCA have not been elucidated. To test this conjecture, we investigated the role of TYMS in 5-FU resistance and its regulation by FOXM1 and E2F1 in response to 5-FU in CCA.

Results

A strong correlated overexpression of TYMS and FOXM1 in CCA tissues

Previous cDNA array studies have shown overexpression of FOXM1 mRNA in *O. viverrini*-associated CCA[11]. To investigate further the role and regulation of TYMS and FOXM1 in *O. viverrini*-associated CCA, the expression of TYMS and FOXM1 was determined by immunohistochemistry (IHC) in CCA tissue arrays. We found that FOXM1 expression was upregulated in 78% (88/113) and TYMS in 48% (54/113) of all *O. viverrini*-associated cases ($n = 113$) (Fig. 1; Supplementary Figs. S1, S2, S3). Notably, the results highlighted that FOXM1 is commonly overexpressed in CCA, suggesting its involvement in CCA tumorigenesis. This finding also suggested that the FOXM1–TYMS axis might have a wider role in tumour progression, such as chemosensitivity, as TYMS is a cellular target of 5-FU, the first-line chemotherapeutic drug for CCA.

Correlated baseline expression of FOXM1 and TYMS in CCA cell lines

To explore the relationship between FOXM1, E2F1 and TYMS expression and their functional roles in CCA, western blot and real-time quantitative PCR (qPCR) analyses were performed to determine the baseline steady-state expression levels of FOXM1 and TYMS, as well as one of their known regulator E2F1, in four CCA cell lines[25]. Consistent with the IHC results, western blot analysis revealed that in general FOXM1 was highly expressed and displayed good correlations with TYMS in CCA cells (Fig. 2a). Expression of E2F1 differed between the four cell lines and had little correlation with that of FOXM1 and TYMS, suggesting that FOXM1 and TYMS expression is not related to E2F1. Interestingly, TYMS expression was higher and FOXM1 expression lower in HuCCA compared to the other three CCA cell lines, KKU-D131, KKU-213 and KKU-214 (Fig. 2a). The mRNA levels of FOXM1, E2F1 and TYMS demonstrated good correlations with their protein levels in these CCA cells (Fig. 2b), indicating that the expression of these proteins are regulated primarily at the transcriptional level. Interestingly, the TYMS mRNA expression levels also demonstrated positive relationships with the FOXM1 in all but the HuCCA cell line, while E2F1 expression levels again did not appear to be associated with those of FOXM1 and TYMS in these CCA cell lines (Fig. 2b). Together, these results suggest that TYMS expression is regulated by FOXM1 but not by E2F1 in CCA cells. The discordance between FOXM1 and TYMS expression levels in HuCCA also suggests that TYMS expression is not coupled to FOXM1 regulation in this cell line.

HuCCA is a highly 5-FU-resistant CCA cell line

As TYMS is the direct cellular target of 5-FU, we next examined the four CCA cell lines, HuCCA, KKU-D131, KKU-213 and KKU-214, for their sensitivity to 5-FU using sulforhodamine B (SRB) assay. Viability of all CCA cell lines decreased in a dose-dependent manner after treatment with

A

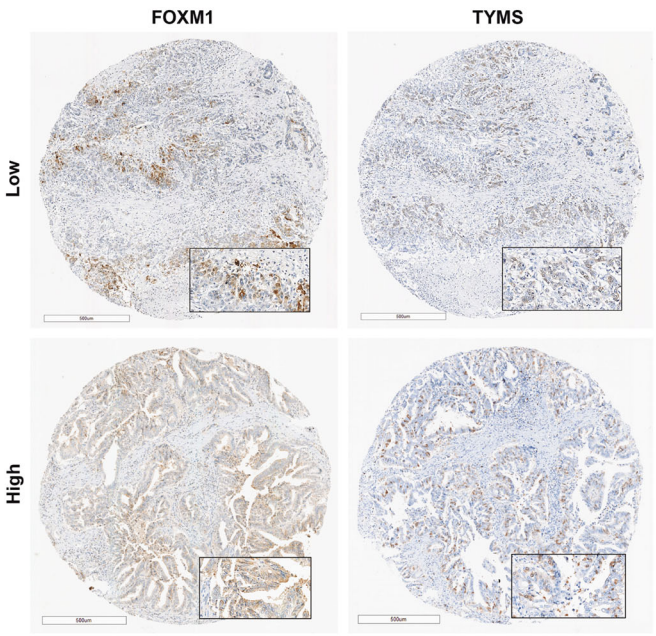

B

FOXM1 * TYMS Crosstabulation

Count

		TYMS		
		Negative	Positive	Total
FOXM1	Negative	19	6	25
	Positive	40	48	88
Total		59	54	113

Chi-Square Tests

	Value	df	Asymp. Sig. (2-sided)	Exact Sig. (2-sided)	Exact Sig. (1-sided)
Pearson Chi-Square	7.280(b)	1	.007		
Continuity Correction(a)	6.108	1	.013		
Likelihood Ratio	7.610	1	.006		
Fisher's Exact Test				.012	.006
Linear-by-Linear Association	7.216	1	.007		
N of Valid Cases	113				

a Computated only for a 2x2 table

b 0 cells (.0%) have expected count less than 5. The minimum expected count is 11.95.

Fig. 1 Correlation of FOXM1 and TYMS expression in CCA tissues. CCA tissue arrays were prepared from 113 *O. viverrini*-associated CCA cases using tissue microdissection techniques. **a** Representative immunohistochemical staining images showing correlated FOXM1 (top) and TYMS (bottom) expression. **b** Staining results and Chi-square analysis. Chi-square statistical analysis was used to test the correlations between TYMS and FOXM1 expression of CCA patients using GraphPad Prism 7.0 and and SPSS 16.0. In statistical analysis, $*p < 0.05$ was considered as significant

5-FU after 24, 48 and 72 h; HuCCA remained the more resistant line compared with the other three and exhibited the highest IC50 (Fig. 3a; Supplementary Figs. S4, S5). We next examined the sensitivity of the CCA cells to 5-FU by clonogenic assays. Consistently, clonogenic assays revealed that HuCCA was the most resistant cell line (Fig. 3b; Supplementary Fig. S6). The results also showed that these CCA cell lines are relatively resistant to 5-FU treatment, consistent with the observations in the clinic that most CCAs are resistant to genotoxic chemotherapy[8–10].

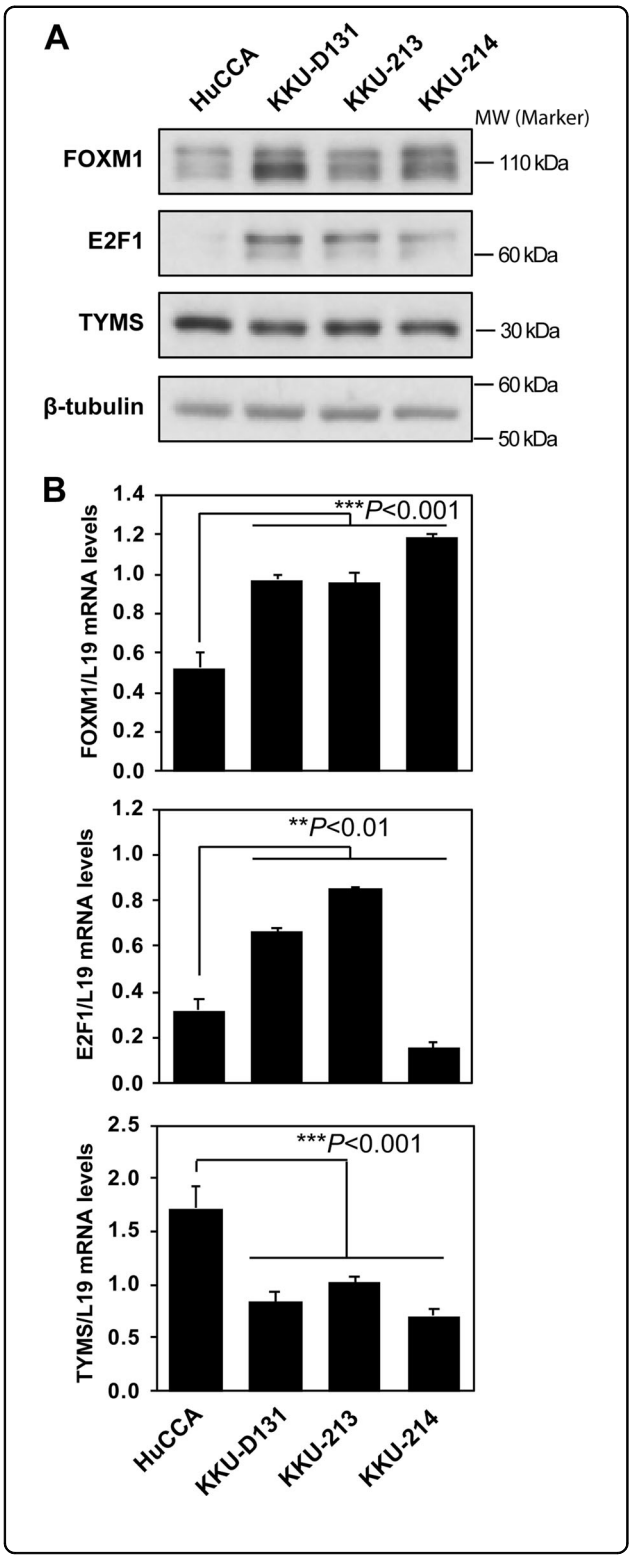

Fig. 2 Baseline expression of FOXM1, E2F1 and TYMS in CCA cells. CCA cells were harvested and the expression of FOXM1, E2F1 and TYMS at the translation and transcription levels were investigated using (**a**) western blot and (**b**) RT-qPCR. The latter assay was carried out in triplicate, and data are presented as means ± S.E.M. Expression of each gene was normalized relative to L19. The RT-qPCR data were analysed by one-way ANOVA with Fisher's Least Significant Difference (LSD) post-test. Double and triple asterisks (** and ***) indicate significant difference at $p < 0.01$ and $p < 0.001$, respectively, from HuCCA ($n = 3$)

Coordinated FOXM1 and TYMS expression upon 5-FU-treatment in CCA cell lines

Since TYMS is an important target for 5-FU treatment and has previously been shown to be regulated by FOXM1 and E2F1, we therefore hypothesized that the expression levels of these proteins regulate 5-FU sensitivity. To test this conjecture, the four very 5-FU-resistant CCA cell lines were treated with a high dose of 100 μM 5-FU (see Fig. 3) over the course of 48 h, and the expression levels of FOXM1, E2F1 and TYMS proteins were examined by western blot analysis (Fig. 3c). Expression of FOXM1 in all four cell lines increased transient in a time-dependent manner and its expression level was the highest at 24 h posttreatment and declined thereafter, concomitant with a reduction in cell proliferation rates (Fig. 3a). This kinetics of FOXM1 expression is consistent with other cancer cells following treatment with genotoxic agents[13,22,26–29]. Similarly, the expression of TYMS mirrored that of FOXM1 but at a slower kinetics in the CCA lines, except for HuCCA where TYMS was expressed consistently at comparatively higher levels throughout the time course. The active metabolite of 5-FU, FdUMP, binds to TYMS to form an inactive slower migrating FdUMP–TYMS complex, which inhibits the conversion of dUMP to dTMP. Notably, using a high dose of 100 μM 5-FU to treat the CCA cells, the majority of the TYMS proteins were in the FdUMP-complexed inactive slower migrating (higher) forms following 5-FU treatment, and this lack of active unligated TYMS would lead to dNTP shortage and the cytotoxic DNA damage. Expression of E2F1 in all cell lines did not show good correlations with either FOXM1 or TYMS, indicating further that E2F1 does not control FOXM1 and TYMS expression or vice versa in response to 5-FU in these CCA cells. These results also further suggest that FOXM1 regulates TYMS expression in CCA cells, except for the resistant HuCCA.

Silencing of FOXM1 reduced the 5-FU resistance and TYMS expression in KKU-D131 but not in HuCCA cells

To further investigate the role of FOXM1 in modulating the sensitivity of 5-FU in CCA cells, western blot analysis was performed on the most sensitive KKU-D131 and resistant HuCCA cells in the presence and absence of FOXM1 depletion. The result revealed that TYMS expression decreased upon FOXM1 depletion

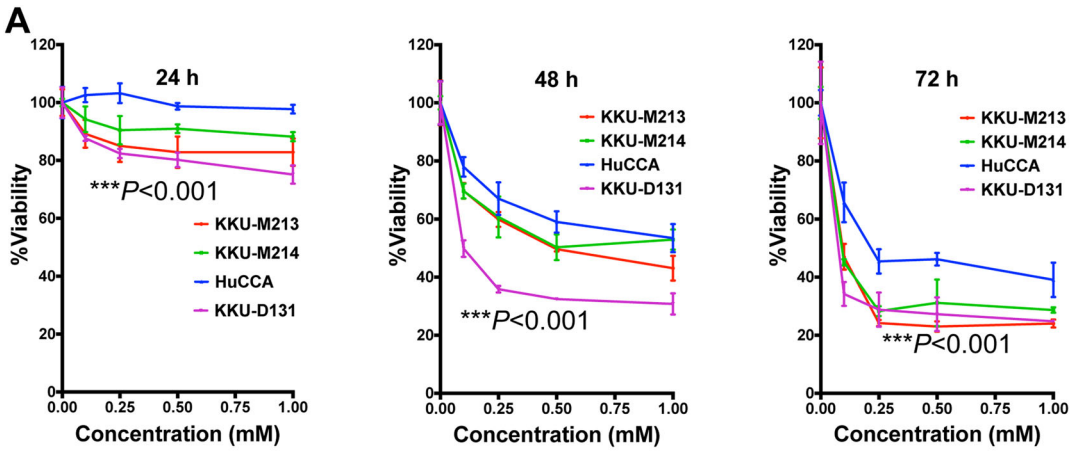

CCA cell lines	IC_{50} at 48 h (mM)	IC_{50} at 72 h (mM)
KKU-D131	0.013	0.008
KKU-M213	0.023	0.011
KKU-M214	0.033	0.014
HuCCA	0.042	0.026

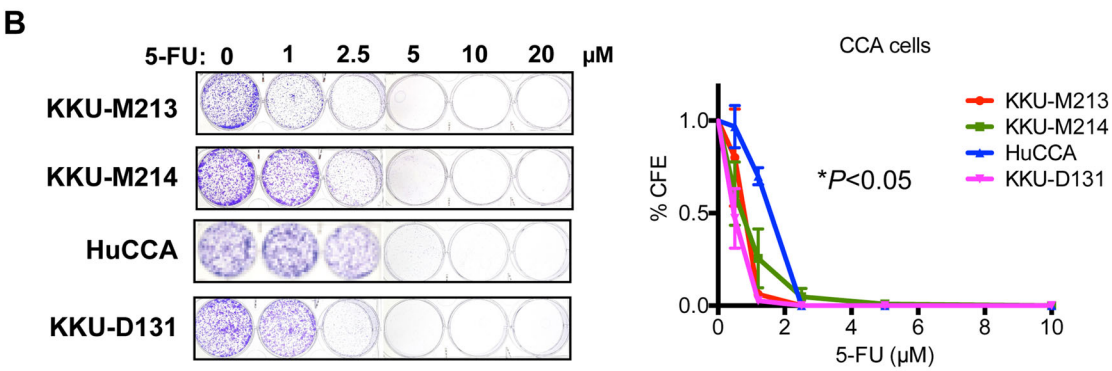

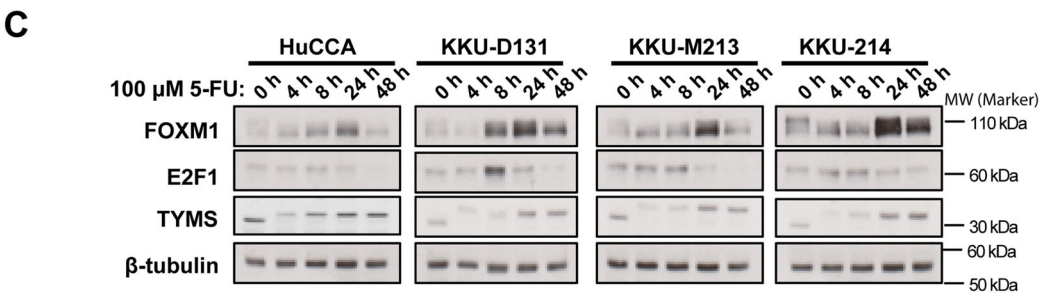

Fig. 3 (See legend on next page.)

(see figure on previous page)
Fig. 3 5-FU treatment suppresses proliferation of CCA cells. CCA cells of HuCCA, KKU213, KKU214 and KKU-D131 lines were treated with different concentrations of 5-FU using DMSO as a vehicle. **a** Cell proliferation was assessed at 24, 48 and 72 h after 5-FU treatment using SRB assay. The experiment was carried out in triplicates and data are presented as means of the percentage of untreated control. The cell viability data were analysed by two-way ANOVA with Fisher's Least Significant Difference (LSD) post-test ($n = 3$). The asterisks (***) indicate significant difference at $p < 0.001$. The IC50 for each CCA cell line at 48 and 72 h are shown (Supplementary Fig. S4). **b** The CCA cells were analysed for their sensitivity to 5-FU by clonogenic assays. After 48 h of incubation with the drugs, cells were cultured in fresh media, grown for around 14 days and stained with crystal violet. The graphs are representative of six experiments. Representative clonogenic images show the effects of 5-FU treatment (Supplementary Fig. S6). Data were analysed by two-way ANOVA with Fisher's Least Significant Difference (LSD) post-test. The asterisk (*) indicates significant difference at $p < 0.05$. **c** Expression of FOXM1, E2F1 and TYMS in 5-FU-treated CCA cell lines in response to 5-FU. The CCA cell lines were treated with 100 μM of 5-FU over a period of 48 h. Cells were trypsinized at specific times and the expression of FOXM1, E2F1 and TYMS was determined using western blotting. β-Tubulin was used as a loading control. Representative western blot images are shown

using small interfering RNA (siRNA) in the sensitive KKU-D131 but not in the resistant HuCCA cells, suggesting that TYMS is, at least partially, regulated by FOXM1 in the sensitive but not in the resistant CCA cells (Fig. 4a). By contrast, FOXM1 knockdown did not cause any substantial changes in E2F1 levels in both cell lines, further confirming that FOXM1 does not regulate E2F1. Clonogenic assay was then performed to investigate the effects of FOXM1 depletion on 5-FU sensitivity in HuCCA and KKU-D131 cells (Fig. 4b). Silencing of FOXM1 did not overtly affect 5-FU sensitivity of the resistant HuCCA cell line but caused a decrease in the clonogenicity of KKU-D131 (Fig. 4b), suggesting that FOXM1 plays a significant role in modulating TYMS expression and hence 5-FU sensitivity in the sensitive but not in the resistant CCA cells. FOXM1 was next overexpressed in KKU-D131 and HuCCA cells. The control and FOXM1-overexpressing CCA cells were then tested for their sensitivity to 5-FU. Western blot analysis revealed that FOXM1 was overexpressed in the FOXM1-transfected KKU-D131 and HuCCA cells, and TYMS expression was not affected by FOXM1 overexpression (Fig. 5a). In concordance, clonogenic assay showed that ectopic overexpression of FOXM1 did not alter the sensitivity of either KKU-D131 or HuCCA cells to 5-FU (Fig. 5b). These results indicated that, although FOXM1 plays a vital role in the proliferation and 5-FU sensitivity of the KKU-D131, FOXM1 is already highly expressed and further overexpression would not induce additional TYMS expression and thereby 5-FU resistance. This notion is consistent with our earlier findings that FOXM1 is overexpressed in most CCA patient samples (Fig. 1) and cell lines (Fig. 2).

Silencing of TYMS sensitizes both HuCCA and KKU-D131 cells to 5-FU treatment

In order to verify that TYMS expression is involved in the modulation of 5-FU sensitivity in CCA cells, TYMS expression was silenced using siRNA in both the 5-FU-resistant HuCCA and 5-FU-sensitive KKU-D131 cells, and the effects of TYMS knockdown on 5-FU sensitivity investigated using clonogenic assay. As shown in Fig. 6a, siRNA efficiently silenced the expression of the TYMS protein. Silencing of TYMS effectively sensitized both HuCCA and KKU-D131 to 5-FU, even at the lowest concentrations (e.g., 1 μM), confirming that TYMS is the target of 5-FU and its levels modulate 5-FU sensitivity in both the sensitive and resistant CCA cells (Fig. 6b; Supplementary Fig. S7). Unexpectedly, TYMS knockdown also resulted in a downregulation of FOXM1 expression (Fig. 6a), suggesting that TYMS might have a role in controlling the FOXM1 expression and FOXM1 as a sensor for TYMS activity and DNA damage, probably through the induction of DNA damage via blockage of replication fork progression. In addition, silencing of E2F1 by siRNA was also performed because expression of TYMS has previously been shown to be regulated by E2F1; however, E2F1 silencing did not affect the sensitivity of either HuCCA or KKU-D131 to 5-FU (Fig. 6b; Supplementary Fig. S7). Collectively, these data showed that TYMS expression levels determine the drug sensitivity in both sensitive and resistant CCA cells. In addition, the findings also supported the idea that FOXM1 regulates TYMS expression and thereby 5-FU sensitivity in CCA cells and that the uncoupling between FOXM1 and TYMS expression is linked to refractory to 5-FU in CCA cells.

FOXM1 modulates TYMS levels and 5-FU response in CCA cells

To further test the hypothesis that FOXM1 modulates 5-FU response through regulating TYMS expression levels in CCA, KKU-D131 and HuCCA cells were treated with a lower dose (20 μM) of 5-FU, which has differential cytotoxic effects on the comparatively more sensitive and resistant CCA cells (Fig. 7). As expected, in the comparatively more sensitive KKU-D131 both FOXM1 and TYMS protein and mRNA expression increased coordinately reaching a peak at 24 h post-treatment and decreased thereafter at 48 h. By contrast, despite the induction of FOXM1 expression in response to 5-FU in the resistant HuCCA cells, the expression of

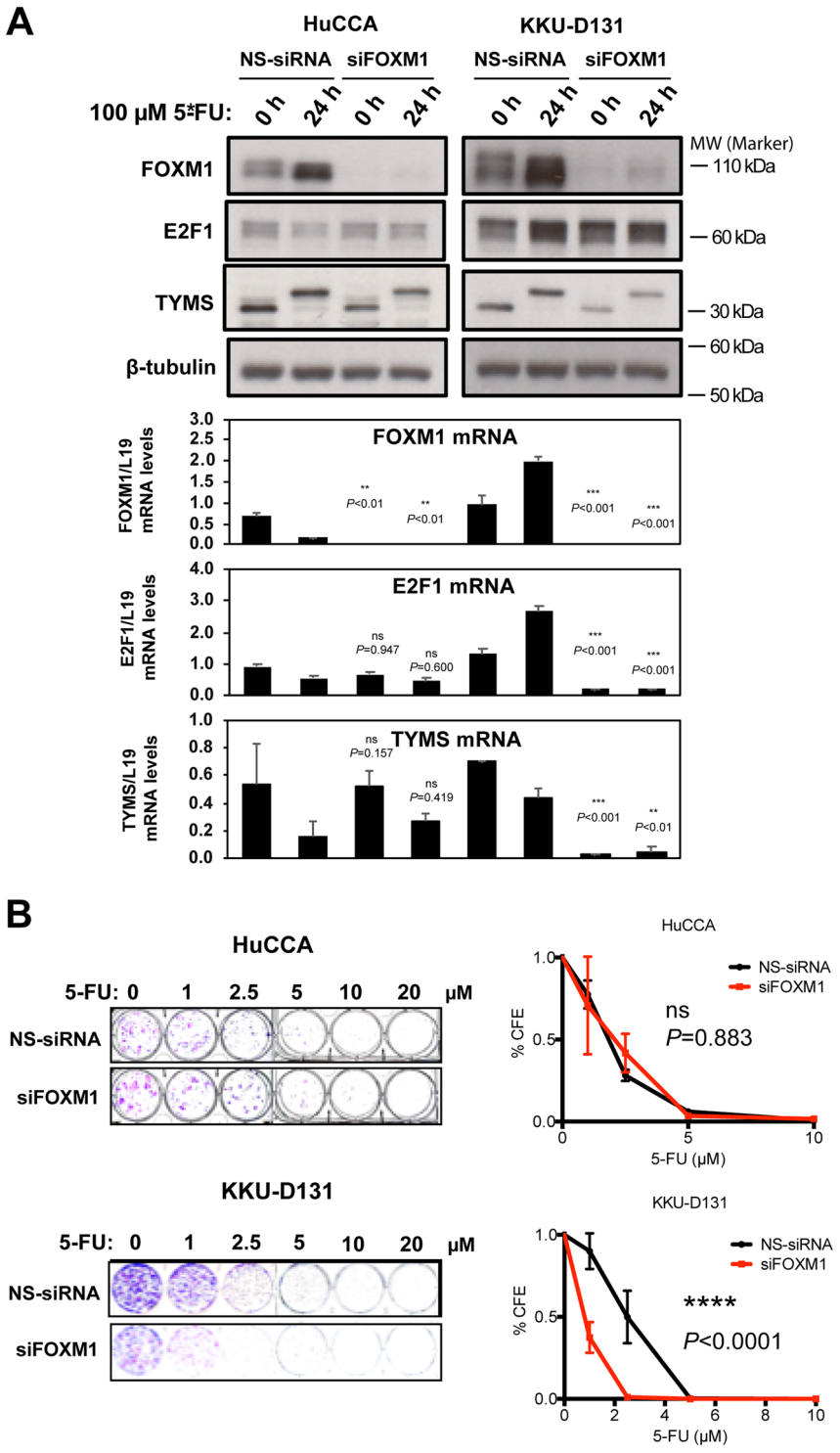

Fig. 4 (See legend on next page.)

(see figure on previous page)

Fig. 4 Effects of FOXM1 silencing on CCA cells in response to 5-FU treatment. FOXM1 expression in HuCCA and KKU-D131 cells was silenced using siRNA (siFOXM1) and non-silencing siRNA (NS-siRNA) was used as control. After 24 h, CCA cells were reseeded and grown overnight. **a** After treatment with 100 μM 5-FU for 24 h, cells were harvested and the expression levels of FOXM1, E2F1 and TYMS were determined by western blot and RT-qPCR analysis. Western blot was performed using β-tubulin as loading control (upper panel). Expression of FOXM1, E2F1 and TYMS mRNA was also determined by RT-qPCR analysis using L19 as an internal control (lower panel). Data are presented as mean ± SEM ($n > 3$). RT-qPCR data were analysed by unpaired *t* tests. Double and triple asterisks (** and ***) indicate significant difference at $p < 0.01$ and $p < 0.001$, respectively, from the non-targeting siRNA-treated control cells; 'ns' indicates no significant difference. **b** Effect of FOXM1 silencing on 5-FU sensitivity was also investigated using clonogenic assays. Representative clonogenic images show the effects of FOXM1 silencing on the outcome of 5-FU treatment. Data are presented as mean ± SEM ($n = 3$) and were analysed by two-way ANOVA. The asterisks (****) indicate significant difference at $p < 0.0001$ from the non-targeting siRNA-treated control cells; 'ns' indicates no significant difference

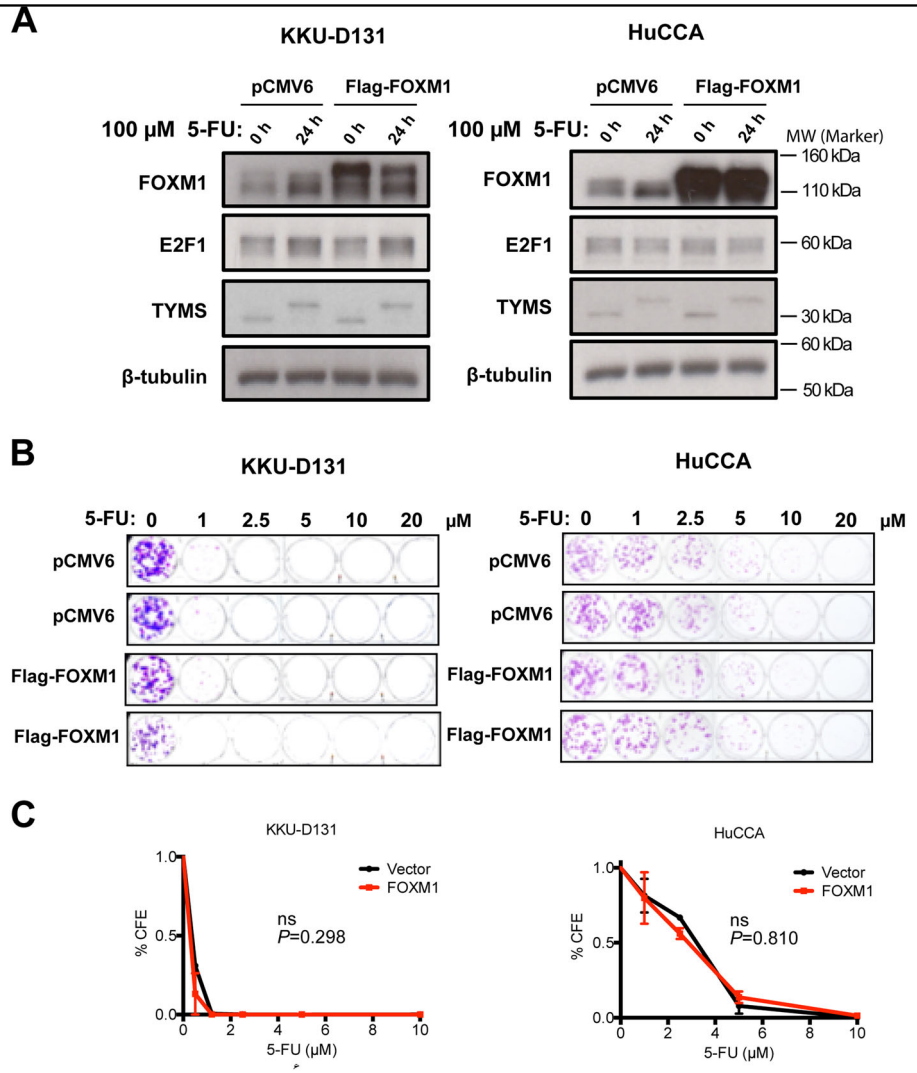

Fig. 5 Effects of ectopic expression of FOXM1 in KKU-D131 and HuCCA cells in response to 5-FU treatment. FOXM1 expression in KKU-D131 cells was induced by transfection with FOXM1-pcDNA3.1 plasmid DNA. Plasmid DNA from parental vector was used as transfection controls. After 24 h, CCA cells were reseeded and grown overnight. **a** After treatment with 100 μM 5-FU for 24 h, cells were harvested and the expression levels of FOXM1, E2F1 and TYMS was determined by western blot analysis using β-tubulin as loading control. **b** Effects of FOXM1 overexpression on 5-FU toxicity was also investigated using a clonogenic assay. Representative clonogenic assay images show the effects of FOXM1 overexpression upon 5-FU treatment. **c** Data are presented as mean ± SEM ($n = 3$) and were analysed by two-way ANOVA. No significant difference is indicated by 'ns'

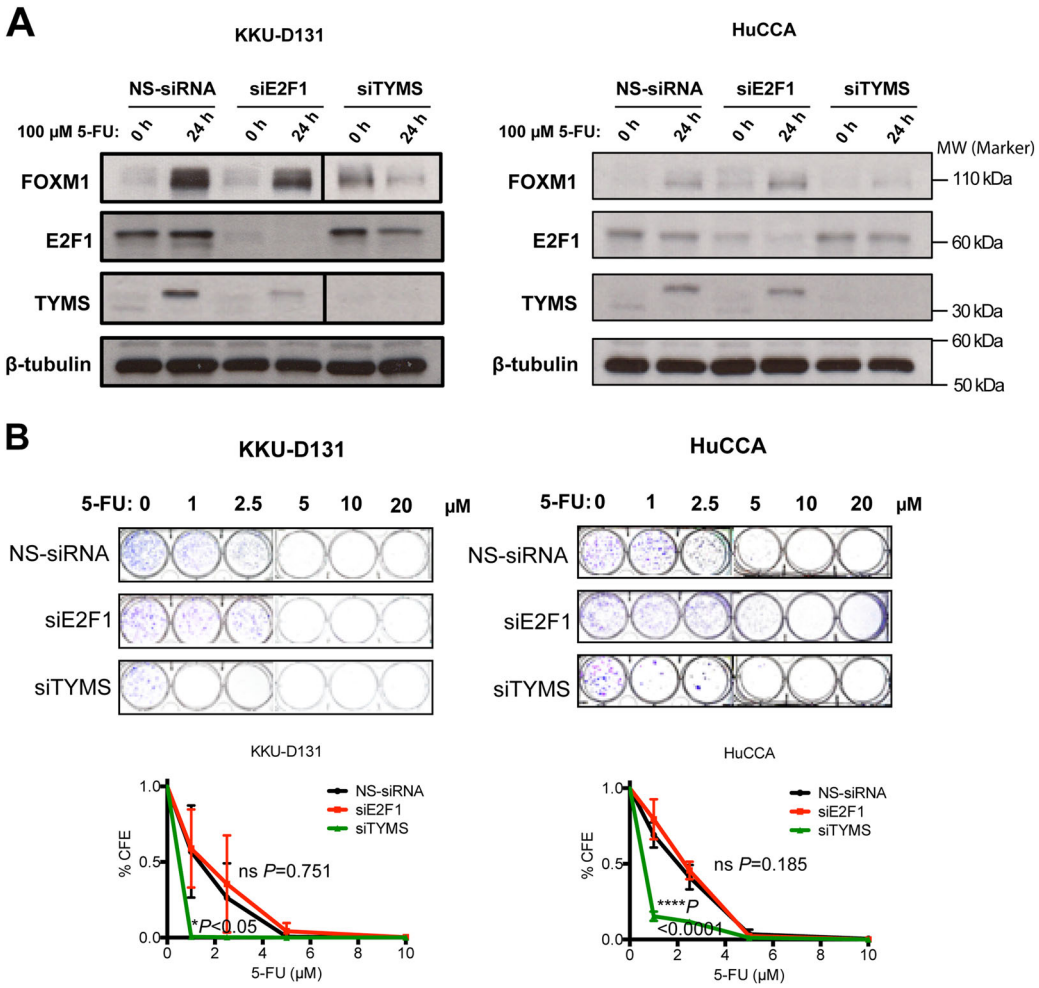

Fig. 6 Effects of E2F1 and TYMS silencing on 5-FU treatment of CCA cells. Either E2F1 or TYMS expression in HuCCA cell was silenced using siRNA (siE2F1 or siTS). Non-silencing siRNA (NS-siRNA) was used as a control. After 24 h, HuCCA cells were reseeded and grown overnight. **a** After treatment with 100 μM 5-FU for 24 h, cells were harvested and the expression of FOXM1, E2F1 and TYMS was determined by western blot analysis using β-tubulin as loading control. **b** Effects of E2F1 and TYMS silencing on 5-FU toxicity was also investigated using a clonogenic assay. Representative clonogenic assay images show the effect on 5-FU treatment of silencing of either E2F1 or TYMS. Data are presented as mean ± SEM ($n = 3$) and were analysed by two-way ANOVA. Single and triple asterisks (* and ****) indicates significant difference at $p < 0.05$ and $p < 0.001$, respectively, from the non-targeting siRNA-treated control cells; 'ns' indicates no significant difference

TYMS remained constantly high throughout the time course.

Critically, in the sensitive KKU-D131 cells the majority of the TYMS proteins were in the FdUMP-complexed inactive slower migrating forms especially after the coordinated downregulation of FOXM1 and TYMS expression at 48 h following 5-FU treatment, and this lack of active unligated TYMS would lead to cytotoxic DNA damage. By comparison, in HuCCA cells the levels of TYMS remained relatively stable over the time course with a substantial proportion remaining in the uncomplexed and active faster migrating species, and the cells could still be able to process the dUMP to dTMP conversion for DNA replication (Fig. 7).

Differential binding of FOXM1 to endogenous TYMS promoter in 5-FU-sensitive and -resistant CCA cells

We next investigated the regulation of TYMS by FOXM1 at the promoter level. To this end, we first identified the putative FOXM1-binding regions from previously published FOXM1 chromatin-Immunoprecipitation–sequencing (ChIP-Seq) studies (Fig. 8). Both HuCCA and KKU-D131 cells were either untreated or treated with 5-FU for 24 and 48 h. To confirm further that FOXM1 binds to the endogenous *TYMS* promoter, we studied the occupancy of the endogenous *TYMS* promoter by FOXM1 using ChIP in the absence and presence of 24 or 48 h of 5-FU treatment in both cell lines. The ChIP analysis showed that

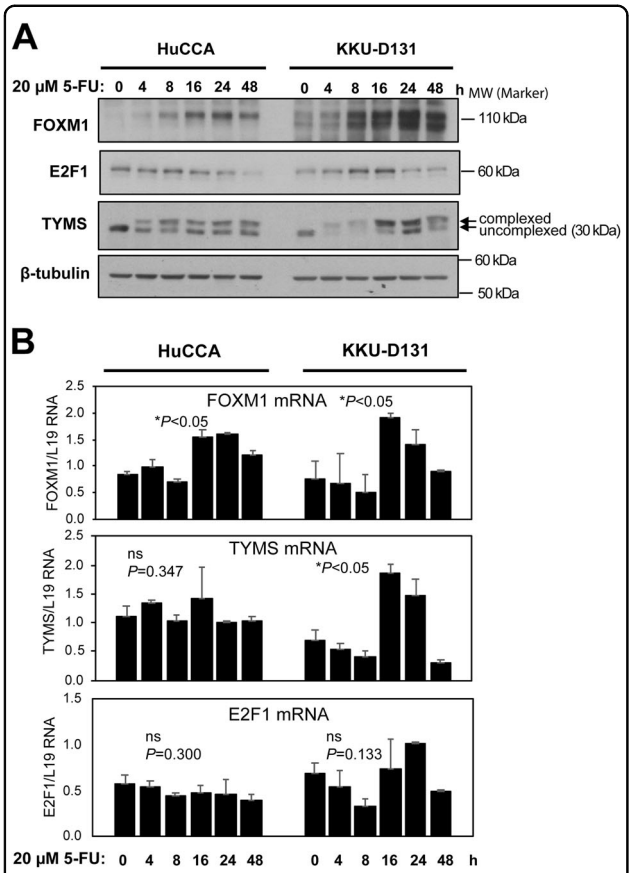

Fig. 7 Expression of FOXM1, E2F1 and TYMS in CCA cell lines treated with a lower 20-μM dose of 5-FU. HuCCA and KKU-D131, the resistant and sensitive cell lines, respectively, were treated with 20 μM of 5-FU over a period of 48 h. Cells were trypsinized at specific times and the expression of FOXM1, E2F1 and TYMS was determined using western blotting. β-Tubulin was used as a loading control. **a** Expression of FOXM1, E2F1 and TYMS was determined by western blot analysis using β-tubulin as loading control. **b** Expression of FOXM1, E2F1 and TYMS mRNA was determined by RT-qPCR analysis using L19 as an internal control. Data are presented as mean ± SEM ($n > 3$). The RT-qPCR data were analysed by one-way ANOVA. The asterisk (*) indicates significant difference at $p < 0.05$

FOXM1 is recruited to the endogenous Forkhead response element (FHRE) in both HuCCA and KKU-D131 cells and its binding to the FHRE increases substantially in KKU-D131 but not in HuCCA in response to 5-FU (Fig. 8; Supplementary Fig. S8). Together, these findings suggest that *TYMS* is a direct transcriptional target of FOXM1 in CCA cells and that the incapacity of FOXM1 to modulate TYMS expression is due its inability to be efficiently recruited by the promoter of *TYMS*.

Discussion

Surgery is the most effective treatment strategy for all potentially resectable intrahepatic CCAs[30]. However, owing to the late presentation and/or the advanced stages of most patients, CCA tumours are often not amenable to resection and chemotherapy. 5-FU either alone or in combination with other drugs is one of the most frequently used first-line regimens for CCA treatment. Nevertheless, the outcome is often sub-optimal because CCA patients are commonly intrinsic resistant or will become refractory after initial 5-FU treatment, leading to disease recurrence[8,31]. As TYMS is a key target of 5-FU, the possible mechanism of 5-FU resistance in CCA is likely to involve TYMS[16] and its putative regulators FOXM1[14] and E2F1[32].

To test this conjecture, we first investigated FOXM1 expression by IHC in CCA tissue arrays and found that FOXM1 is highly expressed in almost all CCA cases, consistent with previously published mRNA expression profiling analyses[11,33]. FOXM1 has previously been shown to be a key genotoxic drug sensor and a regulator of chemotherapeutic resistance in cancer[13,15,26–29,34]. For instance, in breast cancer, FOXM1 expression is consistently higher in epirubicin (MCF-7^{EpiR}) and cisplatin (MCF-7^{CisR}) resistant cells compared to the parental sensitive breast cancer MCF-7 cells[13,22,28]. Moreover, drug treatment downregulates FOXM1 expression at both the transcriptional and post-translational levels in the sensitive breast cancer, whereas FOXM1 expression remains at high levels in the resistant cells[13,22,26,27,29,34]. Furthermore, depletion of FOXM1 has been shown to sensitize breast cancer cells to genotoxic agents[13,22]. In agreement with this idea, high levels of FOXM1 expression have also been found to convey poor prognosis in breast cancer patients[13,22,35]. Taken together with these previous observations, our IHC led us to investigate the hypothesis that FOXM1 regulates TYMS to modulate 5-FU sensitivity. Notably, our finding that FOXM1 is overexpressed in almost all CCA cases (95%) is in concordance with previous observations that most CCAs are resistant to conventional chemotherapy[8,31]. However, owing to the lack of comprehensive clinical follow-up data and the late presentation of the patients, the correlations between FOXM1/TYMS expression and 5-FU sensitivity were pursued in CCA cell culture models and not in patient samples.

In vitro clonogenic and proliferative studies showed that all CCA cell lines tested are highly resistant to 5-FU, consistent with the previous published CCA patient results[8,31]. These studies also identified HuCCA as the most 5-FU resistant among four human CCA cell lines (e.g., HuCCA, KKU-213, KKU-214 and KKU-D131). Western blot and quantitative reverse transcriptase PCR (qRT-PCR) analyses also unveil a discordance between FOXM1 and TYMS expression at the base line level in this highly 5-FU-resistant HuCCA line when compared with the other comparatively more sensitive CCA cells. Upon treatment with high doses of 5-FU, expression of FOXM1 in all four cell lines increased transiently in a

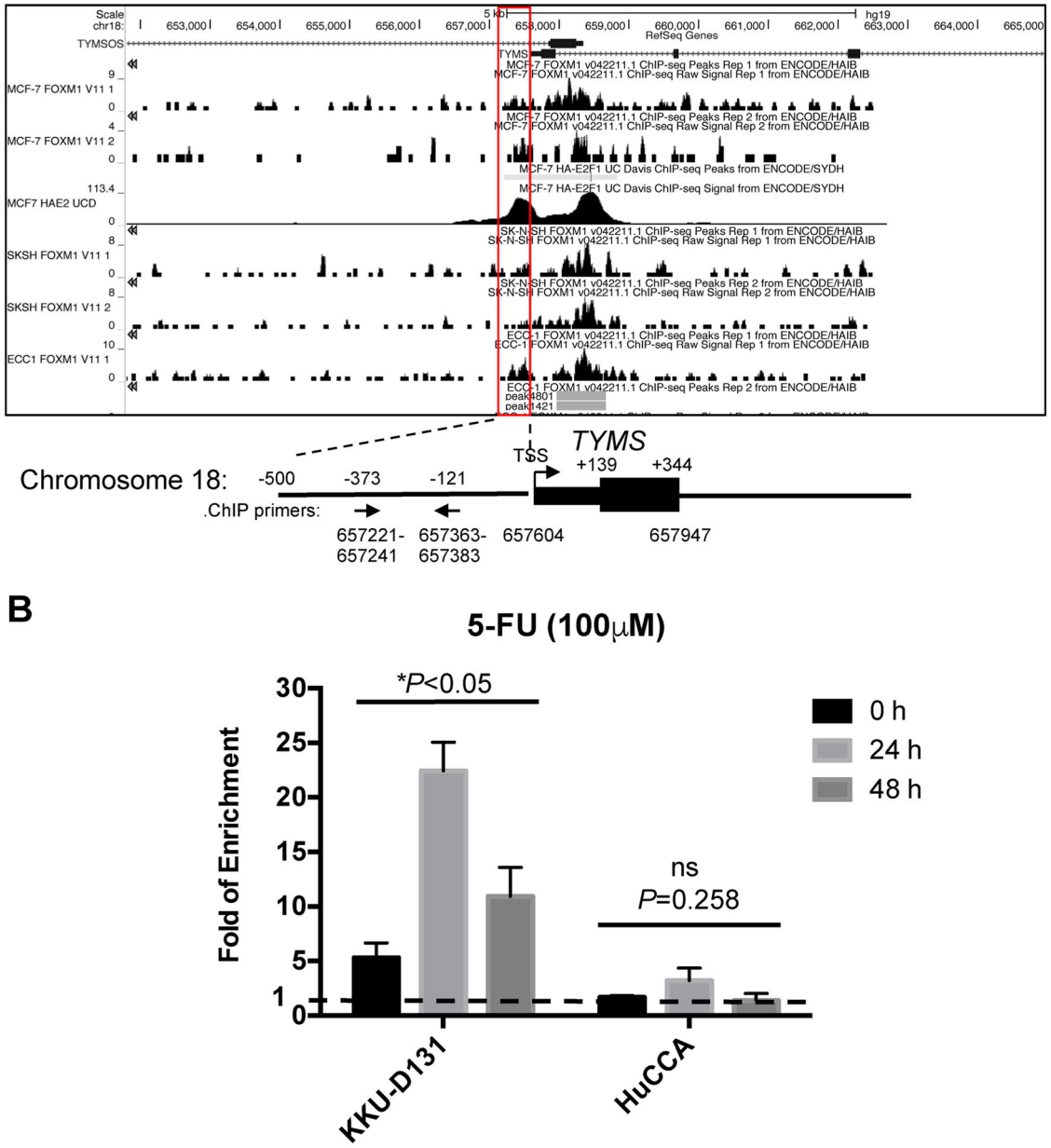

Fig. 8 Analysis of FOXM1 binding on human TYMS promoter a FOXM1-binding site on human TYMS promoter. ENCODE (the Encyclopedia of DNA Elements) project ChIP sequencing data of FOXM1 binding in the MCF-7, SKSH and ECC1 cells were used for predicting global genome-binding profiles for FOXM1 using the Integrative Genomics Viewer (Version 2.3.88) and the hg19 UCSC Genome Browser[50]. The predicted binding profiles of FOXM1 and the locations of the designed ChIP primer pairs are aligned to the human TYMS promoter. **b** KKU-D131 and HuCCA cells treated with 100 nM 5-FU for 0, 24 and 48 h were used for chromatin immunoprecipitation assays using the IgG as negative control and anti-FOXM1 antibody. After reversal of cross-linking, the co-immunoprecipitated DNA was amplified by qRT–PCR, using primers amplifying the FOXM1 binding-site-containing region. Data are presented as mean ± SEM ($n = 4$, each with >3 replicates) and were analysed by two-way ANOVA (Supplementary Fig. S7). The asterisk (*) indicates significant difference at $p < 0.05$ and 'ns' no significant difference

time-dependent manner with the expression levels highest at 24 h and declined thereafter, concomitant with a reduction in cell proliferation and viability rates (Fig. 3). This kinetics of FOXM1 expression is analogous to those observed in drug-sensitive cancer cells upon genotoxic drug treatments, suggesting that FOXM1 is also a sensor for 5-FU induced DNA damage in CCA cells[13,22,26,27,29,34]. While FOXM1 and TYMS expression was coordinately

modulated in response to 5-FU treatment in the 5-FU sensitive CCA cell lines, TYMS expression remained comparatively high throughout the time course in the resistant HuCCA cells, indicating a potential uncoupling between FOXM1 and TYMS expression in the resistant HuCCA cells. This conjecture is supported by our siRNA silencing analysis, which shows that FOXM1 depletion only reduces TYMS expression and 5-FU sensitivity in KKU-D131 but not in the highly resistant HuCCA cells. Based on the results, we conclude that TYMS expression is linked to 5-FU sensitivity, implying that TYMS overexpression plays a major role in 5-FU resistance. Consistent with this finding, previous studies have shown overexpression of TYMS as a 5-FU-resistance mechanism[36–38].

Notably, the 5-FU sensitivity and TYMS expression in HuCCA was not affected by FOXM1 silencing, suggesting that HuCCA is not sensitive to regulation by FOXM1. In concordance, ChIP analysis shows that in response to 5-FU, the binding of FOXM1 increases transiently before dropping to basal levels in the KKU-D131 cells but remains constantly low in the resistant HuCCA cells. These findings confirm that *TYMS* is a direct transcriptional target of FOXM1 in CCA cells and that FOXM1 fails to modulate TYMS expression in the resistant CCA cells because of its inability to be efficiently recruited to the *TYMS* promoter. This result is consistent with a recent FOXK1-ChIP-Seq analysis which shows the *TYMS* promoter contains FHRE[39]. The strong and significant correlations between FOXM1 and TYMS expression in CCA patient samples, further suggest that FOXM1 controls TYMS expression.

Time course experiments with a lower dose (20 μM) of 5-FU provide further evidence to support the notion that FOXM1 modulates TYMS expression levels and therefore 5-FU sensitivity in response to the drug. They also illustrate that the uncoupling of the FOXM1–TYMS axis allows a consistent level of unligated active TYMS to mediate DNA replication. This notion is supported by the fact that TYMS depletion by siRNA rendered the 5-FU resistance HuCCA cells sensitive to 5-FU treatment in clonogenic assays (Fig. 6). Our siRNA depletion studies also indicate that E2F1 is not involved in the regulation of TYMS and FOXM1 in CCA cells. In concordance, others have also found that TYMS is not regulated by E2F1 in other cell models[40].

Interestingly, downregulation of FOXM1 was observed in TYMS knocked down HuCCA cell line. This observation might be explained by the fact that TYMS can suppress the 5-FU-induced DNA damage and expression of p53, which can in turn repress FOXM1 expression[41–43]. These results suggest that FOXM1 functions as a sensor of 5-FU-induced DNA damage and its regulation of TYMS determines 5-FU response in CCA. In agreement, FOXM1 has been shown to be a sensor of genotoxic agents and a modulator of their response. Accordingly, FOXM1 has been demonstrated to be regulated by SUMOylation and ubiquitination in response to genotoxic drug treatments and the ubiquitination-conjugating enzymes, RNF8 and RNF168, and the deconjugating enzyme OTUB1 play a crucial role in mediating this response by regulating FOXM1 expression at the post-translational levels[27,29,34].

Interestingly, in contrast, overexpression of FOXM1 in both the 5-FU-sensitive and -resistant CCA cells does not affect TYMS expression nor 5-FU sensitivity, further confirming that in most CCA cells FOXM1 is already overexpressed at high levels. This observation is consistent with our IHC finding and previous gene expression profiling results[11,33]. FOXM1 overexpression could be a feature of CCA tumorigenesis, and therefore, FOXM1 and its gene transcription signature can be exploited as a useful biomarker for early CCA diagnosis. The mechanism for FOXM1 overexpression in CCA is unclear; however, exome sequencing has identified TP53 gene mutation as an event that may contribute to the initiation of *O. viverrini*-related CCA[44]. FOXM1, a gene highly expressed in CCA[11,33], is one of the targets of p53-mediated repression[22,45]. Furthermore, the molecular mechanism of tumorigenesis for *O. viverrini*-associated CCA has been linked to inflammation-induced DNA damage[46,47], and this could lead to the selection of p53-mutated and FOXM1-overexpressing CCA cells.

Collectively, our data provide evidence to show that FOXM1 regulates TYMS to modulate 5-FU sensitivity in CCA cells and that the high FOXM1 expression confers 5-FU resistance in most of these CCA cells through promoting high levels of TYMS expression (e.g., in KKU-M213, KKU-M214 and KKU-D131 cells). Moreover, we also found an alternative and novel mechanism for further 5-FU resistance, which is the uncoupling of the regulation of TYMS by FOXM1 (e.g., HuCCA). In support of the idea that the uncoupling of the regulation of TYMS by FOXM1 is uniquely important for 5-FU insensitivity in HuCCA cells, our preliminary data show that, despite HuCCA being the most resistant to 5-FU treatment among all the CCA cells tested, it is one of the more, if not most, sensitive to epirubicin and paclitaxel treatment (Supplementary Fig. S9). This is consistent with our previous finding that epirubicin and paclitaxel target DNA repair and mitotic genes via FOXM1 (e.g., NBS1 and KIF20A, respectively) to modulate their drug sensitivity[13,35]. Moreover, although overexpression of FOXM1 does not have any effect on 5-FU sensitivity in HuCCA, its ectopic expression can confer resistance to epirubicin and paclitaxel, respectively (Supplementary Fig. S10). These findings also propose the possibility of using alternative FOXM1-targeting cytotoxic agents to treat 5-FU-resistant

cancer cells that have FOXM1–TYMS regulation uncoupled and lower FOXM1 expression.

In conclusion, our results evidently show that FOXM1, but not E2F-1, modulates TYMS expression and thereby 5-FU sensitivity in CCA cells. Our data also demonstrate that the FOXM1–TYMS axis plays a major role in mediating 5-FU sensitivity in CCA cells and its uncoupling may be linked to 5-FU resistance. Our findings suggest the FOXM1–TYMS axis is a determinant of 5-FU response and a target for designing more effective treatment for CCA patients. Since FOXM1 is overexpressed in almost all CCAs and may be essential for CCA tumorigenesis, FOXM1 and its downstream transcriptional signature might also be useful for prognosis prediction of CCA.

Materials and methods

Chemicals and reagents

SRB and 5-FU were purchased from Sigma Aldrich (Irvine, UK). Rabbit anti-FOXM1 (C-20) and β-Tubulin (H-235) antibodies were from Santa Cruz Biotechnology (Santa Cruz, CA, USA). Rabbit anti-TYMS was obtained from Cell Signaling Technology (New England Biolabs Ltd. Hitchin, UK). Rabbit anti-E2F1 was purchased from Abcam (Cambridge, UK) and horseradish peroxidase (HRP)-conjugated secondary antibodies from Dako (Glostrup, Denmark) and Jackson ImmunoResearch (West Grove, PA, USA). Western Lightning® Plus-ECL was acquired from Perkin Elmer (PerkinElmer Ltd, Beaconsfield, UK) and SYBR Select Master Mix from Applied Biosystems (Fisher Scientific UK Ltd, Loughborough, UK).

Human CCA cell lines

Four human CCA cell lines were used in this study. KKU-213 (mixed papillary and non-papillary CCA) and KKU-214 (well-differentiated CCA) were established from Thai CCA patients as described previously[17]. HuCCA was established from Thai patient with intrahepatic CCA[48] and KKU-D131 CCA cell line was recently established from a Thai CCA patient. All cell lines were cultured in Dulbecco's modified Eagle's medium supplemented with 10% foetal calf serum (FCS) (First Link Ltd, Birmingham, UK), 2 mmol/L glutamine, 100 U/mL penicillin and 100 μg/mL streptomycin (Sigma-Aldrich, Poole, UK). All cell lines were maintained at 37 °C in in a humidified incubator with 10% CO_2.

IHC staining

IHC was performed as described elsewhere[49]. In brief, CCA tissue array slides were constructed at the Department Pathology, Faculty Medicine, Khon Kaen University, Thailand. All cancerous tissues were obtained from CCA patients who underwent surgery at Srinagarind Hospital, Khon Kaen Province, Thailand. All patients did not receive any chemotherapy prior to surgery. Tissue was deparaffinized and antigens were unmasked by autoclaving with sodium citrate buffer (10 mM sodium citrate, 0.05% Tween 20, pH 6.0). Thereafter, slides were immersed in 3% H_2O_2 for 10 min for endogenous peroxidase removal. Then non-specific binding was blocked by incubating with 5% FCS for 1 h at room temperature. Slides were then immersed with either rabbit anti-FOXM1 or TYMS (1:200) in 1% FCS overnight at 4 °C. After washing with phosphate-buffered saline (PBS) for 3 times, slides were incubated with 1:1000 HRP-conjugated secondary antibody for 1 h at room temperature. Immunoreactivity was developed by using 3,3-diaminobenzidine and slides were counterstained with Mayer's haematoxylin. The expression was categorized as 0 = negative (either negative staining or positive <10% of CCA tissue area) and 1 = positive (positive staining >10% of the CCA tissue area) by 3 investigators and consensus scoring by at least two out of the three was chosen as definitive grading score.

Cell viability assay

Cell viability was investigated by SRB colorimetric assay. CCA cell lines were plated in 96-well plate at 2000 cells per well and incubated overnight. In the following day, CCA cell lines were treated with various concentrations of 5-FU in dimethyl sulphoxide (DMSO) for 24, 48 and 72 h. All plates were kept in humidified incubator at 37 °C and 10% CO_2. Then cells were fixed with cold 40% (w/v) trichloroacetic acid and incubated for 1 h at 4 °C. After washing 5 times with slow running tap water, 100 μL of 0.4% SRB in 1% acetic acid was added and incubated at room temperature for 1 h. Then unbound dye was removed by washing with 1% acetic acid and left to air-dry overnight. Finally, SRB dye was dissolved with 10 mM Tris buffer and placed on a rotator for 30 min. The optical density at 492 nm were measured using the Sunrise plate reader (Tecan Group Ltd, Mannedorf, Switzerland).

Clonogenic assay

CCA cells were seeded (1000 cells/well) in duplicate into 6-well plate. Then cells were treated with either vehicle (DMSO) or 5-FU for 48 h. Culture media was changed every 2 days without further treatment. For harvesting, media was removed and then colonies were washed with PBS and fixed with 4% paraformaldehyde for 15 min at room temperature. After washing with PBS for 3 times, colonies were stained with 0.5% crystal violet for 30 min. Finally, solution was removed and plates were washed with tap water for 5 times and left to dry overnight. Digital images of colonies were taken using digital camera.

Cell transfection

For gene silencing, HuCCA and KKU-D131 were plated in at sub-confluent densities. The following day, HuCCA and KKU-D131 were transfected with ON-TARGET plus siRNAs (GE Dharmacon) targeting FOXM1, E2F1, or TYMS using oligofectamine (Invitrogen, UK) following the manufacturer's protocol. Non-Targeting siRNA pool (GE Dharmacon) was used as transfection control. For gene overexpression study, either pcDNA3.1 plasmid DNA or pcDNA3.1-FOXM1 plasmid DNA were transfected into HuCCA or KKU-D131 using X-tremeGENE HP (Roche Diagnostics Ltd, Burgess Hill, UK) according to the manufacturer's protocol. Cells were harvested at 24 h post-transfection for further experiment.

Western blot analysis

Protein was extracted from cell pellets using 2 volumes of RIPA buffer (50 mM Tris-HCl, 150 mM NaCl, 1% NP-40, 5 mM EDTA, 1 mM dithiothreitol, 1 mM NaF, 2 mM phenylmethylsulfonyl fluoride, 1 mM sodium orthovanadate) with protease inhibitor cocktail. Protein (20 µg) were separated by sodium dodecyl sulphate-polyacrylamide gel electrophoresis and then transferred to a nitrocellulose membrane. After blocking with 5% bovine serum albumin in Tris buffered solution with 0.05% Tween-20 (TBST, pH 7.5), membranes were incubated with primary antibodies overnight at 4 °C. After washing with 0.05% TBST, membranes were incubated with secondary antibodies and chemiluminescence reaction was developed using Western Lightning® Plus-ECL. β-Tubulin was used as loading control.

RNA extraction, cDNA synthesis and real-time qPCR

mRNA was extracted from cell pellets using the RNeasy Mini Kit (Qiagen Ltd, Crawley, UK) and mRNA was reversed-transcribed to cDNA using the SuperScript III First-Strand Synthesis System (Invitrogen). Real-time qPCR analysis was performed in triplicate using SYBR Select Master Mix and specific primers (Supplementary Figure S11) according to the manufacturer's instructions. The qRT-PCR conditions were as follows: 95 °C for 10 min for enzyme activation, followed by 40 cycles of denaturing at 95 °C for 3 s and primer annealing and cDNA amplification at 60 °C for 30 s. Relative gene expression was calculated and normalized by L19.

Statistical analysis

Data are expressed as mean ± SD. Chi-square statistical analysis were used to test the correlations between TYMS and FOXM1 expression of CCA patients, respectively, using GraphPad Prism 7.0 (GraphPad Software Inc., La Jolla, CA, USA) and SPSS 16.0 (Imperial College London, Software Shop, UK); $p < 0.05$ was considered as statistically significant. For comparisons between groups of more than two unpaired values, analysis of variance was used, and $p < 0.05$ was considered as statistically significant.

Acknowledgements

S.Z. and P.S.-G. are post-doctoral research associates supported by the Medical Research Council (MRC) of UK (MR/N012097/1). C.-F.L. is a post-doctoral research associate supported by CRUK (C37/A187840). S.Y. and S.T. are both PhD students and research assistants supported by Imperial College IC Trust. E.W.-F.L.'s work is supported by MRC (MR/N012097/1), CRUK (C37/A12011;C37/A18784), Breast Cancer Now (2012MayPR070; 2012NovPhD016), the Cancer Research UK Imperial Centre, Imperial ECMC and NIHR Imperial BRC. S.W. is supported by the Senior Research Scholar Grant, Thailand Research Fund and Khon Kaen University for (RTA5780012), the Thailand Research Fund and Medical Research Council-UK (Newton Fund) project no. DBG5980004. K.I. and S.P. were supported by the Thailand Research Fund and KKU Joint Funding though the Royal Golden Jubilee PhD. Program (grant no. PHD/0166/2553). This study was also supported by grants from the Thailand Research Fund (DBG5980004) and Khon Kaen University research funding (KKU#591005). We thank the research assistants at the Faculty of Medicine, Khon Kaen University for technical support.

Author details

[1]Department of Surgery and Cancer, Imperial College London, Imperial College London, Hammersmith Hospital Campus, London W12 0NN, UK. [2]Biomedical Science Program, Graduate School, Khon Kaen University, Khon Kaen 40002, Thailand. [3]Cholangiocarcinoma Research Institute, Khon Kaen University, Khon Kaen 40002, Thailand. [4]Department of Biochemistry, Faculty of Medicine, Khon Kaen University, Khon Kaen 40002, Thailand. [5]Department of Pathology, Faculty of Medicine, Khon Kaen University, Khon Kaen 40002, Thailand. [6]Department of Surgery, Faculty of Medicine, Khon Kaen University, Khon Kaen, Thailand. [7]Department of Parasitology, Faculty of Medicine, Khon Kaen University, Khon Kaen, Thailand

Conflict of interest

The authors declare that they have no conflict of interest.

Supplementary Information accompanies this paper at (https://doi.org/10.1038/s41419-018-1235-0).

Received: 11 June 2018 Revised: 1 November 2018 Accepted: 23 November 2018
Published online: 11 December 2018

References

1. IARC Working Group on the Evaluation of Carcinogenic Risk to Humans. in *IARC Monographs on the Evaluation of Carcinogenic Risks to Humans*, Vol. 100B. 342–370 (IARC, Lyon, 2012).
2. Sripa, B. et al. The tumorigenic liver fluke *Opisthorchis viverrini*–multiple pathways to cancer. *Trends Parasitol.* **28**, 395–407 (2012).
3. Chamadol, N. et al. Histological confirmation of periductal fibrosis from ultrasound diagnosis in cholangiocarcinoma patients. *J. Hepatobiliary Pancreat. Sci.* **21**, 316–322 (2014).
4. Prakobwong, S. et al. Time profiles of the expression of metalloproteinases, tissue inhibitors of metalloproteases, cytokines and collagens in hamsters infected with *Opisthorchis viverrini* with special reference to peribiliary fibrosis and liver injury. *Int. J. Parasitol.* **39**, 825–835 (2009).
5. Pinlaor, S. et al. Mechanism of NO-mediated oxidative and nitrative DNA damage in hamsters infected with *Opisthorchis viverrini*: a model of inflammation-mediated carcinogenesis. *Nitric Oxide* **11**, 175–183 (2004).
6. Khan, S. A. et al. Guidelines for the diagnosis and treatment of cholangiocarcinoma: consensus document. *Gut* **51**(Suppl 6), VI1–VI9 (2002).
7. Anderson, C. D., Pinson, C. W., Berlin, J. & Chari, R. S. Diagnosis and treatment of cholangiocarcinoma. *Oncologist* **9**, 43–57 (2004).

8. Ramirez-Merino, N., Aix, S. P. & Cortes-Funes, H. Chemotherapy for cholangiocarcinoma: an update. *World J. Gastrointest. Oncol.* **5**, 171–176 (2013).
9. Chong, D. Q. & Zhu, A. X. The landscape of targeted therapies for cholangiocarcinoma: current status and emerging targets. *Oncotarget* **7**, 46750–46767 (2016).
10. Yao, D., Kunam, V. K. & Li, X. A review of the clinical diagnosis and therapy of cholangiocarcinoma. *J. Int. Med. Res.* **42**, 3–16 (2014).
11. Jinawath, N. et al. Comparison of gene expression profiles between *Opisthorchis viverrini* and non-*Opisthorchis viverrini* associated human intrahepatic cholangiocarcinoma. *Hepatology* **44**, 1025–1038 (2006).
12. Koo, C. Y., Muir, K. W. & Lam, E. W. FOXM1: from cancer initiation to progression and treatment. *Biochim. Biophys. Acta* **1819**, 28–37 (2012).
13. Khongkow, P. et al. FOXM1 targets NBS1 to regulate DNA damage-induced senescence and epirubicin resistance. *Oncogene* **33**, 4144–4155 (2014).
14. Liu, X. et al. MicroRNA-149 increases the sensitivity of colorectal cancer cells to 5-fluorouracil by targeting forkhead box transcription factor FOXM1. *Cell Physiol. Biochem.* **39**, 617–629 (2016).
15. Myatt, S. S. & Lam, E. W. The emerging roles of forkhead box (Fox) proteins in cancer. *Nat. Rev. Cancer* **7**, 847–859 (2007).
16. Longley, D. B., Harkin, D. P. & Johnston, P. G. 5-fluorouracil: mechanisms of action and clinical strategies. *Nat. Rev. Cancer* **3**, 330–338 (2003).
17. Tepsiri, N. et al. Drug sensitivity and drug resistance profiles of human intrahepatic cholangiocarcinoma cell lines. *World J. Gastroenterol.* **11**, 2748–2753 (2005).
18. Hahnvajanawong, C. et al. Orotate phosphoribosyl transferase mRNA expression and the response of cholangiocarcinoma to 5-fluorouracil. *World J. Gastroenterol.* **18**, 3955–3961 (2012).
19. Denechaud, P. D., Fajas, L. & Giralt, A. E2F1, a novel regulator of metabolism. *Front. Endocrinol. (Lausanne)* **8**, 311 (2017).
20. Zona, S., Bella, L., Burton, M. J., Nestal de Moraes, G. & Lam, E. W. FOXM1: an emerging master regulator of DNA damage response and genotoxic agent resistance. *Biochim. Biophys. Acta* **1839**, 1316–1322 (2014).
21. Yan, L. H. et al. Overexpression of E2F1 in human gastric carcinoma is involved in anti-cancer drug resistance. *BMC Cancer* **14**, 904 (2014).
22. Millour, J. et al. ATM and p53 regulate FOXM1 expression via E2F in breast cancer epirubicin treatment and resistance. *Mol. Cancer Ther.* **10**, 1046–1058 (2011).
23. de Olano, N. et al. The p38 MAPK-MK2 axis regulates E2F1 and FOXM1 expression after epirubicin treatment. *Mol. Cancer Res.* **10**, 1189–1202 (2012).
24. Kasahara, M. et al. Thymidylate synthase expression correlates closely with E2F1 expression in colon cancer. *Clin. Cancer Res.* **6**, 2707–2711 (2000).
25. Liu, H. et al. Herbal formula Huang Qin Ge Gen Tang enhances 5-fluorouracil antitumor activity through modulation of the E2F1/TS pathway. *Cell Commun. Signal.* **16**, 7 (2018).
26. Monteiro, L. J. et al. The Forkhead Box M1 protein regulates BRIP1 expression and DNA damage repair in epirubicin treatment. *Oncogene* **32**, 4634–4645 (2013).
27. Myatt, S. S. et al. SUMOylation inhibits FOXM1 activity and delays mitotic transition. *Oncogene* **33**, 4316–4329 (2014).
28. Kwok, J. M. et al. FOXM1 confers acquired cisplatin resistance in breast cancer cells. *Mol. Cancer Res.* **8**, 24–34 (2010).
29. Karunarathna, U. et al. OTUB1 inhibits the ubiquitination and degradation of FOXM1 in breast cancer and epirubicin resistance. *Oncogene* **35**, 1433–1444 (2016).
30. Bektas, H. et al. Surgical treatment for intrahepatic cholangiocarcinoma in Europe: a single center experience. *J. Hepatobiliary Pancreat. Sci.* **22**, 131–137 (2015).
31. Hezel, A. F. & Zhu, A. X. Systemic therapy for biliary tract cancers. *Oncologist* **13**, 415–423 (2008).
32. Ishida, S. et al. Role for E2F in control of both DNA replication and mitotic functions as revealed from DNA microarray analysis. *Mol. Cell Biol.* **21**, 4684–4699 (2001).
33. Obama, K. et al. Genome-wide analysis of gene expression in human intrahepatic cholangiocarcinoma. *Hepatology* **41**, 1339–1348 (2005).
34. Kongsema, M. et al. RNF168 cooperates with RNF8 to mediate FOXM1 ubiquitination and degradation in breast cancer epirubicin treatment. *Oncogenesis* **5**, e252 (2016).
35. Khongkow, P. et al. Paclitaxel targets FOXM1 to regulate KIF20A in mitotic catastrophe and breast cancer paclitaxel resistance. *Oncogene* **35**, 990–1002 (2016).
36. Burdelski, C. et al. Overexpression of thymidylate synthase (TYMS) is associated with aggressive tumor features and early PSA recurrence in prostate cancer. *Oncotarget* **6**, 8377–8387 (2015).
37. Peters, G. J. et al. Induction of thymidylate synthase as a 5-fluorouracil resistance mechanism. *Biochim. Biophys. Acta* **1587**, 194–205 (2002).
38. Copur, S., Aiba, K., Drake, J. C., Allegra, C. J. & Chu, E. Thymidylate synthase gene amplification in human colon cancer cell lines resistant to 5-fluorouracil. *Biochem. Pharmacol.* **49**, 1419–1426 (1995).
39. Grant, G. D. et al. Identification of cell cycle-regulated genes periodically expressed in U2OS cells and their regulation by FOXM1 and E2F transcription factors. *Mol. Biol. Cell* **24**, 3634–3650 (2013).
40. Nakajima, T. et al. Activation of B-Myb by E2F1 in hepatocellular carcinoma. *Hepatol. Res.* **38**, 886–895 (2008).
41. Ju, J., Pedersen-Lane, J., Maley, F. & Chu, E. Regulation of p53 expression by thymidylate synthase. *Proc. Natl Acad. Sci. USA* **96**, 3769–3774 (1999).
42. Liu, J. et al. Thymidylate synthase as a translational regulator of cellular gene expression. *Biochim. Biophys. Acta* **1587**, 174–182 (2002).
43. Chu, E. et al. Thymidylate synthase protein and p53 mRNA form an in vivo ribonucleoprotein complex. *Mol. Cell Biol.* **19**, 1582–1594 (1999).
44. Ong, C. K. et al. Exome sequencing of liver fluke-associated cholangiocarcinoma. *Nat. Genet.* **44**, 690–693 (2012).
45. Barsotti, A. M. & Prives, C. Pro-proliferative FoxM1 is a target of p53-mediated repression. *Oncogene* **28**, 4295–4305 (2009).
46. Prakobwong, S. et al. Involvement of MMP-9 in peribiliary fibrosis and cholangiocarcinogenesis via Rac1-dependent DNA damage in a hamster model. *Int. J. Cancer* **127**, 2576–2587 (2010).
47. Yongvanit, P., Pinlaor, S. & Bartsch, H. Oxidative and nitrative DNA damage: key events in opisthorchiasis-induced carcinogenesis. *Parasitol. Int.* **61**, 130–135 (2012).
48. Sirisinha, S. et al. Establishment and characterization of a cholangiocarcinoma cell line from a Thai patient with intrahepatic bile duct cancer. *Asian Pac. J. Allergy Immunol.* **9**, 153–157 (1991).
49. Haonon, O. et al. Upregulation of 14-3-3 eta in chronic liver fluke infection is a potential diagnostic marker of cholangiocarcinoma. *Proteomics Clin. Appl.* **10**, 248–256 (2016).
50. The ENCODE Project Consortium. An integrated encyclopedia of DNA elements in the human genome. *Nature* **489**, 57–74 (2012)..

INVITED REVIEW
doi: 10.2306/scienceasia1513-1874.2018.44S.011

ScienceAsia 44S (2018): **11–18**

Translational cancer research towards Thailand 4.0

Kanlayanee Sawanyawisuth[a], Chaisiri Wongkham[a], Chawalit Pairojkul[b], Sopit Wongkham[a,c,*]

[a] Department of Biochemistry, Faculty of Medicine, Khon Kaen University, Khon Kaen 40002 Thailand
[b] Department of Pathology, Faculty of Medicine, Khon Kaen University, Khon Kaen 40002 Thailand
[c] Center for Translational Medicine, Faculty of Medicine, Khon Kaen University, Khon Kaen 40002 Thailand

[*]Corresponding author, e-mail: sopit@kku.ac.th

ABSTRACT: Cancer is still a major cause of mortality in the Thai population. The heterogeneity and complexity of cancer make this disease often result in ineffective treatment and a fatal outcome. Primary prevention for a known-risk cancer is one way to minimize the number of new cancer cases; however, effective treatment with reasonable cost-effectiveness is important for cancer patients. Basic and preclinical cancer research are necessary for better and deeper understanding of the nature of cancer. Several research initiatives should be implemented to translate the preclinical developments to clinical outcome. High specificity and sensitivity of tumour markers in serum or secretory fluids are helpful for diagnosis of cancer before advanced, high cost, or invasive diagnoses are implemented. A set of potential markers instead of a single marker should be researched to increase the diagnostic power of the tests for a particular cancer. Simplicity, low cost, and highly effective diagnostic power of the test is also required to validate a test for clinical use. The knowledge generated at the molecular level together with the advanced technologies of next-generation sequencing, cellular and molecular biology, and computational biology, provide a new trend of precise treatment against individual cancers. Histoculture drug response assays or in vitro chemo-sensitivity assays, genomic profiling of tumours by next-generation sequencing, drug repositioning for cancer, and chimeric antigen receptor T-cell therapy are exciting approaches that lead to precise and effective therapy for cancer patients. In this review, several new directions for the precise diagnosis and effective treatments of cancer are highlighted.

KEYWORDS: precision medicine, histoculture drug response assay, repurposing drugs, CAR T-cell

INTRODUCTION

Cancer is considered a leading cause of death worldwide in developed and developing countries, including Thailand. The number of cancer cases and deaths is expected to grow rapidly. As noted in GLOBOCAN 2012, approximately 8 million people died of cancer and 14 million new cases were recorded worldwide[1]. The most commonly diagnosed cancer in each country varied considerably. Based on GLOBOCAN 2012, prostate cancer was the most common cancer among males in North and South America, and Europe while the leading cancers among males varied substantially in Africa and Asia[2]. Breast cancer was the most common cancer among females in North America, Europe and Oceania, whereas breast and cervical cancers were the most frequently found cancers in Africa and most of Asia. According to the World Health Organization, the numbers of new cancer cases are expected to rise by about 70% over the next 20 years[3].

Cancer is also the highest cause of death of Thais. The mortality rates of the Thai population in 2015, analysed from the Health Information System Development Office, Ministry of Public Health of Thailand (www.hiso.or.th) revealed that 417 per 100 000 Thais died because of cancer, followed by kidney failure (100), accident (98) and diabetes mellitus (75) (Fig. 1). Among all cancer deaths, lung cancer was highest in the north, while liver cancer was extremely high in the north-east. Breast and cervical cancers seemed to be distributed over the country with lower rates in the north-east and the south (Fig. 2). Except for cervical cancer that seems to have been stable for a couple years, mortality rates of all major cancers in Thailand have an increasing trend. This may be due to the changes of lifestyle that increases exposure and accesses to risk factors, decreases physical activity, and changes eating habits and behaviour.

Thailand is now facing an ageing society. Low birth rates and longevity of the elderly population moves Thailand towards an ageing society. Of any developing country in East Asia and Pacific, Thailand together with China, has the highest share

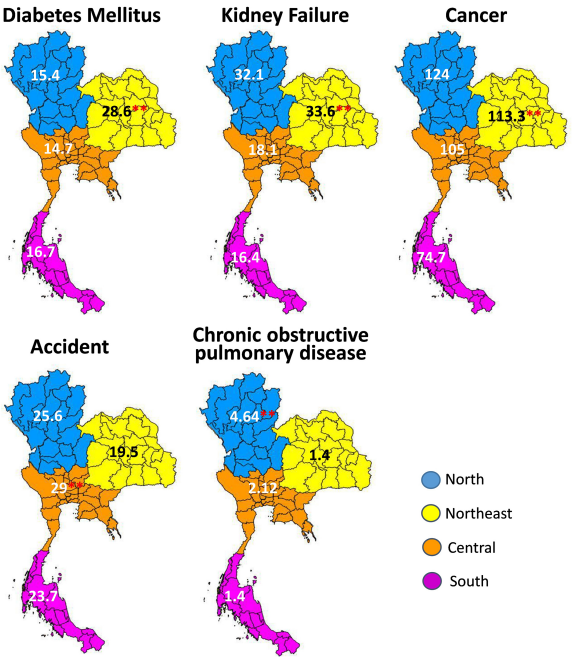

Fig. 1 The major causes of mortality in the Thai population, in 2015. The geographical distribution of mortality rates of the major causes of death in the Thai population in 2015. Cancer was the highest cause of death, followed by kidney failure and accidents. The numbers are rates of mortality per 100 000 persons; ** indicates the highest mortality rate. Data from the Health Information System Development Office, Ministry of Public Health of Thailand (www.hiso.or.th).

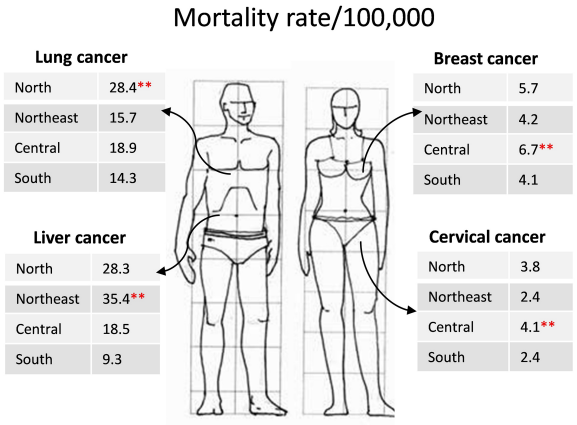

Fig. 2 Four major causes of cancer death in the Thai population in 2015. The leading cancers among Thai males in 2015 was liver cancer, followed by lung cancer, whereas those in Thai females was breast cancer and cervical cancer. The numbers indicate rates of mortality per 100 000 persons and ** indicates the highest mortality rate. Modified figure from http://how2drawrunggg.blogspot.com/2014/01/humanscale-1-7-4-normal-7-dialistic-8.html.

of elderly people[4]. As the occurrence of cancer increases with age, it can be presumed that there will be a growing cancer incidence and mortality in the Thai population and the rising of healthcare expense for cancer patients in the next decade. Besides the primary prevention, effective diagnosis, treatments and care for cancer patients should be considered. The research and development to achieve an early and definite diagnosis as well as effective treatments for cancer patients should be intensively evaluated. This article is intended to share the perspective of cutting-edge biomedical research that may ultimately contribute to specific diagnosis and better treatments for cancer patients towards Thailand 4.0.

INNOVATION OF TUMOUR MARKERS FOR DIAGNOSIS AND PROGNOSIS OF CANCER

Cancer is a group of diseases that can occur in any tissue or organ with a common characteristic—uncontrolled cell growth. Cancer cells divide uncontrollably, form masses and in the advanced stage, metastasize to distant organs. Most fatal cancers are slow growing and have no specific symptoms at the beginning, thus almost all patients are diagnosed when cancers have metastasized. The potentially curative treatment is surgical resection, however, this can only be offered effectively for early stage cancers. Early detection of cancer is, thus crucial to reduce morbidity and mortality. Advanced imaging techniques such as X-rays, CT scans, MRI scans, PET scans, and ultrasound scans are used to detect tumour masses. These techniques, however, have limited sensitivity in detecting small masses or metastatic foci and are very much dependent on the experience of the operators. In addition, they are available only to a limited number of patients due to their high cost. Tumour markers then play a key role for primary diagnosis of suspected cancer in persons before using invasive or high cost diagnostic technologies.

Tumour associated markers are substances produced by a tumour itself or by the body as a response to the tumour. These biomarkers can be detected in tumour tissues and its microenvironments or body fluids, such as whole blood, serum, urine, and saliva. Several biomolecules reflecting the biological processes of cancer cells can be used as tumour markers. They can be proteins, glycoproteins, DNA, long non-coding RNA (lncRNAs), mi-

croRNAs (miRNAs), metabolites, tumour associated macrophages and fibroblasts, circulating tumour cells and white blood cells. Tumour markers are of benefit not only for diagnosis, but also for prognosis and prediction of drug response. Some markers are good for screening as a health checkup. Long-term surveillance should be provided for a person who is positive for these markers. An early stage cancer, may then be diagnosed during follow up. Some tumour markers are of benefit for cancer diagnosis. These markers should be determined in combination with other investigations for definite diagnosis of a particular cancer. The prognostic markers are suitable to provide the information for clinicians to select the appropriate and effective treatment for patients. These markers mostly reflect the clinical manifestations of patients and are associated with patient survival or tumour staging. Some tumour markers are associated with drug responses or idiosyncratic genetic problems and can be used to predict the responsiveness of patients to the drug treatment.

The present high-throughput and large-scale analytical technologies, i.e., genomics, transcriptomics, proteomics and metabolomics, offer researchers an opportunity to discover a number of potential markers that could be used for diagnosis, prognosis or prediction of treatment responses for an individual patient. While many of them even hold a promising potential to use in clinical practice, many of them may not identify a particular type of cancer. As cancer is heterogeneous, it is well accepted that a combination markers may have better diagnostic power than a single marker. Using a ratio of two serum proteins may have high diagnostic and predictive powers in several cancer types. A comparison of serum proteomes from cholangiocarcinoma (CCA) patients and healthy controls, differential amounts of $\alpha_1\beta$-glycoprotein (A1BG) and afamin (AFM) were identified in sera from CCA patients[5]. Determination of these two serum proteins in a single blood test as an A1BG/AFM ratio could differentiate CCA patients with 84% sensitivity and 88% specificity. Besides, the albumin to γ-glutamyltransferase ratio[6] and the aspartate aminotransferase to neutrophil ratio[7] was proposed as a potential prognostic markers for CCA. A suitable combination of markers can give a precise diagnosis for a specific cancer type with satisfactory sensitivity and specificity for clinical implications. Most researchers selected the markers as a combination based on the physiological functions of those particular molecules. Machine learning decisions can effectively assist researchers in selecting a combination of potential markers with designed specificity and sensitivity. Using a decision tree diagram built by the C4.5 algorithm, 2 of the 8 diagnostic markers were selected to distinguish CCA patients from non-CCA subjects with sensitivity, specificity and accuracy $\geqslant$ 95% [8]. With the high sensitivity, specificity and accuracy, a simple blood test could be the way to replace the biopsy; the gold standard for detecting cancer.

Based on a search on Pubmed from 2000–2017, there were 645 publications published by authors from Thailand on markers and cancers. Only a limited number of these, however, could be translated to clinical practice. To discover novel and high impact tumour markers available in clinical practice, collaboration and integration of knowledge among different disciplines are the keys to success. Biomolecular researchers, clinicians, biostatisticians, bio-informaticians, granting agencies and private sectors should join hands and set up a national project to innovate development of diagnostic tests for cancers that have a high incidence in Thailand. Evaluation of the usefulness of candidate tumour markers in routine pathological diagnosis is the next step needed to analyse their values. Systematic reviews and meta-analyses should be evaluated to clarify the impact of the potential markers for particular cancers and to prevent over-diagnoses. The detection techniques and the cohorts of studies with appropriate clinical data and precise sample collections are of importance and should be considered. A nationwide biobank to collect bio-samples taken with standard protocols should be set to support the discovery of novel tumour markers. In parallel, the non- or low invasive sample collection techniques, as well as the simple and affordable determination methods should be taken into account. Finally, towards the Thailand 4.0 policy, the possibility of the determination of the manufacture of tumour markers as commercially available test kits should be assessed.

PRECISION MEDICINE: AN UPCOMING APPROACH FOR EFFECTIVE TREATMENT OF CANCER

Many efforts and huge budgets have been invested to discover new drugs for cancer treatment. Low response rates and short overall survival, however, are still the norm. High recurrence rates and drug resistance are the main problems of ineffective treatments using either chemotherapy or targeted therapies. Furthermore, patients with similar cancer

types frequently exhibit different drug responses to the same drug treatment. This observation has lately been shown to be the different molecular signatures of cancer in individuals that takes into account the diverse drug responses in individual patients. Not only the histopathology and clinical features of the cancer, but the specific molecular features of the cancer that drive and regulate the behaviour of cancer in a particular individual. Several studies have indicated different molecular signatures among individual persons with similar cancer types. For example, different expression patterns in transcriptomes, epigenomes and mutations were reported recently among cholangiocarcinoma patients from liver fluke and non-liver fluke associated cancers[9–12]. A "one-size-fits-all approach", in which the treatment strategies are developed for the average person, therefore, may not be not effective. To face this fact, an upcoming approach of 'precision medicine', in which the treatment is arranged according to individual variability in genes, environment, and lifestyle of each person, is recommended[13]. The cancers could be classified according to their expression profiles to predict the drug responsiveness of cancer in an individual as a good or poor response to the cancer. This is not only to increase the response rate and cost-effectiveness of the outcome but also avoids the opposite adverse effect of cytotoxic drugs for those who will not tolerate the treatment. This approach provides clinicians and researchers a means to predict more accurately the best treatment that will effectively work for individual cancer patient.

Precision medicine holds promise for improving treatment for cancer and many other diseases. Precision medicine is still young in Thailand. To establish this approach, physicians and medical scientists have to prepare many aspects in the drive for "precision medicine for cancer" in the country towards Thailand 4.0. Basic research is needed for a better understanding of biology, molecular signature sand underlying mechanisms of specific types of cancer in Thai patients. This information is of value not only for improving the treatment but also for diagnosis and prevention. As Thailand 4.0 targets a high value economy, basic research is necessary to analyse and filter the potential genes that may reflect the prognosis and drug response. Special cellular and molecular technologies, such as histoculture drug response assays, organoid and patient tissues derived xenograft models, RNA sequencing (RNAseq), and data mining are required.

IN VITRO-GUIDED THERAPY IMPROVES RESPONSIVENESS TO DRUG THERAPY IN CANCER PATIENTS

The histoculture drug response assay (HDRA) or in vitro chemo-sensitivity assay were developed in considering the urgent need for chemo-resistance prediction in cancer patients. Several clinical studies including colorectal, gastric and lung cancers revealed that inhibition rates obtained with HDRA can predict clinical responses to chemotherapy[14,15]. A study reported in Ref. 16, demonstrated that HDRA appeared to be useful to cancer patients for prediction of responses to chemotherapy. In this study, tumours from 329 various cancer patients who underwent chemotherapy were cultured and tested with different chemo-drugs for 5 days. The overall survivals were compared between patients with HDRA guided therapy and those with empiric therapy. The results indicated that the overall survivals in patients treated with HDRA guided therapy were significantly prolonged compared to those with empiric therapy. Similar results were obtained in a report of 359 lung cancer patients studied[17]. Using HDRA to evaluate the chemo-sensitivities of lung tumour tissues to several chemotherapeutic drugs, patients who received HDRA guided therapy are reported. They found that the evaluability and predictability of HDRA were high and could be used to predict clinical responses. Several studies demonstrated the strong association of in vitro and in vivo effects[17], however, it is hard to exclude selection bias and confounding as an influence on the results. Future research should be conducted with well-designed randomized trials to measure survival outcomes.

HDRA is a representative of an in vitro drug response test for anticancer agents in individuals before starting the chemotherapy. It provides a reliable drug sensitivity test with a simple and low cost method. The advantages of the HDRA over other single cells suspension methods may be due to good cell viability and a more natural patient environment. Future investigation on the profit of HDRA guided treatment may provide a place for HDRA to be an adjuvant investigation for targeted or second- or third-line chemotherapies. As the biological and molecular characteristics of each cancer type differ, it is suggested that before implementation of HDRA in routine clinical practice, it should be verified whether HDRA is applicable and useful for the specific cancer type under consideration. Furthermore, one should be aware that primary culture

is sometimes not successful due to contamination, non-growth or fibroblast overgrowth. In addition, HDRA requires a large amount of tissue which may limit the application of HDRA in clinical practice.

GENOMIC PROFILING OF TUMOURS LEADS TO PERSONALIZED-PRECISION THERAPY FOR CANCER PATIENTS

Cancer can be considered as a genome defect disease. Accumulation of genomic alterations, i.e., activation of oncogenes, suppression of tumour suppressor genes, mutation of several genes and alteration in epigenetics that transform normal cells to uncontrolled cancer cells are all possibilities. Basic and clinical cancer research have identified a number of mechanisms associated with cancer development and progression. The present advanced technology in sequencing, commonly known as next-generation sequencing (NGS), not only provides in-depth understanding of the genomic land-scape of cancers but also enables the identification of crucial genetic pathways that may be the molecular therapeutic targets. NGS makes it possible to have routine genomic studies of tumours in clinical practice. This allows clinicians and scientists to improve the prognosis of clinical outcomes in individuals and leads to further development of precision therapy.

The use of imatinib, the kinase inhibitor, for the treatment of chronic myelogenous leukaemias (CML) was the pioneer example for molecular driven therapy. Treatment with imatinib in CML patients who harboured BCR-ABL1 chromosomal translocation significantly improved their survival almost similar to those of general population[18]. Similarly, HER2-targeted therapies for patients with metastatic HER2-positive breast cancer dramatically increased a median survival to almost 5 years[19] and improved the cure rates of early-stage HER2-positive breast cancer by 35–50%[20]. Currently, therapies targeting 11 somatic aberrations of tumours in 10 different cancer types were identified[21]. Targeting the clinically validated predictive biomarkers has proven to benefit not only a specific type of tumour but also to benefit other tumours that possess similar genetic alterations. For example, the use of RAF and MEK inhibitors in cutaneous melanoma patients with BRAF V600 mutations effectively improved survivals of these patients[22]. BRAF V600 mutations, however, were also evident in non-melanoma cancer patients who may obtain benefit from the same treatment. Currently, the clinical activities of these inhibitors have been identified in lung and thyroid cancers as well as in hairy cell leukaemia[23,24]. A common molecular subtypes of intrahepatic cholangiocarcinoma and hepatocellular carcinoma from Thai patients was demonstrated recently[25], even these two cancers are clinically different with etiological and biological heterogeneity. In this context, targeted therapy should be prescribed for selected subsets of patients according to the genomic alterations of the tumour regardless of tumour type or tumour origin. Hence a new taxonomy of human cancers based on genomic profiling of abnormal mutation has been suggested to complement current histology-based classifications[26].

Advances in NGS technologies have generated a large volume of data supporting somatic alterations in cancer that can be targeted for precision cancer therapy. Genomic profiling of tumours could identify the most appropriate targeted therapy to an individual patient who harbours a particular genetic profile or molecular feature. Broadening the use of targeted therapy in a larger cohort with multiple types of tumours will maximize the utilization of precision medicine in cancer. Other factors, however, may alter the responsiveness of cancer to targeted therapy and have to be taken into account. Genomic variants and the tumour microenvironment of an individual may modulate the sensitivity of the patient to a specific inhibitor of targeted therapy. These factors may signify the complexity of genomic data and decision-making for clinical implications. Finally, collaborative genome-driven clinical trials should be initiated worldwide to refine a better understanding of the roles of these genomic aberrations in association with disease pathogenesis, drug response and resistance that may lead to discovery of new drug target.

DRUG REPOSITIONING AS A PROMISING STRATEGY FOR NEW ANTICANCER AGENTS

Drug repositioning or drug repurposing for the identification of new therapeutic indications is the goal for already approved drugs. This approach is a promising strategy for drug discovery and development, as the traditional drug discovery approach is more time consuming and expensive. The repositioning is not only faster and cheaper to translate from bench to clinic but is also a benefit for patients as it reduces safety risks and accelerates successful access to treatment[27,28]. Drug repurposing, however, is not completely safe or ready to use as biological activity, pharmacokinetics, and clinical observations such as adverse effects, new dosing and scheduling in a new set of patients, are needed

to be fully analysed.

Currently, there are several reports on using existing drugs as antitumor agents. For example, metformin, a standard drug for diabetes, has been reported to reduce the carcinogenic risk and inhibit tumour cell growth in endometrial, breast and ovarian cancers. The efficacy of metformin for the treatment of these cancers has been suggested in preclinical studies and clinical trials. In addition, the combination of metformin and doxorubicin, a chemotherapeutic agent, effectively inhibited growth of breast cancer stem cells and cancer cells in culture[29]. The treatment in a xenograft mouse model not only reduced tumour mass but also prevents relapse of cancer. The study supported the rationale of using a combination of metformin and chemo-drugs to improve treatment of breast cancer patients. In the experience of the present authors, metformin exhibited significantly anti-proliferative activity on cholangiocarcinoma cells in a dose and time dependent fashion[30]. Furthermore, a low dose of metformin could potentially increase anoikis and inhibit migration and invasion of cancer cells. These findings encourage the repurposing of metformin in clinical trials to improve treatment of this cancer. Several anti-parasitic drugs were also investigated for their efficacies to repurpose as anticancer agents; such as mebendazole, chloroquine, and artesunate. Anticancer activity of mebendazole as an anthelmintic drug that has been used extensively for gastro-intestinal parasitic infections in humans, has been shown effective in preclinical studies in various types of cancers, e.g., lung, brain, melanoma and cholangiocarcinoma[31–33].

Recently, computational techniques and methods have been proposed for repositioning of cancer drugs. It can be 'on-target' repositioning when known pharmacological activity is applied to a different clinical application or 'off-target' repositioning, if a new mechanism has been identified for a known drug. There are different approaches to re-investigate known drugs for cancer treatment, i.e., target based, drug based and disease based[34]. Computational and experimental methods are needed to search for the potential repurposing drugs. Computational technologies are helpful to integrate data from various sources, i.e., pharmacologic, genomic, phenotypic, chemical and clinical information. Prediction of drug-disease responses could be obtained using bio-informatic technologies, machine learning-based models, biological network analysis and text-mining research. For validation of candidate compounds suggested by computational analyses, both in vitro and in vivo are necessary to be performed. Deeper understanding of genomics and molecular pathways and drug activity associated with cancer are essential to support the potential application of drug repurposing in personalized therapy.

Drug repurposing for cancer in Thailand is still young and most of research is at the preclinical level. A number of natural and synthetic compounds with anticancer activities have been reported. None, however, have been continuously validated and translated to patients. A collaborative network among investigators with different expertise including computational researchers, bio-informaticians, cell biologists and molecular biologists, as well as clinicians should be set up. Research programs, new tools and approaches for managing data should be developed from databases of Thai patients. These issues are necessary to fully realize the promise of drug repurposing in personalized medicine.

Immunotherapy for cancer

In general, immune cells can recognize cancer cells and eradicate them. Cancer cells, however, can develop a system to evade immune response and hence cancer develops. Over the past several years, immunotherapy for cancer has emerged and the most advanced and furthest in clinical implication is Chimeric Antigen Receptor (CAR) T-cell therapy. The principal of this approach is to strengthen the power of a patient's immune system to attack tumours by engineering the T-cells themselves to enhance the immune response against a specific tumour antigen. The common procedure involves, (i) genetically modifying T-cells from the patient to express a CAR on their cell membranes, (ii) expand these T-cells in vitro, and (iii) reinfuse the CAR T-cells into the patient. Second and third generation CAR-Ts have additional co-stimulatory domains that further enhance the immune response[35]. Until recently, CAR T-cell therapy has shown huge remission rates, largely in patients with advanced blood cancers. In 2017, two CAR T-cell therapies were approved by the Food and Drug Administration (FDA); one for the treatment of children with acute lymphoblastic leukaemia and the other for adults with advanced lymphomas. Whether CAR T-cell therapy will be effective against solid tumours, is still questionable[36].

The ability to rewire an immune system to fight cancer is an alternative therapy and a new hope for cancer patients. Immunotherapy for cancer is still in its infancy in the scientific world and

in Thailand. There are several factors that are of concern clinically; the biomarker that could be targeted by a specific CAR T-cell therapy, the adverse consequences associated with autoimmune disease, and the tumour microenvironment, all of which could interfere with treatment outcomes[37].

COMMENTS

Recent advanced technologies in molecular biology, NGS and computational biology, that provide several new directions for the precise diagnosis and effective treatment of cancer are being developed. Basic and molecular research efforts in cancer biology in Thailand are solid, some of which are at the edge of translation to clinical practice. To translate the knowledge from preclinical sciences to clinical practice, new partnerships and network of scientists in various specialities, as well as people from universities, pharmaceutical companies, and others should be formed. Several national research programs aimed towards patient outcome should be developed. The Science Society of Thailand may create a stage where lead scientists in different fields can meet and develop national programs to be submitted to the government sectors that are responsible for this issue. To accelerate the translation period, many aspects have to be generated in parallel. A national biobank for cancer research, NGS service, a database for genetic profiling of cancers from Thai patients, and animal facilities for cancer research, should be developed.

Acknowledgements: This work is supported by the Thailand Research Fund and Medical Research Council-UK (Newton Fund) to C. Pairojkul (DBG5980004). We would like to acknowledge Prof. James A. Will, University of Wisconsin for editing of the manuscript via the Faculty of Medicine Publication Clinic (ID88-60MD), Khon Kaen University, Thailand.

REFERENCES

1. Ferlay J, Soerjomataram I, Ervik M, Dikshit R, Eser S, Mathers C, et al (2013) *GLOBOCAN 2012 v1.0, Cancer Incidence and Mortality Worldwide: IARC CancerBase No. 11*, International Agency for Reseach on Cancer, Lyon, France, http://globocan.iarc.fr.
2. Torre LA, Siegel RL, Ward EM, Jemal A (2016) Global cancer incidence and mortality reates and trends–an update. *Canc Epidemiol Biomarkers Prev* **25**, 16–27.
3. MNT Editorial Team (2016) Cancer: What you need to know. *Medical News Today*, Healthline Media UK Ltd, Brighton, UK, www.medicalnewstoday.com/info/cancer-oncology.
4. World Bank (2016) *Thailand Economic Monitor: Aging Society and Economy—June 2016*, World Bank Group, Washington, DC.
5. Tolek A, Wongkham C, Proungvitaya S, Silsirivanit A, Roytrakul S, Khuntikeo N, Wongkham S (2012) Serum $\alpha_1\beta$-glycoprotein and afamin ratio as potential diagnostic and prognostic markers in cholangiocarcinoma. *Exp Biol Med* **237**, 1142–9.
6. Jing CY, Fu YP, Shen HJ, Zheng SS, Lin JJ, Yi Y, et al (2017) Albumin to gamma-glutamyltransferase ratio as a prognostic indicator in intrahepatic cholangiocarcinoma after curative resection. *Oncotarget* **8**, 13293–303.
7. Liu L, Wang W, Zhang Y, Long J, Zhang Z, Li Q, et al (2017) Declined preoperative aspartate aminotransferase to neutrophil ratio index predicts poor prognosis in patients with intrahepatic cholangiocarcinoma after hepatectomy. *Canc Res Treat* **50**, 538–50.
8. Pattanapairoj S, Silsirivanit A, Muisuk K, Seubwai W, Cha'on U, Vaeteewoottacharn K, et al (2015) Improve discrimination power of serum markers for diagnosis of cholangiocarcinoma using data mining-based approach. *Clin Biochem* **48**, 668–73.
9. Jinawath N, Chamgramol Y, Furukawa Y, Obama K, Tsunoda T, Sripa B, et al (2006) Comparison of gene expression profiles between *Opisthorchis viverrini* and non-*Opisthorchis viverrini* associated human intrahepatic cholangiocarcinoma. *Hepatology* **44**, 1025–38.
10. Chan-on W, Nairismägi ML, Ong CK, Lim WK, Dima S, Pairojkul C, et al (2013) Exome sequencing identifies distinct mutational patterns in liver fluke–related and non-infection-related bile duct cancers. *Nat Genet* **45**, 1474–8.
11. Ong CK, Subimerb C, Pairojkul C, Wongkham S, Cutcutache I, Yu W, et al (2012) Exome sequencing of liver fluke–associated cholangiocarcinoma. *Nat Genet* **44**, 690–3.
12. Jusakul A, Cutcutache I, Yong CH, Lim JQ, Huang MN, Padmanabhan N, et al (2017) Whole-genome and epigenomic landscapes of etiologically distinct subtypes of cholangiocarcinoma. *Canc Discov* **7**, 1116–35.
13. National Library of Medicine (2018) *Genetics Home Reference*, NLM, National Institutes of Health, US Department of Health and Human Services, Bethesda, MD, https://ghr.nlm.nih.gov.
14. Kubota T, Sasano N, Abe O, Nakao I, Kawamura E, Saito T, et al (1995) Potential of the histoculture drug-response assay to contribute to cancer patient survival. *Clin Canc Res* **1**, 1537–43.
15. Furukawa T, Kubota T, Hoffman RM (1995) Clinical applications of the histoculture drug response assay. *Clin Canc Res* **1**, 305–11.
16. Udelnow A, Schönfelder M, Würl P, Halloul Z, Meyer F, Lippert H, Mroczkowski P (2013) In vitro chemosensitivity assay guided chemotherapy is associated

with prolonged overall survival in cancer patients. *Pol J Surg* **85**, 340–7.
17. Yoshimasu T, Oura S, Hirai I, Tamaki T, Kokawa Y, Hata K, et al (2007) Data acquisition for the histoculture drug response assay in lung cancer. *J Thorac Cardiovasc Surg* **133**, 303–8.
18. Bower H, Björkholm M, Dickman PW, Höglund M, Lambert PC, Andersson TML (2016) Life expectancy of patients with chronic myeloid leukemia approaches the life expectancy of the general population. *J Clin Oncol* **34**, 2851–7.
19. Swain SM, Baselga J, Kim SB, Ro J, Semiglazov V, Campone M, et al (2015) Pertuzumab, trastuzumab, and docetaxel in HER2-positive metastatic breast cancer. *New Engl J Med* **372**, 724–34.
20. Piccart-Gebhart MJ, Procter M, Leyland-Jones B, Goldhirsch A, Untch M, Smith I, et al (2005) Trastuzumab after adjuvant chemotherapy in HER2-positive breast cancer. *New Engl J Med* **353**, 1659–72.
21. Hyman DM, Taylor BS, Baselga J (2017) Implementing genome-driven oncology. *Cell* **168**, 584–99.
22. Brose MS, Cabanillas ME, Cohen EEW, Wirth LJ, Riehl T, Yue H, et al (2016) Vemurafenib in patients with *BRAF*^{V600E}-positive metastatic or unresectable papillary thyroid cancer refractory to radioactive iodine: a non-randomised, multicentre, open-label, phase 2 trial. *Lancet Oncol* **17**, 1272–82.
23. Planchard D, Kim TM, Mazieres J, Quoix E, Riely G, Barlesi F, et al (2016) Dabrafenib in patients with *BRAF*^{V600E}-positive advanced non-small-cell lung cancer: a single-arm, multicentre, open-label, phase 2 trial. *Lancet Oncol* **17**, 642–50.
24. Tiacci E, Park JH, De Carolis L, Chung SS, Broccoli A, Scott S, et al (2015) Targeting mutant BRAF in relapsed or refractory hairy cell leukemia. *New Engl J Med* **373**, 1733–47.
25. Chaisaingmongkol J, Budhu A, Dang H, Rabibhadana S, Pupacdi B, Kwon SM, et al (2017) Common molecular subtypes among asian hepatocellular carcinoma and cholangiocarcinoma. *Canc Cell* **32**, 57–70.e3.
26. Hoadley KA, Yau C, Wolf DM, Cherniack AD, Tamborero D, Ng S, et al (2014) Multiplatform analysis of 12 cancer types reveals molecular classification within and across tissues of origin. *Cell* **158**, 929–44.
27. Langedijk J, Mantel-Teeuwisse AK, Slijkerman DS, Schutjens MH (2015) Drug repositioning and repurposing: terminology and definitions in literature. *Drug Discov Today* **20**, 1027–34.
28. Ashburn TT, Thor KB (2004) Drug repositioning: identifying and developing new uses for existing drugs. *Nat Rev Drug Discov* **3**, 673–83.
29. Hirsch HA, Iliopoulos D, Tsichlis PN, Struhl K (2009) Metformin selectively targets cancer stem cells, and acts together with chemotherapy to block tumor growth and prolong remission. *Canc Res* **69**, 7507–11.
30. Saengboonmee C, Seubwai W, Cha'on U, Sawanyawisuth K, Wongkham S, Wongkham C (2017) Metformin exerts antiproliferative and anti-metastatic effects against cholangiocarcinoma cells by targeting STAT3 and NF-kB. *Anticanc Res* **37**, 115–23.
31. Mukhopadhyay T, Sasaki J, Ramesh R, Roth JA (2002) Mebendazole elicits a potent antitumor effect on human cancer cell lines both in vitro and in vivo. *Clin Canc Res* **8**, 2963–9.
32. Bai RY, Staedtke V, Aprhys CM, Gallia GL, Riggins GJ (2011) Antiparasitic mebendazole shows survival benefit in 2 preclinical models of glioblastoma multiforme. *Neuro Oncol* **13**, 974–82.
33. Sawanyawisuth K, Williamson T, Wongkham S, Riggins GJ (2014) Effect of the antiparasitic drug mebendazole on cholangiocarcinoma growth. *Southeast Asian J Trop Med Publ Health* **45**, 1264–70.
34. Würth R, Thellung S, Bajetto A, Mazzanti M, Florio T, Barbieri F (2016) Drug-repositioning opportunities for cancer therapy: novel molecular targets for known compounds. *Drug Discov Today* **21**, 190–9.
35. Rodríguez Fernández C (2018) A cure for cancer? How CAR-T therapy is revolutionizing oncology. *Labiotech.eu Reviews*, Labiotech UG, Berlin, Germany, https://labiotech.eu/car-t-therapy-cancer-review.
36. National Cancer Institute (2017) *CAR T Cells: Engineering Patients' Immune Cells to Treat Their Cancers*, National Cancer Institute at the National Institutes of Health, US Department of Health and Human Services, Bethesda, MD, https://www.cancer.gov/about-cancer/treatment/research/car-t-cells.
37. Smith AJ, Oertle J, Warren D, Prato D (2016) Chimeric antigen receptor (CAR) T cell therapy for malignant cancers: Summary and perspective. *J Cell Immunother* **2**, 59–68.

Molecular Oncology

FEBS PRESS science publishing by scientists

O-GlcNAc-induced nuclear translocation of hnRNP-K is associated with progression and metastasis of cholangiocarcinoma

Chatchai Phoomak[1,2], Dayoung Park[3,4], Atit Silsirivanit[1,2,5], Kanlayanee Sawanyawisuth[1,2], Kulthida Vaeteewoottacharn[1,2,5], Marutpong Detarya[1,2], Chaisiri Wongkham[1,2], Carlito B. Lebrilla[4] and Sopit Wongkham[1,2,5]

1 Department of Biochemistry, Faculty of Medicine, Khon Kaen University, Thailand
2 Cholangiocarcinoma Research Institute, Khon Kaen University, Thailand
3 Department of Surgery, Beth Israel Deaconess Medical Center, Harvard Medical School, Boston, MA, USA
4 Department of Chemistry, University of California, Davis, CA, USA
5 Center for Translational Medicine, Faculty of Medicine, Khon Kaen University, Thailand

Keywords
bile duct cancer; heterogeneous nuclear ribonucleoprotein-K; metastasis; O-GlcNAcylated proteins

Correspondence
S. Wongkham, Department of Biochemistry, Faculty of Medicine, Khon Kaen University, Khon Kaen 40002, Thailand
Tel/Fax: +66-43-348-386
E-mail: sopit@kku.ac.th
and
C. B. Lebrilla, Department of Chemistry, University of California, Davis, Davis, CA 95616, USA
Fax: +1-530-752-8995
Tel: +1-530-752-6364
E-mail: cblebrilla@ucdavis.edu

(Received 26 June 2018, revised 6 October 2018, accepted 3 November 2018, available online 10 January 2019)

doi:10.1002/1878-0261.12406

O-GlcNAcylation is a key post-translational modification that modifies the functions of proteins. Associations between O-GlcNAcylation, shorter survival of cholangiocarcinoma (CCA) patients, and increased migration/invasion of CCA cell lines have been reported. However, the specific O-GlcNAcylated proteins (OGPs) that participate in promotion of CCA progression are poorly understood. OGPs were isolated from human CCA cell lines, KKU-213 and KKU-214, using a click chemistry-based enzymatic labeling system, identified using LC-MS/MS, and searched against an OGP database. From the proteomic analysis, a total of 21 OGPs related to cancer progression were identified, of which 12 have not been previously reported. Among these, hnRNP-K, a multifaceted RNA- and DNA-binding protein known as a pre-mRNA-binding protein, was one of the most abundantly expressed, suggesting its involvement in CCA progression. O-GlcNAcylation of hnRNP-K was further verified by anti-OGP/anti-hnRNP-K immunoprecipitations and sWGA pull-down assays. The perpetuation of CCA by hnRNP-K was evaluated using siRNA, which revealed modulation of cyclin D1, XIAP, EMT markers, and MMP2 and MMP7 expression. In native CCA cells, hnRNP-K was primarily localized in the nucleus; however, when O-GlcNAcylation was suppressed, hnRNP-K was retained in the cytoplasm. These data signify an association between nuclear accumulation of hnRNP-K and the migratory capabilities of CCA cells. In human CCA tissues, expression of nuclear hnRNP-K was positively correlated with high O-GlcNAcylation levels, metastatic stage, and shorter survival of CCA patients. This study demonstrates the significance of O-GlcNAcylation on the nuclear translocation of hnRNP-K and its impact on the progression of CCA.

Abbreviations
CCA, cholangiocarcinoma; EMT, epithelial to mesenchymal transition; GlcNAc, N-acetylglucosamine; hnRNP-K, heterogeneous nuclear ribonucleoprotein-K; IHC, immunohistochemistry; MMP, matrix metalloproteinase; OGA, O-GlcNAcase; OGPs, O-GlcNAcylated proteins; OGT, O-GlcNAc transferase; sWGA, succinylated wheat germ agglutinin.

Molecular Oncology **13** (2019) 338–357

1. Introduction

O-GlcNAcylation is a post-translational modification of proteins in which a single sugar, N-acetylglucosamine (GlcNAc), is covalently attached to the hydroxyl group of a serine or threonine residue on a polypeptide. The bioassembly is a dynamic process catalyzed by two enzymes, O-GlcNAc transferase (OGT) and O-GlcNAcase (OGA), which adds and removes the GlcNAc to and from the protein, respectively (Hart *et al.*, 2007). Protein properties and functions are known to be modulated via O-GlcNAcylation, for example, phosphorylation, interactions, degradation, and localization. Several evidences have indicated the association of aberrant O-GlcNAcylation with many human diseases including cancer (Hart *et al.*, 2011; Singh *et al.*, 2015; Zachara and Hart, 2006). The significance of O-GlcNAcylation in cancer metastasis has been demonstrated *in vitro* and *in vivo*. Suppression of OGT using shRNA resulted in inhibition of metastasis in xenografted mouse models of breast cancer (Ferrer *et al.*, 2017; Gu *et al.*, 2010), cervical cancer (Ali *et al.*, 2017), and prostate cancer (Lynch *et al.*, 2012).

We have previously reported the correlation of high O-GlcNAcylation levels with shorter survival of cholangiocarcinoma (CCA) patients (Phoomak *et al.*, 2012). Specifically, increased O-GlcNAcylation of vimentin, a major intermediate filament protein, persuaded its stability and is implicated in the aggression of CCA cells. In addition, promotion of CCA aggressiveness under high glucose conditions was shown to be via elevation of OGT and O-GlcNAcylation (Phoomak *et al.*, 2017). On the other hand, suppression of OGT with siRNA significantly reduced cell migration and invasion of CCA cells (Phoomak *et al.*, 2016). According to the O-GlcNAcylated proteins database (dbOGAP) (Wang *et al.*, 2011), there are only about 800 O-GlcNAcylated proteins reported at present. In this context, there may be a number of O-GlcNAcylated proteins (OGPs) associated with progression of cancer that remain unidentified. Historically, progress has been hampered in part by the technical difficulties in detection of OGPs (Hart *et al.*, 2007). However, with the recent development of more sophisticated mass spectrometric methods in combination with biochemical tools, including enhancement of OGPs using OGA inhibitors, identification of OGPs has been markedly improved (Hart *et al.*, 2007).

This study was aimed to determine novel OGPs that modulate progression of CCA cells. OGPs were first globally enriched and labeled using Click-iT™ *O*-GlcNAc Enzymatic Labeling System, and then identified using Q Exactive Plus Orbitrap mass spectrometry. Heterogeneous nuclear ribonucleoprotein-K (hnRNP-K) was selected and validated for its O-GlcNAcylation status and involvement in CCA progression. The signal pathways related to hnRNP-K in association with migration and invasion activities of CCA cells were subsequently determined. Specifically, O-GlcNAcylation of hnRNP-K was implicated in mediation of nuclear translocation in addition to migration of CCA cells. Moreover, association of O-GlcNAcylation levels and hnRNP-K expression was observed in tumor tissues of CCA patients in association with metastatic stage and shorter survival of patients. Significantly, these results implicate hnRNP-K O-GlcNAcylation as a promising therapeutic target to suppress CCA progression.

2. Materials and methods

2.1. Antibodies and reagents

Antibodies were purchased from various sources: anti-O-GlcNAc (RL-2, MA1-072) from Pierce Biotechnology (Rockford, IL, USA); anti-hnRNP-K (H-300, sc-25373), anticyclin D1 (H-295, sc-753), anti-XIAP (H-202, sc-11426), anti-MMP2 (H-76, sc-10736), anti-MMP7 (JL07, sc-80205), and anti-OGT (F-12, sc-74546) from Santa Cruz Biotechnology (Santa Cruz, CA, USA); anticleaved caspase 3 (D175, 5A1E, #9664), anti-E-cadherin (24E10, #3195), anticlaudin-1 (D5H1D, #13255), antivimentin (D21H3, #5741), and antislug (C19G7, #9585) from Cell Signaling (Danvers, MA, USA); PUGNAc (O-(2-acetamido-2-deoxy-d-glucopyranosylidene) amino-N-phenylcarbamate) from Sigma-Aldrich (St. Louis, MO, USA).

2.2. CCA cell culture and CCA tissues

CCA cell lines (KKU-100, KKU-213, and KKU-214) were obtained from the Japanese Collection of Research Bioresources (JCBR) Cell Bank (Osaka, Japan). MMNK1, an immortal cholangiocyte cell line, was a gift from Kobayashi N. (Maruyama *et al.*, 2004). Cells were cultured in DMEM—Dulbecco's modified Eagle's medium (DMEM) (Gibco, Grand Island, NY, USA) supplemented with 10% FBS and 1% antibiotic–antimycotic under standard protocol. Transient enhancement of O-GlcNAcylation was performed by culturing cells in the presence of 20 μM PUGNAc for 24 h prior to further experiments.

The immunohistochemistry (IHC) experiments were performed using formalin-fixed paraffin-embed liver

tissues from histologically proven CCA patients. Each subject gave informed consent, and the study protocol was certified by the Ethics Committee for Human Research at Khon Kaen University (HE581369).

2.3. Identification of O-GlcNAcylated proteins

The Click-iT™ O-GlcNAc Enzymatic Labeling System (Invitrogen, Carlsbad, CA, USA) was used to detect the OGPs in CCA cells. As shown in Fig. S1, cells were homogenized and N-linked glycans were released as described previously (Park *et al.*, 2016). Protein (2 mg) was trypsinized with 1 μg trypsin at 37°C overnight. The peptides were enriched with C-18 column (Discovery® DSC-18, 52603U, Sigma) as standard protocol for solid-phase extraction (Yang *et al.*, 2016). O-GlcNAcylated peptides were enzymatically labeled with azido-modified galactose (GalNAz) by mutant β-1,4-galactosyltransferase (Gal-T1 (Y289L)). The labeled peptides were tagged with biotin-alkyne by Click-iT™ Biotin Protein Analysis Detection Kit (Invitrogen). The complex was then pulled down with streptavidin–agarose resin (Thermo Scientific, Waltham, MA, USA) at 4 °C overnight. The peptides were cleaved by mild β-elimination and Michael addition (BEMAD; 1.5% triethylamine, 20 mM dithiothreitol, pH 12-12.5 with NaOH). The reaction was incubated at 54 °C for 4 h with shaking and stopped by addition of 2% trifluoroacetic acid. The peptides were enriched and analyzed using a Q Exactive Plus Orbitrap mass spectrometer (Thermo Scientific; Park *et al.*, 2015). A 60-min binary gradient was applied using 0.1% (v/v) formic acid in (A) water and (B) acetonitrile. The parameters of protein identification were set as follows: spray voltage 2.2 kV; ion transfer capillary temperature 200 °C; MS automatic gain control 1×10^6; MS maximum injection time 30 ms; MS/MS automatic gain control 5×10^4; MS/MS maximum injection time 50 ms; isolation width 1.6; normalized collision energy 27; charge state preference 2–8. The proteomics data were analyzed by X!Tandem (Craig and Beavis, 2004). Identified proteins were matched to the human proteome (SWISSPROT) and the Database of O-GlcNAcylated Proteins and Sites (dbOGAP) (Wang *et al.*, 2011).

2.4. Transient suppression of hnRNP-K expression using specific siRNA

hnRNP-K expression in CCA cells was suppressed using siRNA (Zhang *et al.*, 2016b) as previously reported (Phoomak *et al.*, 2016). Cells treated with scramble siRNA (Negative Control siRNA, 1027310, Qiagen, Hilden, Germany) were used as the control.

2.5. Cell proliferation

Viable cells were measured using the WST-8 proliferation assay (Cell Counting Kit-8 (CCK-8), Dojindo Molecular Technologies, Inc., Rockville, MD, USA) according to the manufacturer's guidelines. The absorbance of soluble WST-8 formazan was measured at 450 nm. Cell numbers were calculated as % of control cells.

2.6. Cell migration and invasion

CCA cells (40 000 cells) were placed into the upper chamber of a 8.0 μm pore size transwell-cell culture inserts (Corning Incorporated, Corning, NY, USA) for migration and invasion assays as previously described (Phoomak *et al.*, 2016). Cells were allowed to migrate or invade: 9 h for KKU-213 and 24 h for KKU-214. The migrated and invaded cells underneath the filter were stained and counted under a microscope with 10× objective lens. Experiments were performed in triplicate, and cells from 5 microscopic fields/insert were determined and calculated as % of control.

2.7. Immunoprecipitation

Cell lysate was prepared and immunoprecipitation was performed as previously described (Phoomak *et al.*, 2016). Briefly, cell lysates (500 μg) were immunoprecipitated with 2 μg anti-O-GlcNAc or anti-hnRNP-K at 4 °C, overnight. The immunoprecipitated complex was separated and solubilized in SDS sample buffer prior to SDS/PAGE and western blotting.

2.8. Succinylated wheat germ agglutinin (sWGA) pull-down assay

The sWGA pull-down assay was performed as previously described (Kang *et al.*, 2009). In brief, 500 μg of cell lysates was incubated with 40 μL of agarose-conjugated sWGA (Vector Laboratories, Burlingame, CA, USA) with or without 0.25 M GlcNAc at 4 °C, overnight. The precipitates were washed four times with NET lysis buffer and boiled in SDS sample buffer.

2.9. SDS/PAGE and western blot analysis

Cells were lysed in lysis buffer (1% NP-40, 150 mM NaCl, 50 mM Tris/HCl pH 7.4) containing 5 μM PUGNAc, phosphatase, and protease inhibitors. The SDS/PAGE and western blot were performed as previously

described (Phoomak *et al.*, 2016). The ECL™ Prime Western Blotting Detection System and the images were analyzed using an ImageQuant LAS 4000 mini image analyzer and ImageQuant™ TL analysis software (GE Healthcare, Buckinghamshire, UK).

2.10. Immunocytofluorescence

Cells were prepared for immunocytofluorescence as previously described (Phoomak *et al.*, 2016). After fixation, cells were then incubated with 1:100 anti-hnRNP-K overnight at 4 °C and with 1:200 anti-rabbit-IgG-PE (Santa Cruz) for 1 h at room temperature. To visualize nuclei, cells were stained with 1:10 000 Hoechst 33342 (Molecular Probes, Invitrogen, Paisley, UK). The fluorescence image was taken using a ZEISS LSM 800 Confocal Laser Scanning Microscope (Zeiss, Oberkochen, Germany).

2.11. Immunohistochemistry

Expression of hnRNP-K and OGP in CCA tissues was determined using immunohistochemistry (IHC) staining according to the standard protocol. The signals were amplified using the EnVision-system-HRP (Dako, Glostrup, Denmark). The immunoreactivity signals were developed using diaminobenzidine (Sigma-Aldrich). The IHC score was determined as described previously (Phoomak *et al.*, 2017). Two independent assessors scored the levels of IHC staining signal blindly without prior knowledge of clinical parameters.

2.12. Statistical analysis

All statistics were analyzed using the GraphPad Prism® 5.0 software (GraphPad software, Inc., La Jolla, CA, USA). Student's *t*-test was used to compare parameters between two samples. The correlation between OGP level and hnRNP-K expression in CCA patient tissues was determined using Fisher's exact test, Mann–Whitney test, and Spearman's rank correlation test. Differences were considered statistically significant if $P < 0.05$.

3. Results

3.1. Increasing O-GlcNAcylation enhances migration and invasion abilities of CCA cells

As PUGNAc, an inhibitor of OGA was used to enrich the O-GlcNAcylation in CCA cells, we first determined whether PUGNAc treatment could increase O-GlcNAcylation and enhance progression of CCA cells. CCA cells (KKU-213 and KKU-214) were treated with PUGNAc for 24 h, and the OGP level together with migration and invasion abilities of CCA cells treated with or without PUGNAc was determined. As shown in Fig. 1A, suppression of OGA activity using PUGNAc increased the levels of OGP in CCA cells 2.5-fold in KKU-213 and 3.0-fold in KKU-214, respectively. PUGNAc treatment also significantly enhanced the relative migratory ability to 165% in KKU-213 and to 175% in KKU-214 compared with the control cells (Fig. 1B). Similar results were also observed for the invasion ability. PUGNAc treatment increased invasion of KKU-213 to 175% and of KKU-214 to 150% compared with those of control cells (Fig. 1C).

3.2. Novel O-GlcNAcylated proteins related to progression of CCA cells were revealed by enzymatic labeling and mass spectrometry analysis

To increase the sensitivity of OGP detection, O-GlcNAcylated peptides were labeled with GalNAz by GalT1 (Y289L) and tagged with biotin-alkyne. The labeled peptides were then analyzed by mass spectrometry (Fig. S1). Over 100 OGPs were identified in cell lysates from KKU-213 and KKU-214 (Tables S1), of which the major OGPs were found in the cytoplasm and nucleus (Fig. S2A).

To classify the OGPs that are related to progression of CCA cells, the primary list of OGPs obtained from mass spectrometry were filtered according to the following parameters: (1) it was present in both KKU-213 and KKU-214 cells, and (2) it had at least one predicted O-GlcNAcylation site (based on dbOGAP). There were 21 OGPs that passed these criteria. The description, cellular localization, and functions of these OGPs are listed according to the intensity of the peptides in Table 1. Twelve OGPs listed may be novel OGPs as their O-GlcNAcylation has not been identified (Fig. S2B). The involvement of these OGPs in biological processes is summarized in Fig. S2C.

3.3. Immunoprecipitation reveals O-GlcNAc modification of hnRNP-K

hnRNP-K, a multifaceted RNA- and DNA-binding protein associated with pre-mRNA, mRNA metabolism and transport (Dejgaard and Leffers, 1996; Lu and Gao, 2016), has been shown to contribute to metastasis in several cancer types (Chung *et al.*, 2014; Gao *et al.*, 2013; Zhang *et al.*, 2016b; Zhou *et al.*, 2010). Moreover, hnRNP-K possesses multiple Ser/Thr sites that are predicted to be O-GlcNAcylated.

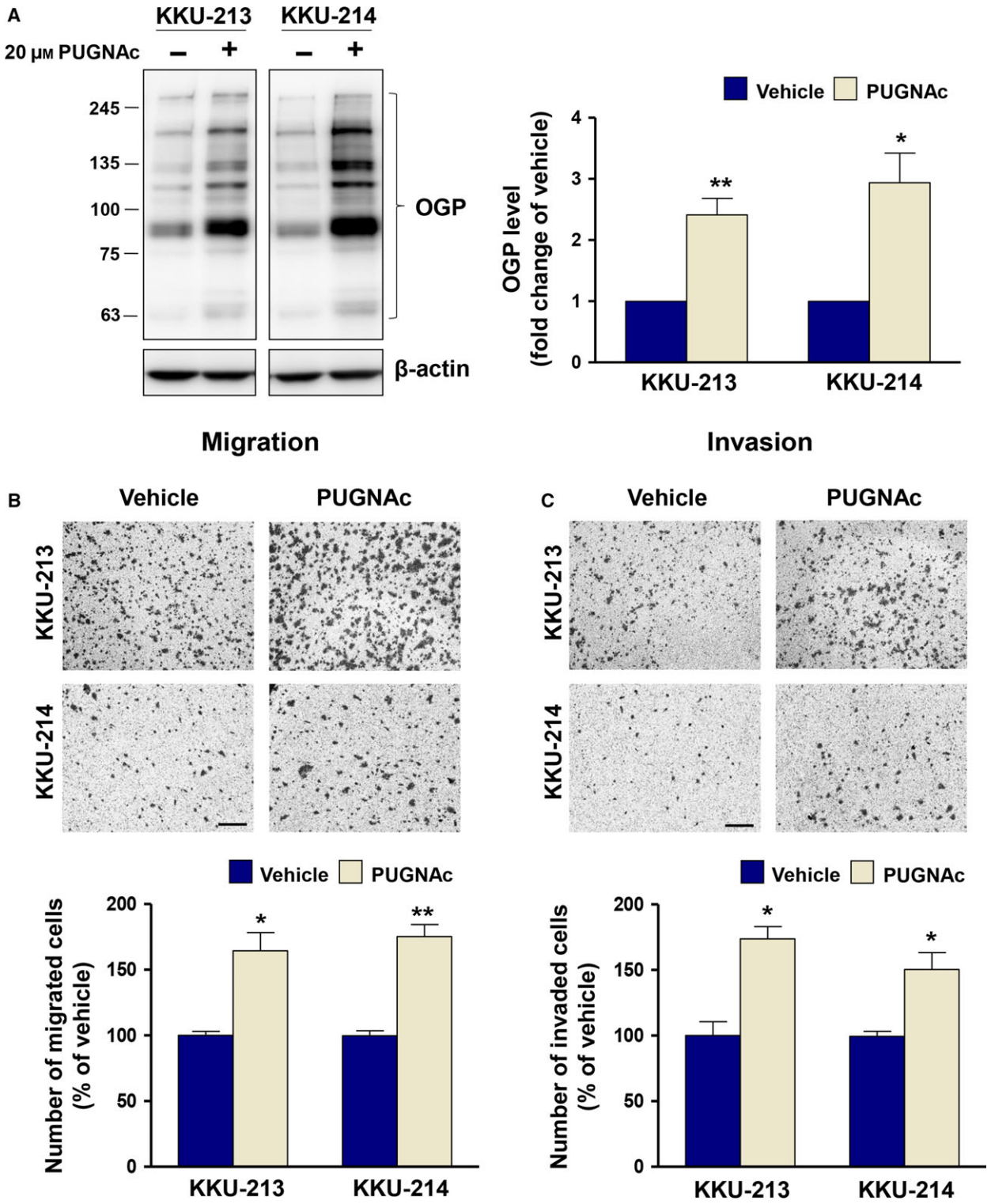

Fig. 1. O-GlcNAcylation promotes CCA migration and invasion. CCA cells, KKU-213 and KKU-214, were treated with 20 μM PUGNAc for 24 h. (A) OGP levels were determined using western blot. (B) Migration and (C) invasion abilities of PUGNAc-treated CCA cells were compared with those of the vehicle control cells. The results represent one of two independent experiments (mean ± SEM, $*P < 0.05$; $**P < 0.01$, Students' *t*-test). The images shown are 100 × magnification with 50 μm of scale bar.

Table 1. List of O-GlcNAcylated proteins related with proliferation and progression of cancer.

UniProt accession	Gene name	Protein description	log(intensity)[a]	Cellular compartment[b]	Function	Reference
Reported O-GlcNAcylated proteins						
P60709	ACTB	Actin, beta	8.33	Cytoplasm	–	–
P16403	HIST1H1C	Histone cluster 1 H1c	7.78	Nucleus	Proliferation Migration Invasion	Song *et al.* (2008)
P10412	HIST1H1E	Histone cluster 1 H1e	7.74	Nucleus	Proliferation	Lee *et al.* (2013)
P16401	HIST1H1B	Histone cluster 1 H1b	7.69	Nucleus	Carcinogenesis	Khachaturov *et al.* (2014)
P02545	LMNA	Lamin A/C	7.56	Nucleus	Proliferation Migration Invasion	Kong *et al.* (2012)
P06748	NPM1	Nucleophosmin (nucleolar phosphoprotein B23 numatrin)	7.49	Cytoplasm Nucleus	Proliferation Migration Invasion	Ching *et al.* (2015)
P22626	NRNPA2B1	Heterogeneous nuclear ribonucleoprotein A2/B1	7.32	Nucleus	Proliferation Migration Invasion	Chen *et al.* (2014)
Q09666	AHNAK	AHNAK nucleoprotein	7.10	Nucleus	Proliferation Migration Invasion	Sudo *et al.* (2014)
P07355	ANXA2	Annexin A2	7.07	Membrane Cytoplasm Nucleus	Proliferation Migration Invasion	Chaudhary *et al.* (2014) and Wang *et al.* (2015)
Unreported O-GlcNAcylated proteins						
P46939	UTRN	Utrophin	8.49	Membrane Cytoplasm	Proliferation	Li *et al.* (2007)
Q5QNW6	HIST2H2BF	Histone cluster 2 H2bf	8.43	Nucleus	–	–
P62805	HIST1H4A	Histone cluster 2 H4a	8.16	Nucleus	Proliferation	Yan-Fang *et al.* (2015)
B9ZVM9	TCP10L2	T-complex protein 10A homolog 2	7.95	Nucleus	Proliferation	(Shen *et al.*, 2015)
Q16695	HIST3H3	Histone cluster 3 H3	7.50	Nucleus	Proliferation	(Xu *et al.*, 2014)
P08195	SLC3A2	Solute carrier family 3 (amino acid transporter heavy chain), member 2	7.09	Membrane Cytoplasm Nucleus	Proliferation Migration Invasion	Fei *et al.* (2014), Santiago-Gomez *et al.* (2013) and Yang *et al.* (2007)
Q16819	MEP1A	Meprin A subunit alpha	6.96	Membrane	Migration Invasion	Minder *et al.* (2012)
P61978	HNRNPK	Heterogeneous nuclear ribonucleoprotein-K	6.81	Cytoplasm Nucleus	Proliferation Migration Invasion	Chung *et al.* (2014) and Gao *et al.* (2013)
P27824	CANX	Calnexin	6.73	Cytoplasm	Carcinogenesis Metastasis	Dissemond *et al.* (2004)
Q08170	SRSF4	Serine/arginine-rich splicing factor 4	6.26	Nucleus	Proliferation	Gabriel *et al.* (2015)
Q5T200	ZC3H13	Zinc finger CCCH-type containing 13			–	–
Q7Z7G8	VPS13B	Vacuolar protein sorting 13 homolog B			–	–

[a]Log (intensity) of identified OGPs in KKU-213.
[b]According to GeneCards®: The Human Gene Database.

Therefore, hnRNP-K was selected for verification of its O-GlcNAc modification and involvement in CCA progression.

To prove the modification of O-GlcNAc on hnRNP-K, an immunoprecipitation assay was performed. Cell lysates of CCA cells treated with PUGNAc or vehicle were subjected to immunoprecipitation using anti-OGP. Immunoprecipitation using mouse immunoglobulin (IgG) as an isotype control was used to clarify the specificity of the anti-OGP. As shown in Fig. 2A, PUGNAc

treatment increased the expression level of OGPs and signal of hnRNP-K in the immunoprecipitated-OGP from both KKU-213 and KKU-214 cells. Similar results were obtained for the reversed-immunoprecipitation using anti-hnRNP-K (Fig. 2B). In both cell lines, the signal of OGP was higher in the immunoprecipitate of hnRNP-K from PUGNAc-treated cells than that from the control cells. These data demonstrated the O-GlcNAc modification of hnRNP-K. As succinylated wheat germ agglutinin (sWGA) specifically recognizes the sugar moiety of GlcNAc, an sWGA pull-down assay was performed to further ensure that hnRNP-K was O-GlcNAcylated. As shown in Fig. 2C, the signal of hnRNP-K in the sWGA pull-down precipitate from PUGNAc-treated cells was higher than that of the control cells. The specific interaction between O-GlcNAcylated hnRNP-K and sWGA was assured by the neutralization of sWGA with GlcNAc. The signals of O-GlcNAcylated hnRNP-K, sWGA-conjugated proteins, and O-GlcNAcylated proteins were diminished in the GlcNAc-neutralized sWGA condition. In addition, the level of O-GlcNAcylation of hnRNP-K was elevated when cellular O-GlcNAcylation was increased. Collectively, these results indicate the O-GlcNAcylation of hnRNP-K.

3.4. hnRNP-K is required for cell proliferation, migration, and invasion of CCA cells

We next investigated the involvement of hnRNP-K in CCA progression, indicated namely by increases in cell proliferation, migration, and invasion. To this end, the expression of hnRNP-K was transiently suppressed by siRNA, and cell proliferation, migration, and invasion were determined in comparison with those of the scramble control cells. The si-hnRNP-K transfection could reduce the expression of hnRNP-K to 30% of the control cells in KKU-213 and to 25% in KKU-214 (Fig. 3A). Proliferation rates of KKU-213 and KKU-214 were significantly decreased when the expression of hnRNP-K was suppressed for 48 h (Fig. 3B). Moreover, diminution of hnRNP-K expression markedly decreased the motility of CCA cells to 36% of the control cells in KKU-213 and to 27% in KKU-214 (Fig. 3C). Similar effects were also observed for the invasion ability of CCA cells. The invasion ability of si-hnRNP-K-treated cells was 50% and 15% of the control cells in KKU-213 and KKU-214, respectively (Fig. 3D). These data indicated the association of hnRNP-K with the proliferation, migration and invasion of CCA cells. To ensure that the observed effects of hnRNP-K on migration and invasion were not due to changes in growth rates, we parallelly measured cell proliferation. As shown in Fig. S3, there were no growth differences between si-hnRNP-K- and scramble siRNA-treated cells during the time of assays. Thus, si-hnRNP-K conferred decreases in migration and invasion without affecting cell growth.

3.5. Key markers related to growth and metastasis proteins are influenced by hnRNP-K

Given that hnRNP-K is a multifaceted RNA- and DNA-binding protein, we further examined the influence of hnRNP-K on key effector proteins related to these malignant phenotypes: cyclin D1 for cell proliferation, XIAP for antiapoptosis, cleaved caspase 3 for cell apoptosis, E-cadherin and claudin-1 for epithelial markers, vimentin and slug for mesenchymal markers, and MMP2 and MMP7 for invasion activity. Specifically, the expression of cyclin D1 and XIAP was investigated after hnRNP-K was suppressed by siRNA for 24, 48, and 72 h. Compared to the control cells, the expression of cyclin D1 and XIAP in si-hnRNP-K-treated KKU-213 and si-hnRNP-K-treated-KKU-214 cells decreased along with hnRNP-K expression until 72 h (Fig. 4A). In addition, the level of cleaved caspase 3 increased with time in si-hnRNP-K-treated cells. The quantitative data are shown in Fig. 4B.

To determine the effect of hnRNP-K on the effector proteins related to cell migration and invasion, the expression of epithelial to mesenchymal transition (EMT) markers (e.g., E-cadherin, claudin-1, vimentin, and slug), and matrix metalloproteinase (MMP) 2 and MMP7 was determined in si-hnRNP-K-treated cells in comparison with those of the scramble control cells. As shown in Fig. 4C,D, the expression levels of E-cadherin and claudin-1 increased whereas those of vimentin and slug decreased in si-hnRNP-K-treated cells. On the other hand, while si-hnRNP-K treatment suppressed the MMP2 expression after 24 h of treatment, expression of MMP7 gradually decreased with time. These data demonstrated that hnRNP-K influenced cell migration and invasion in association with the expression of EMT, MMP2, and MMP7.

To emphasize the connection of O-GlcNAcylation levels, hnRNP-K and its downstream signals, the expression level of O-GlcNAcylation, hnRNP-K, cyclin D1, XIAP, and EMT markers was determined in CCA cell lines, KKU-100, which shows lower migration activity versus KKU-213. As shown in Fig. 4E, compared to KKU-213, KKU-100 exhibited not only lower levels of O-GlcNAcylation but also lower levels of hnRNP-K and the effector molecules related to migration and invasion.

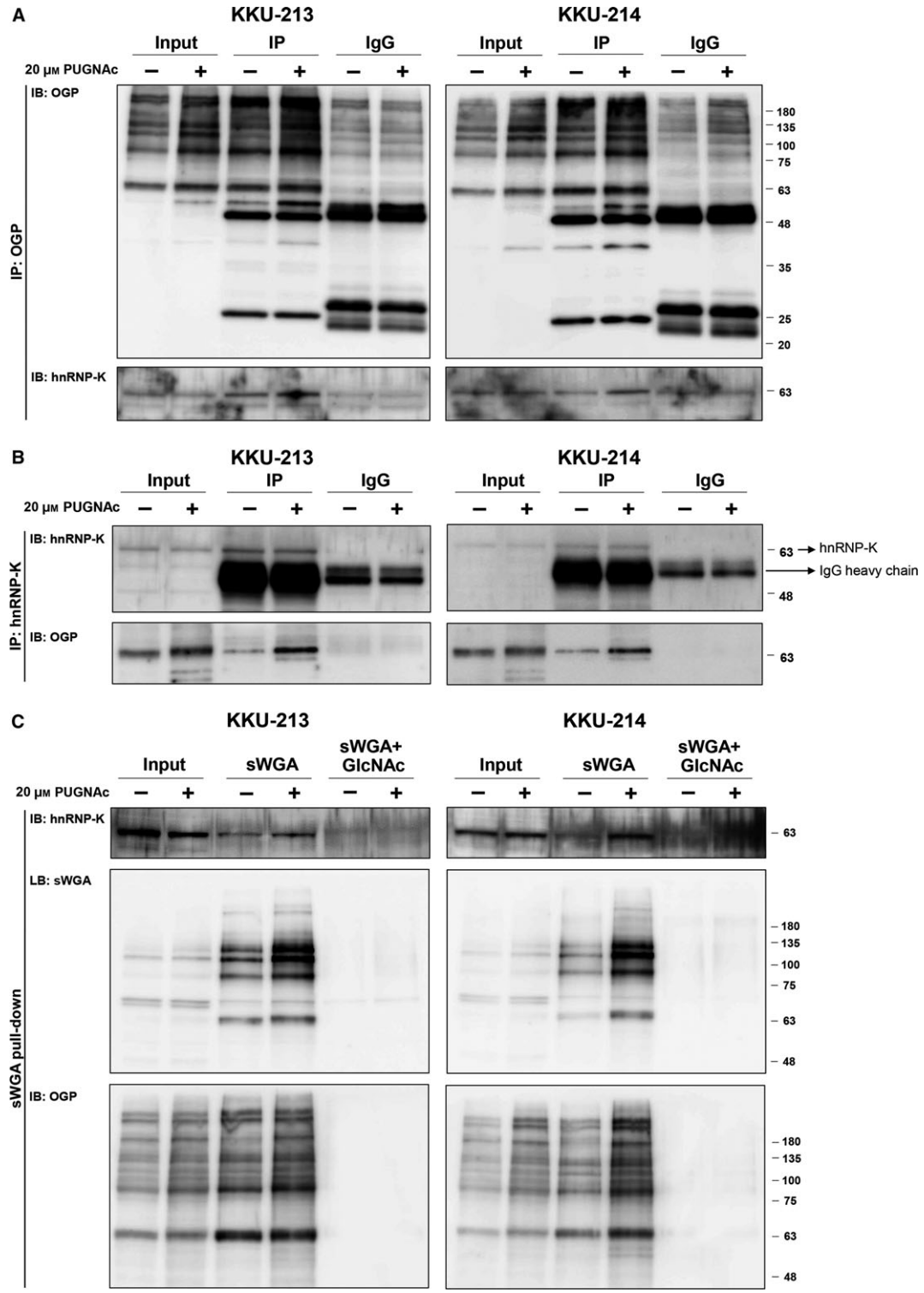

Fig. 2. Validation of hnRNP-K O-GlcNAcylation. CCA cells (KKU-213 and KKU-214) were treated with PUGNAc or vehicle for 24 h. The cell lysates were immunoprecipitated with either (A) anti-OGP or (B) anti-hnRNP-K and probed with anti-hnRNP-K and anti-OGP. Human immunoglobulin G (IgG) isotype was used as the controls of the specificity of the antibodies that were used in the immunoprecipitation assay. (C) The sWGA pull-down assay was performed using sWGA-conjugated agarose and probed with anti-hnRNP-K, sWGA, and anti-OGP. GlcNAc neutralization was used to examine the specific binding of sWGA to the OGPs.

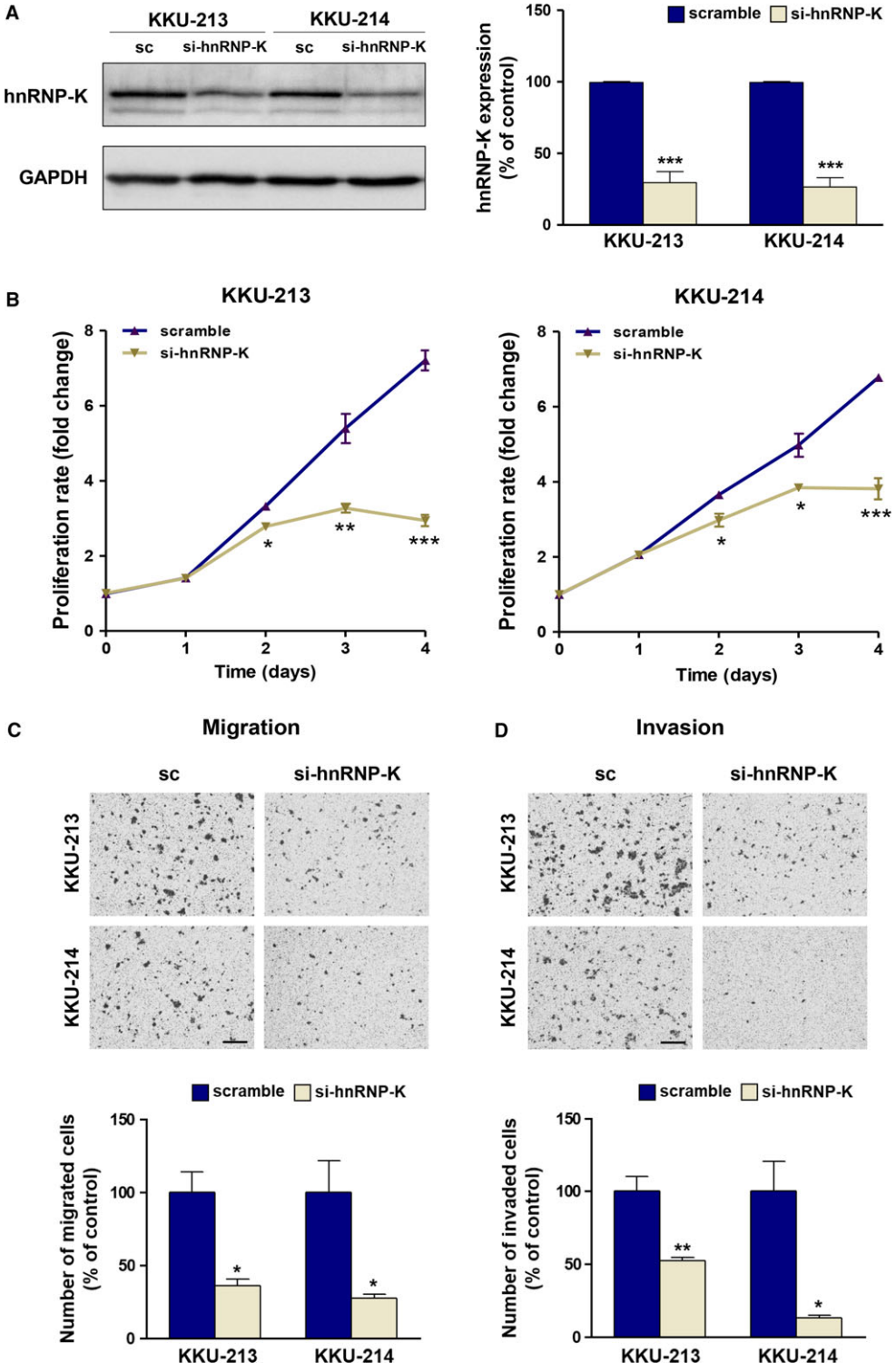

Fig. 3. Suppression of hnRNP-K reduces proliferation, migration, and invasion of CCA cells. The expression of hnRNP-K was transiently suppressed by siRNA for 48 h prior to the migration and invasion assays. (A) The expression of hnRNP-K was determined using western blot. (B) Cell proliferation, (C) migration, and (D) invasion abilities of si-hnRNP-K-treated CCA cells were compared with those of the scramble siRNA (sc)-treated cells. The migration and invasion assays were conducted for 9 h in KKU-213 and 24 h in KKU-214. The images shown are 100 × magnification with 50 μm scale bar. Data are mean ± SEM (*$P < 0.05$; **$P < 0.01$; ***$P < 0.001$, Students' *t*-test).

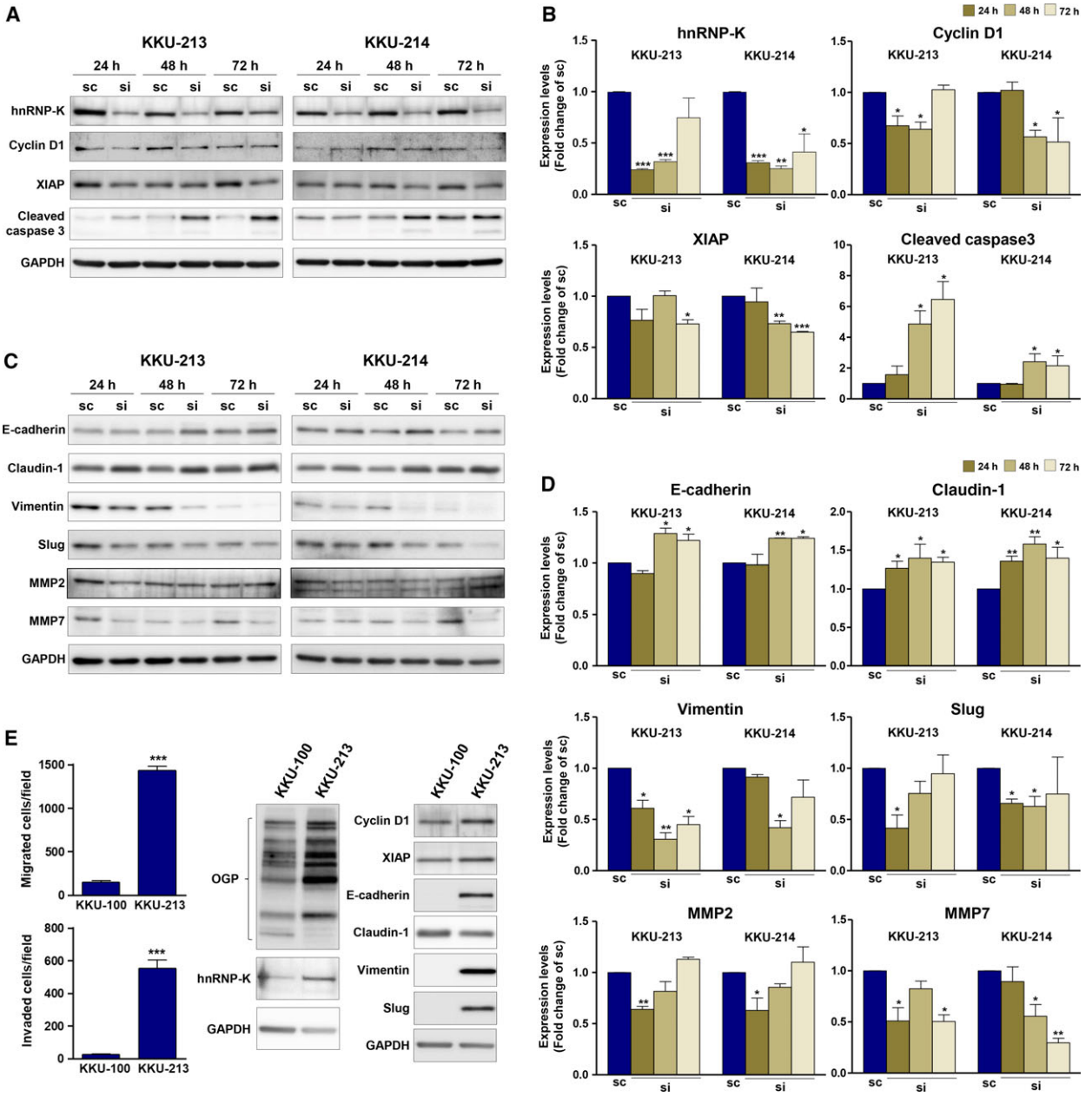

Fig. 4. hnRNP-K mediates the expression of growth- and metastasis-related proteins in CCA cells. CCA cell lines, KKU-213 and KKU-214, were treated with si-hnRNP-K for 24, 48, and 72 h. The expression levels of growth- and metastasis-related proteins were determined using western blot. Expression of GAPDH was used as an internal control. The expression of (A) hnRNP-K, cyclin D1, XIAP, and cleaved caspase 3 as well as (C) EMT markers (E-cadherin, claudin-1, vimentin, and slug), and MMP2 and MMP7 was determined in si-hnRNP-K-treated cells in comparison with those of scramble control cells. B and D are the quantitative analysis of (A) and (C) presented as mean ± SD from two independent experiments. (E) The endogenous expression of hnRNP-K and its downstream targets was compared in 2 CCA cell lines (KKU-100 and KKU-213) with different migration/invasion abilities and O-GlcNAcylation levels. (*$P < 0.05$; **$P < 0.01$, Students' *t*-test)

To investigate whether enhancing O-GlcNAcylation of hnRNP-K could support the migratory activity of cells, two additional cell lines with low hnRNP-K expression were enrolled, MMNK1, an immortal cholangiocyte, and KKU-100. Their migration was measured with si-hnRNP-K treatment and in the presence or absence of PUGNAc. While siRNA of hnRNP-K was used to suppress the expression of hnRNP-K, PUGNAc treatment enhanced the levels of OGPs in both cell lines (Fig. S4). Suppression of

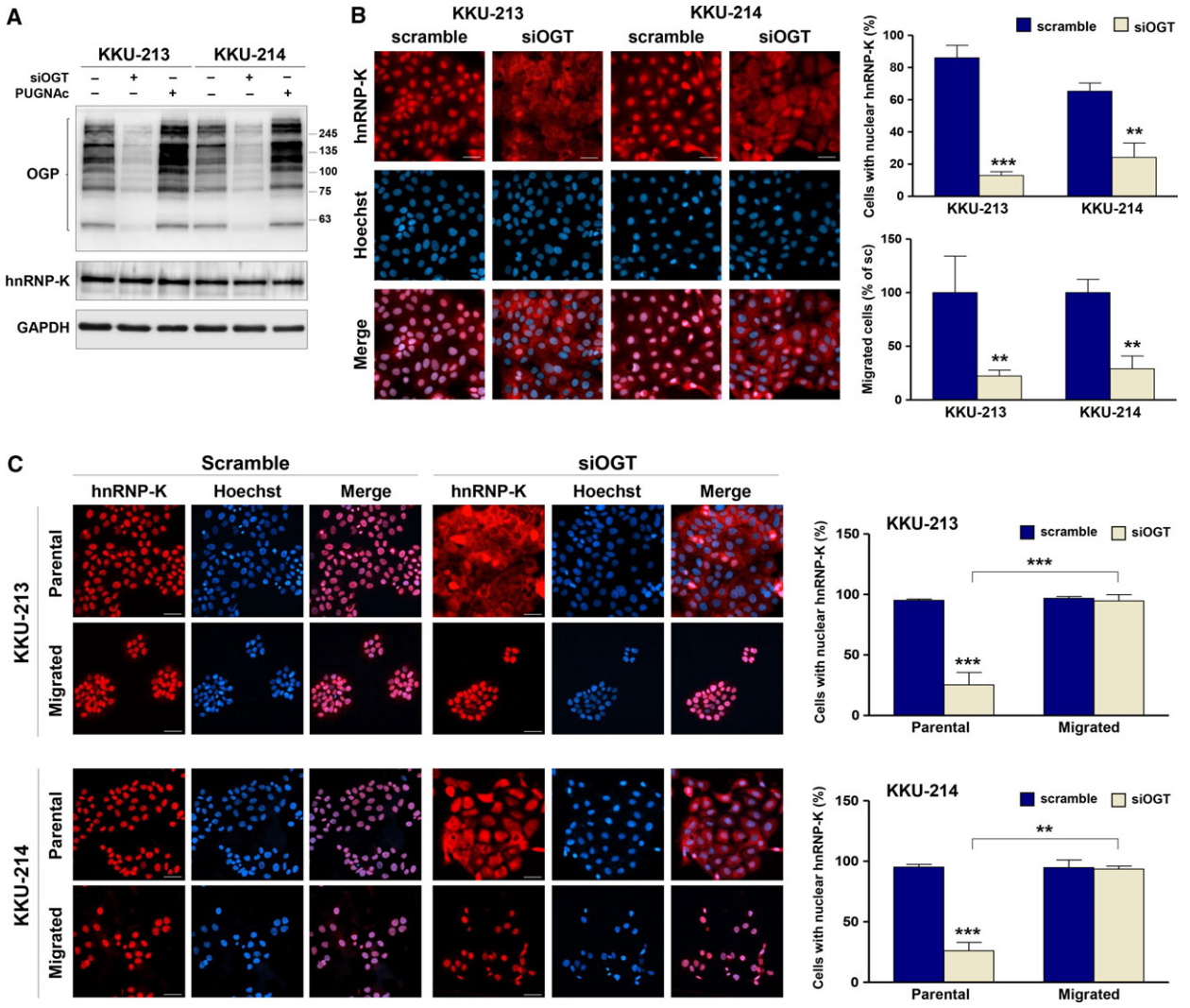

Fig. 5. hnRNP-K nuclear localization is regulated by O-GlcNAcylation and correlated with migratory activity of CCA cells. (A) The expression of OGT was suppressed by siRNA for 24 h. Expression levels of OGP and hnRNP-K in siOGT- and PUGNAc-treated cells were compared with those of control cells using western blot analysis. (B) Localization of hnRNP-K and nuclei was observed using immunocytofluorescent staining. hnRNP-K was stained using PE (red), and cell nuclei were visualized using Hoechst 33342 (blue). Nuclear localization of hnRNP-K is demonstrated by the purple nuclei in the merged images. The quantification of scramble siRNA- and siOGT-treated cells with nuclear hnRNP-K is shown in the upper panel graph. The migratory ability of cells treated with scramble siRNA and siOGT is shown in the lower panel graph. (C) The scramble siRNA- and siOGT-treated cells were allowed to migrate to the lower chamber in a Transwell culture system for 48 h. Localization of hnRNP-K was determined in the parental and migrated cells using immunocytofluorescent staining. Cells with nuclear hnRNP-K were counted as shown in the graphs. The images are 200 × magnification and scale bars = 20 μm. Data are mean ± SD with $^{**}P < 0.01$; $^{***}P < 0.001$ (Students' *t*-test).

hnRNP-K expression decreased the migratory activity of MMNK1 and KKU-100 cells to 50% and 30% of the control cells, respectively. On the other hand, elevating O-GlcNAcylation by PUGNAc treatment increased the migratory ability of both the control and si-hnRNP-K-treated cells. Similar effects were observed in MMNK1 and KKU-100. Together, these results support our finding that O-GlcNAcylation and hnRNP-K are associated with migratory ability regardless of cell type.

3.6. O-GlcNAcylation of hnRNP-K activates the nuclear translocation of hnRNP-K

To investigate the effect of O-GlcNAcylation on the function of hnRNP-K, the level of O-GlcNAcylation

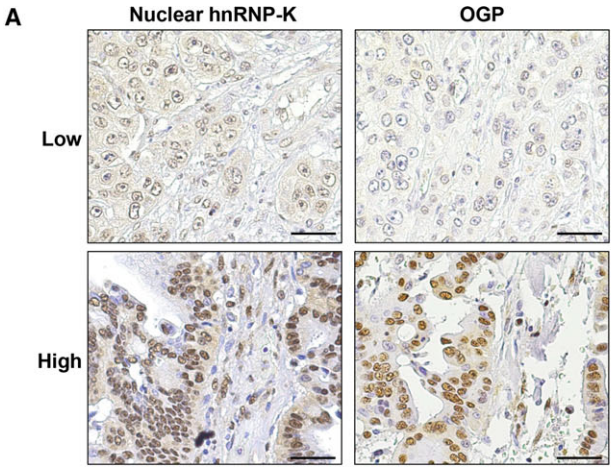

B

		Nuclear hnRNP-K		*P*-value
		low	high	
OGP	Low	14 (47%)	3 (10%)	0.008
	high	4 (13%)	9 (30%)	

Fisher's Exact Test (2-sided)

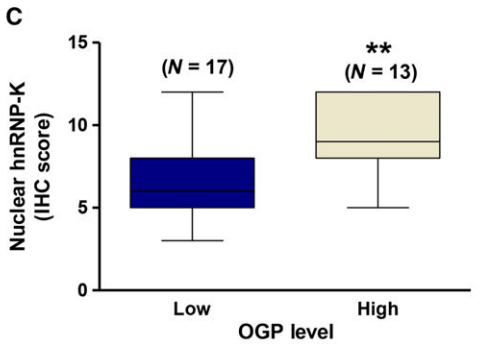

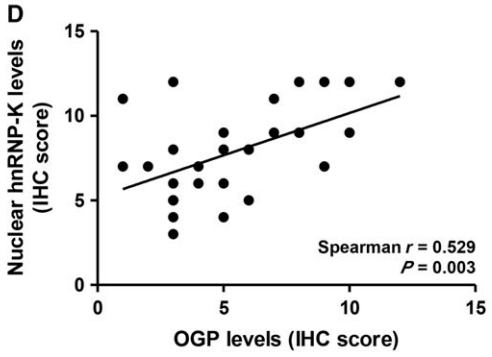

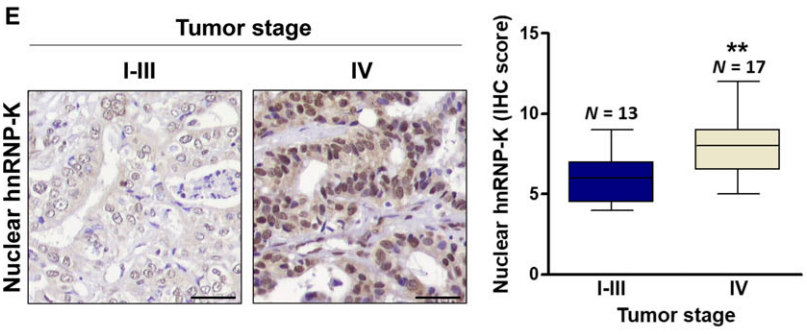

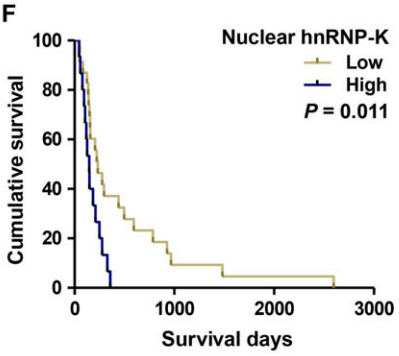

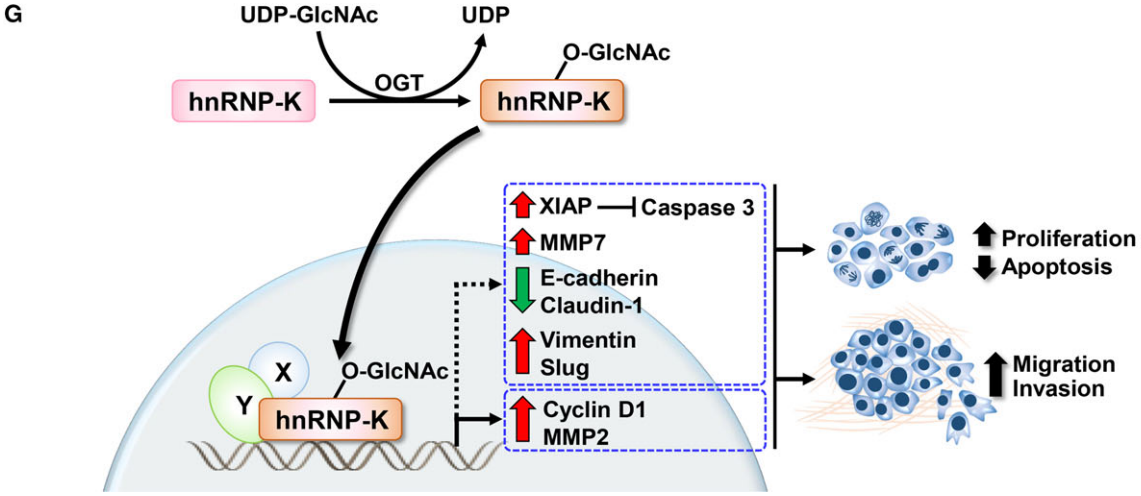

Fig. 6. The expression and localization of hnRNP-K in CCA tissues correlated with OGP levels. (A) IHC staining of hnRNP-K and OGP in two representative pairs of CCA tissues. (B) The correlations between hnRNP-K expression and OGP were analyzed by Fisher's exact test ($N = 30$). (C) Mean expression of hnRNP-K in nucleus of the high OGP group was significantly higher than those of the low OGP group (**$P < 0.01$; Mann–Whitney test). (D) The positive correlation between nuclear hnRNP-K and OGP levels was shown by Spearman's rank correlation test. (E) Nuclear hnRNP-K in CCA patient tissues with stage I-III and IV were compared. (F) High level of nuclear hnRNP-K was correlated with shorter CCA patients with high nuclear hnRNP-K level exhibited the shorter survival (median survival = 147 days, 95% CI = 106–187 days), than those with low nuclear hnRNP-K level (median survival = 233 days, 95% CI = 128-338 days) ($P = 0.011$, Kaplan–Meier plot and log-rank test). The IHC images are showed in 200 × magnification with 20 μm of scale bar. (G) Schematic diagram presents molecular mechanism by which O-GlcNAcylation regulated nuclear translocation of hnRNP-K in association with progression of CCA.

was monitored using siOGT and PUGNAc. As shown in Fig. 5A, siOGT treatment reduced cellular O-GlcNAcylation whereas PUGNAc treatment increased the level of O-GlcNAcylation in both KKU-213 and KKU-214. However, neither treatments affected hnRNP-K expression. This observation implied that O-GlcNAcylation may not affect the expression and stability of hnRNP-K.

As hnRNP-K is a transcription factor and the translocation from cytoplasm to nucleus is an important process for proper functioning of hnRNP-K, we next explored the effect of O-GlcNAcylation on the nuclear translocation of hnRNP-K. Cellular localization of hnRNP-K was determined in siOGT-treated cells using hnRNP-K immunocytofluorescence: hnRNP-K was stained using PE (red) and cell nuclei were visualized using Hoechst 33342 (blue). As shown in Fig. 5B, almost all of the positive hnRNP-K signals of scramble control cells were located in the nucleus (red nuclei of the hnRNP-K staining; purple nuclei of the merged images). Suppression of O-GlcNAcylation in siOGT-treated cells retained hnRNP-K signals in the cytoplasm (red cytoplasmic stain with blue nuclei of the merged images). The number of cells with positive nuclear hnRNP-K was significantly reduced in siOGT-treated cells in both KKU-213 ($P < 0.001$) and KKU-214 ($P < 0.01$; Fig. 5B). The siOGT treatment also significantly decreased migratory activity of both cell lines. These data suggested that O-GlcNAcylation modulates the nuclear localization of hnRNP-K, which may in turn influence the migratory ability of CCA cells.

To affirm the connection between O-GlcNAcylation and nuclear localization of hnRNP-K, the expression and localization of hnRNP-K in KKU-100 were coevaluated using immunofluorescent staining. As shown in Fig. S5A-B, the number of KKU-100 cells with nuclear hnRNP-K was significantly lower than that of KKU-213 and KKU-214 ($P < 0.05$). The difference corresponded with the level of O-GlcNAcylation and hnRNP-K expression. In addition, increased O-GlcNAcylation by PUGNAc treatment in KKU-100 resulted in a higher proportion of cells with nuclear hnRNP-K (Fig. S5C). These data are consistent with those observed in KKU-213 and KKU-214 cells in that O-GlcNAcylation conferred the nuclear translocation of hnRNP-K.

3.7. Migratory enhancement of CCA cells is correlated with nuclear translocation of hnRNP-K

To connect the nuclear translocation of hnRNP-K with the migratory ability of CCA cells, the localization of hnRNP-K in the parental and migrated cells was determined. CCA cells were transfected with scramble siRNA or siOGT for 24 h and allowed to migrate to the lower chamber of a Transwell system for 48 h. Localization of hnRNP-K in the parental cells and the migrated cells in the lower chamber were detected using immunocytofluorescent staining. As shown in Fig. 5C, almost all the parental and migrated si-scramble-treated cells possessed nuclear hnRNP-K (purple nuclei). Suppression of O-GlcNAcylation using siOGT, however, resulted in the retention of hnRNP-K in the cytoplasm (pink cytoplasm with blue nuclei) and significantly reduced the number of cells with nuclear hnRNP-K ($P < 0.001$). Furthermore, when siOGT-treated cells were allowed to migrate to the lower compartment of the Boyden chamber, it was found that only the fraction of cells with nuclear hnRNP-K could migrate to the lower chamber. These data emphasized the association of nuclear hnRNP-K and migratory activity of CCA cells.

3.8. Expression of nuclear hnRNP-K in CCA tissues positively correlates with O-GlcNAcylation levels

Upon observation of O-GlcNAc-mediated nuclear translocation of hnRNP-K in CCA cell lines, we then verified whether this association could be observed in tumor tissues of CCA patients. The expression levels of OGP and hnRNP-K with nuclear localization were determined in 30 cases of CCA tissues using IHC, semiquantitated according to the intensity and

frequency of the positive signal with IHC scores. hnRNP-K and OGP were generally observed in both the nucleus and cytoplasm of CCA tissues but nuclear staining with different intensities was predominantly observed (Fig. 6A). Expression of nuclear hnRNP-K and OGP was categorized according to the median of IHC scores as low or high levels, and the correlation of these two factors was analyzed. Positive correlations between number of CCA cells with nuclear hnRNP-K and those with OGP expression were observed (Fig. 6B, Fisher's exact test). CCA tissues with high nuclear hnRNP-K expression also had high OGP expression. In addition, higher expression of nuclear hnRNP-K was observed in CCA tissues with high OGP expression than those with low OGP expression (Fig. 6C, Mann–Whitney test). Correlations between the expression levels of nuclear OGP and those of nuclear hnRNP-K are shown by Spearman rank correlation with $r = 0.529$ (Fig. 6D).

3.9. High expression of tissue nuclear hnRNP-K is associated with metastatic stage and poor clinical outcome of CCA patients

To implicate the clinical significance of hnRNP-K in CCA, expression of tissue hnRNP-K and clinicopathological features of CCA patients were determined in 38 CCA subjects. Nuclear hnRNP-K expression was categorized as low or high based on median IHC score, and univariate analysis was performed. CCA tissues with metastatic stage (stage IV) exhibited higher levels of nuclear hnRNP-K than those with nonmetastatic stages (stages I–III) (Table 2, Fig. 6E). The Kaplan–Meier analysis indicated that patients whose tumor possessed high nuclear hnRNP-K had significantly shorter survival than those possessed low nuclear hnRNP-K (Fig. 6F, $P = 0.011$, log-rank analysis). Univariate Cox proportional hazard-regression analysis was next performed to determine the influence of nuclear hnRNP-K levels and clinicopathological characteristics on overall survival of CCA patients. As shown in Table 3, high level of nuclear hnRNP-K was significantly correlated with overall survival ($P = 0.014$) and an independent prognostic factor of CCA (HR = 2.540, 95% CI = 1.213–5.317, $P = 0.013$).

Table 2. The correlation between nuclear hnRNP-K levels and clinicopathological data of CCA patients.

	Nuclear hnRNP-K		
Variables (*N*)	Low	High	*P*-value
Age (38)			
≤ 56 (21)	13	8	0.847
> 56 (17)	10	7	
Sex (38)			
Male (25)	16	9	0.544
Female (13)	7	6	
Histological type (38)			
Papillary (11)	7	4	0.802
Nonpapillary (27)	16	11	
CCA stage (30)			
I–III (13)	12	1	0.001*
IV (17)	5	12	

*$P < 0.001$, Fisher's exact test (two-sided).

4. Discussion

Several O-GlcNAcylated proteins (OGPs) have been reported for their roles in cancer proliferation, metastasis, metabolism, angiogenesis, stress response, replicative immortality, and resistance to apoptosis (Ma and Vosseller, 2013). Although it is likely that there are more cancer-related OGPs involved in these processes, many remain unidentified. In this study, we used Click-iT™ O-GlcNAc Enzymatic Labeling System and mass spectrometry to reveal OGPs that are related to the progression of CCA. Among these, hnRNP-K was shown to be O-GlcNAcylated and associated with

Table 3. Univariate and multivariate analysis of factors influencing overall survival in CCA patients

	Univariate analysis			Multivariate analysis		
Variables (*N*)	HR	95% CI	*P*-value	HR	95% CI	*P*-value
Age (38)						
≤ 56 (21)	1					
> 56 (17)	0.741	0.384-1.428	0.370			
Sex (38)						
Male (25)	1					
Female (13)	1.302	0.650-2.609	0.456			
Histological type (38)						
Papillary (11)	1			1		
Nonpapillary (27)	1.353	0.676-2.706	0.393	1.439	0.702-2.949	0.320
CCA stage (30)						
I–III (13)	1					
IV (17)	1.850	0.835-4.102	0.130			
Nuclear hnRNP-K (38)						
Low (23)	1			1		
High (15)	2.528	1.208-5.294	0.014*	2.540	1.213-5.317	0.013*

CI, confidence interval; HR, hazard ratio.
*$P < 0.05$, Cox proportional hazard-regression test.

malignant progression phenotypes of CCA cells. In addition, this study is the first demonstration that O-GlcNAc modification has an impact on nuclear translocation of hnRNP-K and mediates the migratory ability of CCA cells. The association of O-GlcNAcylation and the nuclear translocation of hnRNP-K with metastasis and poor patient outcome were also demonstrated.

The contribution of O-GlcNAcylation in the progression of CCA has been sequentially reported (Phoomak *et al.*, 2012, 2016, 2017). Immunohistochemistry of OGP, OGT, and OGA in tumor tissues from patients revealed that CCA tissues had increased expression of OGPs which resulted from the increase of OGT and decrease of OGA expression. Correlation of high OGPs in CCA tissues with poor clinical outcomes of CCA patients was observed (Phoomak *et al.*, 2012). Recently, O-GlcNAcylation was shown to enhance progressive phenotypes of CCA cells by increasing high mannose N-linked glycans at the cell surface through regulation of FOXO3 and MAN1A1 expression (Phoomak *et al.*, 2018). The connection of O-GlcNAcylation to the migration and invasion abilities of CCA cells was shown to be partly via activation of nuclear translocation of NF-κB (Phoomak *et al.*, 2016). Reducing the cellular O-GlcNAcylation by siOGT, however, suppressed migration and invasion abilities of CCA cells to a lower extent than the inactivation of NF-κB (Phoomak *et al.*, 2016). This implies that there might be other O-GlcNAcylated proteins together with NF-κB that modulate progression of CCA cells. In the present study, novel OGPs that associated with progressive phenotypes of CCA were explored.

O-GlcNAc is particularly difficult to detect due to biological and technical challenges. First, cells contain high levels of hydrolase enzymes which can rapidly remove O-GlcNAc when cells are damaged or lysed, resulting in loss of O-GlcNAc during protein isolation (Greis and Hart, 1998; Hart *et al.*, 2007). Second, O-GlcNAc appears on a protein at substoichiometric amounts and easily falls off when it is ionized in a mass spectrometer (Greis and Hart, 1998). Third, the signal of O-GlcNAcylated peptides, if remained, is almost always suppressed by the higher abundance of unmodified peptides (Greis and Hart, 1998). To determine the OGPs that modulate progression of CCA cells, we first increased the signal of OGPs by inhibiting the activity of OGA (an enzyme that removes GlcNAc from the proteins) with PUGNAc. The treatment did increase OGP levels in both CCA cell lines (Fig. 1A) and enhanced the progressive phenotypes of CCA cells. These results support the association of O-GlcNAcylation and progression of CCA cells. The sensitivity to detect O-GlcNAcylated peptides was elevated using Click-iT™ *O*-GlcNAc Enzymatic Labeling System, which stabilized the GlcNAc moieties on the peptide by GalNAz labeling. The system allowed us to select and detect only O-GlcNAcylated peptides for mass spectrometric analysis. In this study, there were over 100 OGPs detected, of which 21 were commonly found in both CCA cell lines, KKU-213 and KKU-214 (Table 1).

The OGPs found in this study were checked against a curated database of experimentally verified O-GlcNAcylated proteins using the Database of O-GlcNAcylated Proteins and Sites (dbOGAP) (Wang *et al.*, 2011). Twelve proteins were identified as novel OGPs. Among these, hnRNP-K, a member of the RNA/DNA-binding protein family, was selected for further verification (Lu and Gao, 2016). hnRNP-K has a unique RNA- and DNA-binding component of ribonucleoproteins, which is involved in several cellular processes, including chromatin remodeling, transcription, mRNA processing, translation, nuclear transport, signal transduction, and DNA repair (Gao *et al.*, 2013; Lu and Gao, 2016). It can be further modified by several post-translational modifications, including phosphorylation, that regulates its function and interactions with different binding partners (Barboro *et al.*, 2014a). There are several studies that have indicated the significant roles of hnRNP-K in the development and progression of several cancers, including cancers of the bladder (Chen *et al.*, 2017), breast (Dhanjal *et al.*, 2014), colon (Zhang *et al.*, 2016b), pancreas (Zhou *et al.*, 2010), prostate (Barboro *et al.*, 2014b), lung (Li *et al.*, 2011), cervix (Zhang *et al.*, 2016a), and liver (Xiao *et al.*, 2013).

In the present study, we demonstrated that hnRNP-K expression is related to cell proliferation, migration, and invasion which are hallmarks of cancer progression. Silencing of hnRNP-K expression with specific siRNA significantly decreased cell growth, migration, and invasion of both CCA cell lines tested. Suppression of hnRNP-K expression decreased the key effectors of cell growth (cyclin D1 and XIAP) and increased the level of cleaved caspase 3, a marker of apoptosis (Fig. 4A,B). The impact of hnRNP-K on cell proliferation was firstly shown in colon (Sugimasa *et al.*, 2015), liver, and bladder cancers (Chen *et al.*, 2017; Xiao *et al.*, 2013). In the current study, hnRNP-K was shown to be involved in cell migration and invasion of CCA cells. Reduced hnRNP-K expression significantly diminished the migration and invasion abilities of CCA cells and decreased the expression of the effector markers of migration and invasion—EMT

markers (cadherin, claudin-1, vimentin, slug) and metastasis-related proteins (MMP2, MMP7). The association of these markers and progressive phenotypes has been reported in several cancer cells (Chung *et al.*, 2014; Gao *et al.*, 2013; Zhang *et al.*, 2016b; Zhou *et al.*, 2010). Cyclin D1 and MMP2 have been demonstrated to be the direct downstream targets of hnRNP-K. Decreased expression of cyclin D1 was shown in hnRNP-K suppressing bladder cancer cells (Chen *et al.*, 2017). In addition, increased transcription activity and mRNA level of MMP2 were shown in hnRNP-K enhancing colorectal cancer cell lines (Zhu *et al.*, 2017). Whether the EMT markers (cadherin, claudin-1, vimentin, slug) and MMP7 are direct downstream targets of hnRNP-K remain to be explored.

The connection of O-GlcNAcylation, hnRNP-K, and progression of CCA cells was further supported by the study of KKU-100 which exhibited lower migration and invasion activities than KKU-213. The levels of O-GlcNAcylation and hnRNP-K expression as well as the downstream signals of cell proliferation and EMT markers related to hnRNP-K were also lower in KKU-100 than those in KKU-213. The association of hnRNP-K and O-GlcNAcylation with cell migration is irrespective of cell type, as monitoring of hnRNP-K expression or O-GlcNAcylation levels was also able to affect the migratory ability of the immortal cholangiocyte, MMNK1 and a less aggressive CCA cell line, KKU-100 (Fig. S4). These collective results establish a correlation between the expression of hnRNP-K and O-GlcNAcylation with the migratory ability of CCA cells.

For this study, hnRNP-K was justified as a novel OGP based on the analysis using Database of O-GlcNAcylated Proteins and Sites (dbOGAP) (Wang *et al.*, 2011). However, more recently, O-GlcNAcylation of hnRNP-K has been identified and reported previously in breast cancer (Champattanachai *et al.*, 2013; Drougat *et al.*, 2012). The modulation of O-GlcNAc on hnRNP-K was confirmed by anti-OGP and anti-hnRNP-K immunoprecipitation as well as sWGA pull-down assays (Fig. 2). In agreement with this phenomenon, the elevation of O-GlcNAcylation by PUGNAc treatment also increased the level of O-GlcNAcylated hnRNP-K in CCA cells. This evidence provides a link between global O-GlcNAcylation and O-GlcNAcylated hnRNP-K.

Even though the modification of hnRNP-K by O-GlcNAcylation has been shown, the effect of O-GlcNAcylation on the regulation of hnRNP-K expression and action is unknown. The present study reported for the first time the effect of GlcNAc modification on the nuclear translocation of hnRNP-K. The O-GlcNAcylation of CCA cells was modulated using siOGT or PUGNAc treatment. Treated cells with siOGT significantly decreased O-GlcNAcylation levels whereas PUGNAc treatment reversed the observation (Fig. 5A). Modulating levels of O-GlcNAcylation have no effect on the expression of hnRNP-K but did affect the O-GlcNAcylated level of hnRNP-K (Fig. 2). As hnRNP-K action is in the nucleus, we then investigated the effect of O-GlcNAcylation on nuclear translocation of hnRNP-K. To visualize nuclear hnRNP-K in relation with O-GlcNAcylation, the immunocytofluorescence of hnRNP-K was assessed in CCA cells treated with scramble siRNA or siOGT. As demonstrated in Fig. 5B, suppression of O-GlcNAcylation by siOGT in KKU-213 and KKU-214 cells significantly reduced the number of cells with positive nuclear hnRNP-K. Conversely, increased O-GlcNAcylation in KKU-100 by PUGNAc treatment increased the number of cells with nuclear hnRNP-K (Fig. S5C). O-GlcNAc-induced nuclear translocation of other proteins besides hnRNP-K has also been observed, for example, NF-kB in CCA (Phoomak *et al.*, 2016) and lung cancer (Yang *et al.*, 2008); hnRNP-A1 (Roth and Khalaila, 2017) and β-catenin in colorectal cancer (Olivier-Van Stichelen *et al.*, 2012).

The significance of nuclear localization of hnRNP-K was linked to migration of CCA cells by the observation that almost all migrated cells of siOGT-treated cells had nuclear hnRNP-K. The positive associations of O-GlcNAcylation and nuclear hnRNP-K as well as progressive phenotypes were also evident in tumor tissues from CCA patients (Fig. 6A–D). High level of nuclear hnRNP-K in CCA tissues was associated with metastatic stage and shorter survival of CCA patients. The association of hnRNP-K with poor prognosis has also been reported in colon cancer (Carpenter *et al.*, 2006).

Collectively, the results above demonstrated the function of O-GlcNAcylation on nuclear translocation of hnRNP-K. Whether this association is the direct effect of O-GlcNAcylation on hnRNP-K, however, is still obscure. It has been shown that nuclear translocation of hnRNP-K is mediated via activation of Akt (Barboro *et al.*, 2014b; Li *et al.*, 2011), which is also regulated by O-GlcNAcylation (Phoomak *et al.*, 2016). In CCA cells, the association of nuclear translocation of hnRNP-K and O-GlcNAcylation is possibly the direct effect of O-GlcNAcylation on hnRNP-K or formed indirectly via Akt activation. Further experiments using site-directed mutagenesis of O-GlcNAcylation on hnRNP-K are required for the complete

understanding of the precise role of O-GlcNAcylation on nuclear translocation of hnRNP-K.

Our results also underscore the impact of nuclear translocation of hnRNP-K on the migratory ability of CCA cells. First, siOGT treatment inhibited nuclear translocation of hnRNP-K and concurrently decreased migration of CCA cells. Second, almost all migrated cells detected in migration assay had positive nuclear hnRNP-K. These findings prompt further development of inhibitors of hnRNP-K nuclear translocation to diminish CCA progression.

5. Conclusion

Primarily in the nucleus and cytoplasm, 12 novel OGPs associated with progression of cancer were revealed in CCA cells. Of these, hnRNP-K was validated for its O-GlcNAc modification and its molecular mechanism in promoting progression of CCA (Fig. 6E). The impact of hnRNP-K on progressive phenotypes—cell growth, migration, and invasion—was emphasized. O-GlcNAcylation was proved to be necessary for nuclear translocation of hnRNP-K that subsequently activates several downstream targets of hnRNP-K (cyclin D1, XIAP, caspase 3, EMT markers, and MMP2 and MMP7). Expression of nuclear hnRNP-K in tumor tissues predicted the metastatic stage and associated with poor patient outcome. Inhibition of nuclear translocation of hnRNP-K may be a new strategy for CCA treatment.

Acknowledgements

This project was cosupported by the National Research University Grant, Khon Kaen University, for CW (NRU592009), the Thailand Research Fund and Medical Research Council-UK (Newton Fund) project no. DBG5980004 and a scholarship under the Post-Doctoral Training Program from Research Affairs and Graduate School, Khon Kaen University, Thailand, to CP and SW (59151). CBL and DP would like to thank the US National Institutes of Health for support (R01GM049077).

Conflict of interest

The authors declare no conflict of interest.

Author contributions

CP, DP, AS, KS, CBL, and SW conceived and designed experiments; CP, DP, AS, and MD performed experiments; CP and DP prepared the figures; CP, DP, AS, KS, KV, and CW analyzed data; CP, DP, CBL, and SW wrote the manuscript. All authors participated in the interpretation of the studies and reviewed the manuscript.

References

Ali A, Kim SH, Kim MJ, Choi MY, Kang SS, Cho GJ, Kim YS, Choi JY and Choi WS (2017) O-GlcNAcylation of NF-kappaB promotes lung metastasis of cervical cancer cells via upregulation of CXCR4 expression. *Mol Cells* **40**, 476–484.

Barboro P, Ferrari N and Balbi C (2014a) Emerging roles of heterogeneous nuclear ribonucleoprotein K (hnRNP K) in cancer progression. *Cancer Lett* **352**, 152–159.

Barboro P, Salvi S, Rubagotti A, Boccardo S, Spina B, Truini M, Carmignani G, Introini C, Ferrari N, Boccardo F *et al.* (2014b) Prostate cancer: prognostic significance of the association of heterogeneous nuclear ribonucleoprotein K and androgen receptor expression. *Int J Oncol* **44**, 1589–1598.

Carpenter B, McKay M, Dundas SR, Lawrie LC, Telfer C and Murray GI (2006) Heterogeneous nuclear ribonucleoprotein K is over expressed, aberrantly localised and is associated with poor prognosis in colorectal cancer. *Br J Cancer* **95**, 921–927.

Champattanachai V, Netsirisawan P, Chaiyawat P, Phueaouan T, Charoenwattanasatien R, Chokchaichamnankit D, Punyarit P, Srisomsap C and Svasti J (2013) Proteomic analysis and abrogated expression of O-GlcNAcylated proteins associated with primary breast cancer. *Proteomics* **13**, 2088–2099.

Chaudhary P, Thamake SI, Shetty P and Vishwanatha JK (2014) Inhibition of triple-negative and Herceptin-resistant breast cancer cell proliferation and migration by Annexin A2 antibodies. *Br J Cancer* **111**, 2328–2341.

Chen X, Gu P, Xie R, Han J, Liu H, Wang B, Xie W, Xie W, Zhong G, Chen C *et al.* (2017) Heterogeneous nuclear ribonucleoprotein K is associated with poor prognosis and regulates proliferation and apoptosis in bladder cancer. *J Cell Mol Med* **21**, 1266–1279.

Chen CY, Yang SC, Lee KH, Yang X, Wei LY, Chow LP, Wang TC, Hong TM, Lin JC, Kuan C *et al.* (2014) The antitumor agent PBT-1 directly targets HSP90 and hnRNP A2/B1 and inhibits lung adenocarcinoma growth and metastasis. *J Med Chem* **57**, 677–685.

Ching RH, Lau EY, Ling PM, Lee JM, Ma MK, Cheng BY, Lo RC, Ng IO and Lee TK (2015) Phosphorylation of nucleophosmin at threonine 234/237 is associated with HCC metastasis. *Oncotarget* **6**, 43483–43495.

Chung IC, Chen LC, Chung AK, Chao M, Huang HY, Hsueh C, Tsang NM, Chang KP, Liang Y, Li HP *et al.* (2014) Matrix metalloproteinase 12 is induced by

heterogeneous nuclear ribonucleoprotein K and promotes migration and invasion in nasopharyngeal carcinoma. *BMC Cancer* **14**, 348.

Craig R and Beavis RC (2004) TANDEM: matching proteins with tandem mass spectra. *Bioinformatics* **20**, 1466–1467.

Dejgaard K and Leffers H (1996) Characterisation of the nucleic-acid-binding activity of KH domains. Different properties of different domains. *Eur J Biochem* **241**, 425–431.

Dhanjal JK, Nigam N, Sharma S, Chaudhary A, Kaul SC, Grover A and Wadhwa R (2014) Embelin inhibits TNF-alpha converting enzyme and cancer cell metastasis: molecular dynamics and experimental evidence. *BMC Cancer* **14**, 775.

Dissemond J, Busch M, Kothen T, Mors J, Weimann TK, Lindeke A, Goos M and Wagner SN (2004) Differential downregulation of endoplasmic reticulum-residing chaperones calnexin and calreticulin in human metastatic melanoma. *Cancer Lett* **203**, 225–231.

Drougat L, Olivier-Van Stichelen S, Mortuaire M, Foulquier F, Lacoste AS, Michalski JC, Lefebvre T and Vercoutter-Edouart AS (2012) Characterization of O-GlcNAc cycling and proteomic identification of differentially O-GlcNAcylated proteins during G1/S transition. *Biochim Biophys Acta* **1820**, 1839–1848.

Fei F, Li X, Xu L, Li D, Zhang Z, Guo X, Yang H, Chen Z and Xing J (2014) CD147-CD98hc complex contributes to poor prognosis of non-small cell lung cancer patients through promoting cell proliferation via the PI3K/Akt signaling pathway. *Ann Surg Oncol* **21**, 4359–4368.

Ferrer CM, Lu TY, Bacigalupa ZA, Katsetos CD, Sinclair DA and Reginato MJ (2017) O-GlcNAcylation regulates breast cancer metastasis via SIRT1 modulation of FOXM1 pathway. *Oncogene* **36**, 559–569.

Gabriel M, Delforge Y, Deward A, Habraken Y, Hennuy B, Piette J, Klinck R, Chabot B, Colige A and Lambert C (2015) Role of the splicing factor SRSF4 in cisplatin-induced modifications of pre-mRNA splicing and apoptosis. *BMC Cancer* **15**, 227.

Gao R, Yu Y, Inoue A, Widodo N, Kaul SC and Wadhwa R (2013) Heterogeneous nuclear ribonucleoprotein K (hnRNP-K) promotes tumor metastasis by induction of genes involved in extracellular matrix, cell movement, and angiogenesis. *J Biol Chem* **288**, 15046–15056.

Greis KD and Hart GW (1998) Analytical methods for the study of O-GlcNAc glycoproteins and glycopeptides. *Methods Mol Biol* **76**, 19–33.

Gu Y, Mi W, Ge Y, Liu H, Fan Q, Han C, Yang J, Han F, Lu X and Yu W (2010) GlcNAcylation plays an essential role in breast cancer metastasis. *Cancer Res* **70**, 6344–6351.

Hart GW, Housley MP and Slawson C (2007) Cycling of O-linked beta-N-acetylglucosamine on nucleocytoplasmic proteins. *Nature* **446**, 1017–1022.

Hart GW, Slawson C, Ramirez-Correa G and Lagerlof O (2011) Cross talk between O-GlcNAcylation and phosphorylation: roles in signaling, transcription, and chronic disease. *Annu Rev Biochem* **80**, 825–858.

Kang JG, Park SY, Ji S, Jang I, Park S, Kim HS, Kim SM, Yook JI, Park YI, Roth J *et al.* (2009) O-GlcNAc protein modification in cancer cells increases in response to glucose deprivation through glycogen degradation. *J Biol Chem* **284**, 34777–34784.

Khachaturov V, Xiao GQ, Kinoshita Y, Unger PD and Burstein DE (2014) Histone H1.5, a novel prostatic cancer marker: an immunohistochemical study. *Hum Pathol* **45**, 2115–2119.

Kong L, Schafer G, Bu H, Zhang Y, Zhang Y and Klocker H (2012) Lamin A/C protein is overexpressed in tissue-invading prostate cancer and promotes prostate cancer cell growth, migration and invasion through the PI3K/AKT/PTEN pathway. *Carcinogenesis* **33**, 751–759.

Lee LR, Teng PN, Nguyen H, Hood BL, Kavandi L, Wang G, Turbov JM, Thaete LG, Hamilton CA, Maxwell GL *et al.* (2013) Progesterone enhances calcitriol antitumor activity by upregulating vitamin D receptor expression and promoting apoptosis in endometrial cancer cells. *Cancer Prev Res (Phila)* **6**, 731–743.

Li Y, Huang J, Zhao YL, He J, Wang W, Davies KE, Nose V and Xiao S (2007) UTRN on chromosome 6q24 is mutated in multiple tumors. *Oncogene* **26**, 6220–6228.

Li LP, Lu CH, Chen ZP, Ge F, Wang T, Wang W, Xiao CL, Yin XF, Liu L, He JX *et al.* (2011) Subcellular proteomics revealed the epithelial-mesenchymal transition phenotype in lung cancer. *Proteomics* **11**, 429–439.

Lu J and Gao FH (2016) Role and molecular mechanism of heterogeneous nuclear ribonucleoprotein K in tumor development and progression. *Biomed Rep* **4**, 657–663.

Lynch TP, Ferrer CM, Jackson SR, Shahriari KS, Vosseller K and Reginato MJ (2012) Critical role of O-Linked beta-N-acetylglucosamine transferase in prostate cancer invasion, angiogenesis, and metastasis. *J Biol Chem* **287**, 11070–11081.

Ma Z and Vosseller K (2013) O-GlcNAc in cancer biology. *Amino Acids* **45**, 719–733.

Maruyama M, Kobayashi N, Westerman KA, Sakaguchi M, Allain JE, Totsugawa T, Okitsu T, Fukazawa T, Weber A, Stolz DB *et al.* (2004) Establishment of a highly differentiated immortalized human cholangiocyte cell line with SV40T and hTERT. *Transplantation* **77**, 446–451.

Minder P, Bayha E, Becker-Pauly C and Sterchi EE (2012) Meprinalpha transactivates the epidermal growth factor receptor (EGFR) via ligand shedding, thereby enhancing colorectal cancer cell proliferation and migration. *J Biol Chem* **287**, 35201–35211.

Olivier-Van Stichelen S, Guinez C, Mir AM, Perez-Cervera Y, Liu C, Michalski JC and Lefebvre T (2012) The hexosamine biosynthetic pathway and O-GlcNAcylation drive the expression of beta-catenin and cell proliferation. *Am J Physiol Endocrinol Metab* **302**, E417–E424.

Park D, Arabyan N, Williams CC, Song T, Mitra A, Weimer BC, Maverakis E and Lebrilla CB (2016) Salmonella Typhimurium enzymatically landscapes the host intestinal epithelial cell (IEC) surface glycome to increase invasion. *Mol Cell Proteomics* **15**, 3653–3664.

Park D, Brune KA, Mitra A, Marusina AI, Maverakis E and Lebrilla CB (2015) Characteristic changes in cell surface glycosylation accompany intestinal epithelial cell (IEC) differentiation: high mannose structures dominate the cell surface glycome of undifferentiated enterocytes. *Mol Cell Proteomics* **14**, 2910–2921.

Phoomak C, Silsirivanit A, Park D, Sawanyawisuth K, Vaeteewoottacharn K, Wongkham C, Lam EW, Pairojkul C, Lebrilla CB and Wongkham S (2018) O-GlcNAcylation mediates metastasis of cholangiocarcinoma through FOXO3 and MAN1A1. *Oncogene* **37**, 5648–5665.

Phoomak C, Silsirivanit A, Wongkham C, Sripa B, Puapairoj A and Wongkham S (2012) Overexpression of O-GlcNAc-transferase associates with aggressiveness of mass-forming cholangiocarcinoma. *Asian Pac J Cancer Prev* **13**(Suppl), 101–105.

Phoomak C, Vaeteewoottacharn K, Sawanyawisuth K, Seubwai W, Wongkham C, Silsirivanit A and Wongkham S (2016) Mechanistic insights of O-GlcNAcylation that promote progression of cholangiocarcinoma cells via nuclear translocation of NF-kappaB. *Sci Rep* **6**, 27853.

Phoomak C, Vaeteewoottacharn K, Silsirivanit A, Saengboonmee C, Seubwai W, Sawanyawisuth K, Wongkham C and Wongkham S (2017) High glucose levels boost the aggressiveness of highly metastatic cholangiocarcinoma cells via O-GlcNAcylation. *Sci Rep* **7**, 43842.

Roth S and Khalaila I (2017) The effect of O-GlcNAcylation on hnRNP A1 translocation and interaction with transportin 1. *Exp Cell Res* **350**, 210–217.

Santiago-Gomez A, Barrasa JI, Olmo N, Lecona E, Burghardt H, Palacin M, Lizarbe MA and Turnay J (2013) 4F2hc-silencing impairs tumorigenicity of HeLa cells via modulation of galectin-3 and beta-catenin signaling, and MMP-2 expression. *Biochim Biophys Acta* **1833**, 2045–2056.

Shen S, Zuo J, Feng H, Bai M, Wang C, Wei Y, Li Y, Le Y, Wu J, Yu L *et al.* (2015) TCP10L synergizes with MAD1 in transcriptional suppression and cell cycle arrest through mutual interaction. *BMB Rep* **49**, 325–330.

Singh JP, Zhang K, Wu J and Yang X (2015) O-GlcNAc signaling in cancer metabolism and epigenetics. *Cancer Lett* **356**, 244–250.

Song D, Chaerkady R, Tan AC, Garcia-Garcia E, Nalli A, Suarez-Gauthier A, Lopez-Rios F, Zhang XF, Solomon A, Tong J *et al.* (2008) Antitumor activity and molecular effects of the novel heat shock protein 90 inhibitor, IPI-504, in pancreatic cancer. *Mol Cancer Ther* **7**, 3275–3284.

Sudo H, Tsuji AB, Sugyo A, Abe M, Hino O and Saga T (2014) AHNAK is highly expressed and plays a key role in cell migration and invasion in mesothelioma. *Int J Oncol* **44**, 530–538.

Sugimasa H, Taniue K, Kurimoto A, Takeda Y, Kawasaki Y and Akiyama T (2015) Heterogeneous nuclear ribonucleoprotein K upregulates the kinetochore complex component NUF2 and promotes the tumorigenicity of colon cancer cells. *Biochem Biophys Res Commun* **459**, 29–35.

Wang J, Torii M, Liu H, Hart GW and Hu ZZ (2011) dbOGAP – an integrated bioinformatics resource for protein O-GlcNAcylation. *BMC Bioinformatics* **12**, 91.

Wang T, Yuan J, Zhang J, Tian R, Ji W, Zhou Y, Yang Y, Song W, Zhang F and Niu R (2015) Anxa2 binds to STAT3 and promotes epithelial to mesenchymal transition in breast cancer cells. *Oncotarget* **6**, 30975–30992.

Xiao Z, Ko HL, Goh EH, Wang B and Ren EC (2013) hnRNP K suppresses apoptosis independent of p53 status by maintaining high levels of endogenous caspase inhibitors. *Carcinogenesis* **34**, 1458–1467.

Xu LX, Li ZH, Tao YF, Li RH, Fang F, Zhao H, Li G, Li YH, Wang J, Feng X *et al.* (2014) Histone acetyltransferase inhibitor II induces apoptosis in glioma cell lines via the p53 signaling pathway. *J Exp Clin Cancer Res* **33**, 108.

Yan-Fang T, Zhi-Heng L, Li-Xiao X, Fang F, Jun L, Gang L, Lan C, Na-Na W, Xiao-Juan D, Li-Chao S *et al.* (2015) Molecular mechanism of the cell death induced by the histone deacetylase pan inhibitor LBH589 (Panobinostat) in Wilms tumor cells. *PLoS One* **10**, e0126566.

Yang N, Goonatilleke E, Park D, Song T, Fan G and Lebrilla CB (2016) Quantitation of site-specific glycosylation in manufactured recombinant monoclonal antibody drugs. *Anal Chem* **88**, 7091–7100.

Yang WH, Park SY, Nam HW, Kim DH, Kang JG, Kang ES, Kim YS, Lee HC, Kim KS and Cho JW (2008) NFkappaB activation is associated with its O-

GlcNAcylation state under hyperglycemic conditions. *Proc Natl Acad Sci USA* **105**, 17345–17350.

Yang H, Zou W, Li Y, Chen B and Xin X (2007) Bridge linkage role played by CD98hc of anti-tumor drug resistance and cancer metastasis on cisplatin-resistant ovarian cancer cells. *Cancer Biol Ther* **6**, 942–947.

Zachara NE, Hart GW (2006) Cell signaling, the essential role of O-GlcNAc! *Biochim Biophys Acta* **1761**, 599–617.

Zhang L, Feng J, Kong S, Wu M, Xi Z, Zhang B, Fu W, Lao Y, Tan H and Xu H (2016a) Nujiangexathone A, a novel compound from Garcinia nujiangensis, suppresses cervical cancer growth by targeting hnRNPK. *Cancer Lett* **380**, 447–456.

Zhang Z, Zhou C, Chang Y, Zhang Z, Hu Y, Zhang F, Lu Y, Zheng L, Zhang W, Li X *et al.* (2016b) Long non-coding RNA CASC11 interacts with hnRNP-K and activates the WNT/beta-catenin pathway to promote growth and metastasis in colorectal cancer. *Cancer Lett* **376**, 62–73.

Zhou R, Shanas R, Nelson MA, Bhattacharyya A and Shi J (2010) Increased expression of the heterogeneous nuclear ribonucleoprotein K in pancreatic cancer and its association with the mutant p53. *Int J Cancer* **126**, 395–404.

Zhu XH, Wang JM, Yang SS, Wang FF, Hu JL, Xin SN, Men H, Lu GF, Lan XL, Zhang D *et al.* (2017) Down-regulation of DAB2IP promotes colorectal cancer invasion and metastasis by translocating hnRNPK into nucleus to enhance the transcription of MMP2. *Int J Cancer* **141**, 172–183.

Supporting information

Additional supporting information may be found online in the Supporting Information section at the end of the article.

Table S1. List of identified OGPs in CCA cells.

Fig. S1. Identification of O-GlcNAcylated proteins using Click-iT™O-GlcNAc Enzymatic Labeling System and mass spectrometry.

Fig. S2. Predicted O-GlcNAcylated proteins in CCA cells.

Fig. S3. Cell proliferation during migration and invasion assays.

Fig. S4. Effect of hnRNP-K and O-GlcNAcylation on cell migration.

Fig. S5. Expression and localization of hnRNP-K in CCA cell lines.

Taylor & Francis
Taylor & Francis Group

Expert Review of Anticancer Therapy

ISSN: 1473-7140 (Print) 1744-8328 (Online) Journal homepage: http://www.tandfonline.com/loi/iery20

Prognostic biomarkers for cholangiocarcinoma and their clinical implications

Charupong Saengboonmee, Kanlayanee Sawanyawisuth, Yaovalux Chamgramol & Sopit Wongkham

To cite this article: Charupong Saengboonmee, Kanlayanee Sawanyawisuth, Yaovalux Chamgramol & Sopit Wongkham (2018): Prognostic biomarkers for cholangiocarcinoma and their clinical implications, Expert Review of Anticancer Therapy, DOI: 10.1080/14737140.2018.1467760

To link to this article: https://doi.org/10.1080/14737140.2018.1467760

Accepted author version posted online: 20 Apr 2018.
Published online: 26 Apr 2018.

EXPERT REVIEW OF ANTICANCER THERAPY, 2018
https://doi.org/10.1080/14737140.2018.1467760

Taylor & Francis
Taylor & Francis Group

REVIEW

Prognostic biomarkers for cholangiocarcinoma and their clinical implications

Charupong Saengboonmee[a,b], Kanlayanee Sawanyawisuth[a,b], Yaovalux Chamgramol[b,c] and Sopit Wongkham[a,b]

[a]Department of Biochemistry, Faculty of Medicine, Khon Kaen University, Khon Kaen, Thailand; [b]Cholangiocarcinoma Research Institute, Khon Kaen University, Khon Kaen, Thailand; [c]Department of Pathology, Faculty of Medicine, Khon Kaen University, Khon Kaen, Thailand

ABSTRACT

Introduction: Cholangiocarcinoma (CCA) is a poorly prognostic cancer with limited treatment options. Most patients have unresectable tumors when they are diagnosed and the chemotherapies provided are of limited benefit. Prognostic markers are therefore necessary to predict the disease outcome, risk of relapse, or to suggest the best treatment option.

Areas covered: This article provides an up-to-date review of biomarkers with promising characteristics to be prognostic markers for CCA reported in the past 5 years. The biomarkers are sub-classified into tissue and serum markers. Proteins, RNAs, peripheral blood cells etc., that are associated with aggressive phenotypes, signal pathways, chemo-drug resistance, and those that reflect the survival time of CCA patients are evaluated for their prognostic prediction values.

Expert commentary: CCAs are heterogeneous tumors of different histo-pathological subtypes and genetic influences and, therefore, potential markers should be validated in larger collectives with varied epidemiological backgrounds. A systematic review and meta-analysis should be done to clarify the impact of the reported biomolecules for their potential prognostic values. Non- or low-invasive sample collections, as well as the simple and affordable determination methods, should be constructed to make the prognostic biomarkers available in clinical practice.

ARTICLE HISTORY
Received 10 December 2017
Accepted 18 April 2018

KEYWORDS
CA19-9; diagnosis; drug resistance; miRNAs; neutrophil-to-lymphocyte ratio; non-coding RNA; overall survival; signaling pathways; tumor microenvironment; tumor stromal

1. Cholangiocarcinoma: incidence and clinical manifestations

Cholangiocarcinoma (CCA) is a malignancy of bile duct epithelia. The incidence of CCA accounts for 15% of all primary liver cancers and 3% for all gastrointestinal malignancies [1]. Considering CCA as a rare cancer, its incidence is nevertheless increasing globally. The highest incidence of CCA is in Southeast Asia, especially in the Northeast of Thailand, while the lowest incidence is in Australia [1,2]. The risk factors for choangiocarcinogenesis are varied geographically. Primary sclerosing cholanigitis is a well-known risk factor in the Western countries, 10–15% of which later develop CCA. The high-risk group for CCA in Southeast and East Asia is, in contrast, associated with the infection of liver flukes, *Opisthorchis viverrini* in the Southeast and *Clonorchis sinensis* in East Asia [3,4].

CCA is classified into three types according to its anatomical location: the intrahepatic (iCCA), perihilar (pCCA), and distal (dCCA) CCAs. iCCA is considered as the second most common primary liver cancer after hepatocellular carcinoma (HCC). pCCA and dCCA are extrahepatic CCA (eCCA), of which pCCA is the most frequent type reported [5]. Risk factors for iCCA and eCCA are common but the etiology and cells of origin may be different. In addition, liver fluke and non-liver fluke associated CCAs also exhibited different genetic mutations and gene expression profiles [6]. Hence, the genetic background, molecular expression, and biological behaviors of CCAs among each type are different [6–8]. These facts imply that the potential biomarkers or therapeutic targets raised from one type of CCA may not be beneficial to all CCAs even with similar subtypes.

CCA is highly fatal. The potentially curative treatment is surgical resection [2]. Only one third of CCA patients, however, are diagnosed at an early stage and are therefore amenable to curative surgical intervention [9]. The rest of CCA patients usually present with an advanced stage, loco-regional invasion or distant metastasis, for all of which, surgical intervention is an unlikely cure. Alternative treatments such as systemic chemotherapy and loco-regional therapies still have roles for survival time improvement even though with limited effectiveness. The transarterial chemoembolization for localized unresectable iCCA has improved median overall survival time to 12–15 months while the standard-of-care chemotherapy regimen of gemcitabine and cisplatin provided median overall survival times of less than a year [10–12]. The other approaches such as targeted therapy and immunotherapy for CCA are ongoing in the clinical trials [13].

2. Significance of prognostic markers for cancer treatment

Most of the morbidity and mortality of CCA comes from metastasis, therefore, prognostic markers to follow up the treatment outcomes after resection and to predict those who will benefit from the treatment are needed.

CONTACT Sopit Wongkham sopit@kku.ac.th Department of Biochemistry, Faculty of Medicine, Khon Kaen University, Khon Kaen, Thailand, 40002

Biomolecules that reflect the biological processes of cancer cells can be used as biomarkers and upregulation of these markers may imply clinical manifestations of patients. For example, an increase of motility-associated molecules may reflect the metastatic potential of cancer cells and imply a poor prognosis and short survival time of the patients. In addition, the rising level of a biomarker after surgical resection may suggest recurrence of the disease. For example, carbohydrate antigen 19–9 (CA-19–9) and carcinoembryonic antigen (CEA) are potentially used to indicate the risk of a recurrent tumor when their levels have risen. Biomarkers that are associated with therapeutic responsiveness are also beneficial in clinical practice as they signify the success of treatment and suggest effective management. The prognosis of CCA after treatment with any modality is associated with many factors including the genetic and epigenetic background, gene expression pattern of tumor, surgical procedure or responsiveness to chemotherapy or loco-regional intervention, and the recurrence of tumors after resection. To achieve an accurate prognostic prediction for CCA, in terms of an overall survival (OS) time, disease-free survival (DFS), and recurrent rate, *etc*. involves several stated factors. At present, none is the best representative.

The attempts to discover an effective prognostic biomarker for CCA have been occurring for several decades and some of promising candidates have been reported. Various types of biomolecules, nucleic acid, proteins, and glycoproteins associated with CCA progression have been discovered and suggested as candidates for prognostic markers for CCA. The correlation between the expression levels of these candidates with clinico-pathological characteristics and survival of patients has provided evidence for the values of these markers for the prognosis of CCA. Most of the candidates were discovered using immunohistochemistry, some of which could be detected in serum. The latter group is an ideal prognostic marker for a follow-up purpose as serum collection is convenient and less invasive. In this sense, validation of biomarkers in serum or secretory fluids should not be neglected when a tissue marker is identified.

In this review, the biomarkers are sub-classified according to the sources of samples from tissue and serum markers. The functional molecules related to the prognosis of CCA in the recent 5 years are evaluated.

3. Tissue biomarkers as prognostic-predictive markers of CCA

Overexpression or aberrant expression of many molecules in CCA tissues identified by immunohistochemistry or other techniques have been proposed to be prognostic markers for CCA. Tissue markers have become a prototype for cancer biomarkers since their association with cancer cells or the cancer microenvironment are definitely proven. Most of these markers were identified at the protein level and some were validated at the mRNA level. The recent tissue markers reported for CCA are summarized in Table 1.

3.1. Cell surface molecules

Several surface molecules, for example, clusters of differentiation (CD) 155, CD44, CD97, CD98, and EpCAM, *etc*., play significant roles in cancer progression. These molecules are associated with cell motility and transcellular signaling that modulate tumor behavior. Thus, the associations of surface molecules with cancer progression and poor prognosis of patients are frequently found. CD155, an immunoglobulin-like adhesion molecule, known as the poliovirus receptor, is associated with cell proliferation, migration, metastasis, and tumor immunity of CCA [14]. Upregulation of CD155 in CCA tissues has been associated with histological grading, lymph node metastasis, the expression of vascular endothelial growth factor (VEGF), and microvascular density (MVD). Expression of CD155 was related to a shorter DFS and OS of patients and was suggested to be an independent prognostic marker for CCA [14]. High expression of CD44, a transmembrane protein involved in glutathione synthesis for redox balance and survival of cancer cells in CCA tissues, was correlated with clinico-pathological features and an OS of patients [15]. Patients with tissue CD44 positive had a significantly shorter OS survival than those with CD44 negative. Moreover, the patients with high CD44 and negative phospho-p38 mitogen-activated protein kinase (MAPK) expressions in CCA tissues had a significantly shorter OS compared to those with low CD44 and positive phospho-p38 MAPK expressions [16]. High expression of CD98, involved in tumor growth, was associated with expression of CD34, an L-type amino acid transporter, and Ki-67, a proliferation marker, and was proposed to be an independent prognostic factor for CCA [17]. In addition, CD55 and CD97 were recently reported for their associations with poor histological grading, lymph node metastasis, venous invasion, and shorter OS of CCA patients [18].

3.2. Receptor proteins

Receptor proteins and their partners are the other key proteins that are straightforwardly associated with cancer growth and progression. Mostly, they are the upstream of signaling pathways that regulate the biological process of cancer cells, and usually investigated for their significances in prognostic prediction and as therapeutic targets. A group of sophisticated receptor proteins of the tyrosine kinase receptor family was found in several cancers including CCA. Recent studies showed various tyrosine kinase receptors and their associated proteins as potential prognostic markers. For examples, CCA patients with a high expression of C-met, a member of tyrosine kinase receptor family, exhibited shorter OS and DFS than those with low expression [19]. High expression of fibroblast growth factor receptor (FGFR4) in tumor tissues from iCCA, pCCA, and dCCA patients was associated with poor prognosis of iCCA and pCCA patients and recommended to be an independent prognostic marker for iCCA [20]. Ephrin B2, a member of Ephrin receptor tyrosine kinase family, was associated with phosphorylation of focal adhesion kinase (FAK), the downstream signaling molecule of Ephrin [21]. The migration of CCA cell lines increased after FAK activation. The

Table 1. Summary of potential tissue biomarkers of cholangiocarcinoma prognosis.

Name	Associated biological function	Associated clinicopathological features	Associated prognostic values	Type of CCA[a] and number of cases	Geographical origin of CCA	Ref.
Cell surface molecule						
CD155	Adhesion, proliferation, migration, metastasis, tumor immunity	Histological grading, LN metastasis, MVD	DFS, OS	90	China	[14]
CD44	Redox balance, cell survival	ND	OS	iCCA: 85, iCCA: 97	Thailand	[15,16]
CD98	Proliferation, L-type amino acid transporter	ND	OS	139	Japan	[17]
CD55	ND	Histological grading, LN metastasis, venous invasion	OS	iCCA: 71	China	[18]
CD97	ND	Histological grading, LN metastasis, venous invasion	OS	iCCA: 71	China	[18]
EpCAM	ND	Number of tumor nodule	DFS, OS	iCCA: 40	France	[35]
Receptor proteins and partners						
C-met	Tyrosine kinase receptor	TNM staging	DFS, OS	291	China	[19]
Fibroblast growth factor receptor	Tyrosine kinase receptor, proliferation, invasion, EMT	MVD	OS	iCCA: 83, pCCA: 75 dCCA: 41	China	[20]
Ephrin B2	Tyrosine kinase receptor, Migration	Metastasis	ND	50	Thailand	[21]
Signaling molecules and regulators						
Interleukin-6	ND	ND	DFS, OS	iCCA: 72	Japan	[22,23]
Interleukin-8	ND	MVD, TNM staging	OS	pCCA:62	China	[51]
Interleukin-17		ND	DFS, OS	ICC: 72	Japan	[23]
Tumor necrosis factor α-induced protein 3	ND	TNM staging	OS	22	China	[24]
Suppressor of cytokine signaling 3 (SOCS3) (low)	ND	Tumor differentiation	OS	22	China	[24]
Ring finger protein 43 (RNF43) (low)	wnt/β-catenin signaling pathway regulator	ND	OS	iCCA: 50	Thailand	[26]
SOX4	Transcriptional factor, EMT	Expression of EGFR and HER2	OS	iCCA58, eCCA: 94	China	[29]
Mucins						
Mucin 5AC	ND	Tumor size, LN metastasis, TNM staging	OS	iCCA: 179, iCCA: 62	Thailand Japan	[31,32,33]
Mucin 4	ND	ND	OS	249	China and Japan	[34]
Miscellaneous proteins						
Transferrin receptor-I	Accumulation of labile iron pool	Metastasis	OS	49	Thailand	[37]
High-mobility group AT-hook 2 (HMGA2)	Growth, differentiation, apoptosis, neoplastic transformation	Mutated p53 expression, decreased p16 expression, LN metastasis	OS	68	USA	[39]
LIM and SH3 protein (LASP) 1	Proliferation, migration, invasion, tumorigenesis	Tumor size, differentiation, LN metastasis, TNM staging	OS	40	China	[41]
B7-H4	ND	Histological differentiation, lymph node metastasis and staging, low CD8 + T cell infiltration	DFS, OS	137	China	[42]
Hepatoma-derived growth factor (HDGF)	Proliferation, invasion, angiogenesis	MVD, LN invasion, metastasis, TNM staging	OS	iCCA: 83	China	[43]
Phosphorylated 4E-binding protein 1 (p-4E-BP1)	ND	Histological differentiation, LN metastasis	DFS, OS	pCCA: 61	China	[45]
Ki-67	ND	TNM staging	OS	pCCA: 35	China	[46]
Mesenchymal-epithelial transition factor (MET)	ND	ND	OS	pCCA:248	Japan	[47]
Recepteur d'origine nantais (RON)	ND	ND	OS	pCCA:248	Japan	[47]
Sex determining region Y-box (Sox9)	Migration, Invasion	ND	OS	iCCA: 43	Japan	[48]
Matrix metalloproteinase −11	Invasion	ND	OS	30	Thailand	[49]

(*Continued*)

Table 1. (Continued).

Name	Associated biological function	Associated clinicopathological features	Associated prognostic values	Type of CCA[a] and number of cases	Geographical origin of CCA	Ref.
Matrix metalloproteinase −9	Invasion	ND	OS	pCCA:62	China	[50,51]
Eye absent homolog (EYA) 4 (low)	Proliferation, invasion, tumorigenesis	Tumor number, local invasion, LN metastasis, tumor differentiation	DFS, OS	iCCA: 112	China	[75]
Metastasis suppressor 1 (MSST1) (low)	Migration	Tumor size, LN metastasis, TNM staging	OS	iCCA: 93	China	[80]
Lysil oxidase-like 2 (LOXL2)	Extracellular matrix remodeling enzyme	ND	DFS, OS	iCCA	France	[36]
AT-rich interactive domain 1A (ARID1A) (low)	ND	Tumor nodules, venous invasion, recurrence	DFS, OS	iCCA: 57	China	[78]
Secreted frizzled related protein-1 (SFRP1) (low)	ND	ND	DFS, OS	iCCA: 50	Japan	[82]
Co-expression of natural killer group 2 member D (NKG2D) ligands (low)	ND	ND	DFS, OS	eCCA: 82	Japan	[85]
Non-coding RNA						
lncRNA H19	Proliferation, anti-apoptosis, EMT, migration, invasion	Tumor size, TNM staging,	DFS, OS	56	China	[53]
PANDAR	Proliferation, anti-apoptosis, EMT	Lymph node metastasis, TNM staging	OS	67	China	[54]
miR-29a	ND	Lymph node metastasis, clinical staging, histological differentiation	OS	125	China	[60]

• The poor prognosis is associated with upregulation of those biomarkers, otherwise specified.
• Abbreviation; ND: not determined in the study; LN: lymph node; MVD: microvascular density; TNM: tumor-lymph node-metastasis staging; EGFR: epidermal growth factor receptor; HER: human epidermal growth factor; EMT: epithelial-mesenchymal transition; DFS: disease free survival; OS: overall survival
[a] Type of CCA as specified.

association of Ephrin B2 over-expression in CCA tissues and metastatic status of CCA patients was also notable. Although, the functions of tyrosine kinase receptor family and their direct association with aggressiveness of cancer and poor prognosis of patients are well known, the clinical implications may be limited because the post-translational modifications, for example, phosphorylation, of the receptors more directly reveal their active status than the expression levels.

3.3. Signaling molecules and regulators

The signaling molecules including cytokines, intracellular signaling molecules and their regulators are important in cancer progression and frequently associated with the prognosis of patients. Association of various interleukins (IL), for example, IL1, IL2, and IL6, *etc*., with progression and severity of cancers has been repeatedly reported. IL6 is a multifunctional cytokine that acts as both a pro- and an anti-inflammatory cytokine. Increased levels of IL6 promote neo-angiogenesis, inhibit cancer cell apoptosis, and deregulate tumor microenvironment. As a result, high levels of IL6 in cancers is associated with elevated cancer risk, tumor stage, treatment response, and severity of symptoms in several cancer types [22]. High expressions of interleukin-6 (IL6) in tumor tissue and IL17 in peritumoral cells of CCA corresponded to the shorter OS and DFS of CCA patients [23]. The expression of suppressors of cytokine signaling 3 (SOCS3) was down-regulated in cancer cells compared with the peritumoral tissues [24]. Conversely, the regulator protein of SOCS3 expression, the tumor necrosis factor α-induced protein 3 (TNFAIP3 or A20), was increased in CCA cells. The inverse of these two proteins were observed in CCA and significantly correlated with poor prognosis of CCA patients. Patients with high expression of A20 and low expression of SOCS3 had a dramatically low OS rate. Expression of A20 was related with tumor-lymph node-metastasis (TNM) staging while SOCS3 was associated with tumor differentiation. This suggested A20 and SOCS3 as prognostic markers for CCA.

Ring finger protein 43 (RNF43), a ring finger E3 ligase that negatively regulates Wingless-related integration site (wnt)/β-catenin signaling pathway, mutates in ~9.3% of iCCA. The involvements of RNF43 in suppression of cell proliferation, enhanced cell apoptosis, and being a potential prognostic indicator for the clinical assessment of gastric cancer were demonstrated [25]. The prognostic value of RNF43 in iCCA was reported [26]. RNF43 mRNA and protein were reduced in iCCA tissues, and the decreasing of RNF43 mRNA was correlated with the presence of rs2257205 and RNF43 somatic mutation. Thus, the down regulation of RNF43 in iCCA was associated with shorter OS of CCA patients.

Increased expression and activity of a transcription factor, SOX4, a member of the SOX (SRY-related HMG-box) family, contributed to cellular transformation, cell survival, and metastasis in many cancer types. SOX4 is a key regulator of EMT that governs the expression of the epigenetic modifier Ezh2 [27]. Meta-analysis showed that SOX4 expression was about 78% in overall cancer tissues and over-expression of SOX4 was correlated with a poor OS and the pooled hazard ratio [28]. SOX4

was overexpressed in approximately 20% of iCCA and 30% of iCCA and eCCA tissues [29]. The expression of Sox4 was correlated with the expression of EGFR and HER2 in both iCCA and eCCA, and associated with shorter OS of iCCA patients.

3.4. Mucins

Mucins (MUCs), a heterogeneous family of *O*-glycosylated high molecular weight glycoproteins, has been studied for its significance in CCA for decades. MUC1, MUC2, MUC4, MUC5AC, and MUC16 were detected in CCA tissues [30]. MUC5AC was the most studied mucin that has a high potential as a biomarker for CCA. MUC5AC was aberrantly expressed in CCA tissues, associated with a larger tumor size and advanced stage CCA [31]. Moreover, high level of MUC5AC could be detected in the serum of CCA patients and was associated with shorter OS of the patients [32]. High expression of MUC5AC tissues was also associated with lymph node metastasis and shorter survival of patients after curative-intent hepatectomy [33]. The meta-analysis of MUC4 from 5 studies reporting on 249 patients who undergone surgical resection, indicated that positive tissue MUC4 was associated with the poor survival of CCA patients [34].

3.5. Tumor stromal and microenvironment

Molecules of stromal cells can also be the prognostic markers of cancer. As the microenvironment is crucial for supporting cancer survival, therefore the over- or aberrant expressions of molecules in the stromal cells or tumor microenvironment should be explored for discovery of prognostic markers. The report from Sulpice *et al*. [35] indicated that EpCAM, a well-known cancer stem cell marker in HCC, was ubiquitously expressed in iCCA stroma. High expression of EpCAM in non-fibrous liver tissue was related to the worst DFS iCCA patients. Besides, overexpression of lysil oxidase-like 2 (LOXL2), an extracellular matrix remodeling enzyme found in the stroma, was found to be associated with poor OS and DFS of iCCA patients. Moreover, LOXL2 could be an independent prognostic marker with a high hazard ratio of 5.55 [36].

3.6. Intracellular proteins

Various intracellular proteins associated with cancer progression and the poor prognosis of CCA have been reported. Upregulation of transferrin receptor-I in CCA cell lines and patient CCA tissues resulted in an increased accumulation of a labile iron pool was associated with CCA metastasis and shorter OS [37]. The ectopic expression of HMGA2, the non-histone chromosomal high-mobility group (HMG) protein family that acts as architectural transcription regulators, could induce EMT, invasion and metastasis of human epithelial cancers [38]. HMGA2 was also associated with cell growth, differentiation, apoptosis, and neoplastic transformation of CCA cells [39]. Expression of HMGA2 was negatively correlated with p16, a tumor suppressor protein expression, but positively correlated with the mutated p53 expression, lymph node metastasis and shorter OS. HMGA2 was, hence, suggested to be an independent indicator for a poor prognosis of CCA.

LIM and SH3 protein (LASP) 1, a member of a LIM protein subfamily characterized by a LIM motif and a domain of Src homology region 3, functions as an actin-binding protein and cytoskeletal organization. The association of LASP1 with progression and metastatic dissemination was reported in medulloblastoma [40]. In CCA, LASP1 was associated with proliferation, migration, invasion and tumorigenesis of CCA *in vivo* [41]. High expression of LASP1 in CCA tissues was positively correlated with the larger tumor, poor histological differentiation, lymph node metastasis, an advanced TNM stage, and shorter OS of patients. Moreover, suppression of LASP1 increased apoptosis and suppressed proliferation, migration, and invasion of CCA cell lines. LASP1 is, thus, a promising prognostic factor and a candidate for being a therapeutic target.

B7-H4, a member of the B7 superfamily of ligands, has been implicated in tumor immunogenicity and cancer development. Blockade of B7-H4 could allow for antigen-specific clearance of tumor cells, suggesting the therapeutic potential of targeting B7-H4 [42]. High expression of B7-H4 was found in approximately 50% of CCA tissues. An increased level of B7-H4 was associated with poor histological differentiation, lymph node metastasis, staging, poor OS and the early recurrence of tumors. The *in vivo* experiments indicated the association of B7-H4 with the immunomodulation of CCA in which its expression suppressed the infiltration of $CD8^+$ cytotoxic T lymphocyte. Hepatoma-derived growth factor (HDGF), an acidic heparin binding protein was associated with tumor progression in many cancers and promoted proliferation, invasion, and angiogenesis of CCA cells *in vitro* [43]. The expression of HDGF in CCA tissues was associated with MVD, lymphatic invasion, distant metastasis and TNM staging of CCA patients. It, thus was significantly correlated with the shorter OS of CCA patients and might be used as a prognostic marker.

Eukaryotic translation initiation factor 4E (eIF4E)-binding protein 1 (4E-BP1), a member of a family of translation repressor proteins, is a well-known substrate of the mechanistic target of the rapamycin (mTOR) signaling pathway. Phosphorylation of 4E-BP1 (p-4E-BP1) allows translation to proceed. Recently, overexpression of 4E-BP1 was found in many human carcinomas [44]. Expression of p-4E-BP1 in tissue microarrays with pCCA showed that 57.4% of CCA cases had a moderate to high expression of this protein [45]. Moreover, overexpression of p-4E-BP1was also associated with poor differentiation and lymph node metastasis, shorter DFS and OS.

High expressions of Ki-67 and p73 were correlated with the shorter OS of pCCA patients [46]. Ki-67 was correlated with the higher staging of tumor, suggesting the predictive value of Ki67 for a worse prognosis of CCA. A similar observation was reported for mesenchymal-epithelial transition factor (MET) and recepteur d'origine nantais (RON). The positive expressions of MET and RON in pCCA tissues were associated with shorter OS [47]. The positive combination of these proteins may be a worse prognostic biomarker of pCCA patients and the negative staining of either MET or RON may reflect a better prognosis of patients with pCCA. The sex determining region Y-box (Sox9) is required for normal development of the biliary tract, but was decreased in early biliary tract carcinogenesis [48]. The expression of Sox9, however, was increased

in CCA and involved in cell migration and invasion. Correlation of high Sox9 expression and shorter OS of iCCA patients was demonstrated.

The metalloproteinases (MMPs) are enzymes that degrade extracellular matrices. In physiological conditions, these enzymes take part in the remodeling of tissues and play a key role in the wound healing process. In cancer, MMPs were activated to degrade the cancer extracellular matrix, a crucial step for the metastasis. High expression of MMPs in cancer and stromal cells, therefore, can signify the aggressiveness of the tumor. In CCA, MMP-9 and MMP-11 were expressed in CCA tissues and significantly associated with poor OS, but not with any clinicopathological features of CCA patients [49,50]. In addition, the expression of tissue MMP-9 was associated with that of tissue IL8, the expression of which was significantly associated with MVD and TNM staging of CCA patients. Tissue IL8 was noted to be an independent prognostic marker for CCA patients [51].

3.7. Non-coding RNA

A non-coding RNA is a functional RNA molecule that regulates mRNA synthesis at the transcriptional and post-transcriptional level. The non-coding RNAs are transcribed from DNA but not translated into proteins, including microRNAs (miRNA), small interfering RNAs (siRNA), and long non-coding RNAs (lncRNA). These non-coding RNAs are a new emerging target for investigation of their functional roles as well as their potential to be a biomarker, especially in cancer.

3.7.1. Long non-coding RNA (lncRNA)

lncRNAs are the main non-coding RNA transcripts that function in chromatin remodeling, transcriptional and post-transcriptional regulation, and as precursors for siRNAs. The performance of high throughput techniques to profile the transcriptomes of cancer cells compared with normal cells provided many potential lncRNAs that were associated with aggressive functions of cancer cells. The transcriptomic profiling of iCCA showed that EMP1-008, ATF3-008 and RCOR-013 were significantly down regulated in iCCA with metastasis, suggesting the tumor suppressor roles of these lncRNAs [52]. lncRNA H19, the first discovered lnRNA reported in diverse human cancers, was expressed in CCA cell lines and tissues [53]. The *in vitro* study indicated its roles in the proliferation, anti-apoptosis, EMT, migration and invasion of CCA cells. In addition, upregulation of lncRNA H19 in CCA tissues was correlated with tumor size, TNM staging, post-operative recurrence and OS of patients. Another lncRNA, PANDAR, was also highly expressed in CCA cell lines and tissues [54]. The *in vitro* study demonstrated their involvements in cell growth, anti-apoptosis and EMT of CCA cells. High expression of lncRNA-PANDRA in CCA tissues was associated with lymph node metastasis, TNM staging and post-operative recurrence as well as shorter OS of CCA patients. Hence, lncRNA H19 and PANDRA may serve as poor prognostic markers for CCA.

3.7.2. microRNAs (miRNAs)

MicroRNAs are small non-coding RNAs of 22–24 nucleotide-RNAs that regulate post-transcriptional gene expression. These miRNAs are often misregulated in disease states including cancer. With the high specificity, sensitivity, and stability of miRNAs in both body fluids and formalin fixed-paraffin embedded tissues, they provide a great potential for miRNAs as a new class of biomarkers in cancer [55]. Using a custom microarray, 158 differentially expressed miRNAs with a 30-miRNA signature for distinguishing iCCA was established [56]. The expression levels of 3-miRNAs, miR-675-5p, miR-652-3p and miR-338-3p, were strongly associated with the prognosis of iCCA patients and were determined by regression coefficients as risk scores. It was found that patients with high risk scores had significantly shorter OS and DFS medians than those with low risk scores. This 3-miRNA signature was marked as an independent prognostic predictor for iCCA.

The miRNA sequencing data indicated 64 differentially expressed miRNAs between CCA and normal biliary tissues. Among these, miR-122s that modulate the expression of the transcription factor FOXM1were under-expressed [57]. The cDNA microarray analysis revealed 4 times higher FOXM1 mRNA in CCA cells than normal bile duct cells [58]. Overexpression of FOXM1 in CCA tissues was confirmed by immunohistochemistry. It is well known that FOXM1 is involved in tumorigenesis and tumor invasion, and was suggested to be a target for immunotherapy against CCA as FOXM1 derived peptides could induce HLA-A2-restricted T cells. Upregulation of tissue miR-29a was also suggested to be a beneficial prognostic marker for CCA. A significant role of miR-29a either as a tumor promoter or suppressor was evidenced based on cancer types [59]. Using qRT-PCR, miR-29a was shown to be upregulated in CCA tissues and correlated with lymph node metastasis, clinical stage, and a short OS of the patients [60].

4. Serum biomarkers as prognostic-predictive markers of cholangiocarcinoma

An ideal prognostic marker is the biomolecule that has a dynamic expression according to the disease and in response to the treatment. Aside from being less invasive for sample collection, serum biomarkers are superior to the tissue biomarkers for the purpose of monitoring the recurrence of tumors or the patient outcome after treatment. To date, various biomolecules in the blood circulation are revealed as prognostic markers for CCA (Table 2).

4.1. Serum proteins

YKL-40 or chitinase-3-like 1 (ChI3L1), a 40 kDa glycoprotein secreted from monocytes, macropahges, neutrophils, chondrocytes and synovial cells were expressed in many cancer cell lines and related to cell survival, cell proliferation and tumor angiogenesis [61]. High levels of YKL-40 in sera of patients with several types of cancers were reported [62]. In CCA, YKL-40 promoted cell proliferation and migration, and high levels of YKL-40 could be detected in both CCA tissues and plasma [63]. The high expression of YKL-40 in stromal areas of CCA tissues was associated with non-papillary type CCA and shorter OS. Moreover, high levels of YKL-40 in plasma could discriminate CCA patients from healthy subjects and was related with short OS of CCA patients. Thus, YKL-40 could be a potential prognostic biomarker for CCA.

Table 2. Summary of potential serum biomarkers for prognostic predictions of cholangiocarcinoma.

Name	Associated biological function	Associated clinicopathological features	Associated prognostic values	Type of CCA[a] and number of cases	Geographical origin of CCA	Ref.
YKL-40	Proliferation, migration	Non-papillary type	OS	57	Thailand	[63]
Carbohydrate antigen-S27 (CA-S27)	Proliferation, adhesion, migration, invasion	ND	OS	96	Thailand	[64]
Periostin	ND	ND	OS	68	Thailand	[65,66]
C-reactive protein (CRP)	ND	TNM staging	DFS, OS	iCCA: 141 iCCA: 140	Japan China	[67,68]
Osteopontin	ND	Metastasis	OS	107	Germany	[69,70]
α1β-glycoprotein to afamin ratio	ND	Recurrence	OS	64	Thailand	[71]
Albumin to γ-glutamyltransferase	ND	TNM staging	DFS, OS	iCCA: 206	China	[72]
Aspartate aminotransferase to neutrophil	ND	ND	OS	iCCA: 184	China	[73]
lncRNA H19	Proliferation, anti-apoptosis, EMT, migration, invasion	Tumor size, TNM staging, post-operative recurrence	OS	56	China	[53]
lncRNA PANDAR	Growth, anti-apoptosis, EMT	LN metastasis, TNM staging, recurrence	OS	67	China	[54]
miR-29a	ND	Histological differentiation	OS	125	China	[60]
miR26a	ND	Clinical staging, metastasis, histological differentiation	OS	66	China	[74]
CA19-9	ND	Metastasis	OS	106, 1,264, 89, 2,816	Japan, Thailand, China, Japan, Germany, USA, Sweden, Italy, UK, Portugal, USA	[114] [115] [116] [117]

• The poor prognosis is associated with upregulation of those biomarkers, otherwise specified.
• Abbreviation; ND: not determined in this study, LN: lymph node, MVD: microvascular density, TNM: tumor-lymph node-metastasis staging, EMT: epithelial-mesenchymal transition, DFS: disease free survival, OS: overall survival
[a] Type of CCA as specified.

Alterations of glycan structures resulted from incomplete synthesis and neo-syntheses have been repeatedly reported in many cancer types. Carbohydrate antigen-S27 (CA-S27), a new Lewis-a associated modification on MUC5AC, was associated with proliferation, adhesion, migration and invasion of CCA cell lines [64]. CA-S27 was detected in serum at higher levels in sera from CCA patients than those from gastrointestinal malignancies, HCC, benign biliary diseases and healthy controls and hence, it was proposed to be a new diagnostic marker for CCA. Moreover, a high level of serum CA-S27 was significantly associated with shorter OS of CCA patients and the level of serum CA-S27 was dramatically reduced after tumor resection. Therefore, CA-S27 is not only a candidate for being a diagnostic marker for CCA but also is a promising prognostic marker to follow up the recurrence of CCA after surgical resection.

Currently, serum periostin (PN) was suggested to be an independent prognostic marker for iCCA with a hazard ratio of 3.197 [65]. PN is a secreted extracellular matrix protein identified in many cancer types. In iCCA, PN was expressed mainly in tumor stromal fibroblasts and high level of tissue PN expression was associated with poor OS of CCA patients [66]. C-reactive protein (CRP), an acute-phase protein of hepatic origin, was identified as an independent prognosis marker for iCCA [67]. A high level of preoperative serum CRP was associated with tumor staging of CCA patients [68] and was positively correlated with the level of other CCA prognosis-related markers such as CA19–9 and CEA. High levels of CRP in patients at stage I and II were associated with cancer specific survival while in those with stage III and IV were associated with DFS.

Serum osteopontin, a protein involved in many cellular biological processes, was recently reported to correlate with the expression observed in CCA tissues, both cancer and stromal cells [69]. Serum osteopontin was elevated in CCA patients compared with those in healthy controls and patients with PSC. Moreover, the pre- and post-operative levels of osteopontin were associated with poor prognosis of CCA patients. This observation identified serum osteopontin as a marker to estimate the chances of the patients to benefit from surgical resection. The specificity and variables of clinical parameters included in the study, however, were debated [70].

4.2. Ratio of two serum proteins as prognostic markers

It is well accepted that a combination of prognostic markers can improve the power of prognosis. Currently, the ratio of two serum proteins as biomarkers with high diagnostic and predictive powers was frequently reported in several cancer types. Using two-dimensional polyacrylamide gel electrophoresis, 36 proteins that could characterize CCA sera were identified [71]. In a comparison of serum proteomes from CCA patients and healthy controls, α1β-glycoprotein (A1BG) was found to be higher while afamin (AFM) was shown to be lower in sera from CCA patients. The pre-operative serum A1BG/AFM ratio could differentiate CCA patients with 84.4% sensitivity and 87.5% specificity. Moreover, the post-operative patients with a high A1BG/AFM ratio was associated with the infiltration of resection margins and had a significantly worse outcome. The albumin to γ-glutamyltransferase (AGR) [72] and aspartate aminotransferase to neutrophil ratio [73] were

proposed for their potential as a prognostic marker for CCA. γ–Glutamyltransferase, an enzyme expressed on the surface of epithelial cells of glands and ducts, is commonly used as an indicator for hepatobiliary disease and damaged bile ducts. While albumin is a protein synthesized by liver cells and higher serum albumin levels were suggested as a protective factor for cancer patients. AGR was significantly related with the TNM staging, OS and DFS of iCCA patients. AGR was superior to other inflammation based scores and other serological tumor markers in predicting overall survival and recurrence free survival in iCCA patients who underwent curative resection [72]. Additionally, the pre-operative ratio of aspartate aminotransferase to neutrophil was shown to correlate with poor survival of iCCA patients after hepatectomy [73]. It potentially predicted the survival of iCCA in various subgroups such as patients with negative hepatitis B surface antigen and those with a high preoperative level of CA19-9.

4.3. Serum miRNA

The detection of miRNA in circulation highlights the value of miRNAs as diagnostic and prognosis of several diseases including cancer. The level of miR-26a was higher in serum of CCA patients than in healthy controls [74]. The post-operative level of serum miR-26 was significantly reduced compared with the pre-operative serum. A high level of serum miR-26a also correlated with clinical staging, metastasis, histological differentiation, and shorter OS of CCA patients. The statistical analysis indicated miR-26a as an independent prognostic indicator of CCA patients. In contrast, the decreased level of miR-106a was correlated with a poor prognosis of CCA patients. A low level of miR-106a was related to lymph node metastasis and was adversely correlated with the OS of CCA patients. Determinations of miR-26a and miR-106a in the same set of CCA patients, however, have not been done.

5. Biomarkers of the favorable outcomes

Metastasis is a complex cellular process involving numerous signaling pathways, either stimulation of metastasis-promoting genes or inhibition of metastasis suppressor genes. Some biomarkers are correlated with the favorable outcome of CCA patients after treatments. These biomarkers frequently are tumor suppressor proteins or oncogene regulators. High expression levels of these molecules suggest a better OS of CCA patients and may be used as good prognostic markers for CCA.

Eyes absent homolog 4 (EYA4), a member of the EYA gene family, was markedly down regulated in several malignancies. EYA4 mRNA and proteins were remarkably lower in iCCA tumor tissues compared with adjacent non-tumorous tissues [75]. Down regulation of EYA4 was associated with the increase of tumor numbers, local invasion, lymph node metastasis, tumor differentiation and shorter DFS and shorter OS time in iCCA patients who underwent curative hepatectomy. The tumor suppressor function of EYA4 was confirmed *in vitro*. The AT-rich interactive domain 1A (ARID1A) protein, a frequented mutated gene found in CCA, is related to the regulation of proliferation, DNA repair, development, differentiation, and tumor suppression [76]. A systematic review and meta-analysis of ARID1A in cancers indicated the loss of ARID1A related to short survival and to recurrence of cancers. ARID1A was also suggested to be an important potential target for personalized medicine in cancer treatment [77]. Both mRNA and protein levels of ARID1A were lower in iCCA tissues compared with the adjacent paracarcinomatous tissues and normal liver [78]. The low expression of tissue ARID1A was associated with a number of tumor nodules, venous invasion, and tumor recurrence, as well as with shorter OS and DFS of CCA patients. It was suggested that ARID1A might play a role as a tumor suppressor gene and be a favorable prognostic maker in CCA.

An anti-metastatic function of metastasis suppressor 1 (MTSS1), an actin-binding protein, was reported in many human malignancies. The roles of MTSS1 in promoting growth or metastasis, however, were also reported in some cancer types [79]. MTSS1 was barely expressed in iCCA tissues and was associated with increased tumor size, lymph node metastasis and advanced staging, and was correlated significantly with tumor recurrence and poor patient outcome [80]. Over-expression of MSST1 inhibited the migration of CCA cells, *in vitro*. Collectively, absence of MTSS1 expression was suggested to be a useful biomarker in predicting tumor recurrence and prognosis of iCCA.

Secreted frizzled-related proteins (SFRPs) are wnt-antagonists. It was proposed to function as a tumor suppressor as its expression was frequently absent in cancer. Roles of SFRPs in promoting tumor growth, however, were also evident [81]. SFRP1 expression was significantly associated with a better prognosis for CCA patients [82]. Patients with low or negative SFRP1 expression in CCA tissues had poor prognosis or poor DFS. Thus, SFRP1 was suggested to be a candidate for the favorable prognosis of iCCA patients.

It is well known that the immune system modulates growth and progression of tumors. An effective immune response leading to recognition of tumor cells may result in their eradication. The activating receptor natural killer cell lectin-like receptor gene 2D (NKG2D) is a stimulatory immune receptor that is expressed on natural killer (NK) cells, T cells and $CD8^+$ T cells. Binding of NKG2D ligands to the NKG2D receptors on NK and T cells can stimulate an immune response against cells expressing these ligands. Several studies suggest a key role of NKG2D in tumor progression, however, some studies oppose this suggestion [83,84]. There is a limited report on the NKG2D ligand in CCA. NKG2D ligands including MHC class I chain-related proteins A and B (MICA/B), unique long 16 binding protein (ULBP)-1 and ULBP2/5/6 were associated with a better prognosis of eCCA patients [85]. The high expression of MICA/B and ULBP2/5/6 correlated with improved both OS and DFS of patients. In contrast, the high expression of ULBP1 was associated with the improved OS but not DFS. The expression of NKG2D ligands thus reflect the good outcome of CCA patients and may be a prognostic factor for favorable eCCA treatment.

6. Peripheral blood: the alternative way and a new hope

Many studies showed that the stromal cells, that is, tumor associated macrophage (TAM) and cancer associated fibroblast (CAF), supported the growth and the progression of CCA. A high

density of M2-TAM in CCA tissues was associated with the metastatic status of CCA patients [86] and with the recurrence of the disease after resection [87]. The DFS and OS were accordingly shorter in CCA patients with high TAM infiltration. Thus, TAMs and perhaps other white blood cells in the tumor microenvironment might be an indirect indicator for aggressiveness of CCA. Furthermore, it was evident that the level of circulating $CD14^{+}CD16^{+}$ monocytes of CCA patients was correlated with the level of TAM infiltration in tumor tissues and with the poorly differentiated type of CCA [88]. The expression profile of selected genes of peripheral blood leukocytes could be integrated into a prognostic index that significantly correlated with the survival time of CCA patients [89].

In the past decade, the neutrophil-to-lymphocyte ratios (NLR) were used to assess the inflammatory response in many diseases. The prognostic role of NLR has been documented in many cancers including CCA [90,91]. NLR is easy to measure, reproducible, and inexpensive, thus, it could potentially be a simple and inexpensive test for cancer prognosis. A number of reports indicated a high NLR as a poor prognostic predictive marker for CCA in a variety of settings. The NLR ≥ 3 was correlated with lymph node metastasis, poor anti-tumor immunity and shorter DFS and OS in iCCA patients after neoadjuvant chemotherapy and resection [92]. The NLR >5 was reported to reflect the poor chemotherapeutic response and short survival of advanced CCA patients who received palliative treatments [93]. The meta-analysis of 9 studies on NLR in CCA patients showed that higher NLRs had a shorter survival time in surgical, non-surgical and mixed groups [94]. The synthesized hazard ratio of 1.449 (95% CI: 1.296–1.619, $p < 0.001$) was reported to indicate the association of a high NLR with an unfavorable OS. Taken together, it is evident that an elevated pre-operative NLR could reflect predictable poor survival in CCA patients.

7. Biomarkers of therapeutic responsiveness for CCA

Drug resistance is the main problem for cancer treatment in both chemotherapy and targeted therapies. Many underlying mechanisms, for example, drug efflux, DNA damage repair, activation of pro-survival pathways, and ineffective induction of cell death were reported [95,96]. The specific molecules involving drug resistance in cancer could probably identify patients who are good or poor responders and suggest specialty clinicians for an appropriate and effective treatment for an individual patient. This is not only beneficial for a cost-effective outcome but also avoids the unfavorable adverse effect of those who had a little advantage from the cytotoxic drugs.

Impaired drug uptake is one of the important mechanisms for the chemoresistance demonstrated in CCA. The decreased expression of organic cation transporter (OCT) 1, a key molecule to uptake sorafinib in HCC and CCA, caused the resistance to this drug in CCA patients [97]. High expression of the ATP-binding cassette (ABC) superfamily increased the efflux pump of various anticancer drugs resulting in chemo-resistance in many cancers including CCA [98]. The *in vitro* studies revealed several over-expressed molecules associated with the chemo-resistance in CCA cells. The expression of multidrug Resistance Protein 1 (MDR1) was associated with a low sensitivity to 5-fluorouracil (5-FU) of CCA cells, while that of Multidrug Resistance-Associated Protein 1 (MRP1) was associated with the resistance to gemcitabine, one of the standard cytotoxic drugs for CCA [99]. Thymosin-β10 (Tβ10), a molecule involving cell motility, was over-expressed in CCA tissues [100]. 5-FU resistant CCA cells had extremely high expressions of Tβ10 and ABC proteins [101]. Silencing of Tβ10 expression significantly reduced expression of ABC proteins and increased sensitivity to 5-FU. Hence, the expression of Tβ10 was proposed to be a predictive biomarker for 5-FU resistance in CCA. The upregulation of anti-apoptotic protein Bcl-2 and down-regulation of pro-apoptotic protein bax have also been reported in 5-FU and cisplatin resistance CCA cells [102]. In addition, the mutation of a p53 isoform, Δ133p53, in CCA patients treated with 5-FU showed a poor survival outcome [103].

The molecules associated with apoptosis resistance might also reflect the chemo-resistance of cancer cells. The EMT process involved the changes of tumor suppressor genes and oncogenes, which then promoted chemo-resistance of CCA cells were reported [104]. Recently, the oncogenic role of Lipocalin-2 (LCN2), a secreted protein involved in the transport of some hydrophobic substances, has been demonstrated in several malignancies. Suppression of LCN2 expression inhibited CCA cell growth by repression of EMT [105]. These effects were due to the negative regulation of LCN2 on tumor suppressor genes, N-myc downstream regulated gene 1 (NDRG1) and NDRG2. LCN2 concentration in bile was high in patients with CCA and was associated with worse survival in CCA patients [106]. Thus, LCN2 may be a potential diagnostic/prognostic marker for CCA. Presently, immunotherapy has an emerging role in many cancers including CCA. The biomarkers that reflect the response to immunotherapy are also of interest to identify a person who is the candidate for this therapeutic strategy. One of the most studied biomarkers is Programmed-death-1 (PD-1) and its major ligand, Programmed-death Ligand 1 (PD-L1). Clinical trials using monoclonal antibodies targeting these molecules showed promising results in various hematologic and solid cancers [107]. For CCA, PDL1 was expressed in 9–72% in CCA cells and 46–63% in stromal immune cells [108,109]. These suggested that a subgroup of CCA patients PDL1 positive may be a candidate for immune checkpoint inhibitor monotherapy such as prembolizumab. The clinical trials of this agent have been registered and carried on in various kinds of cancers including CCA [110].

8. CA19-9 as prognostic biomarker: old wine in a new bottle

CA19-9, a well-known suggestive serum marker for biliary tract disease, has been used as a single marker or in combination with other markers for diagnosis of biliary tract malignancy for a long time. The specificity of this marker, however, is quite low since its level could be increased in many physiological conditions including the benign biliary tract diseases. This may limit the utility of serum CA19-9 as diagnostic marker for CCA. At present, there are several novel biomarkers with potential diagnostic value reported [reviewed in 30, 111, 112].

The implication of CA19-9 as a prognostic biomarker has drawn attention from researchers and clinicians since its level is usually reduced after surgical resection. In resectable CCA patients, the pre- and post-operative serum CA19-9 levels were significantly correlated with the OS of CCA patients

[113]. Pre-operative CA19-9 (≥ 200 IU/ml) and post-operative CA19-9 (≥ 37 IU/mL) were identified as independent predictors of poor OS in CCA patients. A systematic review and meta-analysis of 2,816 iCCA patients, most of whom were non-resectable, showed that an elevated serum CA19-9 was significantly associated with lymph node metastasis and decreased stage-specific survival. In addition, patients with high pre-operative CA19-9 had decreased long-term survival [114]. This agreed with the report that CA-19-9 ≥ 103 IU/L was correlated with metastasis and short OS of CCA patients [115]. A national cohort analysis of 2,816 iCCA patients in USA [116] revealed that 66.7% had elevated CA19-9 levels with decreased long-term survival. Thus, elevation of CA19-9 was proposed to be an independent predictor for a higher risk of mortality similar to node-positivity, positive-margin resection, and non-chemotherapy treatment and as advice to using the levels of pre- and post-operative serum CA19-9 for predicting patient outcomes.

9. Conclusion

Many attempts have been tried to identify the factors that could predict the prognosis in terms of overall survival time, disease-free survival, recurrent rate, and responsiveness to chemotherapy. A number of biological markers with different characteristics that were associated with cell signaling, aggressiveness, metastasis, cell survival, and drug resistance of CCA were proposed as prognostic markers for CCA. These markers could be cell surface molecules, receptors, signaling molecules, lncRNAs, miRNAs, and immune cells that were identified in tumor tissues, tumor stromal and microenvironment, and sera that reflected the outcome of patients (Figure 1).

10. Expert commentary and five-year view

In a recent decade, various biomolecules were discovered and investigated for their potentials to be prognostic markers of CCA. Many of them hold a promising potential for use in clinical practice. Many studies showed a significant correlation with a therapeutic outcome or survival of CCA patients of cohorts but in specific settings, limited sample sizes, and study designs. Recognizing these concerns, one should consider these results with caution and in detail before translating to clinical practice. Firstly, most of the reports were from a tertiary and single center. Secondly, CCAs are heterogeneous tumors, not only in regards to different locations and histopathological subtypes but also with different genetic influences. Therefore, the potential markers should be validated in larger collectives including patients with varied epidemiological backgrounds.

To date, the high-throughput and large-scale analytical technologies i.e. genomics, transcriptomics, proteomics and metabolomics, allow researchers to identify a significant number of potential markers that can be used for diagnosis, prognosis, or prediction of treatment response. A quality assessment is the next required step and urgently needed. As the sensitivity and specificity of the markers relied on the detection technique and the cohort of study, defining subgroups of CCA patients with appropriate clinical data and precise sample collection are important. Nonetheless, the non- or low-invasive methods of sample collection, as well as the simple and affordable determination methods should be taken into account for making a prognostic biomarker available in clinical practice.

Apart from the search for novel molecules, the trend of study in the next 5 years should focus on the implications of the discovered molecules that have been reported. A systematic review and meta-analysis should be conducted to clarify the impact of potential biomolecules as prognostic markers for CCA. Moreover, analysis of using a combination of different potential markers instead of single marker to predict patient outcomes is suggested. Besides, development of a test kit with a panel of markers for predicting prognosis and treatment response must be seriously evaluated prior to launch into the routine clinical application. For the highest benefit to

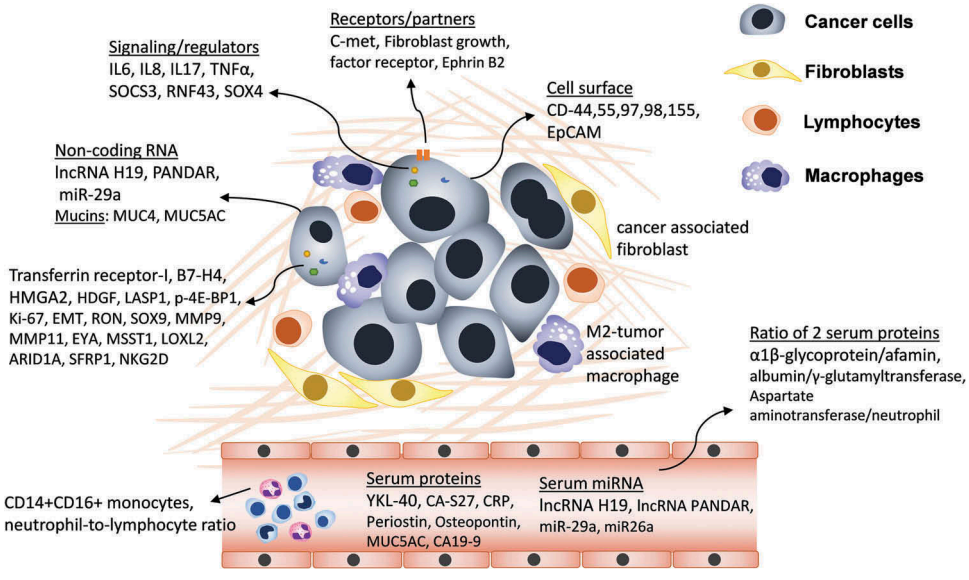

Figure 1. Prognostic predictive markers for CCA. Several biomolecules have been identified in tumor tissues, tumor stromal and microenvironment, and sera that reflected the outcome of patients. These markers could be cell surface molecules, receptors, signaling molecules, lncRNAs, miRNAs, and immune cells.

CCA patients, multidisciplinary collaboration is needed to achieve these goals.

Key issues

- Cholangiocarcinoma (CCA) is a complex malignancy of bile duct epithelia, anatomically classified into three types: intrahepatic, perihilar, and distal CCA. Considered as a rare cancer, the incidence of CCA, however, is increasing globally.
- The strong risk factor in western countries is primary sclerosing cholangitis whereas in Southeast Asia and East Asia it is liver fluke infection. Regarding the different etiologies, CCA developed in patients from different geographical areas exhibited different genetic backgrounds.
- Only one third of CCA patients can achieve surgical resection and the alternative treatments, for example, chemo- or targeted gene therapies might be offered for those whose malignancies are unresectable.
- Not all CCA patients benefit from chemotherapy because CCA has high recurrence rate and high chemo-resistance. Hence, prognostic markers for surveillance of tumor recurrence and those that suggest the best treatment option are necessary for a cost-beneficial and effective treatment.
- In a past decade, many potential molecules in tumor tissues and sera; membrane receptors, signaling proteins, mucins, and non-coding RNAs, as well as peripheral blood cells were reported for the possibility to be prognostic markers for CCA.
- The available biomarker, CA19-9, used as a diagnostic marker for CCA should be re-evaluated for its purpose of prognosis prediction. The application of this marker may be a shortcut for time and budget considerations for biomarker development. The limitation of its low specificity has to be of concern.
- The direction of research in the next 5 years should be focused on the translation of the reported biomarkers for clinical practice. Systematic and meta-analysis of previously reported biomarkers, validation of the markers in a larger and generalized cohort, as well as selection of a panel or combination of potential biomarkers will clarify the impact of these prognostic markers for CCA.

Acknowledgments

We would like to acknowledge Prof. James A. Will of the University of Wisconsin for editing of the manuscript via the Faculty of Medicine Publication Clinic, Khon Kaen University, Thailand; and Dr. C. Phoomak, Department of Biochemistry, Faculty of Medicine, Khon Kaen University, for creating the figure of this presentation.

Funding

This work is supported by The Thailand Research Fund [DBG5980004].

Declaration of interest

The authors have no other relevant affiliations or financial involvement with any organization or entity with a financial interest in or financial conflict with the subject matter or materials discussed in the manuscript apart from those disclosed. Peer reviewers on this manuscript have no relevant financial or other relationships to disclose.

References

Papers of special note have been highlighted as either of interest (•) or of considerable interest (••) to readers.

1. Shaib Y, El-Serag HB. The epidemiology of cholangiocarcinoma. Semin Liver Dis. 2004 May;24(2):115–125. PubMed PMID: 15192785
2. Rizvi S, Khan SA, Hallemeier CL, et al. Cholangiocarcinoma - evolving concepts and therapeutic strategies. Nat Rev Clin Oncol. 2017 Oct 10. DOI:10.1038/nrclinonc.2017.157 [PubMed PMID: 28994423].
3. Sripa B, Pairojkul C. Cholangiocarcinoma: lessons from Thailand. Curr Opin Gastroenterol. 2008 May;24(3):349–356. PubMed PMID: 18408464
4. Banales JM, Cardinale V, Carpino G, et al. Expert consensus document: cholangiocarcinoma: current knowledge and future perspectives consensus statement from the European Network for the Study of Cholangiocarcinoma (ENS-CCA). Nat Rev Gastroenterol Hepatol. 2016 May;13(5):261–280. PubMed PMID: 27095655.
5. Nakeeb A, Pitt HA, Sohn TA, et al. Cholangiocarcinoma. A spectrum of intrahepatic, perihilar, and distal tumors. Ann Surg. 1996 Oct;2244:463–473. discussion 473-5. PubMed PMID: 8857851
6. Jinawath N, Chamgramol Y, Furukawa Y, et al. Comparison of gene expression profiles between Opisthorchis viverrini and non-Opisthorchis viverrini associated human intrahepatic cholangiocarcinoma. Hepatology. 2006 Oct;44(4):1025–1038. PubMed PMID: 17006947.
7. Chan-On W, Nairismagi ML, Ong CK, et al. Exome sequencing identifies distinct mutational patterns in liver fluke-related and non-infection-related bile duct cancers. Nat Genet. 2013 Dec;45 (12):1474–1478. PubMed PMID: 24185513.
8. Ong CK, Subimerb C, Pairojkul C, et al. Exome sequencing of liver fluke-associated cholangiocarcinoma. Nat Genet. 2012 May 06;44 (6):690–693. PubMed PMID: 22561520.
9. Jarnagin WR, Fong Y, DeMatteo RP, et al. Staging, resectability, and outcome in 225 patients with hilar cholangiocarcinoma. Ann Surg. 2001 Oct;2344:507–517. discussion 517-9. PubMed PMID: 11573044
10. Kiefer MV, Albert M, McNally M, et al. Chemoembolization of intrahepatic cholangiocarcinoma with cisplatinum, doxorubicin, mitomycin C, ethiodol, and polyvinyl alcohol: a 2-center study. Cancer. 2011 Apr 01;117(7):1498–1505. PubMed PMID: 21425151.
11. Vogl TJ, Naguib NN, Nour-Eldin NE, et al. Transarterial chemoembolization in the treatment of patients with unresectable cholangiocarcinoma: results and prognostic factors governing treatment success. Int J Cancer. 2012 Aug 01;131(3):733–740. PubMed PMID: 21976289.
12. Valle J, Wasan H, Palmer DH, et al. Cisplatin plus gemcitabine versus gemcitabine for biliary tract cancer. N Engl J Med. 2010 Apr 08;362(14):1273–1281. PubMed PMID: 20375404.
13. Bang YJ, Doi T, Braud FD, et al. 525 Safety and efficacy of pembrolizumab (MK-3475) in patients (pts) with advanced biliary tract cancer: interim results of KEYNOTE-028. Eur J Cancer. 2015; 51. S112. DOI:10.1016/S0959-8049(16)30326-4
14. Huang DW, Huang M, Lin XS, et al. CD155 expression and its correlation with clinicopathologic characteristics, angiogenesis, and prognosis in human cholangiocarcinoma. Onco Targets Ther. 2017;10:3817–3825. . PubMed PMID: 28814880.
15. Kunlabut K, Vaeteewoottacharn K, Wongkham C, et al. Aberrant expression of CD44 in bile duct cancer correlates with poor prognosis. Asian Pac J Cancer Prev. 2012;13(Suppl):95–99. PubMed PMID: 23480770.
16. Thanee M, Loilome W, Techasen A, et al. CD44 variant-dependent redox status regulation in liver fluke-associated cholangiocarcinoma: a target for cholangiocarcinoma treatment. Cancer Sci. 2016 Jul;107(7):991–1000. PubMed PMID: 27176078.
17. Kaira K, Sunose Y, Oriuchi N, et al. CD98 is a promising prognostic biomarker in biliary tract cancer. Hepatobiliary Pancreat Dis Int. 2014 Dec;13(6):654–657. PubMed PMID: 25475870.

18. Meng ZW, Liu MC, Hong HJ, et al. Expression and prognostic value of soluble CD97 and its ligand CD55 in intrahepatic cholangiocarcinoma. Tumour Biol. 2017 Mar;39(3). PubMed PMID: 28345461. DOI:10.1177/1010428317694319
19. Mao ZY, Zhu GQ, Ren L, et al. Prognostic value of C-met expression in cholangiocarcinoma. Technol Cancer Res Treat. 2016 Apr;15 (2):227–233. PubMed PMID: 25873560.
20. Xu YF, Yang XQ, Lu XF, et al. Fibroblast growth factor receptor 4 promotes progression and correlates to poor prognosis in cholangiocarcinoma. Biochem Biophys Res Commun. 2014 Mar 28;446 (1):54–60. PubMed PMID: 24565842.
21. Khansaard W, Techasen A, Namwat N, et al. Increased EphB2 expression predicts cholangiocarcinoma metastasis. Tumour Biol. 2014 Oct;35(10):10031–10041. PubMed PMID: 25012246.
22. Zarogoulidis P, Yarmus L, Darwiche K, et al. Interleukin-6 cytokine: a multifunctional glycoprotein for cancer. Immunome Res. 2013 Aug 12;9(62):16535. PubMed PMID: 24078831.
23. Asukai K, Kawamoto K, Eguchi H, et al. Prognostic impact of peritumoral IL-17-positive cells and IL-17 axis in patients with intrahepatic cholangiocarcinoma. Ann Surg Oncol. 2015 Dec;22(Suppl 3): S1524–S1531. PubMed PMID: 26228109.
24. Wang Y, Wan M, Zhou Q, et al. The prognostic role of SOCS3 and A20 in human cholangiocarcinoma. PLoS One. 2015;10(10): e0141165. .PubMed PMID: 26485275.
25. Niu L, Qin HZ, Xi HQ, et al. RNF43 inhibits cancer cell proliferation and could be a potential prognostic factor for human gastric carcinoma. Cell Physiol Biochem. 2015;36(5):1835–1846. .PubMed PMID: 26184844.
26. Talabnin C, Janthavon P, Thongsom S, et al. Ring finger protein 43 expression is associated with genetic alteration status and poor prognosis among patients with intrahepatic cholangiocarcinoma. Hum Pathol. 2016 Jun;52:47–54. PubMed PMID: 26980022
27. Tiwari N, Tiwari VK, Waldmeier L, et al. Sox4 is a master regulator of epithelial-mesenchymal transition by controlling Ezh2 expression and epigenetic reprogramming. Cancer Cell. 2013 Jun 10;23 (6):768–783. . PubMed PMID: 23764001.
28. Chen J, Ju HL, Yuan XY, et al. SOX4 is a potential prognostic factor in human cancers: a systematic review and meta-analysis. Clin Transl Oncol. 2016 Jan;18(1):65–72. PubMed PMID: 26250764.
29. Wang W, Zhang J, Zhan X, et al. SOX4 is associated with poor prognosis in cholangiocarcinoma. Biochem Biophys Res Commun. 2014 Sep 26;452(3):614–621. PubMed PMID: 25181339.
30. Rahnemai-Azar AA, Weisbrod A, Dillhoff M, et al. Intrahepatic cholangiocarcinoma: molecular markers for diagnosis and prognosis. Surg Oncol. 2017 Jun;26(2):125–137. PubMed PMID: 28577718.
31. Boonla C, Sripa B, Thuwajit P, et al. MUC1 and MUC5AC mucin expression in liver fluke-associated intrahepatic cholangiocarcinoma. World J Gastroenterol. 2005 Aug 28;11(32):4939–4946. PubMed PMID: 16124042.
32. Boonla C, Wongkham S, Sheehan JK, et al. Prognostic value of serum MUC5AC mucin in patients with cholangiocarcinoma. Cancer. 2003 Oct 01;98(7):1438–1443. PubMed PMID: 14508831.
    - ***This article showed for the first time that serum MUC5AC was associated with tumor burden and could be a prognostic-predictor of poor patient outcome.***
33. Abe T, Amano H, Shimamoto F, et al. Prognostic evaluation of mucin-5AC expression in intrahepatic cholangiocarcinoma, mass-forming type, following hepatectomy. Eur J Surg Oncol. 2015 Nov;41(11):1515–1521. PubMed PMID: 26210654.
34. Li B, Tang H, Zhang A, et al. Prognostic role of mucin antigen MUC4 for Cholangiocarcinoma: a meta-analysis. PLoS One. 2016;11(6): e0157878. .PubMed PMID: 27305093.
35. Sulpice L, Rayar M, Turlin B, et al. Epithelial cell adhesion molecule is a prognosis marker for intrahepatic cholangiocarcinoma. J Surg Res. 2014 Nov;192(1):117–123. PubMed PMID: 24909871.
36. Bergeat D, Fautrel A, Turlin B, et al. Impact of stroma LOXL2 overexpression on the prognosis of intrahepatic cholangiocarcinoma. J Surg Res. 2016 Jun 15;203(2):441–450. PubMed PMID: 27363654.
37. Jamnongkan W, Thanan R, Techasen A, et al. Upregulation of transferrin receptor-1 induces cholangiocarcinoma progression via induction of labile iron pool. Tumour Biol. 2017 Jul;39(7). PubMed PMID: 28671021. DOI:10.1177/1010428317717655
38. Morishita A, Zaidi MR, Mitoro A, et al. HMGA2 is a driver of tumor metastasis. Cancer Res. 2013 Jul 15;73(14):4289–4299. PubMed PMID: 23722545.
39. Lee CT, Wu TT, Lohse CM, et al. High-mobility group AT-hook 2: an independent marker of poor prognosis in intrahepatic cholangiocarcinoma. Hum Pathol. 2014 Nov;45(11):2334–2340. PubMed PMID: 25245603.
40. Traenka C, Remke M, Korshunov A, et al. Role of LIM and SH3 protein 1 (LASP1) in the metastatic dissemination of medulloblastoma. Cancer Res. 2010 Oct 15;70(20):8003–8014. PubMed PMID: 20924110.
41. Zhang H, Li Z, Chu B, et al. Upregulated LASP-1 correlates with a malignant phenotype and its potential therapeutic role in human cholangiocarcinoma. Tumour Biol. 2016 Jun;37(6):8305–8315. PubMed PMID: 26729195.
42. Zhao X, Guo F, Li Z, et al. Aberrant expression of B7-H4 correlates with poor prognosis and suppresses tumor-infiltration of CD8+ T lymphocytes in human cholangiocarcinoma. Oncol Rep. 2016 Jul;36 (1):419–427. PubMed PMID: 27177355.
43. Guo S, Liu HD, Liu YF, et al. Hepatoma-derived growth factor: a novel prognostic biomarker in intrahepatic cholangiocarcinoma. Tumour Biol. 2015 Jan;36(1):353–364. PubMed PMID: 25262276.
44. Qin X, Jiang B, Zhang Y. 4E-BP1, a multifactor regulated multifunctional protein. Cell Cycle. 2016;15(6):781–786. PubMed PMID: 26901143
45. Fang Z, Lu L, Tian Z, et al. Overexpression of phosphorylated 4E-binding protein 1 predicts lymph node metastasis and poor prognosis of Chinese patients with hilar cholangiocarcinoma. Med Oncol. 2014 May;31(5):940. PubMed PMID: 24706262.
46. Zhao W, Zhang B, Guo X, et al. Expression of Ki-67, Bax and p73 in patients with hilar cholangiocarcinoma. Cancer Biomark. 2014;14 (4):197–202. .PubMed PMID: 24934361.
47. Watanabe H, Yokoyama Y, Kokuryo T, et al. Prognostic value of hepatocyte growth factor receptor expression in patients with perihilar cholangiocarcinoma. Ann Surg Oncol. 2015 Jul;22 (7):2235–2242. PubMed PMID: 25586241.
48. Matsushima H, Kuroki T, Kitasato A, et al. Sox9 expression in carcinogenesis and its clinical significance in intrahepatic cholangiocarcinoma. Dig Liver Dis. 2015 Dec;47(12):1067–1075. PubMed PMID: 26341967.
49. Tongtawee T, Kaewpitoon SJ, Loyd R, et al. high expression of matrix metalloproteinase-11 indicates poor prognosis in human cholangiocarcinoma. Asian Pac J Cancer Prev. 2015;16(9):3697–3701. PubMed PMID: 25987024.
50. Sun Q, Zhao C, Xia L, et al. High expression of matrix metalloproteinase-9 indicates poor prognosis in human hilar cholangiocarcinoma. Int J Clin Exp Pathol. 2014;7(9):6157–6164. PubMed PMID: 25337264.
51. Sun Q, Li F, Sun F, et al. Interleukin-8 is a prognostic indicator in human hilar cholangiocarcinoma. Int J Clin Exp Pathol. 2015;8 (7):8376–8384. PubMed PMID: 26339407.
52. Lv L, Wei M, Lin P, et al. Integrated mRNA and lncRNA expression profiling for exploring metastatic biomarkers of human intrahepatic cholangiocarcinoma. Am J Cancer Res. 2017;7(3):688–699. PubMed PMID: 28401021.
53. Xu Y, Wang Z, Jiang X, et al. Overexpression of long noncoding RNA H19 indicates a poor prognosis for cholangiocarcinoma and promotes cell migration and invasion by affecting epithelial-mesenchymal transition. Biomed Pharmacother. 2017 Aug;92:17–23. PubMed PMID: 28528181
54. Xu Y, Jiang X, Cui Y. Upregulated long noncoding RNA PANDAR predicts an unfavorable prognosis and promotes tumorigenesis in cholangiocarcinoma. Onco Targets Ther. 2017;10:2873–2883. . PubMed PMID: 28652769.
55. Lan H, Lu H, Wang X, et al. MicroRNAs as potential biomarkers in cancer: opportunities and challenges. Biomed Res Int. 2015;2015:125094. . PubMed PMID: 25874201.
56. Zhang MY, Li SH, Huang GL, et al. Identification of a novel microRNA signature associated with intrahepatic cholangiocarcinoma (ICC) patient prognosis. BMC Cancer. 2015 Feb;18(15):64. PubMed PMID: 25880914.

57. Severino FE, Hashimoto CN, Rodringues MA, et al. Integrative analysis of transcriptome and microRNome profiles in cholangiocarcinoma. J Can Sci Ther. 2017 Aug;9(8):580–588.
58. Yokomine K, Senju S, Nakatsura T, et al. The forkhead box M1 transcription factor as a candidate of target for anti-cancer immunotherapy. Int J Cancer. 2010 May 1;126(9):2153–2163. PubMed PMID: 19688828.
59. Jiang H, Zhang G, Wu JH, et al. Diverse roles of miR-29 in cancer (review). Oncol Rep. 2014 Apr;31(4):1509–1516. PubMed PMID: 24573597.
60. Deng Y, Chen Y. Increased Expression of miR-29a and Its Prognostic Significance in Patients with Cholangiocarcinoma. Oncol Res Treat. 2017;40(3):128–132. PubMed PMID: 28118648
61. Thom I, Andritzky B, Schuch G, et al. Elevated pretreatment serum concentration of YKL-40-an independent prognostic biomarker for poor survival in patients with metastatic nonsmall cell lung cancer. Cancer. 2010 Sep 1;116(17):4114–4121. PubMed PMID: 20564116.
62. Francescone RA, Scully S, Faibish M, et al. Role of YKL-40 in the angiogenesis, radioresistance, and progression of glioblastoma. J Biol Chem. 2011 Apr 29;286(17):15332–15343. PubMed PMID: 21385870.
63. Thongsom S, Chaocharoen W, Silsirivanit A, et al. YKL-40/chitinase-3-like protein 1 is associated with poor prognosis and promotes cell growth and migration of cholangiocarcinoma. Tumour Biol. 2016 Jul;37(7):9451–9463. PubMed PMID: 26781979.
64. Silsirivanit A, Araki N, Wongkham C, et al. CA-S27: a novel Lewis a associated carbohydrate epitope is diagnostic and prognostic for cholangiocarcinoma. Cancer Sci. 2013 Oct;104(10):1278–1284. . PubMed PMID: 23809433.
- ***This article showed that CA-S27 a glycosylated modification of MUC5AC detected in CCA serum had high potential for diagnostic and prognostic purposes for CCA. Serum levels of CA-S27 were correlated with the size of tumor and was a good predictor of CCA recurrence.***
65. Thuwajit C, Thuwajit P, Jamjantra P, et al. Clustering of patients with intrahepatic cholangiocarcinoma based on serum periostin may be predictive of prognosis. Oncol Lett. 2017 Jul;14(1):623–634. PubMed PMID: 28693214.
66. Utispan K, Thuwajit P, Abiko Y, et al. Gene expression profiling of cholangiocarcinoma-derived fibroblast reveals alterations related to tumor progression and indicates periostin as a poor prognostic marker. Mol Cancer. 2010 Jan;24(9):13. PubMed PMID: 20096135.
67. Yoh T, Seo S, Hatano E, et al. A novel biomarker-based preoperative prognostic grading system for predicting survival after surgery for intrahepatic cholangiocarcinoma. Ann Surg Oncol. 2017 May;24(5):1351–1357. PubMed PMID: 28108828.
68. Lin ZY, Liang ZX, Zhuang PL, et al. Intrahepatic cholangiocarcinoma prognostic determination using pre-operative serum C-reactive protein levels. BMC Cancer. 2016 Oct 12;16(1):792. PubMed PMID: 27733196.
69. Loosen SH, Roderburg C, Kauertz KL, et al. Elevated levels of circulating osteopontin are associated with a poor survival after resection of cholangiocarcinoma. . J Hepatol. 2017 Oct;67(4):749–757. . PubMed PMID: 268580.
- ***This recently published article pointed out that serum perostin may be used to subclassify CCA patients who may benefit from surgical resection, and to predict the long-term postoperative outcomes.***
70. Wu H, Zhang H, Hu L-Y, et al. Is osteopontin a promising prognostic biomarker for cholangiocarcinoma? J Hepatol. 2017. DOI:10.1016/j.jhep.2017.08.029
71. Tolek A, Wongkham C, Proungvitaya S, et al. Serum alpha1beta-glycoprotein and afamin ratio as potential diagnostic and prognostic markers in cholangiocarcinoma. Exp Biol Med (Maywood). 2012 Oct;237(10):1142–1149. . PubMed PMID: 23104505.
- ***This article suggested a combintion of a serum protein ratio, A1BG/AFM, as a high sensitivity and specificity diagnostic markers for CCA. The markers reflected the tumor burden and could be a promising prognostic marker to monitor post-operative patients.***
72. Jing CY, Fu YP, Shen HJ, et al. Albumin to gamma-glutamyltransferase ratio as a prognostic indicator in intrahepatic cholangiocarcinoma after curative resection. Oncotarget. 2017 Feb 21;8(8):13293–13303. PubMed PMID: 28076328.
73. Liu L, Wang W, Zhang Y, et al. Declined preoperative aspartate aminotransferase to neutrophil ratio index predicts poor prognosis in patients with intrahepatic cholangiocarcinoma after hepatectomy. Cancer Res Treat. 2017 Jun 01. DOI:10.4143/crt.2017.106 [PubMed PMID: 28602056].
74. Wang LJ, Zhang KL, Zhang N, et al. Serum miR-26a as a diagnostic and prognostic biomarker in cholangiocarcinoma. Oncotarget. 2015 Jul 30;6(21):18631–18640. PubMed PMID: 26087181.
75. Hao XY, Cai JP, Liu X, et al. EYA4 gene functions as a prognostic marker and inhibits the growth of intrahepatic cholangiocarcinoma. Chin J Cancer. 2016 Jul 28;35(1):70. PubMed PMID: 27469137.
76. Ho L, Crabtree GR. Chromatin remodelling during development. Nature. 2010 Jan 28;463(7280):474–484. PubMed PMID: 20110991.
77. Luchini C, Veronese N, Solmi M, et al. Prognostic role and implications of mutation status of tumor suppressor gene ARID1A in cancer: a systematic review and meta-analysis. Oncotarget. 2015 Nov 17;6(36):39088–39097. PubMed PMID: 26384299.
78. Yang SZ, Wang AQ, Du J, et al. Low expression of ARID1A correlates with poor prognosis in intrahepatic cholangiocarcinoma. World J Gastroenterol. 2016 Jul 07;22(25):5814–5821. PubMed PMID: 27433094.
79. Xie F, Ye L, Ta M, et al. MTSS1: a multifunctional protein and its role in cancer invasion and metastasis. Front Biosci (Schol Ed). 2011 1; Jan(3):621–631. PubMed PMID: 21196400.
80. Shi W, Hasimu G, Wang Y, et al. MTSS1 is an independent prognostic biomarker for survival in intrahepatic cholangiocarcinoma patients. Am J Transl Res. 2015;7(10):1974–1983. PubMed PMID: 26692940.
81. Vincent KM, Postovit LM. A pan-cancer analysis of secreted Frizzled-related proteins: re-examining their proposed tumour suppressive function. Sci Rep. 2017 Feb 20;7:42719. PubMed PMID: 28218291.
82. Davaadorj M, Saito Y, Morine Y, et al. Loss of Secreted frizzled-related protein-1 expression is associated with poor prognosis in intrahepatic cholangiocarcinoma. Eur J Surg Oncol. 2017 Feb;43(2):344–350. PubMed PMID: 28062160.
83. de Kruijf EM, Sajet A, VAn Nes JG, et al. NKG2D ligand tumor expression and association with clinical outcome in early breast cancer patients: an observational study. BMC Cancer. 2012 Jan;18(12):24. PubMed PMID: 22257486.
84. Zhang J, Basher F, Wu JD. NKG2D ligands in tumor immunity: two sides of a coin. Front Immunol. 2015;6:97. .PubMed PMID: 25788898.
85. Tsukagoshi M, Wada S, Yokobori T, et al. Overexpression of natural killer group 2 member D ligands predicts favorable prognosis in cholangiocarcinoma. Cancer Sci. 2016 Feb;107(2):116–122. PubMed PMID: 26608587.
86. Thanee M, Loilome W, Techasen A, et al. Quantitative changes in tumor-associated M2 macrophages characterize cholangiocarcinoma and their association with metastasis. Asian Pac J Cancer Prev. 2015;16(7):3043–3050. PubMed PMID: 25854403.
87. Atanasov G, Hau HM, Dietel C, et al. Prognostic significance of macrophage invasion in hilar cholangiocarcinoma. BMC Cancer. 2015 Oct;24(15):790. PubMed PMID: 26497197.
88. Subimerb C, Pinlaor S, Lulitanond V, et al. Circulating CD14(+) CD16(+) monocyte levels predict tissue invasive character of cholangiocarcinoma. Clin Exp Immunol. 2010 Sep;161(3):471–479. PubMed PMID: 20636398.
89. Subimerb C, Wongkham C, Khuntikeo N, et al. Transcriptional profiles of peripheral blood leukocytes identify patients with cholangiocarcinoma and predict outcome. Asian Pac J Cancer Prev. 2014;15(10):4217–4224. PubMed PMID: 24935374.
- ***This article demonstrated that the specific expression profiles of peripheral blood leukocytes could identify patients with CCA and predict patient outcomes.***

90. Faria SS, Fernandes PC Jr., Silva MJ, et al. The neutrophil-to-lymphocyte ratio: a narrative review. Ecancermedicalscience. 2016;10:702. . PubMed PMID: 28105073.
91. Templeton AJ, McNamara MG, Seruga B, et al. Prognostic role of neutrophil-to-lymphocyte ratio in solid tumors: a systematic review and meta-analysis. J Natl Cancer Inst. 2014 Jun;106(6):dju124. PubMed PMID: 24875653.
92. Omichi K, Cloyd JM, Yamashita S, et al. Neutrophil-to-lymphocyte ratio predicts prognosis after neoadjuvant chemotherapy and resection of intrahepatic cholangiocarcinoma. Surgery. 2017 Oct;162(4):752–765. PubMed PMID: 28688518.
93. Lin G, Liu Y, Li S, et al. Elevated neutrophil-to-lymphocyte ratio is an independent poor prognostic factor in patients with intrahepatic cholangiocarcinoma. Oncotarget. 2016 Aug 09;7(32):50963–50971. PubMed PMID: 26918355.
94. Tan DW, Fu Y, Su Q, et al. Prognostic significance of neutrophil to lymphocyte ratio in oncologic outcomes of cholangiocarcinoma: a meta-analysis. Sci Rep. 2016 Oct 03; 6:33789. PubMed PMID: 27694951.

•• ***A meta-analysis of 9 studies evaluated the value of using a simple blood test, the neutrophil-lymphocyte ratio, as prognostic marker for CCA.***

95. Holohan C, Van Schaeybroeck S, Longley DB, et al. Cancer drug resistance: an evolving paradigm. Nat Rev Cancer. 2013 Oct;13 (10):714–726. PubMed PMID: 24060863.
96. Housman G, Byler S, Heerboth S, et al. Drug resistance in cancer: an overview. Cancers (Basel). 2014 Sep 5;6(3):1769–1792. PubMed PMID: 25198391.
97. Herraez E, Lozano E, Macias RI, et al. Expression of SLC22A1 variants may affect the response of hepatocellular carcinoma and cholangiocarcinoma to sorafenib. Hepatology. 2013 Sep;58(3):1065–1073. PubMed PMID: 23532667.
98. Srimunta U, Sawanyawisuth K, Kraiklang R, et al. High expression of ABCC1 indicates poor prognosis in intrahepatic cholangiocarcinoma. Asian Pac J Cancer Prev. 2012;13(Suppl):125–130. PubMed PMID: 23480753.
99. Rau S, Autschbach F, Riedel HD, et al. Expression of the multidrug resistance proteins MRP2 and MRP3 in human cholangiocellular carcinomas. Eur J Clin Invest. 2008 Feb;38(2):134–142. PubMed PMID: 18226047.
100. Sribenja S, Wongkham S, Wongkham C, et al. Roles and mechanisms of beta-thymosins in cell migration and cancer metastasis: an update. Cancer Invest. 2013 Feb;31(2):103–110. PubMed PMID: 23320791.
101. Sribenja S, Natthasirikul N, Vaeteewoottacharn K, et al. Thymosin beta10 as a predictive biomarker of response to 5-fluorouracil chemotherapy in cholangiocarcinoma. Ann Hepatol. 2016 Jul-Aug;15(4):577–585. PubMed PMID: 27236157.
102. Yoon H, Min JK, Lee JW, et al. Acquisition of chemoresistance in intrahepatic cholangiocarcinoma cells by activation of AKT and extracellular signal-regulated kinase (ERK)1/2. Biochem Biophys Res Commun. 2011 Feb 18;405(3):333–337. PubMed PMID: 21130731.
103. Nutthasirikul N, Hahnvajanawong C, Techasen A, et al. Targeting the 133p53 isoform can restore chemosensitivity in 5-fluorouracil-resistant cholangiocarcinoma cells. Int J Oncol. 2015 Dec;47 (6):2153–2164. PubMed PMID: 26459801.
104. Brivio S, Cadamuro M, Fabris L, et al. Epithelial-to-mesenchymal transition and cancer invasiveness: what can we learn from cholangiocarcinoma? J Clin Med. 2015 Dec 19;4(12):2028–2041. PubMed PMID: 26703747.
105. Chiang KC, Yeh TS, Wu RC, et al. Lipocalin 2 (LCN2) is a promising target for cholangiocarcinoma treatment and bile LCN2 level is a potential cholangiocarcinoma diagnostic marker. Sci Rep. 2016 Oct;26(6):36138. PubMed PMID: 27782193.
106. Marin JJG, Lozano E, Herraez E, et al. Chemoresistance and chemosensitization in cholangiocarcinoma. Biochim Biophys Acta. 2017 Jul 07. DOI:10.1016/j.bbadis.2017.06.005 [PubMed PMID: 28600147].
107. Pardoll DM. The blockade of immune checkpoints in cancer immunotherapy. Nat Rev Cancer. 2012 Mar 22;12(4):252–264. PubMed PMID: 22437870.
108. Fontugne J, Augustin J, Pujals A, et al. PD-L1 expression in perihilar and intrahepatic cholangiocarcinoma. Oncotarget. 2017 Apr 11;8 (15):24644–24651. PubMed PMID: 28445951.
109. Walter D, Herrmann E, Schnitzbauer AA, et al. PD-L1 expression in extrahepatic cholangiocarcinoma. Histopathology. 2017 Sep;71 (3):383–392. PubMed PMID: 28419539.
110. Gani F, Nagarajan N, Kim Y, et al. Program death 1 immune checkpoint and tumor microenvironment: implications for patients with intrahepatic cholangiocarcinoma. Ann Surg Oncol. 2016 Aug;23(8):2610–2617. PubMed PMID: 27012989.
111. Silsirivanit A, Sawanyawisufth K, Riggins GJ, et al. Cancer biomarker discovery for cholangiocarcinoma: the high-throughput approaches. J Hepatobiliary Pancreat Sci. 2014 Jun;21(6):388–396. PubMed PMID: 24616382.
112. Macias RIR, Banales JM, Sangro B, et al. The search for novel diagnostic and prognostic biomarkers in cholangiocarcinoma. Biochim Biophys Acta. 2018 Apr;1864(4 Pt B):1468–1477. PubMed PMID: 28782657.
113. Kondo N, Murakami Y, Uemura K, et al. Elevated perioperative serum CA 19-9 levels are independent predictors of poor survival in patients with resectable cholangiocarcinoma. J Surg Oncol. 2014 Sep;110(4):422–429. PubMed PMID: 24889968.
114. Liang B, Zhong L, He Q, et al. Diagnostic accuracy of serum CA19-9 in patients with cholangiocarcinoma: a systematic review and meta-analysis. Med Sci Monit. 2015 Nov;18(21):3555–3563. PubMed PMID: 26576628.

• ***A meta-analysis evaluated value of CA19-9, a well known suggestive but non-specific marker for CCA diagnosis, as a potential prognostic predictor for CCA.***

115. Coelho R, Silva M, Rodrigues-Pinto E, et al. CA 19-9 as a marker of survival and a predictor of metastization in cholangiocarcinoma. GE Port J Gastroenterol. 2017 May;24(3):114–121. PubMed PMID: 28848795.
116. Bergquist JR, Ivanics T, Storlie CB, et al. Implications of CA19-9 elevation for survival, staging, and treatment sequencing in intrahepatic cholangiocarcinoma: a national cohort analysis. J Surg Oncol. 2016 Sep;114(4):475–482. PubMed PMID: 27439662.

cells

MDPI

Article

Establishment of Highly Transplantable Cholangiocarcinoma Cell Lines from a Patient-Derived Xenograft Mouse Model

Kulthida Vaeteewoottacharn [1,2,3], Chawalit Pairojkul [3,4], Ryusho Kariya [1], Kanha Muisuk [5], Kanokwan Imtawil [2], Yaovalux Chamgramol [3,4], Vajarabhongsa Bhudhisawasdi [3,6], Narong Khuntikeo [3,6], Ake Pugkhem [3,6], O-Tur Saeseow [3,6], Atit Silsirivanit [2,3], Chaisiri Wongkham [2,3], Sopit Wongkham [2,3] and Seiji Okada [1,*]

1 Division of Hematopoiesis, Joint Research Center for Human Retrovirus Infection and Graduate School of Medical Sciences, Kumamoto University, Kumamoto 860-0811, Japan; kulthidava@kku.ac.th (K.V.); ryushokariya@gmail.com (R.K.)
2 Department of Biochemistry, Khon Kaen University, Khon Kaen 40002, Thailand; kanoim@kku.ac.th (K.I.); atitsil@kku.ac.th (A.S.); chaisiri@kku.ac.th (C.W.); sopit@kku.ac.th (S.W.)
3 Cholangiocarcinoma Research Institute, Khon Kaen University, Khon Kaen 40002, Thailand; chawalit-pjk2011@hotmail.com (C.P.); cyaova@kku.ac.th (Y.C.); joevajara@gmail.com (V.B.); knaron@kku.ac.th (N.K.); akepug@kku.ac.th (A.P.); otusae@kku.ac.th (O.-T.S.)
4 Department of Pathology, Khon Kaen University, Khon Kaen 40002, Thailand
5 Department of Forensic Sciences, Khon Kaen University, Khon Kaen 40002, Thailand; mkanha@kku.ac.th
6 Department of Surgery, Faculty of Medicine, Khon Kaen University, Khon Kaen 40002, Thailand
* Correspondence: okadas@kumamoto-u.ac.jp; Tel.: +81-9-6373-6522

Received: 28 April 2019; Accepted: 21 May 2019; Published: 23 May 2019

Abstract: Cholangiocarcinoma (CCA) is a deadly malignant tumor of the liver. It is a significant health problem in Thailand. The critical obstacles of CCA diagnosis and treatment are the high heterogeneity of disease and considerable resistance to treatment. Recent multi-omics studies revealed the promising targets for CCA treatment; however, limited models for drug discovery are available. This study aimed to develop a patient-derived xenograft (PDX) model as well as PDX-derived cell lines of CCA for future drug screening. From a total of 16 CCA frozen tissues, 75% (eight intrahepatic and four extrahepatic subtypes) were successfully grown and subpassaged in Balb/c Rag-2$^{-/-}$/Jak3$^{-/-}$ mice. A shorter duration of PDX growth was observed during F0 to F2 transplantation; concomitantly, increased Oct-3/4 and Sox2 were evidenced in 50% and 33%, respectively, of serial PDXs. Only four cell lines were established. The cell lines exhibited either bile duct (KKK-D049 and KKK-D068) or combined hepatobiliary origin (KKK-D131 and KKK-D138). These cell lines acquired high transplantation efficiency in both subcutaneous (100%) and intrasplenic (88%) transplantation models. The subcutaneously transplanted xenograft retained the histological architecture as in the patient tissues. Our models of CCA PDX and PDX-derived cell lines would be a useful platform for CCA precision medicine.

Keywords: cholangiocarcinoma; patient-derived xenograft; cell line; cancer model; precision medicine

1. Introduction

Cholangiocarcinoma (CCA) is a rare subtype of liver cancer for which the highest incidence and mortality have been reported in northeastern Thailand [1,2]. The prognosis of CCA is dismal because of delayed diagnosis and poor response to conventional chemotherapy and targeted treatment [3]. Surgery is the only treatment option that provides a curative outcome [3,4], but limited numbers of the

patients are candidates [5]. Nonetheless, this outcome is influenced by factors such as tumor subtype, complete resection (R0), lymph node involvement, and vascular invasion [6]. Moreover, more than 85% of patients suffer from the disease recurrence [6]. The benefits of postoperative adjuvant treatment from a recent systematic review and meta-analysis are not convincing [7]. Therefore, it is urgently important to develop a novel CCA treatment.

CCA has high heterogeneity in nature [8]. Several risk factors of CCA have been established [9]. A common risk factor for of CCA in Thailand is the presence of a liver fluke, *Opisthorchis viverrini* (*Ov*), through ingestion [1,10]. A unique feature of *Ov*-associated CCA is increased xenobiotic metabolizing gene expression [11]. Mutational analysis of *Ov*-associated CCA identified a distinct signature with higher rates of *TP53*, *SMAD4*, and *ARID1A* mutations but lower frequencies of *IDH1/2* and *BAP1* mutations when compared to other Asian and Western populations [12–14]. These differing characteristics might complicate the usage of newly identified targets for CCA treatment [15–17]. However, the recent advances in multi-omics analyses have led to the identification of the targets for Thai CCA [18,19]. The majority of *Ov*-associated CCAs were gathered in cluster 1 and cluster 2 in Jusakul's study [18]. The molecular signature of cluster 1 showed some degree of similarity to CCA-C1 subgroup in Chaisaingmongkol's study [19] and to the proliferation subclass in Sia's study [17]. Potential usage of Her2/neu (ERBB2) [18] and cycle regulatory molecules [19] as targets for treatment are suggested in these CCA subclasses. Therefore, the development of a model for CCA treatment prediction and validation is urgent.

There are several models for CCA, including a previously established cell line, a cell line-transplanted xenograft, and a genetically engineered mouse model. The limitation of these models is disease homogeneity [20,21]. The generation of a patient-derived model might be better representative of tumor biology. However, primary culture of patient tissue is laborious and less efficient. In highly desmoplastic tumors (e.g., CCA and pancreatic cancer), the overgrowth of stromal cells will reduce the establishment efficiency [22,23]. In our experience, the success rate of cell line establishment from patient-derived primary culture was less than 5%, (unpublished data), comparable to that of pancreatic cancer (7%) [22].

The patient-derived xenograft (PDX) model is a promising tool for the propagation of a patient's tumor in an immunodeficient mouse. This PDX is an invaluable asset for the advancement of cancer precision medicine, particularly for rare and aggressive cancers [24]. A higher success rate of cell line development from PDX has been reported [25–27]. These cell lines show a certain degree of disease heterogeneity [26]. Limited numbers of CCA PDX and PDX-derived cell lines are available [16,27,28]. This prompted us to develop PDX as well as the PDX-derived cell line for high-throughput drug screening. These models might be useful as a platform for future anti-CCA development.

2. Materials and Methods

2.1. Cell Line

Four CCA cell lines—KKU-055, KKU-100 [29], KKU-213, and the hepatocellular carcinoma (HCC) cell line-HuH-7 [30] were selected as reference liver cancer cell lines for current study. KKU-055 and KKU-213 were derived from intrahepatic CCA, while KKU-100 was derived from the extrahepatic (perihilar) CCA [29]. CCA cell lines were obtained from the Japanese Collection of Research Bioresources Cell Bank (Osaka, Japan). HuH-7 was kindly provided by Prof. Kyoko Tsukiyama-Kohara (Kagoshima University, Kagoshima, Japan). Cells were maintained in DMEM (Wako, Osaka, Japan) or RPMI1640 (Wako) as per recommendations. FBS (10%; HyClone, Logan, UT, USA), 100 U/mL penicillin, and 100 µg/mL streptomycin were supplemented in the media. Cultures were maintained at 37 °C in a humidified 5% CO_2 atmosphere.

2.2. CCA Tissue Collection and Storage

Sixteen CCA tissue samples were obtained from the Department of Pathology, Faculty of Medicine, Khon Kaen University, Thailand, after the clinical specimens were obtained from the operating room and the pathological specimens were taken as the standard protocol for pathological staging. All tissue samples were histologically diagnosed; 10 were of intrahepatic CCA (ICC), and six were of the extrahepatic subtype (ECC). The study protocol was reviewed and approved by the Ethical Committee for the Human Research of Khon Kaen University (HE571283), based on the Declaration of Helsinki of 1975. Written informed consent was obtained from each subject. Demographical and pathological characteristics of patients and CCA tissues are listed in Table 1. CCA tissues were cut into 0.5 × 0.5 × 0.5 cm pieces and were stored in the freezing media containing 10% DMSO and 90% FBS, with 3–4 pieces per frozen vial. Tissues were stored at −80 °C until needed.

For transplantation, frozen CCA tissues were thawed and vigorously washed with PBS three times. Tissues were cut into 8–27 mm^3 pieces (2–3 mm each dimension). Non-viable cells were removed. Each tissue was divided into two parts: (1) for transplantation and (2) for molecular characterization and paraffin-embedded tissue preparation. Tissues were transplanted into flank areas of Balb/c Rag-2/Jak3 double-deficient (Balb/c RJ) [31] or Balb/c nude Rag-2/Jak3-deficient (Nude RJ) mice [32] subcutaneously. Implanted tissues were observed three times a week and were removed when the masses reached 8–10 mm in diameter. Xenograft tumors from mice were sub-divided into four parts: (1) for serial transplantation, (2) for frozen tissue stock, (3) for cell line development, and (4) for histological purposes. All experimental protocols were approved by The Institutional Animal Care and Use Committee, Kumamoto University, Japan.

Table 1. Characteristics of patients and cholangiocarcinoma tissues.

Code	Gender	Age	Subtype	TMN **	Stage **	*Ov* #	PDX ##	Histological Classification
D039	F	66	ICC	T3N0M0	III	No	−	WD, papillo-tubular adenocarcinoma
D042	M	56	ECC	T2bN0M0	II	No	−	Invasive, intraductal papillary carcinoma
D049 *	M	55	ICC	T2bN0M0	II	*Ov*	+	WD, tubular adenocarcinoma
D058	F	64	ICC	T3N1M0	IVA	*Ov*	+	WD, tubular adenocarcinoma
D068 *	M	61	ICC	T2aN1M0	IVA	No	+	WD, tubular adenocarcinoma with micropapillary foci
D070	M	65	ICC	T3N1M0	IVA	No	+	WD, tubular adenocarcinoma
D078	F	44	ECC	T4N1M0	IVA	No	+	WD, tubular adenocarcinoma
D088	F	68	ICC	T3N0M0	III	No	+	MD, tubular adenocarcinoma
D090	F	65	ECC	T2bN0M0	II	No	+	Invasive, intraductal papillary carcinoma
D096	M	45	ECC	T3N1M0	IIIB	No	+	WD, tubular adenocarcinoma
D106	M	54	ECC	T2bN1M0	IIIB	No	+/−	Invasive, intraductal papillary carcinoma
D113	M	70	ICC	T3N0M0	III	No	+	Invasive, intraductal papillary carcinoma
D117	M	58	ICC	T3N1M0	IVA	No	−	WD, tubular adenocarcinoma with micropapillary foci
D119	M	71	ECC	T3N1M0	IIIB	No	+	WD, tubular adenocarcinoma
D131 *	M	66	ICC	T3N1M0	IVA	No	+	WD, tubular adenocarcinoma
D138 *	F	60	ICC	T3N0M0	III	No	+	Adenosquamous carcinoma

* Cell lines were established; ** classification is based on the 7th edition of the AJCC cancer staging classification [33]; # *Opisthorchis viverrini* (*Ov*) is observed in the tissues; ## serial transplanted tissues are successfully established, +/− indicates only F0 tumor was obtained; F: female; M: male; ECC: extrahepatic cholangiocarcinoma; ICC: intrahepatic cholangiocarcinoma; MD: moderately-differentiated subtype; WD: well-differentiated subtype; PDX: patient-derived xenograft.

2.3. Cell Line Establishment

For cell line development, fresh xenograft tissues were prepared as previously described [34]. Cells were cultured in DMEM/F12 (Wako) containing 1–10% FBS and insulin-transferrin-selenium (ITS, Gibco BRL, Carlsbad, CA, USA). Stromal cells were sequentially removed by partial trypsinization and mechanical removal. Cancer cells were subsequently cultured in DMEM containing 10% FBS when becoming morphologically homogenous. All media were supplemented with 100 U/mL penicillin and 100 µg/mL streptomycin. The cultures were maintained at 37 °C in a humidified 5% CO_2 atmosphere. Cells were maintained in vitro culture system at least 6 months to ensure the immortalization properties.

All four newly established cell lines were deposited into the Japanese Cancer Research Resources Bank (JCRB), National Institutes of Biomedical Innovation, Health and Nutrition (NIBIOHN), Osaka, Japan.

2.4. The Expressions of Bile Duct and Hepatocyte-Related Genes

To demonstrate the liver cell origin of the cell lines, the expression profile of bile duct or hepatocyte-related genes including cytokeratin 7 (CK7), CK19, γ-glutamyl transferase (GGT), α-fetoprotein (AFP), and albumin (ALB) were determined as previously described [35]. RNA was isolated from the cell line, and cDNA was prepared as mentioned elsewhere [36]. Alpha-smooth muscle actin (αSMA) primers were used for the exclusion of fibroblast contamination. Primers used in the current experiment are listed in Table S1.

PCR products were separated in 1.5% agarose gel in Tris-Borate-EDTA (TBE) buffer. A gel was stained with ethidium bromide solution (Sigma-Aldrich, St. Louis, MO, USA) and the images were captured by Bio-Rad Gel Doc 2000 (Bio-Rad, Hercules, CA, USA).

2.5. Cell Line Authentication and TP53 Mutation Analysis

To determine the genetic stabilities of the cell lines, 16 short tandem repeats (STR) of cell lines, original tumor tissues, and patient's white blood cells (WBC) were compared using AmpFℓSTR® Identifiler® Plus PCR Amplification Kit (Applied Biosystems, Carlsbad, CA, USA). DNA was extracted by the QIAamp® DNA Micro Kit (QIAGEN, Stanford, CA, USA). PCR products were analyzed using ABI Prism 3130 Genetic Analyzer and GeneMapper® ID Software v3.2 (Applied Biosystems).

TP53 gene mutation was analyzed as previously described in [37]. Briefly, PCR reactions were performed using the HotStarTaq Master Mix Kit (QIAGEN) and the amplification reactions were carried out on a GeneAmp 9700 Thermal cycler (Applied Biosystems) as suggested. Sequencing was achieved by using BigDye Terminator V3.1 cycle sequencing reaction kit (Applied Biosystems) and the Genetic Analyzer ABI 3130 (Applied Biosystems). TP53 sequences were compared to the reference sequence (NC_000017.9) by Lasergene 10.1 (DNASTAR, Madison, WI, USA).

2.6. Xenograft Transplantation of Cell Lines

The xenograft transplantation ability of the cell lines was determined. One to two million cells of each cell line were transplanted subcutaneously into both flanks of Balb/c RJ mice. For intrasplenic transplantation, 5×10^4 cells were injected intrasplenically as previously described [38]. Tissues, spleen, and liver were removed at 1 month after transplantation. Paraffin-embedded tissues were prepared as per standard protocol.

2.7. Histological Characterization and Evaluation

Hematoxylin and eosin staining of the original CCA tissues and transplanted tumors was performed regularly. For immunohistochemistry staining, a standard protocol using citrate buffer retrieval buffer was used. Signals were enhanced by EnVision-system-HRP (Dako, Glostrup, Denmark) or the Vectastain Elite ABC standard kit (Vector Laboratories, Burlingame, CA, USA). Detection was performed using the Histofine® DAB substrate kit (Nichirei Bioscience, Tokyo, Japan).

The sources of antibodies were as follows: anti-CK19 (HPA002465,) was from Sigma-Aldrich, anti-Ki-67 (MIB-1) was from Dako, anti-epithelial cell adhesion molecule (EpCAM, C-10) and anti-Oct-3/4 (C-10) were from Santa Cruz Biotechnology (Dallas, TX, USA), anti-Sox2 (D6D9) was from Cell Signaling Technology (Danvers, MA, USA), and biotinylated goat anti-mouse IgG and biotinylated goat anti-rabbit IgG were from Vector Laboratories.

The comparison of tissue architecture between the original CCA tissue and transplanted tissue was made by the pathologists. The images were taken by the BZ-8100 Biozero fluorescent microscope. For the quantitation, the immunoreactivity signals were quantified by BZ-II Analyzer (Keyence, Osaka, Japan) as previously described [36].

2.8. Statistical Analysis

For the correlation study, Pearson's correlation coefficient (r) was calculated using GraphPad Prism version 6.07 (San Diego, CA, USA).

3. Results

3.1. CCA Patient Tissue Transplantation

From 16 CCA tissues, 10 tissue samples were of the intrahepatic subtype (ICC) while six were of the extrahepatic subtype (ECC) based on the 7th edition of the AJCC cancer staging classification. The most extended storage duration with successful transplantation was 134 days (19–134 days). After defrosting and cleaning, tissues were transplanted into both flanks of Balb/c RJ mice. Thirteen tissue samples (eight ICC and five ECC) successfully grew in the subcutaneous areas of the mice (Table 1). No mass was observed in three mice (D039, D042, and D117). Unfortunately, only 12 tissue samples were successfully transplanted into F1 (Figure 1). D106 formed a tumor in the F0 mouse, but it was lethal to the F1 mouse. We repeated D106 F1 transplantation twice but mice died within a month without a specific cause and alarming signs. The durations of F0 tumor formations ranged from 24 to 194 days. The duration of tumor formation was not related to either tumor cell density evaluated by percentage of CK19 immunoreactivity or the proliferative potential of the tumor cells determined by percentage of Ki-67 positive nuclei (Table S2 and Figure S1).

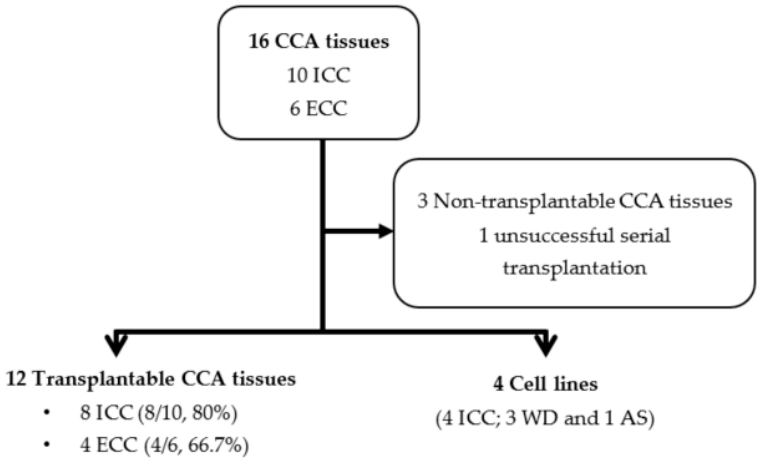

Figure 1. The summary of PDX transplantation and PDX-derived cell line development. CCA: cholangiocarcinoma.

A similar experiment was carried out in nude RJ mice. Three samples were transplanted into both flanks of mice. The transplantation success rate was comparable to those in Balb/c RJ, but F0 growth in nude RJ took approximately 2 weeks longer. Thus, we selected the Balb/c RJ mice for our PDX generation and further testing.

From our protocol, we successfully established the method for generation of the CCA-PDX model, which is highly efficient (67–80% success rate) (Figure 1). The duration of xenograft transplantation was not related to either tumor density or the proliferative capability of the tumor cells indicated by CK19 and Ki-67 immunostaining. Nonetheless, it is worth mentioning that the duration of tumor establishment was shorter when the PDX was serially transplanted (Figure 2). Mean durations of PDX growth in F0, F1, F2, F3, and F4 were 110, 60, 47, 46, and 43 days, respectively. The xenograft tumor growth might be related to the Oct3/4 and Sox2 expressions. Oct-3/4 was detectable in 11 xenografts (92%) and Sox2 was observed in eight xenografts (67%). Interestingly, increased Oct3/4 was observed in 50% of serially transplanted tumors (6/12 xenografts) and increased Sox2 was observed in 33% of tumors (4/12 xenografts). Representative PDXs with Oct-3/4 and Sox2 increments are demonstrated in Figure 3. It should be noted that EpCAM was observed on almost all tumor cell surfaces and no significant alteration of the EpCAM signal was observed in our serially transplanted PDXs (Figure S2).

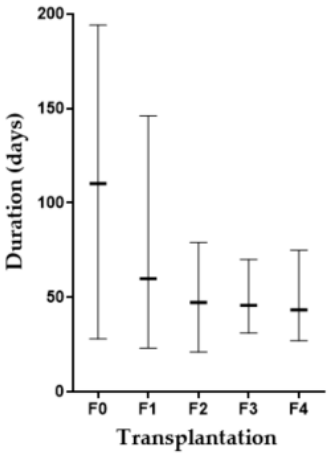

Figure 2. Comparison of PDX growth duration during serial transplantation. Bar indicates the longest to the shortest duration in each generation and - indicates a mean duration.

3.2. Cell Line Establishment and Characterization

Among 12 serially transplantable tissues, four tissues were successfully developed into cell lines. All cell lines were of intrahepatic origin; three were histologically characterized as well-differentiated subtypes (WD; KKK-D049, KKK-D068, and KKK-D131) and one was characterized as a mixed adenosquamous subtype (AS; KKK-D138). KKK-D068 and KKK-D131 were established from the F0-transplanted tumor while KKK-D138 and KKK-D049 were established from the F1 and F2 tumors, respectively. The morphologies of the cell lines are presented in Figure 4a. All cell lines exhibit epithelial-like features with a high nuclear to cytoplasmic ratio. KKK-D049 shows a unique feature of tight clustering. KKK-D068, KKK-D131, and KKK-D138 contain both polygonal and spindle-like cells.

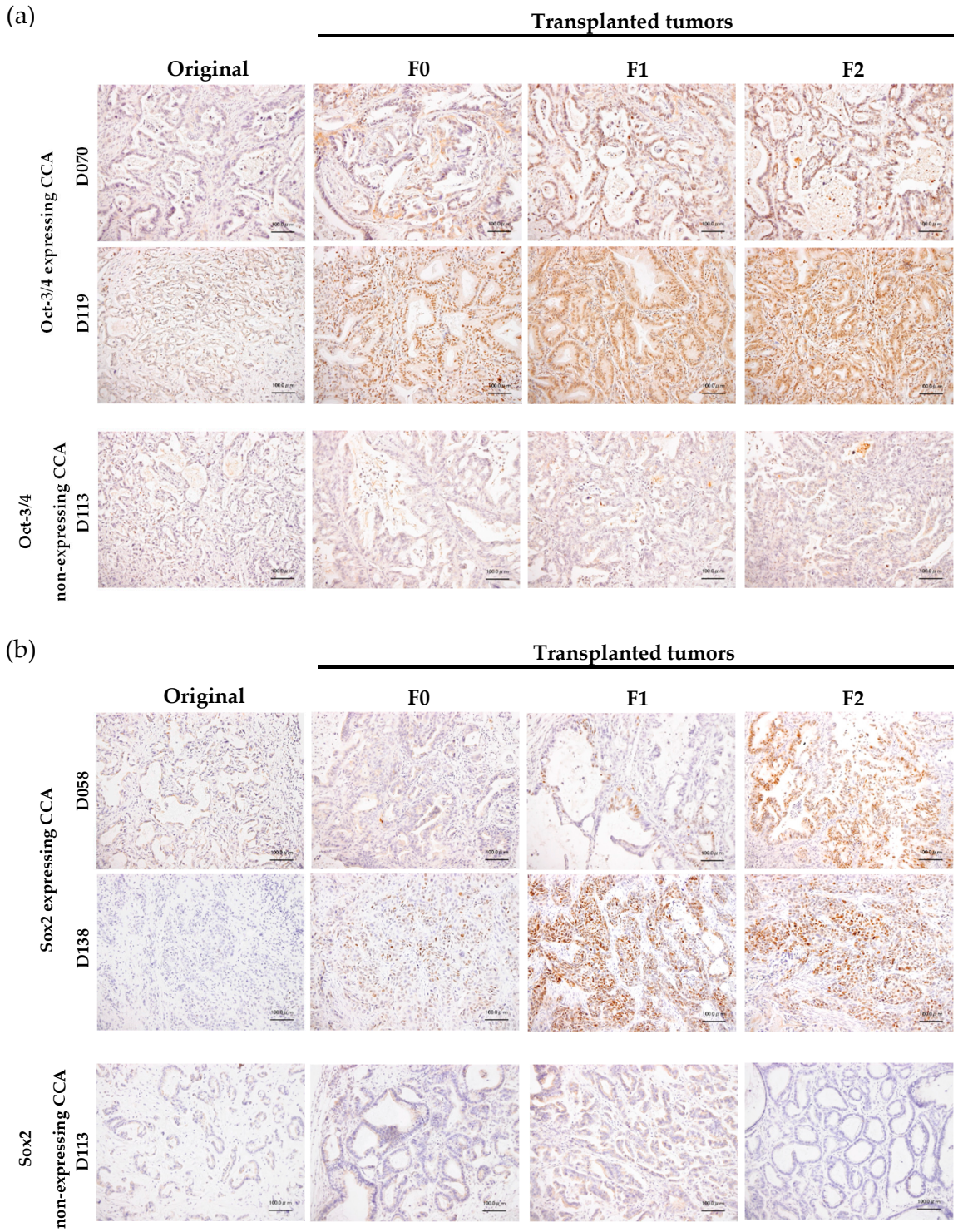

Figure 3. Comparison of Oct-3/4 and Sox2 expressions between original tumor tissue from the patient (original) and serially transplanted tissues (F0, F1, and F2). (**a**) Oct-3/4; (**b**) Sox2 expressions. Representative samples of nuclear expressing and non-expressing CCA are shown. Bar = 100 μm.

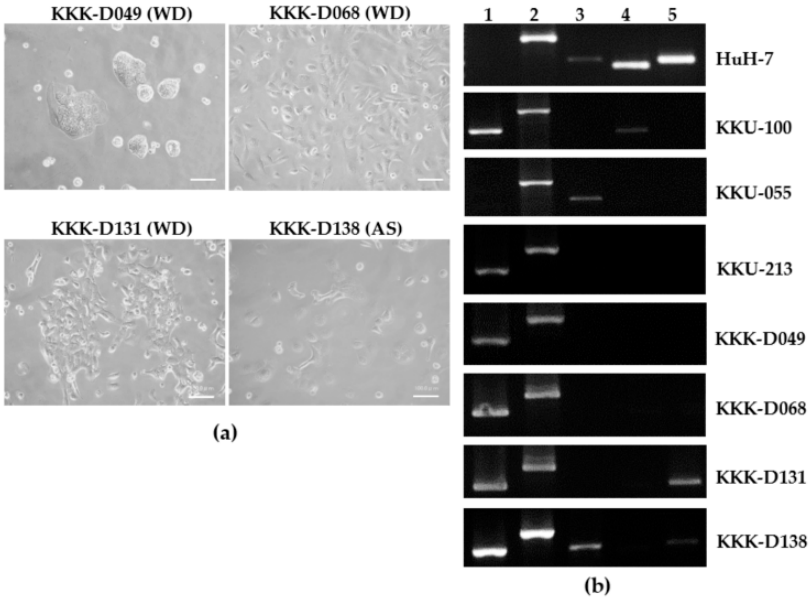

Figure 4. The morphologies (**a**) and gene expression profile (**b**) of PDX-derived CCA cell lines KKK-D-49, KKK-D068, KKK-D131, and KKK-D138. Huh7, KKU-100, KKU-055, and KKU-213 were used as references. WD: well differentiated subtype; AS: adenosquamous subtype; 1: cytokeratin 7 (CK7); 2: CK19, 3: γ-glutamyl transferase (GGT); 4: α-fetoprotein (AFP); 5: albumin (ALB).

The authentications of cell lines were performed by STR analysis (Table 2). DNA from patient's tissue and WBC were used as references. Fifteen STR loci and amelogenin were detected. One locus of D18S51 was lost in the D049 tissue and KKK-D049 cell line. One locus of D16S539 and Y amelogenin was lost in the KKK-D068 cell line but not in D068 tissue. A locus of CSF1PO, TH01, D16S539, D19S433, D5S818, FGA, and Y amelogenin was lost in KKK-D131. A 31.2 locus of D21S11 was lost in KKK-D138.

Further characterization of cell lineage marker was performed using RT-PCR (Figure 4b). Comparisons of the previously developed HCC (HuH-7), CCA (KKU-100, KKU-055, KKU-213) and the newly established cells showed all new cell lines expressed two bile duct markers, CK7, and CK9, similar to the previously established cell lines (KKU-100 and KKU-213); only KKK-D138 expressed GGT. KKK-D131 and KKK-D138 expressed the hepatocyte marker, ALB. None of the newly established cell lines expressed AFP but a previously developed cell line, KKU-100 did. Alpha-SMA was not detectable in any cell lines (data not shown).

TP53 mutation analysis revealed CCC to CGC at codon 72, which will cause missense P72R mutations in KKK-D138 but is not detected in KKK-D068 and KKK-D131. The *TP53* mutation of KKK-D049 has not yet been analyzed.

Table 2. Comparison of STR profiles of CCA tissues, patient WBC, and newly established cell lines.

Loci	D049			D068			D131			D138		
	WBC	**Tissue**	**Cell**	**WBC**	**Tissue**	**Cell**	**WBC**	**Tissue**	**Cell**	**WBC**	**Tissue**	**Cell**
D8S1179	12, 17	12, 17	12, 17	12, 16	12, 16	12, 16	12, 13	12, 13	12, 13	ND **	10, 14	10, 14
D21S11	29, 30	29, 30	29, 30	30, 33.2	30, 33.2	30, 33.2	29	29	29		29, 31.2	29
D7S820 *	8, 10	8, 10	8, 10	8, 10	8, 10	8, 10	8, 11	8, 11	8, 11		10, 11	10, 11
CSF1PO *	11, 12	11, 12	11, 12	11	11	11	12, 13	12, 13, 14	14		10, 11	10, 11
D3S1358	15, 16	15, 16	15, 16	15	15	15	14, 15	14, 15	14, 15		16, 18	16, 18
TH01 *	9	9	9	7	7	7	8, 9.3	8, 9.3	9.3		8, 9.3	8, 9.3
D13S317 *	8, 9	8, 9	8, 9	8, 12	8, 12	8, 12	10, 11	10, 11	10, 11		8, 11	11
D16S539 *	13, 14	13, 14	13, 14	9, 11	9, 11	9	9, 11	9, 11	11		9, 11	9, 11
D2S1338	19, 25	19, 25	19, 25	19	19	19	20, 23	20, 23	20, 23		24, 25	24, 25
D19S433	13, 15.2	13, 15.2	13, 15.2	14, 14.2	14, 14.2	14, 14.2	13.2, 14	13.2, 14	13.2		13.2, 14.2	13.2, 14.2
vWA *	14, 17	14, 17	14, 17	14, 16	14, 16	14, 16	14, 16	14, 16	14, 16		14, 18	14, 18
TPOX *	8, 9	8, 9	8, 9	8, 11	8, 11	8, 11	8, 11	8, 11	8, 11		11	11
D18S51	11, 16	11	11	12	12	12	17	17	17		15	15
D5S818 *	10, 12	10, 12	10, 12	11, 12	11, 12	11, 12	10, 12	10, 12, 13	13		9, 10	9, 10
FGA	23, 24.2	23, 24.2	23, 24.2	23, 25	23, 25	23, 25	19, 21	19, 21	21		18, 24.2	18, 24.2
Amelogenin	X, Y	X, Y	X, Y	X, Y	X, Y	X	X, Y	X, Y	X		X, X	X, X

* Eight markers are common short tandem repeat (STR) markers for cell authentication; ** White blood cells (WBCs) are not available for comparison.

3.3. Cell Line Transplantation

To test the in vivo tumorigenesis properties of the newly developed cell lines, the cell lines were separately injected into both flanks of Balb/c RJ (two mice/cell line, $n = 4$). Tumors were grown in the mice for a month, and tumor masses were observed twice a week. We observed tumor masses from all injected sites (Figure 5a). The successful rate of subcutaneous xenograft was 100% (Table 3).

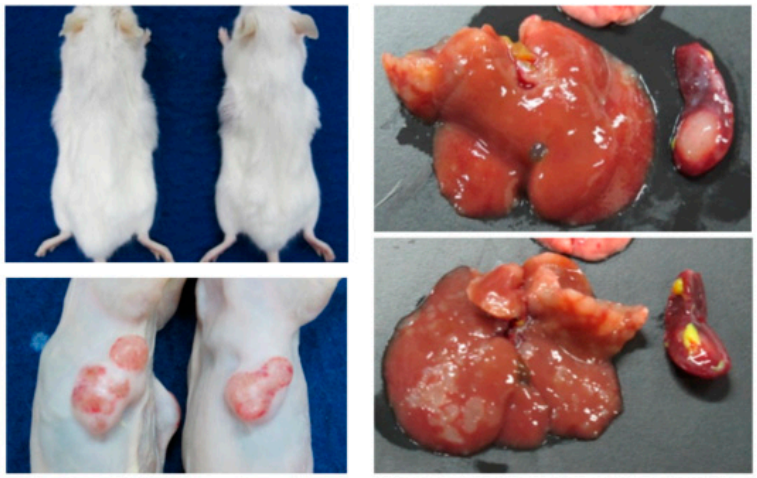

Figure 5. CCA cell line transplantation in subcutaneous (**a**) and intrasplenic (**b**) xenograft mouse models. The representative pictures are from KKK-D068 transplantations.

Table 3. PDX-derived cell line transplantation rate in subcutaneous (SC) and intrasplenic (IS) xenograft mouse model.

Cell Lines	Route	Transplantation Rate (%)
KKK-D049	SC	4/4 (100%)
	IS	1/2 (50%)
KKK-D068	SC	4/4 (100%)
	IS	2/2 (100%)
KKK-D131	SC	4/4 (100%)
	IS	2/2 (100%)
KKK-D138	SC	4/4 (100%)
	IS	2/2 (100%)

The transplantation was further performed in the intrasplenic transplantation model. Fifty thousand cells of each cell line were injected into Balb/c RJ spleen (two mice/cell line, $n = 2$). Spleen, liver, and lungs were removed at 1 month after injection. Tumors were observed in 88% of transplanted livers and spleens (7/8 mice) (Figure 5b). No tumors were detected in one mouse injected with KKK-D049 (Table 3). No tumors were observed in lungs of mice (data not shown).

The subcutaneous tumor masses were prepared for the histological comparison with the tumor tissues from the patients (Figure 6). These transplanted tumors exhibited similar architectures to the original tumors. KKK-D049 showed tubular formation, while KKK-D068, KKK-D131, and KKK-D138 exhibited epithelial like characteristics.

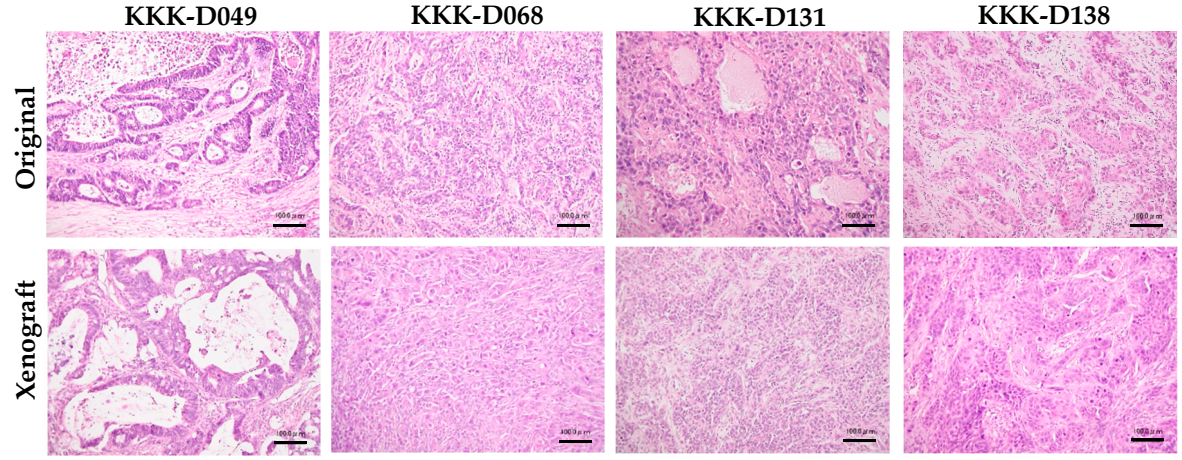

Figure 6. Histological comparison of original tumor tissues from patient (original) and subcutaneous transplanted tissues (xenograft). Bar = 100 μm.

4. Discussion

Cholangiocarcinoma (CCA) is a rare, aggressive tumor of liver found worldwide [1,2]. The world's highest incidence and mortality of CCA are in Thailand, and the disease is a significant health concern. CCA treatment is difficult given the great heterogeneity of the disease. The unique causative agent of *Opisthorchis viverrini* (*Ov*) infection has been demonstrated by distinctive molecular signatures [11–13,18,19]. The typical signatures suggest *Ov*-related CCA might be vulnerable to distinct treatment. Several attempts were made to provide opportunities for *Ov*-related CCA treatment [18,19]. Despite this, pre-clinical models that are patient-representative are limited. Therefore, a model for target validation is urgently required.

Patient-derived xenograft (PDX) models are preclinical models that are ideally developed for the implementation of personalized medicine. PDX models are a powerful tool for cancer propagation that retain disease complexity and heterogeneity [24]. Moreover, PDX-derived cell lines with some degree of cellular heterogeneity are useful tools for the larger scale of drug screening. We have developed the PDX and PDX-derived cell lines which acquire very high efficiency for transplantation in conventional subcutaneous and intrasplenic models.

The newly developed CCA-PDX model is highly efficient, with 75% transplantable efficiency compared to 6–35% engraftment rates in the previously described models [27,28]. This high efficiency is not related to the tumor stage, patient survival, tumor density, or proliferative potential of cells. This might be due to the different genetic backgrounds of the recipient mice. Balb/c RJ or nude RJ mice in our study have no natural killer (NK) cells, but the non-obese diabetic (NOD)/Shi-severe combined immunodeficient (SCID) mice in Cavalloni's study and the athymic C.B17/Icr-scid(scid/scid) mice in Ojima's study retain functional NK cells [27,28]. The roles of NK cells in syngeneic or xenograft tumor rejection are widely accepted [39]. The usefulness of the PDX model has been explored as the resources for cell line development [25–27]. A comparable cell line establishment rate (25% in our study vs. 32% in Ojima's study) was observed, which might be due to the selective power of the PDX model [20]. Increased Oct-3/4 or Sox2 expressing cancer cells were observed during PDX passaging. Similar observations of increased cancer stem cell (CSC) proportions in the PDX model were observed in other cancers [40]. The identification and characterization of CSCs in CCA-PDX are beyond the scope of this study and require more attention.

PDX-derived cell lines developed in this study show some degree of heterogeneity in vitro and in vivo, yet keep the characteristics of tissue organization, which are common in PDX models [25–27]. The loss of the Y chromosome or Y amelogenin was observed in two cell lines (KKK-D068 and KKK-D131). The loss of the Y chromosome is also observed in hepatocellular carcinoma (HCC) [41] and pancreatic cancer [42]. The functional significance of the Y chromosome loss is still under debate.

Our PDX-derived cell lines acquire the expressions of the bile duct or hepatobiliary-related genes. This might suggest a cellular origin, perhaps committed bile duct cells (CK7- and CK19-expressing cells) or bipotential progenitor cells (CK7/CK19 and ALB-expressing cells) [35]. Cellular origins of cell lines require further investigation. The newly established cell lines have very high efficiency for xenotransplantation. Owing the PDX development was in Balb R/J, these cell lines might be adapted to the selection power of the mouse model. Testing of xenotransplantation efficiency in other immunodeficient will be explored.

We propose the platform for anti-cancer drug screening using a PDX-derived cell line, and a PDX mouse model as demonstrated in Figure 7. In cases where immunodeficient mice are not commonly available, cancer tissues might be kept as frozen stock. Transplantation might be performed upon readiness. In parallel, the omics identification of drug targets and the development of PDX-derived cell lines might be performed. This cell line might be useful for high-throughput drug screening or target testing. To validate the information from omics study or high-throughput drug screening, the PDX model may play a critical role. Moreover, this PDX biobank would be a precious resource for future drug development.

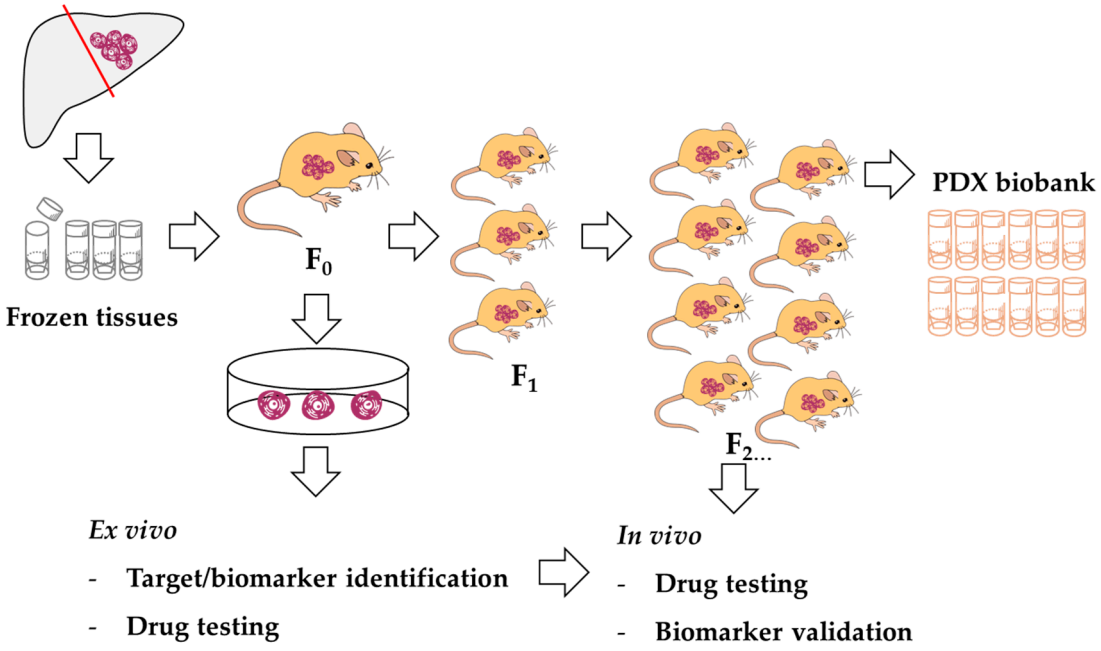

Figure 7. A proposed model of PDX resource usage.

5. Conclusions

In conclusion, in this study we established a highly effective CCA PDX model and highly transplantable PDX-derived cell lines. Cell authentications and characterization have been demonstrated. The cellular heterogeneity and preserved tissue architecture have been confirmed in PDX-derived cell lines and cell line xenografts. These PDX-derived cell lines and PDX models might be a promising platform for anti-CCA development. The advantage of our PDX model for personalized medicine seems to be limited by the long transplantation duration in some cases.

Supplementary Materials: Supplementary materials are available online at http://www.mdpi.com/2073-4409/8/5/496/s1.

Author Contributions: Conceptualization, K.V., C.P., S.W., and S.O.; methodology and investigation, K.V., R.K., K.M., K.I., and Y.C.; surgical specimen preparation and resources, C.P., V.B., N.K., A.P., O.-T.S., and A.S.; data curation, C.P. and Y.C.; writing—original draft preparation, K.V. and S.O.; writing—review and editing, K.V., C.P., S.W., and S.O.; supervision, C.P., V.B., C.W., S.W., and S.O.; funding acquisition, C.P., S.W. and S.O.

Funding: This research was funded by a Grant-in-Aid for Scientific Research from the Ministry of Education, Culture and Sport Science and Technology (MEXT) of Japan (grant number 16K08742); the Thailand Research Fund and the Medical Research Council-UK (Newton Fund) (grant number DBG5980004); the Senior Research Scholar Grant, Thailand Research Fund and Khon Kaen University (grant number RTA5780012); the National Science and Technology Development Agency and the e-Asia Joint Research Program (grant number P1950436).

Acknowledgments: We thank S. Fujikawa for her technical assistance and Y. Kanagawa for her secretarial work. The authors acknowledge the Cholangiocarcinoma Research Institute (CARI), Khon Kaen University, Thailand for providing tissue samples, the Center for Animal Resources and Development (CARD), Kumamoto University, Japan for animal care, and funding from MEXT of Japan, the Thailand Research Fund, the Medical Research Council UK, the National Science and Technology Development Agency, and the e-Asia Joint Research Program.

Conflicts of Interest: The authors declare no conflict of interest.

References

1. Sripa, B.; Pairojkul, C. Cholangiocarcinoma: Lessons from Thailand. *Curr. Opin. Gastroenterol.* **2008**, *24*, 349–356. [CrossRef]
2. Bridgewater, J.; Galle, P.R.; Khan, S.A.; Llovet, J.M.; Park, J.-W.; Patel, T.; Pawlik, T.M.; Gores, G.J. Guidelines for the diagnosis and management of intrahepatic cholangiocarcinoma. *J. Hepatol.* **2014**, *60*, 1268–1289. [CrossRef] [PubMed]
3. Banales, J.M.; Cardinale, V.; Carpino, G.; Marzioni, M.; Andersen, J.B.; Invernizzi, P.; Lind, G.E.; Folseraas, T.; Forbes, S.J.; Fouassier, L.; et al. Expert consensus document: Cholangiocarcinoma: Current knowledge and future perspectives consensus statement from the European Network for the Study of Cholangiocarcinoma (ENS-CCA). *Nat. Rev. Gastroenterol. Hepatol.* **2016**, *13*, 261–280. [CrossRef] [PubMed]
4. Doherty, B.; Nambudiri, V.E.; Palmer, W.C. Update on the Diagnosis and Treatment of Cholangiocarcinoma. *Gastroenterol. Rep.* **2017**, *19*. [CrossRef] [PubMed]
5. Tan, J.C.; Coburn, N.G.; Baxter, N.N.; Kiss, A.; Law, C.H. Surgical management of intrahepatic cholangiocarcinoma—A population-based study. *Ann. Surg. Oncol.* **2008**, *15*, 600–608. [CrossRef]
6. Vogel, A.; Wege, H.; Caca, K.; Nashan, B.; Neumann, U. The Diagnosis and Treatment of Cholangiocarcinoma. *Dtsch. Aerzteblatt Int.* **2014**, *111*, 748–754. [CrossRef]
7. Horgan, A.M.; Amir, E.; Walter, T.; Knox, J.J. Adjuvant Therapy in the Treatment of Biliary Tract Cancer: A Systematic Review and Meta-Analysis. *J. Clin. Oncol.* **2012**, *30*, 1934–1940. [CrossRef] [PubMed]
8. Patel, T. New insights into the molecular pathogenesis of intrahepatic cholangiocarcinoma. *J. Gastroenterol.* **2014**, *49*, 165–172. [CrossRef]
9. Tyson, G.L.; El-Serag, H.B. Risk factors for cholangiocarcinoma. *Hepatology* **2011**, *54*, 173–184. [CrossRef]
10. Sripa, B.; Brindley, P.J.; Mulvenna, J.; Laha, T.; Smout, M.J.; Mairiang, E.; Bethony, J.M.; Loukas, A. The tumorigenic liver fluke Opisthorchis viverrini –multiple pathways to cancer. *Trends Parasitol.* **2012**, *28*, 395–407. [CrossRef]
11. Jinawath, N.; Chamgramol, Y.; Furukawa, Y.; Obama, K.; Tsunoda, T.; Sripa, B.; Pairojkul, C.; Nakamura, Y. Comparison of gene expression profiles between Opisthorchis viverrini and non-Opisthorchis viverrini associated human intrahepatic cholangiocarcinoma. *Hepatology* **2006**, *44*, 1025–1038. [CrossRef]
12. Ong, C.K.; Subimerb, C.; Pairojkul, C.; Wongkham, S.; Cutcutache, I.; Yu, W.; McPherson, J.R.; E Allen, G.; Ng, C.C.Y.; Wong, B.H.; et al. Exome sequencing of liver fluke–associated cholangiocarcinoma. *Nat. Genet.* **2012**, *44*, 690–693. [CrossRef]
13. Chan-On, W.; Nairismägi, M.-L.; Ong, C.K.; Lim, W.K.; Dima, S.; Pairojkul, C.; Lim, K.H.; McPherson, J.R.; Cutcutache, I.; Heng, H.L.; et al. Exome sequencing identifies distinct mutational patterns in liver fluke–related and non-infection-related bile duct cancers. *Nat. Genet.* **2013**, *45*, 1474–1478. [CrossRef]
14. Wardell, C.P.; Fujita, M.; Yamada, T.; Simbolo, M.; Fassan, M.; Karlić, R.; Polak, P.; Kim, J.; Hatanaka, Y.; Maejima, K.; et al. Genomic characterization of biliary tract cancers identifies driver genes and predisposing mutations. *J. Hepatol.* **2018**, *68*, 959–969. [CrossRef]
15. Andersen, J.B.; Spee, B.; Blechacz, B.R.; Avital, I.; Komuta, M.; Barbour, A.; Conner, E.A.; Gillen, M.C.; Roskams, T.; Roberts, L.R.; et al. Genomic and genetic characterization of cholangiocarcinoma identifies therapeutic targets for tyrosine kinase inhibitors. *Gastroenterology* **2012**, *142*, 1021–1031.e15. [CrossRef]

16. Saha, S.K.; Gordan, J.D.; Kleinstiver, B.P.; Vu, P.; Najem, M.S.; Yeo, J.-C.; Shi, L.; Kato, Y.; Levin, R.S.; Webber, J.T.; et al. Isocitrate dehydrogenase mutations confer dasatinib hypersensitivity and SRC-dependence in intrahepatic cholangiocarcinoma. *Cancer Discov.* **2016**, *6*, 727–739. [CrossRef]
17. Sia, D.; Hoshida, Y.; Villanueva, A.; Roayaie, S.; Ferrer, J.; Tabak, B.; Peix, J.; Sole, M.; Tovar, V.; Alsinet, C.; et al. Integrative Molecular Analysis of Intrahepatic Cholangiocarcinoma Reveals 2 Classes That Have Different Outcomes. *Gastroenterology* **2013**, *144*, 829–840. [CrossRef]
18. Jusakul, A.; Cutcutache, I.; Yong, C.H.; Lim, J.Q.; Ni Huang, M.; Padmanabhan, N.; Nellore, V.; Kongpetch, S.; Ng, A.W.T.; Ng, L.M.; et al. Whole-Genome and Epigenomic Landscapes of Etiologically Distinct Subtypes of Cholangiocarcinoma. *Cancer Discov.* **2017**, *7*, 1116–1135. [CrossRef] [PubMed]
19. Chaisaingmongkol, J.; Budhu, A.; Dang, H.; Rabibhadana, S.; Pupacdi, B.; Kwon, S.M.; Forgues, M.; Pomyen, Y.; Bhudhisawasdi, V.; Lertprasertsuke, N.; et al. Common Molecular Subtypes among Asian Hepatocellular Carcinoma and Cholangiocarcinoma. *Cancer Cell* **2017**, *32*, 57–70.e3. [CrossRef] [PubMed]
20. Kopetz, S.; Lemos, R.; Powis, G. The Promise of Patient-Derived Xenografts: The best laid plans of mice and men. *Clin. Cancer Res.* **2012**, *18*, 5160–5162. [CrossRef] [PubMed]
21. Jung, J.; Seol, H.S.; Chang, S. The Generation and Application of Patient-Derived Xenograft Model for Cancer Research. *Cancer Res. Treat. Off. J. Korean Cancer Assoc.* **2018**, *50*, 1–10. [CrossRef]
22. Kim, M.-J.; Kim, M.-S.; Kim, S.J.; An, S.; Park, J.; Park, H.; Lee, J.H.; Song, K.-B.; Hwang, D.W.; Chang, S.; et al. Establishment and characterization of 6 novel patient-derived primary pancreatic ductal adenocarcinoma cell lines from Korean pancreatic cancer patients. *Cancer Cell Int.* **2017**, *17*, 47. [CrossRef]
23. Ku, J.-L.; Yoon, K.-A.; Kim, I.-J.; Kim, W.-H.; Jang, J.-Y.; Suh, K.-S.; Kim, S.-W.; Park, Y.-H.; Hwang, J.-H.; Yoon, Y.-B.; et al. Establishment and characterisation of six human biliary tract cancer cell lines. *Br. J. Cancer* **2002**, *87*, 187–193. [CrossRef]
24. Okada, S.; Vaeteewoottacharn, K.; Kariya, R. Establishment of a Patient-Derived Tumor Xenograft Model and Application for Precision Cancer Medicine. *Chem. Pharm.* **2018**, *66*, 225–230. [CrossRef]
25. Damhofer, H.; A Ebbing, E.; Steins, A.; Welling, L.; A Tol, J.; Krishnadath, K.K.; Van Leusden, T.; Van De Vijver, M.J.; Besselink, M.G.; Busch, O.R.; et al. Establishment of patient-derived xenograft models and cell lines for malignancies of the upper gastrointestinal tract. *J. Transl. Med.* **2015**, *13*, 115. [CrossRef]
26. Pham, K.; Delitto, D.; Knowlton, A.E.; Hartlage, E.R.; Madhavan, R.; Gonzalo, D.H.; Thomas, R.M.; Behrns, K.E.; George, T.J.; Hughes, S.J.; et al. Isolation of Pancreatic Cancer Cells from a Patient-Derived Xenograft Model Allows for Practical Expansion and Preserved Heterogeneity in Culture. *Am. J. Pathol.* **2016**, *186*, 1537–1546. [CrossRef]
27. Ojima, H.; Yoshikawa, D.; Ino, Y.; Shimizu, H.; Miyamoto, M.; Kokubu, A.; Hiraoka, N.; Morofuji, N.; Kondo, T.; Onaya, H.; et al. Establishment of six new human biliary tract carcinoma cell lines and identification of MAGEH1 as a candidate biomarker for predicting the efficacy of gemcitabine treatment. *Cancer Sci.* **2010**, *101*, 882–888. [CrossRef]
28. Cavalloni, G.; Peraldo-Neia, C.; Sassi, F.; Chiorino, G.; Sarotto, I.; Aglietta, M.; Leone, F. Establishment of a patient-derived intrahepatic cholangiocarcinoma xenograft model with KRAS mutation. *BMC Cancer* **2016**, *16*, 288. [CrossRef]
29. Sripa, B.; Leungwattanawanit, S.; Nitta, T.; Wongkham, C.; Bhudhisawasdi, V.; Puapairoj, A.; Sripa, C.; Miwa, M.; Sripa, S.L.B. Establishment and characterization of an opisthorchiasis-associated cholangiocarcinoma cell line (KKU-100). *World J. Gastroenterol.* **2005**, *11*, 3392–3397. [CrossRef]
30. Nakabayashi, H.; Taketa, K.; Miyano, K.; Yamane, T.; Sato, J. Growth of human hepatoma cells lines with differentiated functions in chemically defined medium. *Cancer Res* **1982**, *42*, 3858–3863.
31. Ono, A.; Hattori, S.; Kariya, R.; Iwanaga, S.; Taura, M.; Harada, H.; Suzu, S.; Okada, S. Comparative Study of Human Hematopoietic Cell Engraftment into Balb/c and C57BL/6 Strain of Rag-2/Jak3 Double-Deficient Mice. *J. Biomed. Biotechnol.* **2011**, *2011*, 1–6. [CrossRef]
32. Kariya, R.; Matsuda, K.; Gotoh, K.; Vaeteewoottacharn, K.; Hattori, S.; Okada, S. Establishment of nude mice with complete loss of lymphocytes and NK cells and application for in vivo bio-imaging. *In Vivo* **2014**, *28*, 779–784. [PubMed]
33. Edge, S.B.; Compton, C.C. The American Joint Committee on Cancer: The 7th Edition of the AJCC Cancer Staging Manual and the Future of TNM. *Ann. Surg. Oncol.* **2010**, *17*, 1471–1474. [CrossRef] [PubMed]

34. Puthdee, N.; Vaeteewoottacharn, K.; Seubwai, W.; Wonkchalee, O.; Kaewkong, W.; Juasook, A.; Pinlaor, S.; Pairojkul, C.; Wongkham, C.; Okada, S.; et al. Establishment of an Allo-Transplantable Hamster Cholangiocarcinoma Cell Line and Its Application for In Vivo Screening of Anti-Cancer Drugs. *Korean J. Parasitol.* **2013**, *51*, 711–717. [CrossRef]
35. Cai, J.; Zhao, Y.; Liu, Y.; Ye, F.; Song, Z.; Qin, H.; Meng, S.; Chen, Y.; Zhou, R.; Song, X.; et al. Directed differentiation of human embryonic stem cells into functional hepatic cells. *Hepatology* **2007**, *45*, 1229–1239. [CrossRef]
36. Vaeteewoottacharn, K.; Kariya, R.; Dana, P.; Fujikawa, S.; Matsuda, K.; Ohkuma, K.; Kudo, E.; Kraiklang, R.; Wongkham, C.; Okada, S. Inhibition of carbonic anhydrase potentiates bevacizumab treatment in cholangiocarcinoma. *Tumor Boil.* **2016**, *37*, 9023–9035. [CrossRef]
37. Detection of TP53 Mutations by Direct Sequencing. Available online: http://p53.iarc.fr/protocolsandtools.aspx (accessed on 20 April 2019).
38. Vaeteewoottacharn, K.; Kariya, R.; Pothipan, P.; Fujikawa, S.; Pairojkul, C.; Waraasawapati, S.; Kuwahara, K.; Wongkham, C.; Wongkham, S.; Okada, S. Attenuation of CD47-SIRPalpha Signal in Cholangiocarcinoma Potentiates Tumor-Associated Macrophage-Mediated Phagocytosis and Suppresses Intrahepatic Metastasis. *Transl. Oncol.* **2019**, *12*, 217–225. [CrossRef]
39. Hanna, N. Role of natural killer cells in control of cancer metastasis. *Cancer Metastasis Rev.* **1982**, *1*, 45–64. [CrossRef]
40. Golan, H.; Shukrun, R.; Caspi, R.; Vax, E.; Pode-Shakked, N.; Goldberg, S.; Pleniceanu, O.; Bar-Lev, D.D.; Mark-Danieli, M.; Pri-Chen, S.; et al. In Vivo Expansion of Cancer Stemness Affords Novel Cancer Stem Cell Targets: Malignant Rhabdoid Tumor as an Example. *Stem Cell Rep.* **2018**, *11*, 795–810. [CrossRef]
41. Park, S.-J.; Jeong, S.-Y.; Kim, H.J. Y chromosome loss and other genomic alterations in hepatocellular carcinoma cell lines analyzed by CGH and CGH array. *Cancer Genet. Cytogenet.* **2006**, *166*, 56–64. [CrossRef]
42. Wallrapp, C.; Hähnel, S.; Boeck, W.; Soder, A.; Mincheva, A.; Lichter, P.; Leder, G.; Gansauge, F.; Sorio, C.; Scarpa, A.; et al. Loss of the Y chromosome is a frequent chromosomal imbalance in pancreatic cancer and allows differentiation to chronic pancreatitis. *Int. J. Cancer* **2001**, *91*, 340–344. [CrossRef]